

**IMMUNE AND MULTI-OMIC PROFILING FOR  
MOLECULAR CLASSIFICATION AND BIOMARKER DISCOVERY  
IN SOFT TISSUE SARCOMA**

**Alexander Thomas John Lee**

**The Institute of Cancer Research**

A thesis submitted for the degree of Doctor of Philosophy

August 2019

The work presented in this thesis was completed under the supervision of Dr Robin Jones and Dr Paul Huang in the Molecular and Systems Oncology team at the Institute of Cancer research, London.

I, Dr Alexander Thomas John Lee, confirm that the work presented in this thesis is my own. Where information is derived from other sources, I confirm that this has been indicated in the thesis.

Signed:

Dr Alexander Lee

**Abstract - 4**

**Acknowledgements - 6**

**Table of Abbreviations - 7**

**Publications arising from thesis project -10**

**Table of Chapter Contents - 12**

**List of Tables - 16**

**List of Figures - 18**

## **Abstract**

Soft tissue sarcomas (STS) are a group of over 50 rare cancers of mesenchymal origin. Classification of STS is primarily based on histological characteristics of tumours. Novel biomarkers are required that account for the heterogeneity in clinical phenotype and underlying cancer biology seen within and between histological STS subtypes.

To address the unmet need for new biomarkers, the studies reported in this thesis assembled clinically annotated tumour cohorts for use in tissue profiling experiments. First, we aimed to characterise the immune tumour microenvironment (iTME) of leiomyosarcoma (LMS), undifferentiated pleomorphic sarcoma (UPS) and dedifferentiated liposarcoma (DDLPS) – three STS subtypes characterised by karyotypic complexity - and to assess for association between immune phenotype and clinical outcome. We performed TMA- based IHC profiling of infiltrating immune cells and expression analysis of 21 immune-related genes in a retrospective series of 266 early stage tumours across these 3 subtypes. We found substantial quantitative variation in immune cell infiltration between individual tumours, although differences between the 3 subtype-defined subcohorts were not pronounced. Significant association between improved overall survival and denser immune cell infiltrates was seen in UPS, while no such associations were seen in LMS and DDLPS. Meanwhile, the combination of unsupervised clustering of immune gene expression data with associated IHC-based data, led to the identification of 4 distinct immune-based subgroups that exhibited qualitatively and quantitatively contrasting iTME characteristics, were not restricted by conventional histological subtype classification and were associated with significant differences in prognosis. These hypothesis-generating results indicate that iTME-based prognostic biomarkers warrant further development as risk classifiers in early stage disease both within and across subtypes of karyotypically-complex STS.

The clinical effectiveness of pazopanib, a multitargeted kinase inhibitor with anti-angiogenic and anti-oncogenic activity, in the treatment of advanced STS is limited by the lack of predictive biomarkers and a poor understanding of the clinical mechanisms of drug response and resistance. In a retrospective series of pazopanib-treated patients with advanced STS, we undertook molecular profiling

of pre-treatment tumour specimens which led to the development of an integrated PARSARC (Pazopanib Activity and Response in SARComa) risk classifier. PARSARC consists of the sequential assessment of tumour FGFR1 and PDGFRA protein levels, *TP53* mutational status and expression levels of 229 cancer pathway-related genes that identifies patient subgroups with distinct post-pazopanib outcome, including a subgroup of long-term responders. Comparative analysis of gene expression profiles in tumours that exhibited intrinsic pazopanib resistance and in paired pre-treatment and post-progression samples from a long-term responding patient identified 3 pro-inflammatory cytokines as candidate drivers of clinical pazopanib resistance.

These studies represent discovery data of putative biomarkers that identify subgroups of patients with distinct clinical phenotype that are independent of conventional histological classification. Further studies in independent tumour cohorts are required to provide validation for iTME-based prognostic biomarkers in early stage STS and for the PARSARC classifier as a predictive biomarker for the use of pazopanib in advanced STS.

## **Acknowledgements**

I would like to thank my supervisors, Dr Robin Jones and Dr Paul Huang, for providing me with the opportunity to undertake this research project, and for their continual guidance and encouragement throughout the course of my project. Similar thanks go to Professors Ian Judson and Udai Banerjee in their roles as my back-up supervisors.

My thanks go to Dr Maggie Cheang and her team at the ICR Clinical Trials Statistical Unit for their vital contributions to many of the statistical and bioinformatics analyses included in this project. I am also grateful to Dr Richard Buus and the Breast Cancer Now Ralph Lauren Laboratory, and to Chanthrika Ragulan and the Systems and Precision Cancer Medicine Team at the ICR for their assistance and the use of their NanoString instruments.

I would like to thank all of my colleagues, both past and present, within the Molecular and Systems Oncology team at the ICR and the Sarcoma Unit at the Royal Marsden, for their invaluable advice, assistance, commiserations and celebrations. Particular thanks go to Frank McCarthy for providing me with my formative lab training, Dr Khin Thway for her guidance and stewardship of the histological aspects of my project and Dr Connie Szecei for her input and assistance with microscopy.

I am thankful to my wife Sarah, my parents and the rest of my family for providing me with support, understanding and interest, without which I would not have been able to complete this PhD.

I acknowledge the generous financial support of the NIHR Biomedical Research Centre at the Royal Marsden, The Liddy Shriver Sarcoma Initiative, Sarcoma UK and the Royal Marsden Cancer Charity. I have no competing interests to declare.

## Abbreviations

<b>12wPFR</b>	12 week progression-free rate	<b>CTL</b>	Cytotoxic T lymphocyte
<b>adDFS</b>	Advanced disease-free survival	<b>CTLA-4</b>	Cytotoxic T-lymphocyte-associated protein 4. Also known as: CD152
<b>AJCC</b>	American Joint Committee on Cancer	<b>CTSL</b>	Cathepsin L1 proteinase
<b>ALK</b>	Anaplastic lymphoma kinase	<b>DAVID</b>	Database for Annotation, Visualization and Integrated Discovery
<b>ANOVA</b>	Analysis of variance	<b>DCE-MRI</b>	Dynamic contrast-enhanced magnetic resonance imaging
<b>AS</b>	Angiosarcoma	<b>DDLPS</b>	Dedifferentiated liposarcoma
<b>ASK1</b>	Apoptosis signal-regulating kinase 1 (also: MAP3K5)	<b>DFS</b>	Disease-free survival
<b>ASPS</b>	Alveolar soft part sarcoma	<b>DNE</b>	Dominant negative effect
<b>CAF</b>	Circulating angiogenic factor	<b>DSCRT</b>	Desmoplastic small round cell tumour
<b>CC</b>	Consensus cluster(ing)	<b>DSS</b>	Disease-specific survival
<b>CD137</b>	See: TNFRSF9	<b>EFT</b>	Ewings family tumour
<b>CD274</b>	See: PD-L1	<b>EHE</b>	Epithelioid haemangi endothelioma
<b>CD276</b>	Also known as: B7-H3	<b>EORTC</b>	European Organisation for Research and Treatment of Cancer
<b>CDK2NA</b>	Cyclin-dependent kinase Inhibitor 2A	<b>ESMC</b>	Extraskelatal mesenchymal chondrosarcoma
<b>CDK4</b>	Cyclin-dependent kinase 4	<b>FATHMM-MKL</b>	Functional Analysis through Hidden Markov Models - Multiple Kernel Learning
<b>CGH</b>	Comparative genomic hybridisation	<b>FDG-PET</b>	Fluorodeoxyglucose positron emission tomography
<b>CI</b>	Confidence Interval	<b>FDR</b>	False discovery rate
<b>CINSARC</b>	Complexity index in Sarcomas	<b>FFPE</b>	Formalin-fixed, paraffin-embedded
<b>CONSORT</b>	Consolidated Standards of Reporting Trials	<b>FGFR1</b>	Fibroblast growth factor receptor 1
<b>COSMIC</b>	Catalogue of Somatic Mutations in Cancer	<b>FNCLCC</b>	National Federation of French Cancer Centres
<b>CSF1</b>	Colony-stimulating factor 1	<b>FOXP3</b>	Forkhead box P3
<b>CSF1R</b>	Colony-stimulating factor 1 receptor	<b>GIST</b>	Gastrointestinal stromal tumour
<b>CT</b>	Computerised tomography	<b>H&amp;E</b>	Haematoxylin and eosin
<b>CTA</b>	Cancer testis antigen	<b>HGF</b>	Hepatocyte growth factor

<b>HIF</b>	Hypoxia-inducible factor	<b>MHC</b>	Major histocompatibility complex
<b>HK gene</b>	Housekeeping gene	<b>MLPS</b>	Myxoid liposarcoma
<b>HLA</b>	Human leukocyte antigen	<b>mOS</b>	Median overall survival
<b>HPF</b>	High powered field	<b>mPFS</b>	Median progression-free survival
<b>HR</b>	Hazard ratio	<b>MPNST</b>	Malignant peripheral nerve sheath tumour
<b>ICR</b>	Institute of Cancer Research	<b>mRCC</b>	Metastatic renal cell carcinoma
<b>IDO</b>	Indoleamine 2,3-dioxygenase	<b>MRI</b>	Magnetic resonance imaging
<b>IFN<math>\gamma</math></b>	Inteferon gamma	<b>MRT</b>	Malignant rhabdoid tumour
<b>IHC</b>	Immunohistochemistry	<b>MSI</b>	Microsatellite instability
<b>IL</b>	Interleukin	<b>mTOR</b>	mammalian target of rapamycin
<b>IQR</b>	Interquartile range	<b>NCAM1</b>	Neural cell adhesion molecule 1. Also known as: CD56
<b>iTME</b>	Tumour immune microenvironment	<b>NGS</b>	Next generation sequencing
<b>KIR3DL1</b>	Killer Cell Immunoglobulin Like Receptor, Three Ig Domains And Long Cytoplasmic Tail 1	<b>NKC</b>	Natural killer cell
<b>LAMP3</b>	Lysosome-associated membrane glycoprotein 3	<b>NLR</b>	Neutrophil: lymphocyte ratio
<b>IcPD-L1</b>	Lymphocyte expression of PD-L1	<b>NSCLC</b>	Non-small cell lung carcinoma
<b>LDOC</b>	Low dose oral cyclophosphamide	<b>ORR</b>	Objective response rate
<b>LIF</b>	Leukaemia inhibitory factor	<b>OS</b>	Overall survival
<b>LMS</b>	Leiomyosarcoma	<b>PARSARC</b>	Pazopanib Activity and Response in Sarcoma
<b>LOA</b>	Limits of agreement	<b>PCR</b>	Polymerase chain reaction
<b>LPS</b>	Liposarcoma	<b>PD1</b>	See PDCD1
<b>mAb</b>	Monoclonal antibody	<b>PDCD1</b>	Programmed cell death protein 1. Also known as: PD1, CD279
<b>MAPK</b>	Mitogen-activated protein kinase	<b>PDCD1LG2</b>	Programmed cell death 1 ligand 2. Also known as: PD-L2, B7-DC
<b>max tPD-L1</b>	Maximum score for tumour expression of PD-L1	<b>PDGFRA</b>	Platelet-derived growth factor receptor 1
<b>Mc</b>	Macrophage	<b>PD-L1</b>	Programmed death-ligand 1. Also known as: CD274
<b>MDM2</b>	Mouse double minute 2 homolog	<b>PD-L2</b>	See PDCD1LG2
<b>MDSC</b>	Myeloid-derived suppressor cell	<b>PEComa</b>	Perivascular epithelioid cell neoplasm
<b>MFH</b>	Malignant fibrous histiocytoma	<b>PFI</b>	Progression-free interval

<b>MFS</b>	Myxofibrosarcoma	<b>PFS</b>	Progression-free survival
<b>PMN</b>	Polymorphonuclear neutrophil	<b>Poly PHEN-2</b>	Polymorphism Phenotyping v2
<b>polyPHEN-2</b>	Polymorphism Phenotyping v2	<b>TAM</b>	Tumour-associated macrophage
<b>PR</b>	Partial response	<b>TCGA</b>	The Cancer Genome Atlas
<b>PRF1</b>	Perforin	<b>TCR</b>	T cell receptor
<b>PROVEAN</b>	Protein Variation Effect Analyzer	<b>TGF<math>\beta</math></b>	Tissue growth factor beta
<b>PTEN</b>	Phosphatase and tensin homolog	<b>TIL</b>	Tumour-infiltrating lymphocyte
<b>pTMA</b>	Physical TMA	<b>TIL/core</b>	Number of TIL per 1mm diameter TMA core
<b>RB1</b>	Retinoblastoma 1	<b>TIL/HPF</b>	Number of TIL per x400 high-powered microscopy field
<b>RCT</b>	Randomised controlled trial	<b>TIL/mm<sup>2</sup></b>	Standardised number of TIL per 1mm <sup>2</sup> tumour tissue
<b>RE</b>	Response element	<b>TIM3</b>	T-cell immunoglobulin and mucin-domain containing-3. Also known as: HAVCR2
<b>RECIST</b>	Response Evaluation Criteria in Solid Tumors	<b>TKI</b>	Tyrosine kinase inhibitor
<b>RFS</b>	Relapse-free survival	<b>TLR4</b>	Toll-like receptor 4
<b>RMH</b>	Royal Marsden Hospital	<b>TMA</b>	Tissue microarray
<b>RTK</b>	Receptor tyrosine kinase	<b>TME</b>	Tumour microenvironment
<b>SAM</b>	Significance analysis of microarrays	<b>TNFRSF9</b>	Tumor necrosis factor receptor superfamily member 9. Also known as: CD137; 4-1BB; ILA ( <i>induced by lymphocyte activation</i> )
<b>SCNA</b>	Somatic copy number abnormality	<b>TP3wt</b>	TP53 wildtype
<b>SD</b>	Stable disease	<b>TP53mut</b>	TP53 mutated
<b>SFT</b>	Solitary fibrous tumour	<b>Treg</b>	Regulatory T cell
<b>SIFT</b>	Sorting Intolerant from Tolerant	<b>uLMS</b>	Uterine leiomyosarcoma
<b>SNV</b>	Single nucleotide variant	<b>UPS</b>	Undifferentiated pleomorphic sarcoma
<b>SS</b>	Synovial sarcoma	<b>VEGF</b>	Vascular endothelial growth factor
<b>STAT6</b>	Signal Transducer And Activator Of Transcription 6	<b>VEGFR</b>	Vascular endothelial growth factor receptor
<b>STBSG</b>	Soft Tissue and Bone Sarcoma Group	<b>VTCN1</b>	V-set domain-containing T-cell activation inhibitor 1/ Also known as: B7-H4
<b>STLMS</b>	Soft tissue leiomyosarcoma	<b>vTMA</b>	Virtual TMA
<b>STS</b>	Soft tissue sarcoma	<b>WDLPS</b>	Well differentiated liposarcoma
<b>SUVmax</b>	Maximum standardized uptake value	<b>WHO</b>	World Health Organisation

## **Publications and presentations arising from thesis project**

### **Peer-reviewed primary research papers**

Lee ATJ, Chew W, Smith MJ *et al.* The adequacy of tissue microarrays in the assessment of inter- and intra-tumoural heterogeneity of infiltrating lymphocyte burden in leiomyosarcoma. *Sci Rep* (2019) – *revision in response to reviewers comments submitted. BioRxiv preprint doi.org/10.1101/412387. **This manuscript is based on work reported in Chapter 3***

Lee ATJ, McCarthy F, Elms M. A molecular classifier for pazopanib response in soft tissue sarcoma identifies the IL-8/Src signalling axis as a driver of resistance. *Nat Comms* (2019) – *under revision in response to reviewers comments. **This manuscript includes work reported in Chapters 6 and 7.***

### **Peer-reviewed review articles *\*\*denotes joint first authorship***

Lee ATJ, Jones RL, Huang PH. Pazopanib in advanced soft tissue sarcomas. *Signal Transduct Target Ther* 2019; **4**: 16. doi: 10.1038/s41392-019-0049-6

Lee ATJ, Thway K, Huang PH, Jones RL. Clinical and molecular spectrum of liposarcoma. *J Clin Oncol* 2018; **36**(2): 151-159. doi: 10.1200/JCO.2017.74.9598

Antoniou G\*, Lee ATJ\*, Huang P, Jones RL. Olaratumab in soft tissue sarcoma – Current status and future perspectives. *Eur J Cancer* 2018; **92**:33-39. doi: 10.1016/j.ejca.2017.12.026

Frezza AM, Lee ATJ, Nizri E, Sbaraglia M, Jones R, Gronchi A, Dei Toa AP, Casali PG. 2018 ESMO Sarcoma and GIST Symposium: ‘take-home messages’ in soft tissue sarcoma. *ESMO Open* 2018;**3**:e000390. doi:10.1136/esmoopen-2018-000390

Lima N\*, Lee A\*, Huang P. Progress and Impact of clinical phosphoproteomics on precision oncology. *Transl Cancer Res* 2017;**6**(Suppl 6):S1108-S1114. doi: 10.21037/tcr.2017.07.05

Lee A, Pollack S, Huang P & Jones R. Phase III soft tissue sarcoma trials: Success or Failure? *Curr. Treat. Options Oncol.* 2017; **18**(3):19. Doi: 10.1007/s11864-017-0457-1

Lee A, Huang P, DeMatteo R, & Pollack S. Immunotherapy for Soft Tissue Sarcoma - Tomorrow is Only a Day Away. *Am. Soc. Clin. Oncol. Educ. Book* 2016;**35**;281-90. doi: 10.14694/EDBK\_157439

Lee A, Huang P, Pollack S, Jones R. Drug repositioning in sarcomas and other rare tumours. *EBioMedicine* (2016). doi:10.1016/j.ebiom.2016.03.021

## **Meeting presentations**

Lee ATJ, Szeczei C, Millighetti M, Judson I, Thway K, Jones R, Huang P. The immune microenvironment of leiomyosarcoma, undifferentiated pleomorphic sarcoma and dedifferentiated liposarcoma. Connective Tissue Oncology Society (CTOS) Annual Conference, Rome, Nov 2018.

Lee A. Mobilising FFPE tissue archives for soft tissue sarcoma research. CM-Path Biomarker Symposium Series: The Liquid Biopsy. London, UK, 8th March 2018. Plenary session.

Huang P, Lee ATJ et al. A molecular signature predictive of clinical outcome following pazopanib therapy in advanced soft tissue sarcoma. Mini oral presentation, ESMO Asia 2017 Congress, Singapore, 17-19 November 2017.

Lee A, McCarthy F, Thway K, Morden J, Messiou C, Buus R, Cheang M, Jones R, Huang P. A molecular signature for risk classification following pazopanib therapy in advanced soft tissue sarcoma. ICR Conference, Royal Holloway, UK. June 2017. Poster presentation.

Lee A, Thway K, Pollack S, Judson I, Huang P, Jones R. The accuracy of tissue microarrays in the study of the sarcoma immune microenvironment is dependent on the number of sampled cores. Advances in Sarcomas: From Basic Science to Clinical Translation (AACR), Philadelphia, USA, May 2017. Poster presentation

## **Patents**

Material and methods for stratifying and treating cancers - Lee ATJ, Jones RL, Cheang M, Huang PH

Materials and methods for monitoring the development of resistance of cancers to treatment – Lee ATJ, Huang PH, Elms M

***Both patent submissions relate to work reported in Chapters 6 and 7***

# **Table of Chapters**

<b>CHAPTER 1 – INTRODUCTION</b>	<b>19</b>
1.1 SOFT TISSUE SARCOMAS ARE CLINICALLY AND BIOLOGICALLY HETEROGENEOUS	19
1.2 CLASSIFICATION OF STS	19
1.2.1 <i>Histological classification</i>	19
1.2.2 <i>Genomic Classification</i>	20
1.2.3 <i>Clinico-pathological characteristics of LMS, UPS and DDLPS</i>	24
1.2.4 <i>Emerging molecular classifications</i>	26
1.2.5 <i>Molecular pathology of LMS, UPS and DDLPS</i>	29
1.3 CURRENT STANDARDS OF CARE FOR STS	33
1.3.1 <i>Localised Disease</i>	33
1.3.2 <i>Advanced STS</i>	35
1.4 PAZOPANIB IN THE TREATMENT OF ADVANCED STS	41
1.4.1 <i>Pre-clinical development of pazopanib</i>	41
1.4.2 <i>Early phase clinical development of pazopanib</i>	44
1.4.3 <i>Clinical development of pazopanib for advanced STS</i>	46
1.4.4 <i>Evidence of biomarkers of pazopanib effect</i>	52
1.5 THE IMMUNE SYSTEM IN STS	60
1.5.1 <i>Anti-tumour immunity as therapy and a source of biomarkers</i>	60
1.5.2 <i>The immune microenvironment of STS</i>	72
1.5.3 <i>Immune characteristics of LMS, UPS and DDLPS</i>	86
1.5.4 <i>Clinical investigation of immunotherapy in STS</i>	88
1.5.4 <i>Summary</i>	92
1.6 CANCER BIOMARKERS	93
1.6.1 <i>Prognostic biomarkers</i>	93
1.6.2 <i>Predictive Biomarkers</i>	95
1.7 CONCLUSIONS, HYPOTHESIS AND AIMS	97
<b>CHAPTER 2: MATERIALS AND METHODS</b>	<b>99</b>
2.1 VALIDATION OF TMAS FOR IMMUNE PROFILING	99
2.1.1 <i>Tumour sample selection and processing</i>	99
2.1.2 <i>IHC scoring</i>	100
2.1.3 <i>Statistical analysis</i>	100
2.1.4 <i>Research ethics</i>	102
2.2 PROFILING THE IMMUNE MICROENVIRONMENT IN 3 GENOMICALLY-COMPLEX HISTOLOGICAL SUBTYPES OF STS	103
2.2.1 <i>Patient selection and treatment</i>	103
2.2.2 <i>Tumour sample selection and processing</i>	104
2.2.3 <i>IHC staining and scoring</i>	104

2.2.4 <i>Gene expression analysis</i>	106
2.2.5 <i>Statistical analysis</i>	106
2.3 MOLECULAR RISK CLASSIFICATION AND INVESTIGATION OF RESISTANCE MECHANISMS IN ADVANCED STS TREATED WITH PAZOPANIB	108
2.3.1 <i>Patient selection and treatment</i>	108
2.3.2 <i>Tissue selection and processing</i>	109
2.3.3 <i>IHC</i>	109
2.3.4 <i>TP53 exon sequencing</i>	110
2.3.5 <i>Gene expression analysis</i>	111
2.3.6 <i>Independent evaluation of the biological subgroups on Stanford-LMS dataset</i>	113
2.3.7 <i>Independent Evaluation of identified biomarkers in TCGA-SARC dataset</i>	113
2.3.8 <i>Statistical analysis</i>	114
<b>CHAPTER 3: VALIDATION OF TMAS FOR IMMUNE PROFILING</b>	<b>116</b>
3.1 BACKGROUND AND OBJECTIVES	116
3.2 RESULTS	119
3.2.1 <i>Patient and tumour characteristics</i>	119
3.2.2 <i>LMS are variably infiltrated by T lymphocytes</i>	120
3.3.3 <i>Inter-tumour heterogeneity in TIL burden of LMS greatly outweighs intra-tumour heterogeneity</i>	122
3.2.4 <i>Optimal number of cores to ensure representativeness of tissue microarrays depends on required degree of accuracy</i>	125
3.2.5 <i>Triplicate TMA cores provide adequate sampling for the classification of LMS as containing high or low TIL burden.</i>	129
3.3 DISCUSSION	133
<b>CHAPTER 4: CHARACTERISING THE IMMUNE MICROENVIRONMENT IN GENOMICALLY-COMPLEX STS SUBTYPES</b>	<b>135</b>
4.1 OBJECTIVES	135
4.2 RESULTS	137
4.2.1 <i>Cohort identification</i>	137
4.2.2 <i>Baseline Characteristics</i>	139
4.2.3 <i>Summary of cohort survival</i>	141
4.2.4 <i>IHC-based analysis of immune microenvironment</i>	143
4.2.5 <i>Targeted gene expression-based profiling of the immune microenvironment</i>	152
4.3 DISCUSSION	165
4.4 SUPPLEMENTARY MATERIAL	174
4.4.1 <i>Supplemental Tables</i>	174
4.4.2 <i>Supplemental Figures</i>	178

<b>CHAPTER 5 - PROGNOSTIC ASSOCIATIONS OF THE IMMUNE MICROENVIRONMENT IN STS SUBTYPES WITH COMPLEX KARYOTYPES</b>	<b>204</b>
5.1 BACKGROUND AND OBJECTIVES	204
5.2 RESULTS	205
5.2.1 <i>T lymphocyte infiltration is associated with survival in UPS but not LMS or DDLPS</i>	205
5.2.2 <i>CD68+ macrophage infiltration is associated with survival in UPS but not LMS or DDLPS</i>	207
5.2.3 <i>Tumour and leucocyte PD-L1 expression has contrasting associations with survival depending on STS histological subtype</i>	210
5.2.4 <i>The High Infiltration Immune Cluster is associated with improved overall survival across STS subtypes</i>	213
5.2.5 <i>Immune microenvironment characteristics are independent prognostic factors in STS with complex karyotypes</i>	215
5.3 DISCUSSION	217
5.4 SUPPLEMENTARY MATERIAL	221
5.4.1 <i>Supplemental Figures</i>	221
<b>CHAPTER 6: MOLECULAR RISK CLASSIFICATION FOR PAZOPANIB IN STS</b>	<b>228</b>
6.1 BACKGROUND AND OBJECTIVES	228
6.2 RESULTS	230
6.2.1 <i>Cohort Characteristics</i>	230
6.2.2 <i>FGFR1 and PDGFRA expression</i>	233
6.2.3 <i>TP53 mutations</i>	235
6.2.4 <i>Biclustering analysis identifies biological subgroups variably enriched for histological subtypes or high PDGFRA and low FGFR1 expression</i>	239
6.2.5 <i>High PDGFRA/ Low FGFR1 IHC signature and TP53 mutation are associated with poor outcome following pazopanib therapy</i>	241
6.2.6 <i>Consensus clustering identifies three subgroups with contrasting post-pazopanib outcomes</i>	244
6.2.7 <i>Integration of molecular subgroups into a candidate risk classification model for pazopanib treatment.</i>	247
6.3 DISCUSSION	251
6.4 SUPPLEMENTARY MATERIAL	255
6.4.1 <i>Supplemental Tables</i>	255
6.4.2 <i>Supplemental Figures</i>	258
<b>CHAPTER 7: IDENTIFICATION OF GENES ASSOCIATED WITH PAZOPANIB RESISTANCE</b>	<b>262</b>
7.1 BACKGROUND AND OBJECTIVES	262
7.2 RESULTS	263
7.2.1 <i>Intrinsic pazopanib resistance is associated with upregulation of cytokine signalling and downregulation of cell cycle control and DNA repair pathways</i>	263

<i>7.2.2 Upregulated genes associated with acquired pazopanib resistance in a long-term responding patient</i>	268
<i>7.2.3 Pro-inflammatory cytokine expression is associated with both intrinsic and acquired pazopanib resistance</i>	270
7.3 DISCUSSION	271
<b>CHAPTER 8: CONCLUSIONS AND FUTURE DIRECTIONS</b>	<b>275</b>
<b>REFERENCES</b>	<b>284</b>
<b>APPENDIX 1 – PROSPECTUS STUDY PROTOCOL</b>	<b>319</b>

## **LIST OF TABLES**

### **Chapter 1**

TABLE 1.1: SELECTED EXAMPLES OF RECURRENT GENOMIC ABERRATIONS ASSOCIATED WITH SPECIFIC STS SUBTYPES. ....	21
TABLE 1.2: CURRENT STANDARD SYSTEMIC THERAPIES AND ASSOCIATED LEVEL OF EVIDENCE FOR ADVANCED STS .....	40
TABLE 1.3: SUMMARY OF CLINICAL STUDY DATA ON EFFICACY OF PAZOPANIB IN STS .....	51
TABLE 1.4. OVERVIEW OF CURRENT IHC-BASED PD-L1 BIOMARKER ASSAYS.....	68
TABLE 1.5: SUMMARY OF CANCER IMMUNE SUBTYPES WITHIN >10000 TUMOURS PROFILED BY TCGA.....	71
TABLE 1.6: SUMMARY OF HISTOPATHOLOGY-BASED STUDIES PROFILING TUMOUR PD-L1 EXPRESSION IN STS.....	74
TABLE 1.7: SUMMARY OF HISTOPATHOLOGY-BASED STUDIES PROFILING LYMPHOCYTE INFILTRATION IN STS .....	76
TABLE 1.8: SUMMARY OF HISTOPATHOLOGY-BASED STUDIES PROFILING MACROPHAGE INFILTRATION IN STS.....	78
TABLE 1.9: SUMMARY OF IMMUNE PROFILING DATA IN LMS, UPS AND DDLPS.....	91

### **Chapter 3**

TABLE 3.1: BASELINE CLINICO-PATHOLOGICAL STATUS OF 47 PATIENTS WITH PRIMARY LMS. ....	119
---	-----

### **Chapter 4**

TABLE 4.1: BASELINE CHARACTERISTICS OF LMS, UPS AND DDLPS SUB-COHORTS .....	140
TABLE 4.2: SUMMARY OF FOLLOW-UP AND EVENT RATE IN 3 SUB-COHORTS .....	141
TABLE 4.3: 21 IMMUNE-RELATED GENE PANEL .....	153
TABLE 4.4: SUMMARY OF GENE EXPRESSION, IHC AND HISTOLOGICAL CHARACTERISTICS OF 4 IMMUNE CLUSTERS.....	164

### **Chapter 5**

TABLE 5.1: UNIVARIATE AND MULTIVARIATE SURVIVAL ANALYSIS IN 266 STS COHORT .....	216
TABLE 5.2: UNIVARIATE AND MULTIVARIATE SURVIVAL ANALYSIS IN 72 UPS SUB-COHORT .....	216

### **Chapter 6**

TABLE 6.1: BASELINE CLINICO-PATHOLOGICAL FEATURES OF RMH-SARC COHORT .....	232
TABLE 6.2: FGFR1 AND PDGFRA IHC EXPRESSION LEVELS AND TP53 MUTATION STATUS IN RMH-SARC COHORT .....	237
TABLE 6.3: DESCRIPTION AND PREDICTED FUNCTIONAL EFFECT OF TP53 MUTATIONS IDENTIFIED WITHIN RMH-SARC COHORT.....	238
TABLE 6.4: UNIVARIATE AND MULTIVARIATE ANALYSIS OF PFS AND OS BY CLINICO-PATHOLOGICAL FACTORS, IHC SIGNATURE AND TP53 MUTATIONAL STATUS .....	243

### **Chapter 7**

TABLE 7.1: GENES WITH SIGNIFICANTLY DIFFERENTIAL EXPRESSION IN INTRINSIC RESISTANT F-Lo/P-Hi SUBGROUP WITHIN RMH-SARC .....	264
TABLE 7.2: BIOLOGICAL FUNCTION ANALYSIS OF UPREGULATED GENES IN F-Lo/P-Hi TUMOURS IN RMH-SARC.....	265
TABLE 7.3: BIOLOGICAL FUNCTION ANALYSIS OF DOWNREGULATED GENES IN F-Lo/P-Hi TUMOURS IN RMH-SARC.....	266

## **LIST OF FIGURES**

### **Chapter 1**

FIGURE 1.1: THE SPECTRUM OF GENOMIC CHARACTERISTICS IN STS	22
FIGURE 1.2: KINASE INHIBITORY PROFILE OF PAZOPANIB.	43
FIGURE 1.3: OVERVIEW OF THE IMMUNO-EDITING MODEL IN CANCER	62

### **Chapter 3**

FIGURE 3.1: EVALUATION OF INFILTRATING T AND B LYMPHOCYTE BURDEN IN LMS	121
FIGURE 3.2: ASSESSMENT OF INTER- AND INTRA-TUMOUR HETEROGENEITY OF TIL BURDEN IN LMS	123
FIGURE 3.3: OPTIMAL NUMBER OF TMA CORES RELATES TO REQUIRED DEGREE OF ACCURACY FOR ASSESSMENT OF LYMPHOCYTE INFILTRATION	127
FIGURE 3.4: TRIPPLICATE TMA CORES CAN IDENTIFY TUMOURS AS HAVING A HIGH OR LOW TIL BURDEN, BUT DO NOT ACCURATELY ESTIMATE PRECISE TIL NUMBERS	131

### **Chapter 4**

FIGURE 4.1: CONSORT DIAGRAM OF LMS, UPS AND DDLPS SUB-COHORTS	138
FIGURE 4.2: SWIMMER'S PLOTS OF LMS, UPS AND DDLPS SUB-COHORTS	142
FIGURE 4.3: DISTRIBUTION OF TIL DENSITIES WITHIN STS COHORTS.	145
FIGURE 4.4: DISTRIBUTION OF AVERAGE CD68 SCORES IN LMS, UPS AND DDLPS SUB-COHORTS	147
FIGURE 4.5: DISTRIBUTION OF MAXIMUM TUMOUR PD-L1 SCORES IN LMS, UPS AND DDLPS SUB-COHORTS	149
FIGURE 4.6: PROPORTION OF TUMOURS WITH PRESENCE OR ABSENCE OF PD-L1-STAINING LEUCOCYTES IN LMS, UPS AND DDLPS SUB-COHORTS.	149
FIGURE 4.7: CORRELATION OF EXPRESSION OF 21 IMMUNE-RELATED GENES IN STS COHORT	155
FIGURE 4.8: UNSUPERVISED CLUSTERING OF IMMUNE GENE EXPRESSION DATA IDENTIFIES 4 PAN-SUBTYPE CLUSTERS.	157
FIGURE 4.9: DISTRIBUTION OF BASELINE CLINICO-PATHOLOGICAL CHARACTERISTICS WITHIN 4 IMMUNE CLUSTERS	159
FIGURE 4.10: ASSOCIATION OF GENE EXPRESSION-DERIVED IMMUNE CLUSTERS WITH IHC-BASED IMMUNE MICROENVIRONMENT PARAMETERS	161

### **Chapter 5**

FIGURE 5.1: OVERALL SURVIVAL IN UPS STRATIFIED BY T LYMPHOCYTE INFILTRATION	206
FIGURE 5.2: OVERALL SURVIVAL IN KARYOTYPICALLY-COMPLEX STS WHEN STRATIFIED BY INFILTRATION BY CD68+ MACROPHAGES	209
FIGURE 5.3: OVERALL SURVIVAL IN KARYOTYPICALLY-COMPLEX STS WHEN STRATIFIED BY TUMOUR EXPRESSION OF PD-L1	211
FIGURE 5.4: OVERALL SURVIVAL IN KARYOTYPICALLY-COMPLEX STS WHEN STRATIFIED BY PD-L1 EXPRESSION ON TUMOUR-INFILTRATING LEUCOCYTES	212
FIGURE 5.5: OVERALL SURVIVAL IN KARYOTYPICALLY-COMPLEX STS WHEN STRATIFIED BY IMMUNE-BASED CLUSTERS	214

## Chapter 6

FIGURE 6.1: IDENTIFICATION OF STUDY COHORT AND EXPERIMENTAL PLAN	230
FIGURE 6.2: REPRESENTATIVE IHC IMAGES OF FGFR1 AND PDGFRA EXPRESSION LEVELS IN PRE-PAZOPANIB STS TUMOUR SPECIMEN	234
FIGURE 6.3: TP53 MUTATIONAL STATUS IN RMH-SARC	236
FIGURE 6.4: BICLUSTERING ANALYSIS OF GENE EXPRESSION DATA FROM RMH-SARC IDENTIFIES BIOLOGY-DEFINED PATIENT SUBGROUPS	240
FIGURE 6.5: F-LO/P-HI AND TP53 MUTATED PATIENT SUBGROUPS ARE ASSOCIATED WITH WORSE POST-PAZOPANIB OUTCOME	242
FIGURE 6.6: CONSENSUS CLUSTERING OF GENE EXPRESSION DATA FROM IHCNEGTP53WT PATIENTS IDENTIFIES BIOLOGY-DEFINED INTRINSIC SUBGROUPS	246
FIGURE 6.7: COMBINATION OF FGFR1 AND PDGFRA IHC, TP53 MUTATION STATUS AND GENE EXPRESSION ANALYSIS PROVIDES OPTIMAL RISK CLASSIFICATION	249
FIGURE 6.8: NO PROGNOSTIC ASSOCIATION BETWEEN PARSARC RISK CLASSIFIER AND OVERALL SURVIVAL IN TCGA-SARC DATASET	250

## Chapter 7

FIGURE 7.1: INVOLVEMENT OF GENES DOWNREGULATED IN F-LO/P-HI TUMOURS IN DNA REPAIR AND CELL CYCLE FUNCTIONAL ANNOTATION TERMS	267
FIGURE 7.2: OVERVIEW OF LONG-TERM RESPONDER PATIENT TREATED WITH PAZOPANIB	269
FIGURE 7.3: OVERLAP OF GENES UPREGULATED IN F-LO/P-HI INTRINSIC RESISTANT TUMOURS AND GENES UPREGULATED UPON ACQUISITION OF PAZOPANIB RESISTANCE IN A LONG-TERM RESPONDER (RMH001)	270

## Chapter 8

FIGURE 8.1: STUDY OVERVIEW OF VMPRASS (VALIDATION OF A MOLECULAR SIGNATURE OF PAZOPANIB RESPONSE IN ADVANCED SOFT TISSUE SARCOMA).	279
--	-----

## **Chapter 1 – Introduction**

### **1.1 Soft tissue sarcomas are clinically and biologically heterogeneous**

STS are a group of rare cancers of mesenchymal origin that can arise at practically any anatomical site and affect patients from early childhood through to old age. Although an annual UK incidence of around 3200 new cases per year indicates that STS occurs with a frequency comparable to such conditions as testicular or cervical cancer or multiple myeloma, a unique challenge is presented by the sub-classification of STS into over 50 distinct diagnoses, encompassing a broad range of histological features, clinical phenotype and underlying cancer biology<sup>1</sup>. While subtype-specific research into these rare diseases have resulted in the identification of recurrent molecular characteristics that in turn have led to transformative therapeutic advances in a proportion of subtypes, the majority of STS remains subject to largely generic management approaches that are often associated with low levels of patient benefit. The rarity of STS has often led to the inclusion of many different subtypes in clinical trial cohorts, wherein heterogeneity in underlying tumour biology is a likely determinant of limited efficacy of investigational agents<sup>2</sup>. While it is recognised that certain STS subtypes are associated with greater or lesser sensitivity to chemo- and/or radiotherapy, currently available methods of subtype classification provide only limited guidance for the identification of patient subpopulations most likely to benefit from specific therapies<sup>3</sup>.

### **1.2 Classification of STS**

#### ***1.2.1 Histological classification***

Clinical and histopathological findings remain dominant determinants of STS diagnosis and sub-classification<sup>1</sup>. Recognition of cell and tissue morphology, alongside the use of immunohistochemistry (IHC) in attempt to detect expression of lineage-specific protein expression and determine tissue of origin, is sufficient to meet current diagnostic criteria for a majority of STS subtypes. However, the degree of diagnostic nuance involved in this process demands the input of an experienced specialist sarcoma histopathologist, as there is often diagnostic discrepancy between specialist and non-specialist pathologists. For example, in

a recent report of a mixed STS cohort studied by The Cancer Genome Atlas (TCGA) consortium, 51/237 (21.5%) of tumour samples were subject to diagnostic reassignment following central expert pathology review<sup>4</sup>. Furthermore, atypical morphological features such as epithelioid variants of typically spindle cell-predominant STS subtypes, may misdirect histology-based diagnoses, while dedifferentiated tumours often have lost recognisable morphological or protein expression-based indicators of lineage. Even in the common instances where a confident diagnosis is established, clinico-pathological classification will often insufficiently describe the range of clinical behaviour encompassed within specific STS subtypes. As a result, significant clinical uncertainty related to prognosis and optimal management approach may persist.

### **1.2.2 Genomic Classification**

Incremental advances in genomic characterisation have improved the diagnostic accuracy for certain STS subtypes, and it is increasingly well recognised that, as a group of distinct diseases, STS occupies a spectrum of genomic complexity (**Table 1.1; Figure 1.1**). A proportion of STS subtypes are now characterised by pathognomonic chromosomal alterations that may often occur in the context of an otherwise largely unaltered genome. These recurrent alterations include gene fusions resulting from chromosomal translocation, resulting in fusion proteins that confer oncogenicity through a variety of increasingly well-characterised mechanisms, or specific chromosomal segment amplifications or deletions that result in overexpression or loss of expression of genes with respective oncogenic or tumour suppressor function. Such alterations now serve as diagnostic biomarkers that can be detected by in-situ hybridisation or quantitative polymerase chain reaction (PCR)-based assays or, where validated, correlating protein expression levels as measured by IHC. In one French study of 384 patients with a preliminary histology-based diagnosis of one of 6 STS subtypes with known pathognomonic alterations, molecular testing resulted in change of diagnosis in 14%, including some patients where initial histological diagnosis by an expert pathologist had been categorised as 'certain'<sup>5</sup>. These findings demonstrate the importance of judicious use of ancillary molecular tests in modern STS diagnoses.

Histotype	Common genomic aberration(S)	Involved genes	Oncogenic mechanism	Histological correlates	Associated therapy
<b>Alveolar rhabdomyosarcoma</b>	t(2;13)(p36;14) t(1;13)(p36;q14)	<i>PAX3-FOXO1</i> fusion <i>PAX7-FOXO1</i> fusion	Dysregulated transcription		
<b>Alveolar soft part sarcoma</b>	t(X;17)(p11.2;q25)	<i>TFE3-ASPSCR1</i> fusion	Dysregulated transcription	TFE3 expression	
<b>Synovial sarcoma</b>	t(X;18)(p11;q11) t(X;18)(p11;q11)	<i>SS18-SSX1</i> fusion <i>SS18-SSX2</i> fusion	Dysregulated transcription		EZH2 inhibitors
<b>Myxoid liposarcoma</b>	t(12;16)(q13;p11) t(12;22)(q13;q11-q12)	<i>FUS-DDIT3</i> fusion <i>EWSR1-DDIT3</i> fusion	Dysregulated transcription		
<b>Solitary fibrous tumour</b>	Inv(12)(q13q13)	<i>NAB2-STAT6</i> fusion	Dysregulated transcription	Nuclear STAT6 expression	
<b>Inflammatory myofibroblastic tumor</b>	t(2;19)(p23;p13.1) t(1;2)(q22-23;p23)	<i>TPM4-ALK</i> fusion <i>TPM3-ALK</i> fusion	Dysregulated transcription	ALK expression	ALK inhibitors
<b>Ewing sarcoma</b>	t(11;22)(q24;q12) t(21;22)(q22;q12)	<i>EWSR1-FLI1</i> fusion <i>EWSR1-ERG</i> fusion	Dysregulated transcription		
<b>CIC-rearranged sarcoma</b>	t(4;19)(q35;q13) t(10;19)(q26;q13)	<i>CIC-DUX4</i> fusion	Dysregulated transcription		
<b>Dermatofibrosarcoma</b>	t(17;22)(q22;q13)	<i>COL1A1-PDGFB</i> fusion	Oncogene activation		Imatinib
<b>GIST</b>	Missense/ small InDel	<i>KIT</i> activating mutation <i>PDGFRA</i> activating mutation	Oncogene activation	KIT expression	Imatinib, sunitinib, regorafenib, pazopanib
<b>Well/de-differentiated liposarcoma</b>	12q(13-15) amplification	<i>MDM2</i> and <i>CDK4</i> amplification	Oncogene activation	Ring/giant chromosomes	
<b>MPNST</b>	Truncating mutation Homo/heterozygous deletion	<i>NF1</i> LoF <i>SUZ12/ EED</i> LoF	Loss of tumour suppressor function	Loss of H3K27me3	
<b>Epithelioid sarcoma Malignant rhabdoid tumours</b>	Homozygous deletion Biallelic mutation Epigenetic silencing	<i>SMARCB1</i> LoF	Loss of tumour suppressor function	<i>SMARCB1</i> loss of expression	EZH2 inhibitors
<b>Perivascular epithelioid cell tumours (PEComa)</b>	LOH mutation	<i>TSC1/TSC2</i> LoF	Loss of tumour suppressor function		mTOR inhibitors

**Table 1.1: Selected examples of recurrent genomic aberrations associated with specific STS subtypes.**

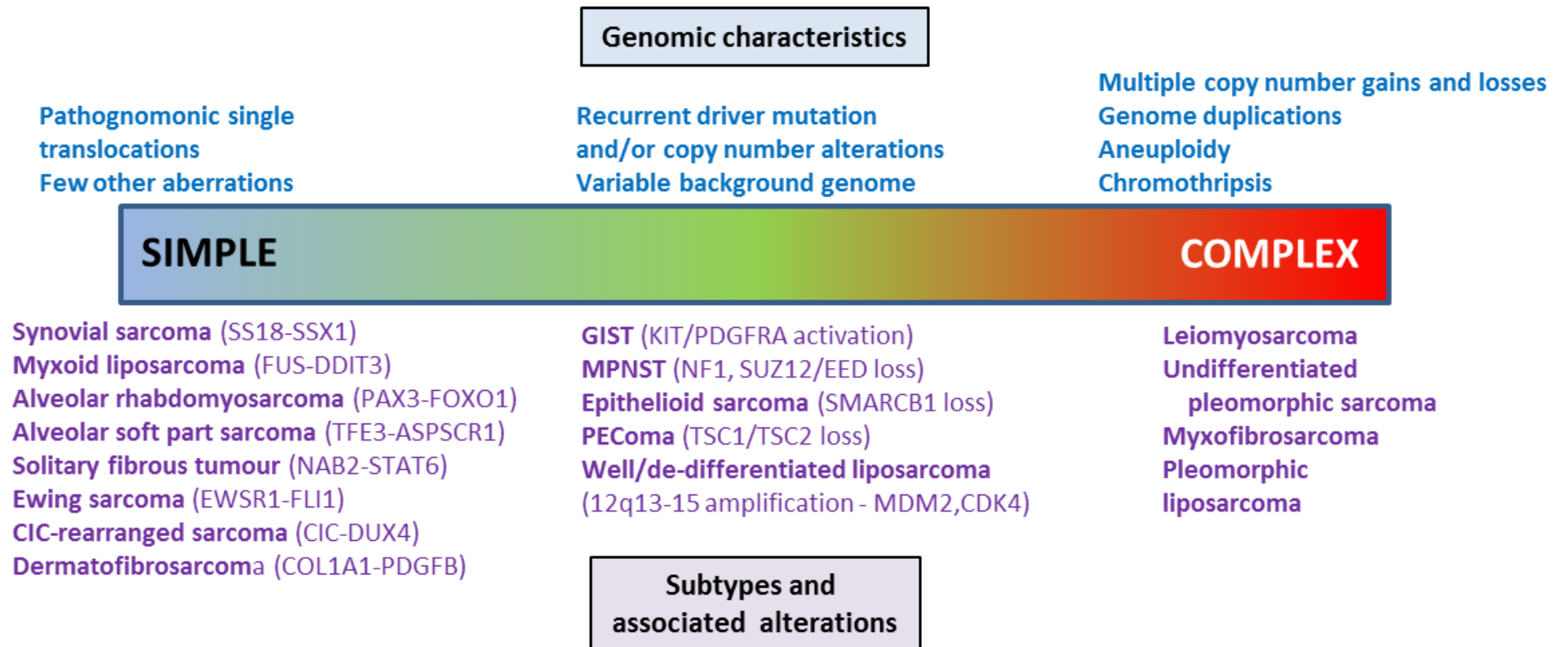


Figure 1.1: The spectrum of genomic characteristics in STS

A smaller number of STS subtypes have been shown to possess recurrent monogenic alterations that play critical roles in cancer biology. The most notable example of this is seen with activating mutations of *KIT* or, less frequently, Platelet-derived growth factor receptor alpha (*PDGFRA*) in gastrointestinal stromal tumours (GIST). Occurring in approximately 85% of GIST (75% *KIT*, 10% *PDGFRA*), these mutations have been shown to be primary drivers of tumour development<sup>6</sup>. Overexpression of *KIT* (also known as CD117), as detected by IHC, serves as a diagnostic biomarker for GIST. Specific mutations of *KIT* or *PDGFRA* have been shown to correlate with clinical parameters such as anatomical site of origin and provide prognostic information as well as predicting for differential sensitivity to tyrosine kinase inhibitor (TKI) therapy<sup>7-10</sup>. *KIT* +/- *PDGFRA* genotyping is now established as part of standard work-up of newly diagnosed GIST, typically through PCR-based assessment for a targeted repertoire of the most commonly occurring mutations.

The characterisation of oncogenic mechanisms associated with these genomic alterations has provided the basis for novel investigative therapeutic strategies, with the most notable success being the targeting of recurrent oncogenic mutations of *KIT* or *PDGFRA* with TKI in GIST<sup>11</sup>. However, many of the recurrent genomic alterations that have been described in various STS subtypes have yet to directly contribute to the development of new therapeutic standards of care. Despite this, the potential value of ongoing investigation for similar recurrent alterations is highlighted by the incorporation of *CIC-DUX4* translocated sarcomas as a distinct diagnostic entity in the updated World Health Organisation (WHO) classification of STS<sup>12</sup>. Representing a previously poorly defined subgroup within the Ewing sarcoma family of tumours, this group of patients were recognised as distinct from others within the same diagnostic bracket in terms of pronounced tumour pleomorphism, preponderance for older male patients, resistance to chemotherapy/ radiotherapy and worse prognosis. The recognition of a shared molecular feature allows for greater diagnostic and prognostic accuracy for these patients and indicates the likelihood of shared driver biology which may be uncovered through focussed research effort.

Beyond the subtypes that are now characterised by highly recurrent translocations, gene fusions or specific monogenic alteration, STS is typified by karyotypic complexity that can variably involve aneuploidy, multiple segmental

gains or losses, whole-genome duplication or chromothripsis<sup>4,13</sup>. Among the heterogeneous genomic landscapes of STS subtypes such as leiomyosarcoma (LMS), myxofibrosarcoma (MFS), malignant peripheral nerve sheath tumours (MPNST) and undifferentiated pleomorphic sarcoma (UPS), loss of the key tumour suppressors *TP53* and/or *RB1*, either through somatic copy number alteration (SCNA) or mutation are among the few specific molecular alterations that have been shown to recur with any notable frequency<sup>4</sup>. Due to this lack of sensitive or specific molecular markers, molecular diagnostic testing has little current role in standard diagnostic work-up for these diseases, where conventional clinico-pathological diagnostic definitions still apply.

### **1.2.3 Clinico-pathological characteristics of LMS, UPS and DDLPS**

#### *LMS*

LMS are sarcomas of smooth muscle lineage and are among the more common of STS histological subtypes, accounting for 10-20% of STS diagnoses<sup>14</sup>. Anatomical site of origin varies and include (in approximate descending order of incidence) the retroperitoneum, large veins (particularly inferior vena cava and large proximal veins of the lower extremities), uterus, other abdominopelvic viscera, soft tissue of the extremities and the skin. LMS of different anatomical sites demonstrate some distinction in terms of clinical phenotype, in terms of risk and pattern of relapse and prognosis. However, inter-individual variation in disease behaviour, treatment response and prognosis largely transcend such anatomical categorisation.

Histologically, LMS typically exhibit intersecting and sharply delineated fascicles of spindle cells that contain abundant eosinophilic cytoplasm and hyperchromatic nuclei. Most LMS express IHC-detectable protein markers associated with smooth muscle lineage, including smooth muscle actin (SMA), desmin and h-caldesmon, although these diagnostic markers have limited specificity for LMS<sup>1</sup>. Features of nuclear pleomorphism, mitosis and extent and appearance of intra-tumoural stroma can vary both between and within individual tumours. Occasionally, regions of dedifferentiation, or osteosarcoma or rhabdomyosarcoma-like components are seen within LMS of otherwise conventional histological appearance.

## *UPS*

UPS is a term now reserved for the description of a group of pleomorphic STS that exhibit no recognisable morphological, IHC or ancillary molecular features of any specific cellular lineage. UPS represent a subset of the now-obsolete diagnosis of malignant fibrous histiocytomas (MFH). MFH is now recognised as encompassing a wide variety of poorly differentiated cancers including those of lipogenic, neurogenic or myogenic lineage, as well as non-sarcomatous neoplasms such as melanoma or sarcomatoid variants of epithelial malignancies. This shift in classification reflects progress in terms of more refined histologic diagnostic criteria, the identification of lineage-specific immunophenotypic markers and the development of other molecular profiling techniques that have demonstrated close similarities between many tumours historically classified as MFH and lineage-specific cancers at genomic and/or gene expression level<sup>15-17</sup>. A consequence of this reclassification, the current incidence of UPS is now significantly below that of historical MFH diagnosis, although still accounts for approximately 10% of all STS<sup>18</sup>.

UPS is a diagnosis of exclusion that requires the absence of morphological, immunophenotypic and ancillary molecular characteristics of poorly differentiated variants of lineage-specific malignancies. Other than being generally high grade, histological appearances of individual UPS are heterogeneous and can consist of variable degrees of cellularity and intra-tumoural fibrous and/or myxoid stroma. As is the case with other karyotypically-complex STS, most UPS occur over the age of 40, with peak incidence between 50-70 years. Little is known about the aetiology of UPS, although a small proportion arise within tissue fields of previous radiotherapy. Clinical features are non-specific but typical presentation involves rapidly and painlessly enlarging deep-seated tumours that most commonly arise in the limbs. UPS is among the most clinically aggressive and poor prognosis STS subtypes, with distant metastasis (typically metachronous) a common occurrence.

## *DDLPS*

Liposarcoma (LPS) are tumours of adipocytic differentiation that consist of 4 principle subtypes (well-differentiated [WDLPS], de-differentiated [DDLPS], myxoid/round cell and pleomorphic) that collectively account for 10-20% of all

STS<sup>19</sup>. WDLPS and DDLPS together account for the majority of LPS and often coexist (WD/DDLPS), reflecting DDLPS's origin as an outgrowth from precursor WDLPS. DDLPS is a more clinically aggressive disease than WDLPS, typically arising in the retroperitoneum in association with a well-differentiated component, and is associated with high rates of local recurrence and distant metastatic disease. In 90% of cases, DDLPS is present at primary presentation, either in association with a WDLPS component of variable proportion, or as a solely dedifferentiated lesion. The remaining 10% of cases of DDLPS occur at relapse, either in association with recurrence of the original WD component or the absence of accompanying WDLPS<sup>20</sup>. Histologically, DDLPS is characterised by highly cellular areas of undifferentiated sarcoma that transitions abruptly within a background of WDLPS, which typically appears as a more recognisably adipocytic proliferation. The origin of DDLPS as a progression of WDLPS is underlined by highly recurrent karyotypic abnormalities that are shared by the two subtypes. Pathognomonic supernumerary ring or giant rod chromosomes are found in both subtypes and consist of amplified segments of 12q13-15<sup>21</sup>.

#### ***1.2.4 Emerging molecular classifications***

Current diagnostic classifications often fail to account for wide variation in clinical behaviours and therapeutic sensitivities that are encountered within individual STS subtypes. This limitation to current classification is particularly pronounced in subtypes typified by greater genomic complexity. Studies that have investigated potential shared genomic or transcriptomic features, either within or across histologically-defined subgroups, have demonstrated the potential to identify STS subgroups defined by recurrent molecular characteristics and that exhibit distinct clinical phenotypes. Molecular profiling of cohorts of subtype-specific STS tumours have demonstrated subgroups within certain histotypes that are defined by shared biological traits and distinct clinical behaviour that are largely independent from conventional clinico-pathological descriptors. Examples of these include LMS subgroups that are defined by contrasting gene expression signatures and subgroups of DDLPS that can be identified by distinct patterns of SCNA and DNA methylation – these are further discussed in **Chapter 1.2.5**. Beyond such evidence of distinct molecular entities that are encompassed within specific STS histotypes, a number of studies have described patterns of shared molecular biology that transcend conventional histological classification and that

identify tumour subgroups that exhibit similar phenotypic behaviour in terms of clinical aggressiveness and, potentially, treatment response. A notable example is that of the complexity index in sarcoma (CINSARC) signature. This 67 gene expression signature was first derived through the analysis of microarray-derived gene expression data from a training cohort of non-translocation-associated STS (39% UPS, 28% LMS, 24%DDLPS, 9% pleomorphic LPS/rhabdomyosarcoma)<sup>22</sup>. Genes that were differentially expressed in association with chromosomal structural abnormality, histological grade and a previously described chromosomal instability-related mRNA signature were selected and shown to be enriched for involvement in maintenance of genomic integrity and mitotic control. A dichotomised CINSARC score based on expression of these selected genes was derived and shown to be independently associated with prognosis, with patients in both a training and validation cohort with a high CINSARC score (i.e. greater genomic instability) shown to have significantly worse metastasis-free survival than those with a low CINSARC score. Intriguingly, the prognostic value of CINSARC is not limited to STS. Similar association between high CINSARC score and poor prognosis has been shown in cohorts of GIST, lymphoma and breast cancers<sup>22,23</sup>, with a recent follow-up study suggesting that CINSARC score performs well as a predictor of poor prognosis across many different cancer types beyond STS<sup>24</sup>. RNA-Seq-based analysis of formalin fixed paraffin embedded (FFPE)-derived tumour material has been shown to be effective in allocating individual tumours to CINSARC-based subgroups, with high levels of concordance in CINSARC group allocation when matched fresh-frozen and FFPE tumour material were used as input for microarray and RNA-Seq-based gene expression analysis respectively<sup>25</sup>. Prospective assessment of CINSARC as a biomarker for response to pre-operative chemotherapy in localised STS is currently underway (NCT02789384). This follows on from the observation that when CINSARC-based stratification was applied to gene expression datasets from 2 cohorts of patients with early stage breast cancer treated with pre-operative chemotherapy within prospective clinical trials, significantly higher rates of pathological complete response (an endpoint validated for surrogacy of relapse and survival in breast cancer) were seen in patients with higher CINSARC scores<sup>26</sup>. These data highlight a biomarker based on aspects of tumour biology (chromosomal instability and mitotic dysregulation) that identifies subgroups of patients with contrasting prognosis across different

STS subtypes and may yet be shown to have predictive value for response to current standard systemic therapy.

TCGA recently reported results of multi-omic profiling of 206 clinically annotated STS representing 5 subtypes characterised by complex karyotypes (DDLPS, UPS, LMS, MPNST and MFS) and one subtype (synovial sarcoma [SS]) with a pathognomonic t(X;18)(p11;q11) translocation that result in the oncogenic SS18-SSX fusion protein<sup>4</sup>. Fresh frozen tissue from predominantly localised tumours sampled at the time of radical resection was used as input for whole exome or genome sequencing, RNA-Seq and miRNA-Seq, DNA copy number analysis through comparative genomic hybridisation (CGH), array-based DNA methylation analysis and reverse-phase protein array (RPPA) analysis of 192 proteins. Integrated unsupervised clustering of all molecular readouts was then performed for the unbiased identification of intrinsic molecular subgroups. The resulting 5 'iClusters' largely reflected histological subtype – all cases of SS clustered together in an iCluster (C4) with relatively uniform patterns of DNA methylation and gene expression that reflect the central role of the SS18-SSX fusion protein in epigenetic dysregulation. One cluster (C1) consisted almost entirely of LMS and was characterised by expression of genes related to myogenic differentiation. The large majority of DDLPS were contained within one of two iClusters (C2 or C3), both of which were typified by high levels of SCNA. Distinguishing between these DDLPS-enriched clusters were contrasting levels of DNA methylation – of these two iClusters, the one with relative hypomethylation (C3) was made up approximately one third DDLPS, with the other two thirds a balanced mix of all other included histotypes. The remaining iCluster (C5) was dominated by UPS but also contained cases of LMS, DDLPS and MFS. This iCluster demonstrated DNA methylation, mRNA and miRNA expression patterns that overlapped with C3, but lacked enrichment in the copy number gains within chromosome 12 that typified C3 and instead demonstrated widespread SCNAs that exhibited no recurring pattern. These data indicate that, even when broad coverage of genomic, transcriptomic and epigenetic features is taken into account, histological subtyping remains a dominant discriminator between individual STS. However, within this is an indication that approximately half of complex-karyotype STS are set apart from subtype-dominated intrinsic subgroups and share molecular features that transcend histological classification.

In summary, histological classification of STS has been augmented by a now-substantial amount of genomic profiling data. From this, a spectrum of genomic complexity is now recognised upon which different histological subtypes tend to localise. While discovery of recurrent genomic abnormalities has in some cases provided a focus for investigation of related oncogenic mechanisms and in others driven transformative therapeutic advances, most have yet to be successfully targeted therapeutically. Meanwhile, a significant proportion of STS can be positioned at the complex end of the genomic spectrum, where few recurrent alterations have been described and have been insufficient to explain observed heterogeneity in clinical phenotype. However, several studies have demonstrated molecular abnormalities that are shared between individual tumours in a manner that does not conform to conventional histological classification of STS but may nevertheless describe subgroups of similar clinical behaviour.

### **1.2.5 Molecular pathology of LMS, UPS and DDLPS**

#### *LMS*

The molecular pathology of LMS is complex and incompletely understood. At a genomic level, varying degrees of karyotypic complexity is a characteristic finding<sup>27</sup>. Partial loss of 10q and 13q, containing *RB1* and *PTEN* respectively, are the most consistently demonstrated SCNAs in LMS, found in 40-80% and 35-80% of cases respectively, and are often co-occurring<sup>28</sup>. Partial or complete deletion of 19p (containing *CDK2NA*, encoding p16<sup>INK4A</sup>) are seen in a minority of patients in a manner that is mutually exclusive to *RB1* loss, indicating that G1/S cell cycle checkpoint dysregulation is an important oncological feature for the majority of LMS. More recent next generation sequencing (NGS)-based genomic profiling studies identify a high frequency of biallelic inactivation of *RB1* and *TP53* through diverse genetic mechanisms that include missense mutation, small insertion/deletions, SCNA and chromosomal rearrangement, indicating a central role for the loss of these two tumour suppressor genes in a large proportion of LMS<sup>4,29,30</sup>. In addition, a high frequency of deletions of genes involved in homologous recombination repair of DNA double-strand breaks has been detected in association genomic changes associated with defective homologous recombination, indicating that significant proportion of LMS may exhibit 'BRCA-ness' that could feasibly be sensitive to therapeutic exploitation<sup>31</sup>. While such

genomic alterations have generally been shown to be unable to discriminate between uterine LMS (uLMS) and non-uterine LMS, the TCGA-SARC study found distinction in terms of methylation and gene expression signatures between tumours from the two anatomically-defined subgroups<sup>4,32-34</sup>. Here, uLMS exhibited higher DNA damage response characteristics while non-uterine LMS had a more prominent HIF1a signalling signature.

Several studies have investigated for the presence of distinct subtypes within LMS at a transcriptomic level. These have reported reproducible findings of 3 transcriptomic subtypes – subtype I has predominant expression of genes related to smooth muscle differentiation, subtype II is enriched for expression of genes related to translation and protein localisation and that disproportionately contained a higher degree of histological features of dedifferentiation, while subtype III predominantly consisted of uLMS and is associated with a colony-stimulating factor 1 (CSF1) protein response signature that had previously been shown to be associated poor clinical outcome in both uLMS and extrauterine LMS<sup>27,32,35</sup>. Comparison of clinical outcomes associated with these subtypes identified better survival outcomes in extrauterine LMS of subtype I, with extrauterine LMS of subtype II having worse outcomes<sup>32</sup>. Collectively, these molecular studies provide an emerging picture of LMS as a disease driven by dysregulation of the cell cycle and loss of p53 function that result from complex genomic aberrations, where divergent gene expression patterns dictate contrasting clinical phenotype. While these findings have yet to translate into the advance development of novel therapeutic approaches, a number of potential strategies, including targeting of PI3K/mTOR signalling or exploitation of homologous recombination deficiency, are suggested for clinical investigation.

### *UPS*

The molecular basis of UPS is poorly understood. As diagnostic classification has shifted away from MFH, it is challenging to accurately contextualise older studies performed in MFH cohorts that likely consisted of a variety of poorly differentiated STS subtypes. Even with modern diagnostic criteria, UPS remains a clinically and histologically heterogeneous disease, a characteristic that has been reflected in the limited available molecular profiling data for this subtype. UPS is characterised at the genomic level by complex karyotypic abnormalities, typically

with numerous copy number gains and losses across the entire genome. As is seen in LMS, alterations of *RB1* and *TP53* through mutation or deletion are the most commonly recurrent genomic feature in UPS, albeit with a lower frequency of biallelic inactivation than in LMS<sup>4,28,36,37</sup>. Truncating mutation of *ATRX* is detectable in approximately 30% of UPS and is associated with alternative lengthening of telomeres<sup>4,38</sup>. Beyond these, a limited number of other recurrent genomic alterations have been described in UPS and include activation of the Hedgehog, Notch or Hippo signal transduction pathways that are respectively implicated in conferring cellular dedifferentiation, maintenance of a stem-like state and dysregulated tissue growth in cancer<sup>4,28,39,40</sup>.

### *DDLPS*

Recognition of the ubiquity of recurrent chromosomal segmental amplification in WD/DDLPS has provided a focus for molecular investigation of these diseases. Several genes located within the 12q amplicon have been implicated in the pathogenesis of WD/DDLPS. Amplification of mouse double minute 2 homolog (*MDM2*), an E3 ubiquitin ligase that plays a key role in the negative regulation of p53 function, is near ubiquitous in WDLPS and results in loss of p53 tumour-suppressor function<sup>41</sup>. Cyclin-dependent kinase 4 (*CDK4*), a critical promoter of progression through G1/S cell cycle checkpoint, is also amplified in 90% of cases and is associated with adverse outcome<sup>42–45</sup>. A range of pharmaceutical inhibitors of MDM2 and CDK4 have been investigated in WD/DDLPS in non-comparative phase I and II protocols with a focus on WD/DDLPS. Reported results from these studies have shown objective response to MDM2 or CDK4 inhibitor monotherapy are rare, although there is some indication of a higher rate of durable disease stabilisation<sup>19</sup>. Both targets remain under active clinical investigation.

Other genes commonly found within the 12q amplicon in WDLPS include HMG2A, an architectural transcription factor capable of DNA remodelling and shown to be sufficient for malignant transformation of human cells<sup>46,47</sup>, and TSPAN31, a gene of currently unknown function that was originally cloned from an UPS cell line and subsequently found to be amplified in a number of STS subtypes<sup>48</sup>. Beyond 12q13-15 amplification, WDLPS typically exhibits an unremarkable genome. Genomic sequencing studies have demonstrated low

rates of somatic mutations with identified variants usually missense single nucleotide variants (SNVs) of undefined functional impact<sup>49-51</sup>.

The molecular mechanisms that lead to the emergence of dedifferentiated, high grade disease within precursor WDLPS are not fully understood but appear to be related to the accumulation of SCNA that contribute to loss of adipocytic differentiation. A number of genes within the 12q13-15 amplicon that can be co-amplified with *MDM2* and *CDK4* have been implicated progression to DDLPS. These include *YEATS4*, a putative transcription factor that is required for suppression of p53 function during normal cell proliferation, and *CPM*, encoding carboxypeptidase M, a proteolytic enzyme involved in the cleavage of growth factor precursors<sup>49,50,52</sup>. Genomic comparisons of paired WD and DD components sampled from the same tumour that clonal divergence of DDLPS is an early event, as evidenced by a low fraction of somatic mutations shared by both components, a greater number of private SCNA in DDLPS components, and continued accumulation of 12q neochromosomes that undergo repeat breakage-fusion-bridge cycles<sup>53</sup>. Truncating fusions of *HMG2A*, an architectural transcription factor involved in adipogenesis, within the 12q amplicon suggest a mechanism of loss of differentiation. In addition, Recurrent co-amplifications of chromosomal segments that contain *ASK1* (6q23) and *C-JUN* (1p32), both inhibitors of peroxisome proliferator-activated receptor gamma (PPAR $\gamma$ ), a key mediator of adipocyte differentiation, have been identified exclusively in de-differentiated components of tumours<sup>54-57</sup>. Comparison of gene expression in WD and DD components identified significantly higher expression of genes involved in lipid metabolism and differentiation in WDLPS, while the highest-ranking genes in DD samples were involved in cell cycle and division, and DNA replication and repair, with homologous recombination-related genes among the most overexpressed. Very few gene expression differences between WDLPS and DDLPS could be explained by detected subtype-specific amplifications and losses, suggesting that epigenetic dysregulation may play a prominent role in driving the development of DDLPS. Supporting this is data from the TCGA-SARC study of 50 DDLPS, wherein unsupervised clustering of DNA methylation dataset identified hyper- and hypo-methylated clusters<sup>4</sup>. Hypermethylated DDLPS was associated with worse survival outcomes and exhibited more genome doublings

and a lower level of expression of leucocyte-related genes wherein inferred Th2 cell content was proportionately greater.

### **1.3 Current standards of care for STS**

#### ***1.3.1 Localised Disease***

Localised disease extent in STS is generally defined by the absence of distant metastasis or preclusion of complete resection by local involvement of critical structures. Formal staging TNM staging criteria distinguish between four main groupings of anatomical site of origin (trunk/extremities, retroperitoneum, head and neck, abdomen and thoracic viscera)<sup>58</sup>, wherein T stage is determined by tumour size and grade (as determined by the three tier French Federation of Cancer Centers Sarcoma Group (FNCLCC) grading system), or by extent of local extension in STS originating from intracavity viscera. Nodal involvement by STS is very unusual except in certain rare subtypes.

Surgical excision with adequate clearance of tumour margins is the primary curative modality in the treatment of localised STS. Limb- and function-sparing wide excision of STS involving the extremities is associated with less morbidity than amputation and produces equivalent oncological outcomes when delivered as part of multidisciplinary care<sup>59</sup>. Optimal extent of resection for retroperitoneal STS, where local recurrence remains a common occurrence even when apparent clear surgical margins are obtained, is yet to be definitively defined – some authors advocate more extensive resection, including tumour-adjacent but macroscopically uninvolved structures<sup>60</sup>. The centralisation of STS surgery in specialist, multi-disciplinary sarcoma centres is associated with improved patient outcomes<sup>61</sup>.

Peri-operative radiotherapy has been shown in randomised trials to reduce rates of local recurrence in the treatment of large, high grade STS of the extremities<sup>62</sup>. Randomised studies comparing pre- or post-operative radiotherapy have demonstrated equivalent oncological outcomes but contrasting toxicity<sup>63</sup>. Post-operative radiotherapy, wherein a larger overall radiation dose is delivered to a larger field, is associated with a higher rate of late toxicities such as soft tissue fibrosis and lymphoedema, while pre-operative treatment is associated with a greater risk of acute surgical wound complication. The role of peri-operative

radiotherapy for retroperitoneal STS is yet to be established, although retrospective series indicate a potential for the improvement of local disease control<sup>64</sup>. Prospective, randomised data will be provided by the now-completed Surgery With or Without Radiation Therapy in Untreated Nonmetastatic Retroperitoneal Sarcoma (STRASS) phase III trial, in which patients with high-risk, operable retroperitoneal STS were allocated to receive either pre-operative radiotherapy or surgery alone (NCT01344018).

Although the high rates of distant disease relapse following resection of localised STS reflect a potential role for effective systemic therapy in the early disease setting, the role of adjuvant chemotherapy in localised STS remains contentious. Over the past 30 years, numerous prospective trials have investigated the adjuvant use of chemotherapies that have recognised activity in advanced disease. A 1997 meta-analysis of data from 14 randomised studies of doxorubicin-based treatment found that adjuvant chemotherapy was associated with a 4% reduction in 10 year recurrence rates with chemotherapy but no significant improvement in overall survival (OS)<sup>65</sup>. Data from 4 subsequent randomised controlled trials (RCTs) that delivered post-operative doxorubicin-ifosfamide in their treatment arms were added in an updated meta-analysis in 2008, and similarly found a 9% reduction in absolute risk of local relapse but no OS benefit<sup>66</sup>. The level of detected benefit was more pronounced in patients with higher risk tumours and/or who received doxorubicin-ifosfamide treatment. Subsequent to this analysis, the European Organisation for Research and Treatment of Cancer (EORTC) performed an RCT in which 351 patients with localised, intermediate- or high-grade STS of any site were treated post-operatively with either no systemic adjuvant therapy or with 5 cycles of doxorubicin-ifosfamide<sup>67</sup>. Post-operative radiotherapy was administered to 74% of patients as per conventional risk-based guidance and irrespective of randomisation arm – radiotherapy followed chemotherapy in the systemic therapy arm. Relapse-free survival (RFS) and OS was not significantly different between patients in the two study arms. Pre-planned and post-hoc subgroup analysis detected a non-significant trend in increased benefit from chemotherapy in terms of RFS in larger, high grade and extremity tumours.

Overall, adjuvant chemotherapy has yet to be shown to produce consistent improvement in RFS or OS in unselected STS populations. Available data have

however been used in some quarters to support the use of anthracycline-based post-operative regimens, especially in patients with tumours with high-risk features and/or in STS subtypes with higher response rates to cytotoxic chemotherapy in advanced disease settings. Given that a large amount of available data from studies that have investigated unselected STS cohorts has yet to unequivocally define the role of adjuvant chemotherapy, alternative approaches that see cohorts selected on the basis of risk profile, histological subtype and/or shared molecular features should be pursued in future studies. However, the limitations of using conventional histological classification to stratify adjuvant trials in STS has been recently indicated by a phase III study which sought to compare the effectiveness of standard, anthracycline-and alkylating agent-based chemotherapy to regimens considered to have subtype-specific activity<sup>68</sup>. In this study, patients with high-risk, localised STS of the extremities or trunk were randomised to receive either anthracycline-based or histotype-tailored pre-operative chemotherapy, with disease-free survival (DFS) the primary efficacy outcome. In contrast to previous trials, the inclusion criteria of this study were strict in terms of tumour size, grade, depth and location. Overall, standard chemotherapy was significantly superior to histotype-tailored regimens. In analysis of subtype-defined subgroups (UPS, SS, MPNST, LMS and myxoid liposarcoma (MLPS)), standard chemotherapy produced numerically superior DFS than all histotype-tailored regimens. These results suggest that alternative means of stratifying patient cohorts are required to identify subgroups who receive the benefit from adjuvant systemic therapy – the ongoing investigation of the CINSARC classifier in this context represents an example of molecular stratification which may yet prove to be a more means of classification.

### **1.3.2 Advanced STS**

Advanced disease, constituting synchronous or metachronous distant metastases or inoperable locally advanced primary tumours, occurs in up to 50% of STS and is the primary determinant of a poor prognosis. The lungs are the main site of metastatic spread for a large majority of STS subtypes, with other common sites including soft tissues, liver, bone or brain, depending upon histological subtype. The resection of metachronous lung metastases in the absence of extrapulmonary disease can be associated with long-term survival in a minority of patients, although high-level clinical trial evidence of benefit is

lacking<sup>69</sup>. Systemic therapy with palliative intent is the mainstay of treatment for patients with synchronous and/or extrapulmonary advanced STS. Doxorubicin was one of the first chemotherapy drugs to produce consistently meaningful response rates in advanced STS and remains a standard for first line therapy. The combination of doxorubicin with a second cytotoxic agent with monotherapy activity has been repeatedly investigated as a means of improving rates of clinical benefit. However, while these more intensive schedules have been variably associated with incremental increase in rates of tumour response (usually at the expense of greater toxicity), no trial has demonstrated robust evidence of prolonged survival compared to doxorubicin alone.

In a notable phase III trial conducted by the EORTC, patients treated with the investigative regimen of dose-intensified doxorubicin in combination with ifosfamide experienced a significantly higher objective response rate (ORR) (26% vs 14%,  $p=0.0006$ ) and longer progression-free survival (PFS) (median PFS 7.4 vs 4.6 months; Hazard Ratio (HR) 0.74; 95% confidence interval (CI) 0.60-0.90;  $p=0.003$ ) compared to patients treated with standard doxorubicin monotherapy in the control arm<sup>70</sup>. However, no significant difference in OS, the primary endpoint of the trial, was detected between the two treatment arms (median OS 14.3 vs 12.8 months; HR 0.83; 95% CI 0.67-1.03;  $p=0.076$ ). Meanwhile, an excess of serious adverse events, including febrile neutropaenia, anaemia, thrombocytopenia and gastrointestinal effects, were seen in the combination treatment group. A later post-hoc subgroup analysis based on enrolled patients for whom central pathology review had been performed found that patients with UPS were less likely to have experienced OS event when treated with combination therapy (HR 0.44 (95% CI 0.25-0.79)). No interaction between treatment arm and tumour grade was found<sup>71</sup>. Reaction to these results has been varied, with some taking the evidence of increased activity of the combination regimen to support its routine first-line use, while others have adopted a more conservative approach of reserving combination therapy for patients where tumour shrinkage is a particular treatment goal. Given the evidence of incremental activity of the combination regimen in this study, it is likely that a currently undefined subgroup of patients also receives survival benefit from intensified first line therapy. While post-hoc analysis indicated that UPS may in particular benefit from combination doxorubicin-ifosfamide, it is possible that

other patients experienced incremental survival but were not detected in subgroup analysis due to lack of statistical power or confounding of OS by post-trial treatment (almost two-thirds of patients in both trial arms received some degree of post-trial therapy, with almost half of patients in the control arm receiving post-protocol ifosfamide). The potential for alternative, molecular classification to identify such subgroups who benefit from intensified therapy has not been explored.

An unprecedented improvement in OS was seen in a randomised phase II study that investigated the addition of olaratumab, a therapeutic monoclonal antibody (mAb) that specifically binds to and inhibits PDGFRA, to standard doxorubicin for the treatment of anthracycline-naïve advanced STS<sup>72</sup>. This study met its primary PFS efficacy endpoint at a pre-stated level of statistical significance, showing a 2-month improvement in median PFS with olaratumab-containing therapy compared to doxorubicin alone (median PFS 6.6 vs 4.1 months; HR 0.67; 95% CI 0.44-1.02; p=0.0615). However, more notable was the dramatic improvement in OS, with those who received olaratumab-containing therapy surviving twice as long as those who received doxorubicin alone (median OS 26.5 vs 14.7 months; HR 0.46; 95% 0.30-0.71; p=0.0003). This finding led to the provisional approval of olaratumab in combination with doxorubicin in the first line treatment of advanced STS, pending the results of a now-completed phase III trial – it has been recently announced that this trial failed to meet its primary OS endpoint, with full reporting of the study awaited. Questions persist from the phase II regarding the mechanism by which olaratumab seemingly delivered an unprecedented OS benefit that dwarves the associated prolongation of disease control. Notably, there was no association between olaratumab-related benefit and tumour expression of PDGFRA, suggesting that olaratumab effect may at least in part extend beyond inhibition of direct PDGFRA-mediated oncogenic signalling<sup>73</sup>. It is currently unclear if the addition of olaratumab to chemotherapy has any subtype-specific effects – in the phase II study, OS benefit was seen in both LMS and heterogenous ‘other’ subtypes subgroups. The potential benefit of adding olaratumab to the combination of gemcitabine and docetaxel in the treatment of advanced STS has also been investigated in a yet-to-be reported randomised phase II trial<sup>74</sup>. Outstanding clinical trial results and any future

translational research may yet identify histological and/or molecular subgroups that are enriched for olaratumab effect.

Beyond anthracycline-based regimens, many other cytotoxic agents have been trialled in advanced STS but with only a small number demonstrating consistent and meaningful single agent efficacy in unselected STS populations (**Table 1.2**). A large majority of STS subtypes are subject to similar treatment pathways for advanced disease, where sequential and generic use of this narrow repertoire of agents is applied regardless of most disease-specific factors. An incremental survival benefit of combination schedules compared to single agent therapies of limited efficacy has been demonstrated in randomised phase II trials in mixed STS populations comparing gemcitabine-docetaxel to gemcitabine alone, or gemcitabine-dacarbazine to dacarbazine alone<sup>75-77</sup>. For a limited proportion of subtypes, the preferential use of certain systemic therapies is supported by a variable degree of clinical trial evidence. In some such cases, including the use of paclitaxel in angiosarcoma (AS) or combination gemcitabine-docetaxel in LMS, prevailing notions of heightened sensitivity are largely based on retrospective or non-comparative prospective data only<sup>75-80</sup>. In other cases, higher-level evidence is available to support the targeted use of specific regimens in certain subtypes and have contributed to several of the more recent drug approvals for STS. Eribulin, a marine-derivative microtubule inhibitor, was initially investigated in STS in a non-comparative phase II trial that stratified patients by histological subtype and found that only patients with LMS or LPS, but not SS or heterogeneous 'other' STS subtypes, met pre-specified efficacy benchmarks<sup>81</sup>. The so-called L-sarcomas were then the focus of a subsequent randomised phase III trial which compared eribulin to dacarbazine in patients with pre-treated advanced disease<sup>82</sup>. While initial efficacy analysis indicated significant improvement in OS but not PFS with eribulin in the overall trial cohort, pre-planned histotype subgroup analysis identified that eribulin benefit was almost entirely limited to patients with LPS, where near identical degrees of PFS and OS gain were seen (PFS HR 0.52; 95% CI 0.35-0.78; p=0.0015, OS HR 0.51; 95% 0.35-0.75; p<0.001), while no significant difference between treatment arms in the LMS subgroup was detected in terms of OS or PFS<sup>83</sup>. These data resulted in the regulatory approval of eribulin for the treatment of advanced LPS only. The clinical development of trabectedin, a different marine-derived cytotoxic agent,

for advanced STS reflected of eribulin, in so much that earlier phase II data identified STS subgroups with greater drug sensitivity that were subsequently confirmed in larger phase III studies that confirmed efficacy<sup>84–86</sup>.

In contrast to these notable examples of successful drug development, a significant number of phase III drug trials in advanced STS over the past 30 years have recruited unselected, mixed STS cohorts, partly as a practical solution to the challenges of recruiting cohorts of patients with rare diagnoses that were of sufficient size to power statistical analysis<sup>2</sup>. Among these studies are numerous examples of novel agents that had shown promising efficacy signals in non-comparative early phase studies yet failed to produce significant survival benefit over standard therapy in larger, randomised trials, ultimately leading to discontinuation of the drugs' development in STS. In contrast to such 'all-comer' RCTs, wherein the heterogeneity of included subtypes and underlying cancer biology likely dilutes any surrogate endpoint-based efficacy signals in earlier phase studies, a greater rate of positive RCT outcomes and subsequent drug approval has been seen with phase III studies that have recruited specific STS subtypes associated with signals of sensitivity in antecedent, non-randomised studies . This finding should be instructive to the design of future drug trials in advanced STS if the rate of conversion of early efficacy signals into proven effect and regulatory approval is to improve.

Drug	Type	Indication	NIH NCI Level of evidence <sup>87</sup>	Refs
Doxorubicin	Anthracycline	1 <sup>st</sup> line	3iiiDiv	88
Doxorubicin + ifosfamide	Anthracycline + alkylating agent	1 <sup>st</sup> line (esp. chemo sensitive subtypes/ bulky disease)	1iiDiii	70
Doxorubicin + Olarutumab	Anthracycline + Anti-PDGFR $\alpha$ mAb	1 <sup>st</sup> line	1iiA	72
Ifosfamide	Alkylating agent	2 <sup>nd</sup> + line	1iiDiv	89–91
Gemcitabine + DTIC	Nucleoside analogue + alkylating agent	2 <sup>nd</sup> + line	1iiA	77
Gemcitabine + docetaxel	Nucleoside analogue + taxane	2 <sup>nd</sup> + line (potentially first line in some subtypes)	1iiDiii	75,76,92
Pazopanib	Multi-targeted kinase inhibitor (activity against VEGFRs, PDGFR $\alpha$ , FGFR1, KIT)	2 <sup>nd</sup> + line in non-adipocytic STS	1iDiii	93
Eribulin	Microtubule inhibitor	2 <sup>nd</sup> + line (after anthracycline)	1iiA	82
Trabectedin	DNA minor groove binder	2-3 <sup>rd</sup> + line (after anthracycline and ifosfamide)	1iiDiii	84–86
Dacarbazine	Alkylating agent	3 <sup>rd</sup> + line	3iiiDiv	94,95
Liposomal doxorubicin	Anthracycline	Kaposi and angiosarcoma Substitute for doxorubicin in most STS	3iiiDiv	78,96,97
Sirolimus	mTOR inhibitor	Malignant PEComa	3iiiDiv	98,99
Paclitaxel	Taxane	Kaposi and angiosarcoma	3iiiDiv	78–80
Crizotinib	Multi-targeted kinase inhibitor (activity against ALK, ROS1, MET)	Inflammatory myofibroblastic tumour	3iiiDiv	100
Imatinib	Multi-targeted kinase inhibitor (activity against KIT, PDGFRA, BCR-ABL)	Dermatofibrosarcoma protuberans	3iiDiv	101

**Table 1.2: Current standard systemic therapies and associated level of evidence for advanced STS**

Replicated with authors permission from Lee *et al.* . Phase III Soft Tissue Sarcoma Trials: Success or Failure? *Curr. Treat. Options in Oncol.* 2017. 18 (3). 19. NIH NCI Levels of evidence are based on Strength of Study Design (1 = RCT, 2= non-randomised, controlled clinical trial, 3=case series or other observational study designs (population-based consecutive series, ii – non-population-based consecutive series, iii – non-consecutive case series)) and Strength of Endpoints (A = overall survival, B = cause-specific mortality, C = quality of life, D = Indirect surrogates (I – event-free survival, ii – disease-free survival, iii – progression-free survival, iv – tumour response))

## 1.4 Pazopanib in the treatment of advanced STS

Pazopanib is an oral multi-target TKI developed by GlaxoSmithKline that has a clinical anti-tumour effect that is thought to be exerted through its selective inhibition of vascular endothelial growth factor receptor (VEGFR)-mediated angiogenesis as well as direct blockade of growth-promoting receptor tyrosine kinases (RTKs) that include PDGFRs, fibroblast growth factor receptors (FGFRs) and KIT<sup>102–106</sup>. After receiving marketing authorisation for the treatment of metastatic renal cell carcinoma, pazopanib became the first and currently only TKI licensed for the treatment of many subtypes of advanced STS. This approval was based on the results of double-blinded, placebo-controlled randomised phase III trial that demonstrated significant prolongation of PFS in patients with pre-treated advanced STS who received pazopanib<sup>93</sup>. However, despite this evidence of anti-tumour effect, no significant difference in OS was observed between pazopanib and placebo-treated patients. The failure of PFS gain to translate to OS benefit has adversely influenced cost assessment of pazopanib for this indication, leading to funding limitations in certain health economies worldwide<sup>107–109</sup>. There is currently an unmet need for predictive biomarkers that are successful in prospectively selecting the subgroup of STS patients most likely to benefit from pazopanib, thus improving the clinical efficiency of the drug.

### 1.4.1 Pre-clinical development of pazopanib

Pazopanib was identified through chemical screening of compounds for inhibition of VEGFR2, a key mediator of tumour angiogenesis<sup>110</sup>. After identification of an initial lead compound by assessing inhibitory action against VEGFR2 kinase activity by direct enzymatic assay, chemical optimisation was undertaken to increase inhibitory potency and improve pharmacokinetic profile in mouse models. Optimised molecules were also shown to have inhibitory potency against VEGFR-1 and -3, as well as closely related RTK including PDGFR-B, c-Kit, FGFR1 and CSF1 receptor (CSF1R). This and further reports on the kinase inhibitory profile of pazopanib are summarised in **Figure 1.2**<sup>102–104</sup>. Pharmacodynamic studies of the biological activity of the drug were performed in a range of *in vitro* and *in vivo* assays<sup>104</sup>. Treatment of cultured human umbilical vein endothelial cells (HUVEC) with pazopanib resulted in potent inhibition of VEGF-mediated phosphorylation of VEGFR2, with associated inhibition of HUVEC proliferation. *In vitro* inhibition of ligand-mediated phosphorylation of c-

Kit and PDGFRB by pazopanib was also shown in human lung cancer and foreskin fibroblast cells respectively, although the drug had no effect on proliferation in an unspecified panel of tumour cells. Inhibition of angiogenesis was demonstrated in mouse models of ocular angiogenesis and subcutaneous implantation of ligand-containing Matrigel plug. The growth of established human xenograft tumours in immunocompromised mice was inhibited on oral pazopanib administration in a dose-dependent manner without apparent toxicity. A steady-state plasma concentration was shown to provide optimal *in vivo* inhibition of VEGFR2 phosphorylation, angiogenesis and xenograft growth, with strong correlation between inhibition of VEGFR2 kinase activity and anti-xenograft effect seen. Further preclinical evidence has indicated that the anti-tumour effect of pazopanib may not solely be mediated by inhibition of angiogenesis, but also through direct effect on tumour cells. A study investigating the effect of pazopanib in human multiple myeloma models found that, in addition to inhibition of endothelial cell proliferation and *in vivo* tumour angiogenesis, the drug also had direct anti-proliferative and pro-apoptotic effect on tumour cells and xenografts<sup>106</sup>. This effect on myeloma cells was in association with downregulation of several cancer-related genes involved in pathways including cytokine and chemokine signalling, cell cycle and insulin-receptor pathways, as well as upregulation of proapoptotic genes. Pazopanib has been shown across a series of studies to act as a pan-RAF inhibitor and exert an anticancer effect through inhibition of mitogen-activated protein kinase (MAPK) pathway signalling in cancer cells in the absence of demonstrable anti-angiogenic effect<sup>111</sup>.

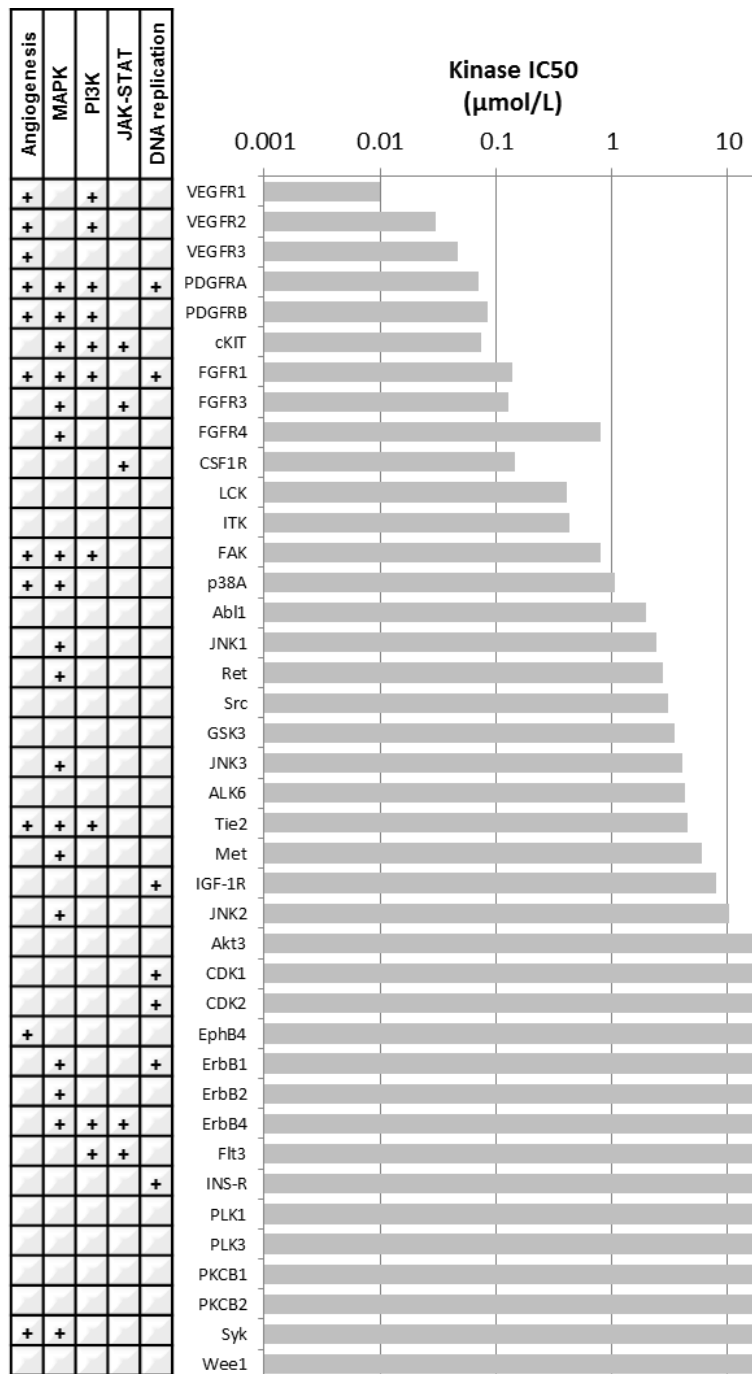


**Figure 1.2: Kinase inhibitory profile of pazopanib.**

Bar graph indicates kinase IC50 of pazopanib against enzymes in a cell-free assay, as reported by Kumar *et al.* Involvement of kinases in canonical oncogenic processes/pathways are indicated in table on the left.

In *in vivo* and xenograft models of a brain-tropic Her2-positive, *BRAF*-mutated breast cancer cell line, pazopanib prevented growth of brain metastasis in association with reduced MAPK pathway activation but no change in markers of angiogenesis. A later study in the same breast cancer xenograft model, showed that inhibition of brain metastasis growth by pazopanib was associated with a reduced number of PDGFRB-expressing, metastasis-associated astrocytes, suggesting a possible role for pazopanib-mediated therapeutic modulation of the tumour microenvironment (TME)<sup>112</sup>. In follow-on studies, a panel of breast cancer and melanoma cell lines with varying *BRAF* mutational status were used in the formation of orthotopic xenografts that were then treated with pazopanib<sup>113</sup>. Here, xenografts with either wildtype or exon 11 mutated *BRAF* showed significant sensitivity to pazopanib, in association with evidence of both reduced MAPK signalling in tumour cells and reduced angiogenesis.

Collectively, these preclinical data demonstrate that pazopanib is a potent inhibitor of several key kinases involved in angiogenic and oncogenic pathways, with an anti-tumour effect that is mediated by both anti-angiogenic and direct anti-cancer cell activity.

#### **1.4.2 Early phase clinical development of pazopanib**

Based on these preclinical findings of anti-tumour effect and proposed optimal dosing, a phase I trial of pazopanib was performed, with 43 patients enrolled in an initial dose-escalation phase and a further 20 patients in a subsequent dose-expansion phase<sup>114</sup>. Pharmacokinetic assessment identified that steady-state exposure was achieved at doses of 800mg or more as a once daily oral dose. In line with toxicities seen with other antiangiogenic TKIs, hypertension was the most common adverse event (grade 3 in 25%), followed by diarrhoea, hair depigmentation, nausea, anorexia and fatigue. Non-severe proteinuria was the most common laboratory abnormality (seen in 52% of patients), followed by a range of non-severe cytopaenias and blood biochemistry disturbances. As no maximally tolerated dose was identified, an oral dose of 800mg once daily was selected for further studies, on the basis that doses >800mg did not increase drug exposure.

Pharmacodynamic analyses in the phase I study demonstrated that plasma VEGF concentrations increased by more than 3-fold in approximately 50% of

treated patients following drug initiation. In a subset of patients who underwent dynamic contrast-enhanced magnetic resonance imaging (DCE-MRI), 7/12 (58%) patients were seen to have >50% reduction in tumour blood flow at day 8 of treatment, and 10/11 (91%) at day 22. Incidence of hypertension was associated with trough drug levels on day 22 of therapy, suggesting that hypertension may act as a pharmacodynamic marker of pazopanib activity.

Assessment of preliminary clinical activity in this study recorded partial response by response evaluation criteria in solid tumours (RECIST) in three patients (2 metastatic renal cell carcinoma (mRCC), 1 pancreatic adenocarcinoma), while stable disease of at least 6 months duration was observed in 14 patients – of note, among these were two patients with chondrosarcoma, one with LMS and one with GIST.

Based on these phase I data, pazopanib was deemed to be a safe and generally well-tolerated drug with an optimal oral dose of 800mg once daily. A further phase I trial to assess pharmacokinetic and pharmacodynamic in 53 patients aged 2-22 years was also undertaken and demonstrated a similar toxicity profile to that seen in adult patients, with one patient with occult brain metastasis experiencing intracranial bleeding<sup>115</sup>. All patients who underwent DCE-MRI evaluation of tumour vascular dynamics demonstrated decreases in tumour blood flow and permeability, while two objective partial responses (one with desmoplastic small round cell tumour) and stable disease >6 months in eight patients (7 with sarcoma) was seen. Early evidence of clinical efficacy prompted further development in mRCC, a cancer with a well-described central role of angiogenesis in tumour development. Subsequent randomised phase III trials demonstrated superior PFS with pazopanib vs placebo in pre-treated patients, and then non-inferior disease control and survival, and favourable quality-of-life outcomes, compared to sunitinib, a different antiangiogenic TKI already approved for first line treatment<sup>116,117</sup>. These studies established pazopanib as a standard of care in mRCC while also providing further data on drug toxicity, confirming severe hypertension as a commonly encountered adverse effect, as well as significant neutropenia and/or liver enzyme derangement in approximately 10%.

### **1.4.3 Clinical development of pazopanib for advanced STS**

Based on evidence of durable disease stabilisation seen in 4/9 patients with sarcoma treated with pazopanib in the initial phase I trial, further development of the drug in this disease context was pursued.

#### *1.4.3.1 EORTC non-comparative phase II trial*

A non-comparative phase II trial of pazopanib was undertaken by the EORTC Soft Tissue and Bone Sarcoma Group (STBSG) in patients with advanced intermediate or high-grade STS with confirmed disease progression who were either ineligible for cytotoxic chemotherapy or who had received fewer than three prior cytotoxic agents for advanced disease<sup>118</sup>. Although this study was non-randomised, patients were prospectively stratified into one of four histologically-defined subgroups: LMS, LPS, SS and a heterogeneous 'other subtypes' group. Primary efficacy endpoint was rate of freedom from disease progression after 12 weeks of treatment (12wPFR), with predefined rates of 40% and 20% determined as reflecting drug activity or inactivity. For each subtype-defined cohort, an initial enrolment of 17 evaluable patients were to be treated at 800mg once daily until disease progression, unacceptable toxicity or withdrawal of consent. If 4/17 patients experienced non-progression at 12 weeks, that subtype cohort was expanded to a total accrual of 37 patients – if 11 or more out of 37 patients were progression-free, this would indicate further investigation of pazopanib in that subgroup would be warranted.

A total of 142 patients were treated within the study. In the LPS arm, only 3 of the first 17 patients showed non-progression at 12 weeks, and so recruitment to this cohort was terminated due to lack of activity. The three other arms continued to complete the second stage of recruitment. Of 44 patients recruited to the 'other subtypes' arm, included diagnoses were undifferentiated sarcoma NOS (n=12), tumour of uncertain differentiation (n=7), MPNST (n=5), vascular tumours (n=5), fibrohistiocytic sarcoma (n=4), solitary fibrous tumour (SFT) (n=3), fibroblastic sarcoma, rhabdomyosarcoma, and GIST (all n=1). Four out of 142 patients were excluded from efficacy analysis due to lack of measurable disease, change of diagnosis to GIST on central histopathology review or lack of objective disease progression prior to commencement of pazopanib. A further 2 patients were not

evaluable due to resection of target lesion or withdrawal due to coronary heart disease, resulting in a total of 136 patients evaluable for efficacy endpoints

Although accrual of the LPS arm was stopped after the first stage of recruitment, two patients who had initially been categorised into one of the other three arms were found on central histopathology review to have LPS. As both of these patients met the 12 week progression-free endpoint, the overall 12wPFR in the LPS arm was 26% (5/19 patients). In the LMS, SS and other subtypes cohorts, 12wPFR was 44% (18/41 patients), 49% (18/37) and 39% (16/41) respectively. Objective partial response per RECIST criteria was seen in 9/136 patients (6.6%) – 5 SS, 3 Other subtypes and 1 LMS. Of these patients, 4 (3 other, 1 SS) experienced disease progression between 253 and 503 days after treatment initiation, while the other 5 (1 LMS, 4 SS) were still progression free at 415 to 812 days. Median PFS was 80 days, 91 days, 161 days and 91 days, and median OS 197 days, 354 days, 310 days and 299 days in the LPS, LMS, SS, and other subtype arms respectively. These PFS and OS rates compared favourably to historic controls for LMS, SS and other subtypes cohorts.

#### *1.4.3.2 PALETTE phase III randomised controlled trial*

Building on the results of the EORTC phase II study, the STBSG, in collaboration with the drug manufacturer, undertook the Pazopanib explored in Soft-Tissue Sarcoma (PALETTE) study, a double-blinded, placebo-controlled phase III RCT<sup>93</sup>. In this international, multicentre trial, adult patients with progressing advanced STS were randomised on a 2:1 basis to receive pazopanib 800mg once daily or placebo until disease progression, unacceptable toxicity or patient withdrawal. On-trial crossover to pazopanib was not permitted for patients who progressed on placebo. Eligibility criteria stipulated that patients must have received between one to four lines of previous systemic therapy, including an anthracycline, for advanced disease. Most common histological subtypes of STS were eligible for enrolment – notably, based on the earlier phase II evidence of limited activity, adipocytic sarcomas were not included in this phase III trial. PFS was the primary statistical endpoint, with a sample size designed to provide 95% power to detect a 15% difference in progression-free rate at 6 months, corresponding to a HR of 0.63. This sample size would also provide 90% power

to detect HR 0.67 for OS, which was included in secondary statistical endpoints along with toxicity and quality of life measures.

Between Oct 2008 and Feb 2010, 369 patients were randomised, with 246 allocated to pazopanib and 123 to placebo. In analysis of the intention-to-treat cohort after a median follow-up of 25 months, a clinically significant 3 month improvement in median PFS was seen with pazopanib (4.6 v. 1.6 months; HR 0.31; 95%CI 0.24-0.40;  $p < 0.0001$ ). There was no significant difference in OS with pazopanib compared to placebo (median OS 12.5 v 10.7 months; HR 0.68; 95% CI 0.67-1.11,  $p = 0.2514$ ). Post-trial systemic treatment was received by 49% and 63% of patients in the pazopanib and placebo arms respectively. Respective best objective response, as determined by external review, in pazopanib and placebo arms were partial response in 6% and 0%, stable disease in 67% and 38%, and disease progression/death in 24% and 62%. Safety and toxicity data were broadly in keeping with earlier pazopanib studies, with fatigue, hypertension, diarrhoea and anorexia among infrequently experience grade 3-4 toxicities. A small excess in decreased left ventricular ejection fraction, thromboembolic events and pneumothorax was observed in the pazopanib arm. One of eight on-treatment deaths in the pazopanib arm – a patient who died of multiorgan failure – was possibly related to study drug treatment. Subsequently reported exploratory health-related quality of life analysis reported that scores for general health status did not significantly differ between pazopanib and placebo-treated patients, while specific toxicity-related measures related to diarrhoea, anorexia, nausea, fatigue and role functioning favoured placebo<sup>119</sup>.

A subsequent post-hoc analysis of the Japanese sub-cohort from the PALETTE study ( $n = 47$ ) demonstrated similar levels of PFS and OS benefit (PFS HR 0.41, 95% CI 0.19-0.90,  $p = 0.002$ ; OS HR 0.87, 95% CI 0.41-1.83,  $p = 0.687$ ) to the overall study population<sup>120</sup>. There was no overall difference in the type or severity of pazopanib-related toxicity within the Japanese sub-cohort and overall study population, although a higher rate of dose reduction and lower average daily dose was experienced by Japanese patients. The lower pazopanib exposure but equivalent efficacy seen in the Japanese cohort potentially suggests contrasting pharmacokinetic profiles between different ethnic groups. However, given that pazopanib dose reduction within these trials study was at investigator discretion, it is possible that the more frequent dose reductions reflect regional variation in

practice. A similar comparison of TKI safety in patients with mRCC treated in an RCT with pazopanib or sunitinib reported similar levels of drug exposure but distinct pattern and severity of adverse events in Asian and non-Asian subgroups<sup>121</sup>. Meanwhile, a phase I study of pazopanib in a Japanese population reported a similar pharmacokinetic profile to the initial phase I<sup>122</sup>. Although these data do not provide a consistent picture of ethnology-related variation in the pharmacokinetic and pharmacodynamics profile of pazopanib, recognised differences in metabolism of many cancer and non-cancer drugs between different ethnic groups indicate the potential for ethnic background to contribute to inter-individual variation in pazopanib exposure and toxicity<sup>123,124</sup>.

A further post-hoc subgroup analysis of data from the PALETTE trial, in combination with data from the preceding phase II, focussed on uterine sarcoma patients treated with pazopanib (n=44, 88.6% LMS, 84.1% high grade)<sup>125</sup>. In this subgroup, who had received a higher degree of pre-treatment ( $\geq 2$  lines prior treatment in 61.3% vs 40.8% in non-uterine sarcomas), an ORR of 11% was seen and was associated with a numerically shorter median PFS and longer median OS compared to pazopanib-treated non-uterine sarcoma from the same studies (mPFS: 3.0 vs 4.5 months, mOS 17.5 vs 11 months). Compared to patients with uterine sarcoma who received placebo within the PALETTE study, patients randomised to pazopanib had significantly longer median PFS (3.0 vs 0.8m,  $p < 0.001$ ) and median OS (17.5 v 7.9m,  $p = 0.038$ ).

The results from the PALETTE study were taken to reflect a clinically-meaningful level of activity and benefit from pazopanib in the eligible population, leading to the drug receiving a license for this indication in the US and Europe in 2012. The subgroup analyses indicate that the efficacy and safety profile of pazopanib is similar in Japanese and non-Japanese populations and that efficacy in uterine sarcomas is broadly equivalent to that in non-uterine sarcomas.

#### *1.4.3.3 Other clinical evidence of pazopanib effect in STS*

Several other prospective and retrospective series provide additional evidence for the efficacy of pazopanib, both in unselected cohorts of mixed histological subtype as well as diagnosis-specific series with a variable focus on epithelioid sarcoma, SFT, desmoplastic round cell tumours, chondrosarcomas and vascular sarcomas. In addition, data has been reported for 211 patients of mixed STS

subtypes treated with pazopanib in an international expanded access program that was conducted following the PALETTE trial<sup>126</sup>. The efficacy data from these studies are summarised in **Table 1.3** and broadly conform with those from the PALETTE study, with infrequent objective responses seen and median PFS and OS following start of pazopanib of around 3-5 and 10-14 months respectively. Of note is a prospective single arm phase II study that provides further information on the efficacy of pazopanib in LPS<sup>127</sup>. Opening following the reporting of the results of the PALETTE study and noting the results of the antecedent phase II where efficacy of pazopanib in the final, centrally-confirmed LPS cut-off was in fact above the predetermined futility cut-off, this multicentre US study treated 41 patients with intermediate or high-grade LPS with pazopanib and reported a 12wPFR of 60%. Median PFS and OS (4.4 and 12.6 months respectively) were consistent with efficacy data for other STS subtypes from the PALETTE study.

In attempt to improve the generally modest activity of pazopanib in unselected advanced STS, a number of reported and ongoing trials have investigated the combination of the drug with various cytotoxic chemotherapy regimens or targeted agents such as histone deacetylase inhibitors<sup>128-131</sup>. While several of these have been associated with unacceptable toxicity and/or insufficient activity in phase I studies, others have progressed to examining efficacy in STS-enriched cohorts. In view of the focus of this project on the licensed indication of pazopanib monotherapy and the lack of convincing evidence of incremental activity of such combinations, further detail of these studies is not explored here.

	Prospective						Retrospective								
Study	Sleijfer 2009 <sup>118</sup>	Van der Graaf 2012 <sup>93</sup>	Frezza 2014 <sup>132</sup>	Benson 2016 <sup>125</sup>	Samuels 2017 <sup>127</sup>	Maruzzo 2015 <sup>133</sup>	Frezza 2018 <sup>134</sup>	Gelderblom 2017 <sup>126</sup>	Jones 2017 <sup>135</sup>	Kollar 2016 <sup>136</sup>	Menegaz 2017 <sup>137</sup>	Nakamura 2016 <sup>138</sup>	Nakano 2015 <sup>139</sup>	Stacchiotti 2014 <sup>140</sup>	Yoo 2015 <sup>141</sup>
Design	Non-comparative phase II	Double blind, placebo-controlled, phase III	Subgroups from pIII and III trials + EAP data	Subgroups from pIII and III trials	Single arm, multicentre US phase II	Single centre case series	Int'l multicentre case series	Int'l multicentre case series based on EAP	Int'l case series	European multicentre case series, inc phase II/III	UK centre case series	Japanese multicentre case series	Japanese centre case series	Italian multicentre series	Korean centre series
N	142	369	9	44	41	13	18	211	8	52	29	156	47	6	43
Subtypes	LMS, SS, LPS, 'Other'	Mixed (LPS excluded)	DSCRT	Uterine sarcoma (89% LMS)	LPS (int/ high grade)	SFT	Epithelioid sarcoma	Mixed	Chondrosarcoma	Vascular sarcomas	DSCRT	Mixed	Mixed	SFT	Mixed
Eligibility	<3 prior lines	1-3 prev lines	≥2nd line	≥2nd line	Any line	1st line	Any line	1-3 prev lines	Any line	Any line	Any line	Any line	Any line	Any line	≥2nd line
Best response: CR or PR	6%	6%	22%	11%	2%	8%	0%	7%	0%	23%	7%	8%	11%	0%	16%
SD	NR	67%	56%	57%	42%	62%	50%	18%	75%	21%	55%	47%	NR	50%	42%
PD	NR	24%	22%	32%	66%	15%	50%	41%	25%	50%	38%	24%	NR	50%	37%
12wPFR *=approx	LMS:44% SS:49% LPS:26% Other:39%	60%*	67%	50%	68%	62%	50%	50%	75%	AS:45%* EHE:60%*	62%	60%*	60%*	50%*	NR
Median PFS (months)	LMS:3.0 SS:5.4 LPS:2.7 Other:3.0	4.6 (vs. 1.6 in placebo arm)	9.2	3	4.4	4.7	3	3	NA	AS: 3.0 EHE: 26.3	5.6	3.6	4.3	3	5
Median OS (months)	LMS:11.8 SS:10.3 LPS:6.6 Other:10.0	12.5 (vs. 10.7 in placebo arm)	15.4	17.5	12.6	13.3	14	11.1	NR	AS: 9.9 EHE 26.3	15.7	11.2	9.6	NR	8.2
Comments	Favourable PFS and OS vs historical control in LMS, SS and Other subgroups	Results led to drug licensing in pre-treated non-adipocytic STS		In PALETTE trial, significantly longer PFS and OS with pazopanib vs placebo	LPS subtypes: 66% DDLPS, 29% MLPS, 5% PleoLPS		Authors conclude limited activity in ES		5/8 Conventional CS 1/8 ESMC 1/8EMC 1/8 clear cell	Equivalent ORR in cutaneous vs non-cutaneous or 1 <sup>st</sup> v 2 <sup>nd</sup> AS		NB 33/156 (21%) LPS			

Table 1.3: Summary of clinical study data on efficacy of pazopanib in STS

#### ***1.4.4 Evidence of biomarkers of pazopanib effect***

The effect of pazopanib in STS is evidenced by the improvement in PFS without associated deterioration in quality of life compared to placebo in a randomised phase III study, as well as reports of post-approval experience in ‘real world’ settings. However, the benefit of pazopanib treatment to individual patients is highly variable and, in the context of infrequent objective tumour responses, often difficult to confirm. Furthermore, despite the RCT evidence of anti-tumour effect in an otherwise poor prognosis patient group with limited further treatment options, no significant difference in OS was seen between pazopanib and placebo-treated patients. The absence of demonstrated OS benefit in an unselected STS population has adversely affected cost effectiveness appraisals of pazopanib, including those by the Scottish Medicines Consortium and the All Wales Medicines Strategy Group. In England, availability of pazopanib for advanced STS through the Cancer Drugs Fund was withdrawn and GSK did not submit for formal NICE appraisal. As such, pazopanib is currently not available through NSH funding within the UK and, similarly, access to the drug is limited in other healthcare economies<sup>107–109</sup>. The ability to prospectively identify patients with advanced STS most likely to benefit from pazopanib therapy would aid clinical decision making, increase the clinical and cost-effectiveness of the drug and improve patient experience and survival outcomes. However, as summarised below, no routinely recorded clinico-pathological parameter or experimental assays have yet been shown to be consistently capable of discriminating between patients who are more or less likely to benefit from pazopanib.

##### ***1.4.4.1 Clinico-pathological parameters***

Pre-planned and post-hoc analysis of the EORTC phase II and III trials of pazopanib have been performed in attempt to identify patient or tumour characteristics that enrich for drug benefit. As discussed above, LPS was identified as a potentially insensitive histological subtype within the phase II study, but subsequent analysis and other studies call into question whether there are subsets of patients with LPS who may respond to treatment<sup>118</sup>. Within the PALETTE study cohort, multivariate analysis identified good performance status and lower histological grade as factors associated with improved outcome, both of which are well-established prognostic factors in STS regardless of pazopanib exposure<sup>93</sup>. Predictive analysis did not detect a significant interaction between

histological subtype and pazopanib benefit, with improved PFS with pazopanib vs placebo seen in all three histological subgroups (LMS, SS, other). Other baseline characteristics including gender, ethnicity and amount of prior treatment were found not to be predictive for OS<sup>142</sup>.

Analysis of patients who received pazopanib within the EORTC phase II and phase III trials and who met PALETTE-eligibility criteria (i.e. non-adipocytic histology, measurable disease, adequate organ function etc.) (n=344) were included in a retrospective analysis that sought to identify baseline factors associated with good outcome following treatment<sup>143</sup>. Here, the authors defined PFS $\geq$  6 months and OS $\geq$ 18 months as long-term response and survival respectively, with 36% of patients showing long term response, 34% long term survival, and 22% both long-term response and survival. Descriptive and multivariate analysis again identified tumour grade and performance status as having prognostic relevance for PFS and OS, as too was the case with baseline blood haemoglobin level. There was no preponderance for any histological subgroup in long-term responder or survivor patient groups. These findings, consistent with results from other case series summarised in **Table 1.3**, indicate that a non-trivial minority of patients across many different STS subtypes attain significant benefit from pazopanib therapy.

#### *1.4.4.2 Radiological biomarkers*

Data from the PALETTE study indicate that the PFS gain seen with pazopanib is associated with a minor increase in objective radiological response compared to placebo (6% vs 0%) but much larger increase in disease stabilisation rates (67 vs 38%)<sup>93</sup>. This implies that pazopanib benefit was predominantly associated with disease stabilisation rather than significant tumour shrinkage. However, given that over a third of patients who received placebo also exhibited stable disease as best response, the difficulty in discerning between intrinsically indolent but pazopanib-resistant disease and true pazopanib-related tumour stabilisation presents a clinical challenge when attempting to appraise early signs of benefit to individual patients. The use of imaging modalities that provide information on changes in tumour physiology beyond dimensional response show promise in assessing pazopanib effect and represent a potential avenue of delineating the heterogeneity of tumour response within the RECIST stable disease category.

Anti-angiogenic therapy can confer therapeutic compromise to tumour blood supply that results in consequent cystic degeneration of solid tumours. Particularly as this process can be associated with an initial inflammation-related increase in tumour dimension, and thus confound RECIST response assessment, the measurement of changes in tumour vascularity as a proxy for anti-tumour effect has been pursued. The initial pazopanib phase I trial used DCE-MRI to measure changes in tumour vascularity in a subset of pazopanib-treated patients – further investigation of this functional MRI modality is required to assess the adequacy of detected vascular alterations as surrogates for survival endpoints. CT-based criteria that account for reduction in tumour density that reflect tumour cell death have been developed by Choi et al<sup>144</sup>. These criteria have been shown to be more sensitive for TKI benefit than RECIST criteria in GIST and have shown promise in other STS subtypes in terms of specificity in predicting pathological response and favourable outcome in patients treated with cytotoxic chemotherapy<sup>145–147</sup>. Remaining questions regarding the reproducibility of Choi response assessment and the surrogacy of Choi response for survival outcomes have so far limited the widespread adoption into routine practice in STS, especially outside of GIST. In a single centre series of 13 patients with advanced SFT treated with pazopanib, assessment of response by Choi criteria identified 4 patients as having a partial response that was categorised as stable disease by RECIST – duration of treatment in these patients (arguably a proxy for duration of disease control) was between 10.7 and 60 months<sup>133</sup>. A further study of pazopanib in a series of 7 patients with advanced SFT found 1 patient with partial response (PR) by Choi criteria and stable disease (SD) by RECIST and who experienced PFS of 15 months<sup>140</sup>. Further information on the utility of Choi criteria, as well functional magnetic resonance imaging (MRI) and fluorodeoxyglucose positron emission tomography (FDG-PET), in predicting pazopanib benefit will be provided by a now-completed window-of-opportunity study of pre-operative treatment in localised STS (NCT01543802)<sup>148</sup>. The potential utility of FDG-PET-CT in this scenario is also informed by small studies that have demonstrated an association in either decrease in maximum standardised uptake value (SUVmax) during therapy and durable disease control, or absence of SUVmax response and lack of clinical benefit<sup>149,150</sup>. These modalities all require significant development prior to potential application as a tool for accurate early detection of pazopanib benefit but feasibly represent an

avenue of distinguishing between responding patients who are likely to benefit from ongoing therapy and those without response who would be better served by a change of therapy.

#### *1.4.4.3 Markers of drug exposure*

Numerous pharmacokinetic factors can influence systemic drug exposure, including oral absorption and metabolism, drug-drug interactions, food-drug interactions and patient characteristics such as age, gender and bodyweight that can relate to variations in volume of distribution. As such, high interpatient variability of plasma exposure of oral anticancer drugs including pazopanib may affect drug efficacy and treatment outcome. Retrospective analyses of clinical trial data on the use of pazopanib in the treatment of mRCC and advanced GIST have reported associations between higher trough levels of plasma pazopanib concentration and longer PFS<sup>151,152</sup>, giving rise to the possibility that variability in drug exposure levels may, at least in part, explain variability in outcome in pazopanib treatment of advanced STS. A prospective cohort study of patients with mRCC or advanced STS or GIST treated with TKIs including pazopanib demonstrated that dose optimisation in response to suboptimal trough drug levels was successful in attaining subsequent adequate trough levels, indicating that dose monitoring and adjustment could represent a path to improved clinical effectiveness of these drugs<sup>153</sup>.

Hypertension is a frequently occurring on-target side effect of pazopanib and correlates with pharmacokinetic degree of drug exposure, and thus has generated interest as a potential biomarker to guide drug dosing or predict treatment effect. However, as has been seen with the use of pazopanib in mRCC, combined analysis of prospective patient data from the EORTC phase II and phase III trial has indicated that development of hypertension during pazopanib therapy was not associated with improved PFS or OS<sup>154,155</sup>. This finding is consistent with data from a single centre, 26 patient case series that found no significant association between suboptimal trough levels of pazopanib and worse PFS following treatment, indicating that drug exposure alone is unable to account for variation in pazopanib effect<sup>156</sup>.

#### 1.4.4.4 Baseline biological markers

Informed by the inhibitory activity of pazopanib against a number of molecular mediators of tumour angiogenesis and the relative ease of using multiplexed antibody arrays to assess for protein levels in blood samples, biomarker research related to pazopanib has so far largely focused on investigation of circulating angiogenic factors (CAFs). This is especially true in mRCC, a disease where dysregulated angiogenic pathways are known to contribute significantly to tumour development and for which pazopanib and other TKIs that target angiogenic mediators are established standards of care. These studies have identified a varying repertoire of CAF or cytokines whose baseline level or change in response to therapy have been associated with differential outcomes following TKI therapy<sup>157</sup>. However, the retrospective nature of many of these studies, and the lack of interaction between biomarker and treatment effect in prospective studies, have limited the extent with which they inform the search for predictive, rather than prognostic, biomarkers for pazopanib. An exception to this was seen in the analysis of prospectively collected pre-treatment blood samples taken from patients with mRCC treated in either a non-comparative phase II or randomised phase III study of pazopanib<sup>158</sup>. After initially screening for association of 17 CAFs with outcome in the phase II cohort, 7 candidates were then taken forward for validation in the phase III cohort. Among these, interleukin (IL)-8 and osteopontin were validated as negative prognostic, but not predictive, biomarkers for PFS. However, the effect of IL-6 level on post-pazopanib outcome was shown to significantly interact with pazopanib exposure, indicating that while patients with raised baseline IL-6 had worse prognosis than those with low IL-6, this was the group in which pazopanib treatment delivered the most benefit. Despite this high-level evidence for baseline circulating IL-6 level for pazopanib in mRCC, this biomarker has not impacted on routine practice so far, for reasons that include the limited analytical replicability of IL-6 assays and the lack of validation in an independent prospective cohort. Elsewhere, studies that have investigated for tumour-based pazopanib biomarkers include retrospective assessment of gene expression mRCC molecular subgroup, hypoxia-inducible factor (HIF) levels or *VHL* mutational status in tissue series – such studies have indicated prognostic associations of the investigated markers but, due to retrospective design and lack of validation, the predictive utility of these remain unproven<sup>159,160</sup>.

Several studies have reported baseline biomarkers with putative predictive associations with pazopanib efficacy in advanced STS patients. Sleijfer et al. examined the serum levels of cytokine and angiogenic factors in a cohort of 85 patients from the EORTC phase II trial and demonstrated that increased baseline plasma levels of pro-angiogenic hepatocyte growth factor (HGF) and basic nerve growth factor (bNGF) were associated with worse PFS in pazopanib treated patients<sup>161</sup>. These findings are consistent with the role of pazopanib as an anti-angiogenic agent and an association of various CAFs with poor post-pazopanib survival, but the impact of the study is limited by high reported false discovery rates combined with lack of validation in independent cohorts.

The ratio of neutrophils to lymphocytes (NLR) in the circulation of patients can serve as an easy-to-measure marker of systemic inflammatory state in cancer patients. High NLR has been shown to be negative prognostic marker in multiple solid tumour types<sup>162</sup>. Blood samples collected at pre-treatment baseline and after 50 days of therapy were used to assess of association between NLR and pazopanib outcome in 333 patients treated with pazopanib within the EORTC phase II and III studies<sup>163</sup>. While elevated NLR at baseline was a poor prognostic marker regardless of treatment with pazopanib or placebo, no observed pattern of change in NLR between baseline and day 50 (stable, >40% increase or decrease) was seen to have any association with PFS or OS. In contrast, in a smaller study of 25 patients treated with pazopanib in several Japanese centres, decrease in NLR from baseline to week 4 of therapy showed a highly significant association with improved PFS while baseline NLR had no prognostic association<sup>164</sup>. This study used a higher cut-off to define high and low NLR patients (based on cohort median NLR value) and did not provide a definition as to what constituted a significant change in NLR during therapy, potentially contributing to discrepancy with the EORTC cohort analysis. Regardless, beyond the consistently observed prognostic association of NLR in STS and other cancers, its role as a potential predictive biomarker for pazopanib appears to have little promise.

In a study by Koehler et al, NGS was used to sequence 405 cancer-related genes in pre-treatment tumour samples from a retrospective cohort of 19 patients with advanced STS treated with anti-angiogenic agents (18 pazopanib and 1 sunitinib)<sup>165</sup>. *TP53* and *RB1* were the only two genes found to be altered in >20%

(in 10 and 6 patients respectively), with all detected mutations of *TP53* predicted to confer loss-of-function (missense mutation of DNA binding and/or tetramerisation domain, or homozygous deletion). While *RB1* mutational status had no association with post pazopanib outcome, patients with *TP53*-mutated tumours were shown to have significantly longer PFS than those with *TP53* wild-type tumours. These data represent the only currently reported tumour-based candidate biomarker for pazopanib in advanced STS and have yet to be validated. The biological basis of any association between *TP53* function and pazopanib response remains to be determined

#### *1.4.4.5 Pre-clinical evidence of markers of pazopanib sensitivity and resistance*

Given that pazopanib selectively inhibits several growth-promoting RTKs, expression levels of these targets in tumour cells are also attractive candidates for evaluation as predictive biomarkers. While translational studies of tumour-based expression of RTKs in pazopanib-treated STS are lacking, several pre-clinical studies have assessed for association between RTK expression and pazopanib effect. In one such study, screening of 14 cell lines representing 8 different sarcoma subtypes identified that only the two malignant rhabdoid tumour (MRT) cell lines demonstrated pazopanib sensitivity<sup>166</sup>. These cell lines were shown to express phosphorylated PDGFRA and FGFR1, both kinase targets of pazopanib. Dual pharmaceutical or RNA interference (RNAi) inhibition led to a synergistic increase in tumour cell apoptosis. Acquired pazopanib resistance was then derived in these cells through culture in the presence of escalating drug dose. Comparison of molecular profiles between parental and resistance cell lines identified significant downregulation of PDGFRA but maintenance of FGFR1 expression and activation. These cells were no longer dependent upon PDGFRA signalling but remained sensitive to FGFR1 inhibition, indicating that loss of PDGFRA could serve as a marker of acquired pazopanib resistance that could potentially be therapeutically targeted with inhibitors of FGFR1. In a follow-up study, further comparative mass spectrometry-based phosphoproteomic characterisation of these paired pazopanib sensitive and resistant cells identified increased activity in cytoskeletal regulatory pathways and downregulation of histone deacetylase activity in pazopanib-resistant cells<sup>167</sup>. Elsewhere, immunoblot and microarray-based comparative proteomic profiling was performed on 4 different synovial cell lines, 3 of which were sensitive to

pazopanib with the other showing primary pazopanib resistance<sup>168</sup>. Increased expression of PDGFRB and phosphoactivation of TKs including FGFR3 and VEGFR1 were shown to be unique to the resistant cell line, while RNAi of PDGFRB, MET and PYK reduced viability of the pazopanib-resistant cells. Collectively, these studies indicate that the relative pazopanib sensitivity of sarcoma cells is reflected and possibly determined by differential expression and phosphorylation of RTKs and pathway signalling proteins. While translational correlates of these findings are lacking, there is an indication that investigation of expression levels of the molecular targets of pazopanib within tumour tissue may yet identify biomarkers for drug effect.

## 1.5 The immune system in STS

### 1.5.1 Anti-tumour immunity as therapy and a source of biomarkers

#### 1.5.1.1 The immuno-editing model

It is now well established that the host immune system may recognise cellular abnormalities that result from the accumulating molecular aberrations required for tumour development and progression. Furthermore, in a subset of patients, effective anti-tumour immune responses can occur either spontaneously or after therapeutic provocation. Significant advancement in the understanding of the complex interaction between cancer cells and the immune system has occurred over the past 10 years, driven by renewed preclinical, translational and clinical research interest. Modern understanding of anti-tumour immunity conforms to the model of immuno-editing as summarised in a seminal 2004 review<sup>169</sup> (**Figure 1.3**). The immuno-editing model reflects a dynamic and deterministic interaction between host immunity and an evolving tumour and can be split into three phases – elimination, equilibrium and escape:

*Elimination* – the developing tumour causes local tissue disruption, releasing tissue factors that drive an acute inflammatory response. Tissue-resident monocyte cells in the TME release cytokines and chemokines that recruit and activate other innate immune cells such as granulocytes, natural killer cells (NKC) and dendritic cells (DC). Infiltrating DCs are activated within the inflammatory milieu and uptake cancer-specific antigenic proteins or peptides released by injured tumour cells. Activated DC migrate to local lymph nodes where they present tumour antigen in a major histocompatibility complex (MHC) class II-restricted fashion alongside upregulated costimulatory factors. Immature, antigen-specific Th1 CD4+ and cytotoxic CD8+ T cells are primed on interaction of their T cell receptor (TCR) with presented antigen-MHC complexes and co-stimulatory factors and undergo functional activation and clonal expansion as they migrate to the TME. Here, the antigen-primed T lymphocytes act as the effector arm of adaptive immunity, recognising their cognate antigens in complex with MHC class I molecules on the surface of tumour cells and killing them via focussed release of cytotoxic granules and ligand-mediated stimulation of apoptotic pathways. If this stage of

immunoediting is completed, the primary tumour will be eradicated before the development of clinically apparent disease and inflammation will resolve.

- *Equilibrium* – the persistence of cytotoxic immune effectors in the TME exerts an evolutionary pressure that selects for tumour clones that, through mutation, transcriptional reprogramming and/or paracrine co-option of host immunosuppressive mechanisms, have acquired the ability to resist immune elimination. Additionally, the failure of inflammation to resolve engenders a chronic inflammatory TME, where the continuous supply of mitogenic growth factors such as tissue growth factor  $\beta$  (TGF-  $\beta$ ) and Th2 helper lymphocyte-related cytokines aimed at promoting tissue repair instead supports the tumour through pro-angiogenic, anti-apoptotic activity that also see modulation of macrophage and lymphocyte populations toward immunosuppressive phenotypes. Other mechanisms of immune resistance may include downregulation of cell-surface expression of MHC-II molecules, this limiting the presence of recognisable antigens, or the co-option of physiological means of immunosuppression, such as recruitment of regulatory T cells, myeloid-derived suppressor cells (MDSC) or alternatively activated M2 macrophages, or upregulation of immune checkpoint proteins, all of which may result in a blunted, anergic lymphocyte and NKC response.

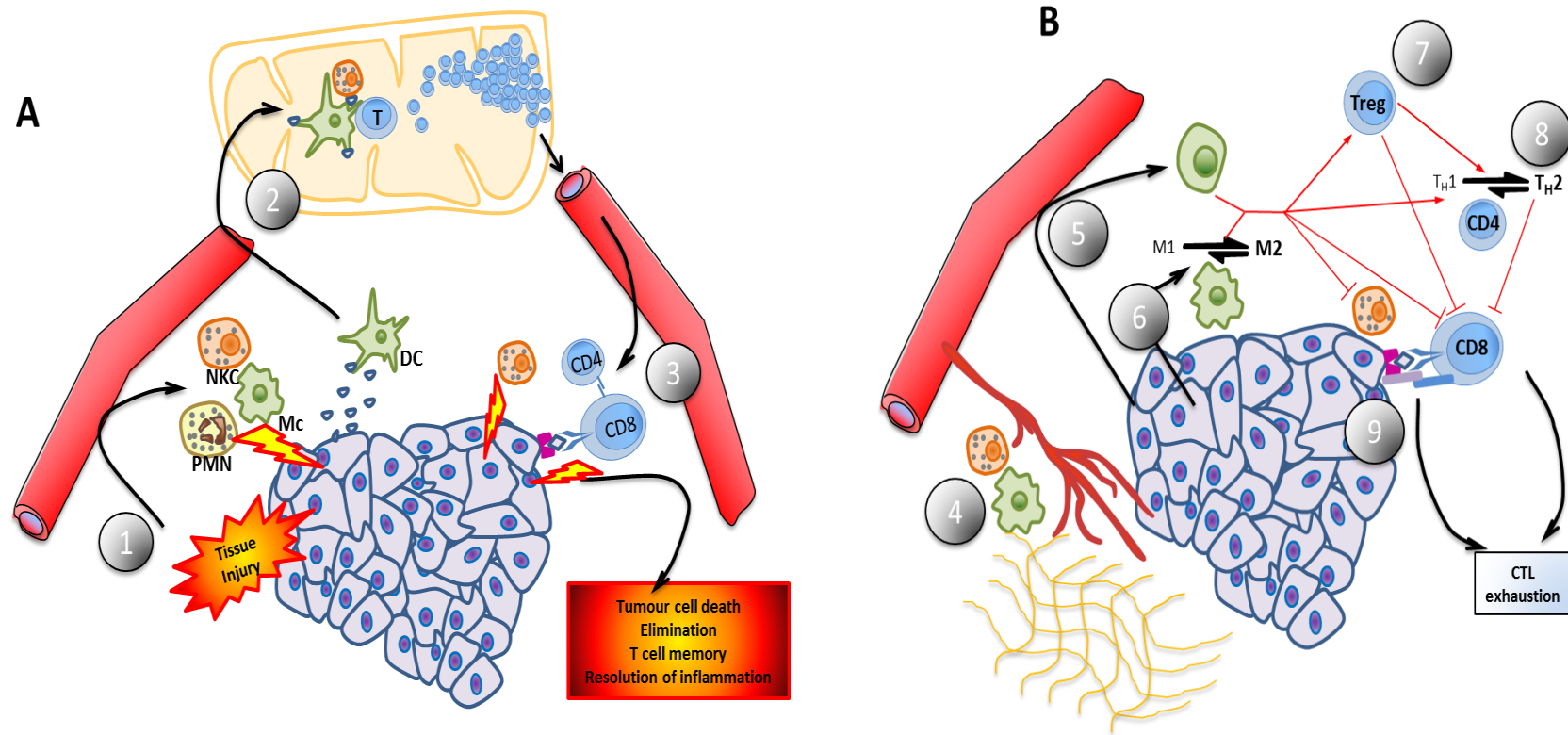


**Figure 1.3: Overview of the immuno-editing model in cancer**  
*(legend overleaf)*

## **A. Immune elimination of tumours**

1. Tissue perturbation by tumour cells triggers acute inflammatory influx, including neutrophils (PMN), macrophages (Mc) and NKC. Limited tumour cell killing by these innate immune cells sees release of antigenic material that is taken up by infiltrating DC.
2. Activated DC migrate via lymphatics to draining lymph nodes where they present tumour antigen to naïve T lymphocytes and NKC. Antigen-specific CD4+ helper and CD8+ cytotoxic T cells (CTL) undergo clonal expansion, enter the circulation and localise to the TME.
3. Antigen-primed CTLs recognise their cognate antigen presented in association with MHC class I molecules on the surface of tumour cells alongside activating co-stimulation from CD4+ T c helper cells. The CTL kill tumour cells through toxic granule release and ligand-dependent apoptotic pathways. Following tumour elimination, local inflammation resolves and antigen-specific memory T cells develop.

## **B. Mechanisms of tumour immune equilibrium and escape.**

4. A chronic inflammatory TME supports tumour survival through supply of mitogenic and anti-apoptotic factors, whilst proteases and metalloproteinases remodel local extracellular matrix, supporting tumour migration and invasion. Angiogenic factors released by extracellular matrix, tumour, immune and stromal cells promote new blood vessel growth.
5. MDSC suppress the anti-tumour actions of NKC and CTL via soluble mediators, as well as promoting the accumulation and immunosuppressive actions of regulatory T lymphocytes (Treg)
6. Plasticity of macrophage phenotype is exploited by the tumour, favouring alternatively activated M2 phenotype, characterised by release of mitogens and survival factors, suppression of CTL and NKC activity and promotion of T<sub>H</sub>2 T helper differentiation.
7. Tregs are CD4+FOXP3+ T lymphocytes that undergo antigen specific priming in lymph nodes and in the TME. Treg inhibit NKC and CTL cytotoxicity directly through release of immunosuppressive cytokines and indirectly through inhibition of antigen presenting cell activation.
8. The chronic inflammatory TME promotes T<sub>H</sub>2 T helper differentiation. This phenotype is functionally characterised by the promotion of tissue repair, humoral immunity and induction of CTL anergy through inhibitory cytokine release and expression of immune checkpoint proteins.
9. The expression of inhibitory immune checkpoint ligands on the surface of tumour and immune cells promote the deactivation and exhaustion of CTL responses. These proteins interact with T cell surface receptors that include PD1, TIM3 and LAG-3 that induce a tolerogenic, exhausted CTL phenotype characterised by significantly limited cytotoxic capabilities.

- *Escape* – immune-resistant tumour clones selected during equilibrium phase acquire the capability to continue developing an increasingly aggressive phenotype, promoted rather than hindered by ongoing immune activity in the TME. Inflammatory and immune factors disrupt the extracellular matrix, promoting metastasis, whilst any previously effective T lymphocyte response is moulded toward an ‘exhausted’ phenotype. The cancer progresses toward overwhelming malignancy unchecked by host immunity.

#### *1.5.1.2 Tumour-infiltrating lymphocytes as cancer biomarkers*

It has long been recognised that the presence of immune cells within the TME can vary significantly both between and within different cancer types<sup>170</sup>. T lymphocytes are the main effector compartment of adaptive cellular immunity and have been shown to play a critical role in anti-tumour immune responses<sup>171</sup>. It is now established that, in a diverse range of solid tumour types, the presence of tumour-infiltrating lymphocytes (TIL) is associated with favourable clinical outcome<sup>172,173</sup>. In a series of studies of the immune microenvironment of colorectal cancers, an ‘Immunoscore’ comprising of a four point measure of density of CD3+ and CD8+ TIL in the centre and invasive margin of early-stage primary tumours has been validated as outperforming conventional TNM staging in terms of predicting DFS and OS<sup>174,175</sup>. This measure has now been taken forward as a tool for stratifying adjuvant therapy in prospective clinical studies<sup>176,177</sup>. Meanwhile, the presence of infiltrating T lymphocytes has been shown to predict improved rates of pathological complete response to pre-operative cytotoxic chemotherapy in certain subtypes of breast cancer<sup>178,179</sup>.

#### *1.5.1.3 Immune checkpoint proteins*

Among the growing number of recognised mechanisms by which cancers may inhibit or attenuate host immune responses, immune checkpoint pathways have gained recent prominence due to the successful therapeutic targeting of two such immune checkpoint proteins – cytotoxic T-lymphocyte protein 4 (CTLA-4) and programmed cell death protein 1 (PD1). CTLA-4 is an immunoglobulin superfamily protein that is expressed on the surface of activated T cells and acts as a negative regulator of T cell function through competing with the costimulatory T cell surface molecule CD28 for binding to ligands expressed on antigen-

presenting cells. PD1 is expressed on T cells during antigen-mediated activation and expansion. PD1 has two known ligands – PD-L1 and PD-L2. PD-L1 can be expressed by both tumour cells and a range of immune cells in response to cytokines including interferon gamma (IFN $\gamma$ ), while PD-L2 expression is largely limited to DCs. On ligand binding, PD1 exerts an inhibitory signal in T cells that acts as part of a physiological negative feedback mechanism that plays an important role in immune homeostasis. This mechanism of T cell exhaustion may also be exploited by cancers to limit anti-tumour immune responses. Inhibitory mAbs that target these immune checkpoint proteins are now established as standard-of-care immunotherapies in a growing range of cancer types. Ipilimumab is an anti-CTLA4 antibody that has been shown to induce durable disease control in approximately 20% of patients with advanced malignant melanoma when used as a monotherapy<sup>180</sup>. An expanding repertoire of antibodies that inhibit the PD1/PD-L1 axis have been shown to bring about tumour response and, in some circumstances, long-lasting disease control and improved OS in cancers that include melanoma, non-small cell lung cancer (NSCLC), Hodgkin lymphoma, bladder and head and neck cancer, either when used as monotherapy or in combination with CTLA-4 targeting agents<sup>181</sup>.

Beyond the PD1/PD-L1 axis and CTLA-4, a number of additional cell surface receptor-ligand interactions are known to contribute to the complex regulation of T cell functional activation and have been implicated in modulating the tumour immune microenvironment toward either pro-inflammatory and anti-tumour or immunosuppressive and tumour-promoting phenotypes. Additional checkpoint inhibitor proteins whose expression is progressively increased during T cell exhaustion include lymphocyte activation gene 3 protein (LAG3, also known as CD223) and T cell immunoglobulin and mucin domain-containing 3 (TIM3, also known as HAVCR2). Both of these proteins have been shown to be expressed on tumour-infiltrating regulatory CD4<sup>+</sup>FOXP3<sup>+</sup> T cells (Treg) and Th1 CD4<sup>+</sup> T cells respectively, suggesting a potential role in immune escape and/or evasion<sup>182,183</sup>. V-set domain-containing T-cell activation inhibitor 1 (VTCN1, also known as B7.H4) is expressed on antigen-presentation cells and, on ligand binding, inhibits pro-inflammatory Th1-type activation of T cells<sup>184</sup>. High levels of tumour cell expression of LAG3, TIM3 and VTCN1 have been reported in multiple cancer types in association with worse clinical outcome, indicating an active role in

promoting an immunosuppressive, tumour-promoting microenvironment<sup>182,185,186</sup>. Inhibitory therapeutic mAbs against these checkpoint proteins are under active clinical investigation as monotherapies or in combination with other checkpoint inhibitors or chemotherapy. Indoleamine 2,3-dioxygenase (IDO) is an enzyme involved in physiological feedback mechanisms that tightly control T cell response against pathogens through tissue depletion of metabolites that result in promotion of Treg activity and suppressing effector T cells<sup>187</sup>. Tumour cells have been shown to express IDO in preclinical models, while overexpression has been detected in multiple cancer types and proposed as a potential mechanism of clinical resistance to immune checkpoint inhibitor therapy<sup>188</sup> – IDO inhibitors are currently being evaluated in clinical trials across multiple cancer types. Meanwhile, a range of co-stimulatory receptors whose signalling promotes survival and activation of T cells and stimulate anti-tumour response are under investigation as targets for agonist therapies that aim to reinvigorate the cytotoxic activation of exhausted TIL. For example, CD137 (also known as 4-1BB and TNFRSF9) is a potent co-stimulatory receptor that is expressed on the surface of T cells and NKC and whose stimulation promotes anti-tumour immune responses in preclinical cancer models<sup>189</sup>. Agonist therapeutic antibodies that target CD137 are under clinical investigation in combination with other therapeutic modalities in a range of cancer types.

#### *1.5.1.4 Emerging concepts of immune subtype as biomarker in cancer*

While the successful targeting of CTLA4 and PD1 signalling axes reflect the tremendous potential of therapeutic manipulation of tumour-immune interactions, intensive clinical investigation has demonstrated that, across all cancer, only a minority of patients will respond to such agents. A broad range of factors are now recognised as contributing to tumour sensitivity or resistance to immune checkpoint inhibitor therapy and include intrinsic tumour factors such as the expression of antigens, the modulation of the immune microenvironment through secretion of chemokines and cytokines that respectively recruit and dictate the functional activation of various immune cell types, vascular and stromal density in the TME and tumour-extrinsic such as patient age, gut microbiome and germline genetics<sup>170,171,190</sup>.

Expression of PD-L1 has been studied extensively as a potential predictive biomarker for anti-PD1/PD-L1 checkpoint inhibitor therapy across a range of tumour types<sup>191</sup>. Overall, such studies have found with some consistency that the efficacy of such agents correlates with the degree of tumour cell expression of PD-L1. Across a number of solid tumour types, PD-L1 measurement is now established as a predictive biomarker, with the indicated use of certain anti-PD1 mAbs limited to patients whose tumours meet IHC-based criteria for PD-L1 positivity<sup>192</sup>. Meanwhile, randomised clinical trial data have indicated that prospectively assessed levels of tumour PD-L1 expression can distinguish between patients with advanced melanoma for whom anti-PD1 monotherapy is equally efficacious to the more toxic combination of anti-PD1 and anti-CTLA4-inhibiting mAbs<sup>193</sup>. Despite these findings, there have been a variety of barriers to the broader adoption of PD-L1 expression as routinely used predictive biomarker. Assessment of PD-L1 by IHC has varied widely between studies in terms of reagents used, scoring methodologies, and definitions of positive/negative thresholds<sup>194</sup>. As summarised in **Table 1.4**, individual anti-PD1 and -PDL1 monoclonal antibodies are accompanied by their own companion diagnostic assay for PD-L1 expression assessment, each using a different diagnostic antibody with individualised assay conditions. Further to this variety in scoring PD-L1 expression, the cellular compartment scored and positive/negative biomarker thresholds vary not only with each assay, but also according to the cancer type and, in some instances, even depending on exposure to prior treatment<sup>195</sup>. This disconcerting variety in methodology speaks to more fundamental limitations to the examination of PD-L1 as an isolated biomarker, where, despite consistent trends of greater PD-L1 expression being associated with higher rates of drug effect, the demonstrated predictive value of such assays often falls considerably beneath that of an idealised biomarker<sup>191</sup>.

A current prevailing notion is that tumours with a high somatic mutation rate are more likely to express mutated proteins that consist of altered peptides that can act as tumour-specific antigens, and thus increase the likelihood of anti-tumour immune response. Supporting evidence for this supposition includes the observation that in early stage colorectal cancer, tumours that exhibit microsatellite instability (MSI) that results from functional impairment of DNA mismatch repair genes are associated with lower rates of tumour recurrence than

		<b>Nivolumab</b>	<b>Pembrolizumab</b>	<b>Durvalumab</b>	<b>Atezolizumab</b>
<b>Target</b>		PD-1	PD-1	PD-L1	PD-L1
<b>Antibody clone</b>		28-8 (Dako)	22C3 (Dako)	SP263 (Ventana)	SP142 (Ventana)
<b>Compartment scored</b>		Membranous	Membranous	TC – M IC – M,C,P	TC – M IC – M,C,P
<b>PD-L1 expression cut-off</b>					
<b>Melanoma</b>	Adjuvant	<b>Any</b>	<b>Any</b>	-	-
	1 <sup>st</sup> line advanced	<b>Any</b>	<b>Any</b>	-	-
	2 <sup>nd</sup> + line advanced	<b>Any</b>	<b>Any</b>	-	-
<b>NSCLC</b>	1 <sup>st</sup> line advanced	<b>Any (w/ ipi)</b>	<b>Any (w/ chemo)</b> <b>50% (mono)</b>	<b>1%</b> <i>(post-chemoRT for unresectable stage III)</i>	<b>50% (TC) or 10% (IC) (w/chemo + bev)</b>
	2 <sup>nd</sup> + line advanced	<b>Any (squamous)</b> <b>1% (adeno)</b>	1%	-	Any
<b>Urothelial</b>	1 <sup>st</sup> line advanced	-	<b>10% (TC + IC)</b> <i>(in cisplatin-ineligible)</i>	-	<b>5% (IC)</b> <i>(in cisplatin-ineligible)</i>
	2 <sup>nd</sup> + line advanced	<b>1%</b>	<b>Any</b>	<b>25% (TC + IC)</b>	<b>5% (IC)</b>
<b>HNSCC</b>	1 <sup>st</sup> line advanced	-	<b>1% (TC+IC)</b> <i>(w/ chemo)</i> <b>20% (TC+IC)</b> <i>(mono)</i>	-	-
	2 <sup>nd</sup> + line advanced	<b>Any</b>	<b>Any</b>	-	-

**Table 1.4. Overview of current IHC-based PD-L1 biomarker assays**

NSCLC = non-small cell lung cancer; HNSCC = head and neck squamous cell carcinoma; TC = tumour cell; IC = Immune cell; M = membranous; C = cytoplasmic; P = punctate; Ipi = ipilimumab; mono = monotherapy; bev = bevacizumab

TNM stage-matched tumours without MSI<sup>196</sup>. Computational analysis of mutations in protein-coding areas of the genome as detected by NGS have demonstrated a correlation between somatic mutation rate and higher number of predicted MHC-stabilising neoantigens in a number of tumour types<sup>197</sup>. More recently, a higher rate of response to immune checkpoint inhibitor therapy has been demonstrated in tumours with a greater somatic mutational burden<sup>198,199</sup>. Such observations, combined with prospective trial evidence of enhanced effect in tumours with DNA mismatch repair protein function, has led to the regulatory approval of anti-PD1 mAbs for the treatment of any solid tumour with demonstrated germline or somatic loss-of-function mutation of mismatch repair genes, loss of protein expression of the same genes and/or MSI<sup>200</sup>. These data highlight a mechanism of increased immune responsiveness that is shared across multiple different tumour types and underpins the first predictive biomarker for cancer immunotherapy that is not restricted by tumour type.

In the face of the diversity in factors that can impact upon the nature of tumour-immune responses, effort has been made to characterise recurrent patterns in immune characteristics that are seen to recur between individual patients with the same or different cancer types and exhibit association with differential clinical behaviour. While the large amount of ongoing research in this area means that concepts of contrasting types of tumour immune responses are likely to evolve rapidly, Chen and Mellman proposed three main categories of cancer-immune phenotypes (T-cell inflamed, immune-excluded and immune desert phenotypes) in a 2017 review that provides a useful framework<sup>171</sup>:

- T-cell inflamed tumours are characterised by the presence of heavy infiltration of tumour parenchyma by CD4+ and CD8+ T lymphocytes, often accompanied by myeloid and monocytic cells and in association with pro-inflammatory and immune effector cytokines. The presence of PD-L1 expression by infiltrating immune cells and/or tumour cells indicate pre-existing T-cell-mediated immune response that has since been attenuated by the developing tumour.
- Immune-excluded tumours contain abundant immune cells, including activated T cells, that are compartmentally restricted to areas of stroma that surround tumour cell nests. The absence of leucocytic infiltration of tumour parenchyma in such tumours suggests a potentially potent immune response that the cancer has rendered ineffective through physical obstruction.
- Tumours with an immune desert phenotype are typified by a paucity of T lymphocytes either in tumour parenchyma or surrounding stroma. While infiltrating myeloid cells may be present, the absence of a vigorous inflammatory response with associated lack of activated T cells reflects a tumour that has avoided provocation of a meaningful immune response.

These concepts have recently been further refined in a study that analysed integrated genomic, epigenomic, transcriptomic, histological and clinical data from over 10000 patients across 33 cancer types (30 non-haematological) studied as part of TCGA<sup>201</sup>. In this study reported by Thorssen *et al*, 5 immune expression signatures representing macrophages/monocytes, overall lymphocytic infiltration, TGF- $\beta$ , IFN- $\gamma$  response and wound healing were selected to perform unsupervised clustering analysis of gene expression data from tumours from all 30 solid tumour types. This identified six distinct 'Immune

Subtypes' that transcended tumour type and were associated with specific genomic and phenotypic features (summarised in **Table 1.5**). These immune subgroups reflect Chen and Melman's notion of contrasting immune phenotypes characterised by the presence or absence of tumour-infiltrating T lymphocytes with varying balance of Th1 or Th2 activated profiles and TCR diversity, alongside immunosuppressive M2-activated tumour-associated macrophages (TAMs) and association with genomic abnormality. Furthermore, enrichment of particular immune phenotypes in certain tumour types was demonstrated, indicating an interaction between lineage-specific factors and the qualitative nature of associated immune response. Specific driver mutations correlated with lower or higher leucocyte levels across all cancers, as did multiple molecular processes at transcriptional, SCNA and epigenetic level. Across all cancers, immune subtypes demonstrated contrasting prognostic associations when adjusted for cancer type. These findings demonstrate that there are recurrent patterns of anti-tumour immunity that retain consistent association with clinical behaviour across multiple cancer types. Further research is required to demonstrate the technical and biological replicability of these findings. The development of these recurrent immune phenotypes into clinically applicable prognostic and predictive biomarkers will require further investigation in prospective clinical studies, as well as optimising related assays for widespread adoption in routine practice.

Immune subtype	Wound healing (C1)	IFN $\gamma$ dominant (C2)	Inflammatory (C3)	Lymphocyte depleted (C4)	Immunologically quiet (C5)	TGF- $\beta$ dominant (C6)
% of cancers	29.9%	32%	29.7%	1.4%	4.8%	2.2%
Macrophage: lymphocyte	Balanced	Lowest	Balanced	High	Highest	High
Th1:Th2	Low	Lowest	High	Minimal CD4+ TIL	Minimal CD4+ TIL	Balanced
Tumour cell proliferation rate	High	High	Low to moderate	Moderate	Low	Moderate
Intra-tumoral genomic heterogeneity	High	Highest	Moderate	Low	Low	Moderate
Outcome association with higher neo-antigen burden	Improved PFI	Improved PFI	Worse PFI	Worse PFI	Worse PFI	Worse PFI
Other features	Elevated expression of angiogenic genes Dominant Th2 lymphocyte profile	Highest M1 proportion Strong CD8 signal High TCR diversity	Elevated Th17 and Th1 genes Low levels of aneuploidy and SCNA	Prominent macrophage signature Th1 suppressed High M2 response	Lowest lymphocyte and highest macrophage proportions response, M2 macrophages dominant	Highest TGF $\beta$ signature High lymphocytic infiltrate (balanced Th1:Th2)
Enriched in cancers (carcinoma unless otherwise stated)	Rectal Squamous Lung Luminal A Breast Squamous head & neck Gastrointestinal (genomic instability subtype)	Breast cancer (highly mutated subtype) Gastric Ovarian Squamous head & neck Cervical	Renal Prostate Pancreatic Papillary thyroid	Adrenocortical Pheochromocytoma Paraganglioma Hepatocellular Gliomas	Gliomas (accounted for 92.7% of immune subtype)	Mixed, no dominant tumour type
Overall association with OS	Less favourable	Less favourable	Most favourable	Least favourable	More favourable	Least favourable
% of included STS	24.9%	14.8%	16.3%	23.0%	0%	7.8%

**Table 1.5: Summary of cancer immune subtypes within >10000 tumours profiled by TCGA**

Based on data and analysis reported by Thorssen et al, wherein genomic data from >10000 cases across 30 solid tumour types collected by TCGA were analysed for common immune phenotypes. Data for 257 patients within TCGA-SARC subset is highlighted. NB 13.2% of TCGA-SARC patients were not assigned to an immune subtype. PFI = progression-free interval

## **1.5.2 The immune microenvironment of STS**

Characterisation of the immune microenvironment of STS has historically been lacking compared to more common solid tumour types. However, recent research efforts have produced data that, whilst limited in terms of quantity and consistency of findings, has contributed to an emerging picture of the quantitative and qualitative differences in immune factors between the microenvironments of individual STS tumours. Collectively, these findings support the existence of contrasting immune phenotypes across and within different STS subtypes in a manner that, in part, appears to associate with extent of genomic complexity. The role of these immune phenotypes in shaping disease biology has yet to be conclusively characterised, but available profiling data, in association with a limited body of clinical evidence from trials of various immunotherapeutic modalities, indicate that sustained translational research effort may yet provide clinically meaningful findings in terms of immune-based biomarkers and therapeutic targets.

### *1.5.2.1 IHC-based assessment of PD-L1 expression in STS*

Over the past 5 years, several studies have reported results of IHC-based profiling of the immune microenvironment in retrospective STS cohorts (**Table 1.6-1.8**). However, recurrent methodological limitations in terms of heterogeneity and size of studies cohorts and varying technical approaches have likely been major contributors to the failure of these studies to provide a consistent picture of the frequency and character of intra-tumoral immune responses and their association with clinical phenotype.

In response to demonstrated prognostic associations in other cancers and a putative role as a predictive biomarker for immune checkpoint therapies, a focus of these STS immune profiling studies has been to establish the extent of expression of PD-L1 in the STS microenvironment<sup>202–213</sup> (**Table 1.6**). These studies have variably included between 50 to 200 tumour samples, among which multiple different STS subtypes have been represented. Additionally, many such studies have also included bone sarcomas and sarcomas of prevalent incidence in childhood or adolescence, resulting in intra- and inter-cohort biological heterogeneity where insufficient numbers for any one subtype were available to power subtype-specific analyses. Further biological heterogeneity between

studies is represented by variable use of tumour sampled from either primary or recurrent disease in the context of varying disease extent and exposure to prior exposure to systemic and/or radiation therapy. Technical variation in methodologies between these studies adds to the challenges of comparing their results. In the absence of an established, standardised IHC assay for PD-L1 expression in STS, a range of different primary antibodies have been used by different studies, giving rise to concerns of the reproducibility and specificity of results. Some studies did not distinguish between PD-L1 expression on tumour cells or infiltrating leucocytes, thus overlooking potential biologically-important distinctions, while others reported only tumour cell staining. Scoring systems for PD-L1 staining vary between studies, as to cut-offs for defining PD-L1 positivity, with some applying permissively low cut-offs largely based on observations of clinically meaningful cut-offs in other cancer types, or have otherwise used semi-quantitative scoring systems that have then been investigated for optimised cut-offs that provide best distinction in terms of clinical outcome.

Meanwhile, the variable use of either whole sections or tumour microarrays (TMAs) indicates inconsistent risk of sampling error across studies. Given this diversity in terms of included tumour biology and methodological approach, it is unsurprising that reported rates of PD-L1 expression within specific STS subtypes have been widely variable between these studies, even when seemingly equivalent definitions of positive PD-L1 expression have been applied. Furthermore, reported associations of PD-L1 with clinical outcome have been inconsistent, with some studies finding a negative association with relapse- and/or survival-based in mixed STS cohorts, some finding such no association in similarly heterogeneous cohorts and yet others reporting improved survival associated with PD-L1 positivity in certain STS subtypes. Where reported, correlation of PD-L1 expression with heavier T cell infiltrates have been recurrently but inconsistently described, while association of higher histological grade and/or more advanced tumour stage with greater PD-L1 expression has only occasionally been demonstrated. If a clearer picture of the frequency and clinical relevance of PD-L1 expression as assessed by IHC is to be achieved for different STS subtypes, further study of larger cohorts are required, wherein heterogeneity of clinico-pathological variables should be

Study		Kim 2013 <sup>202</sup>	D'Angelo 2015 <sup>203</sup>	Movva 2015 <sup>206</sup>	Paydas 2016 <sup>207</sup>	Pollack 2017 <sup>208</sup>	Que 2017 <sup>209</sup>	Boxberg 2017 <sup>210</sup>	Patel 2018 <sup>211</sup>	Kostine 2018 <sup>212</sup>	Shurell 2016 <sup>213</sup>	Van Erp 2017 <sup>204</sup>	Honda 2017 <sup>205</sup>	
N		105	49	196	61	81	163	128	46	100	53	208	106	
Cohort factors	% of cohort	LMS	19%	8%	31%	15%	23%	6%	6%	7%	100%	0%	0%	0%
		UPS	10%	6%	5%	20%	25%	29%	45%	72%	0%	0%	0%	0%
		DDLPS	7%	6%	7%	7%	18%	14%*	0%	17%*	0%	0%	0%	0%
		SS	15%	10%	2%	6%	19%	13%	23%	0%	0%	0%	11%	0%
		MPNST	6%	2%	2%	6%	0%	6%	0%	0%	0%	100%	0%	0%
		AS	5%	8%	3%	0%	0%	3%	18%	0%	0%	0%	0%	100%
		MLPS	10%	0%	3%	2%	15%	NA*	0%	NA*	0%	0%	0%	0%
	Others	RMS: 8% Other: 20%	GIST: 29% Other: 31%	ChondroS: 8% Other: 39%	OsS: 16% EFT: 13% Other: 15%		FS: 18% ASPS: 3% Other: 10%	Other: 8%	Other: 4%			SS: 11%		
	Lesion	NR	100% Primary	NR	Varied	Varied	Primary	100% Primary	100% Primary	75% primary	72% Primary	100% Primary	Primary	
	Disease stage	Varied	64% localised	NR	Varied	Varied	Varied	93% localised	100% localised	Varied	Varied	90% localised	Localised	
	Treatment exposure	NR	Naïve	NR	Varied	Varied	Naïve	Naïve	Naïve	Varied	Varied	Varied	Naïve	
Technical factors	Material used	TMA	Whole section	Whole section	Whole Section	Whole section	Whole section	TMA	Whole section	Whole section	TMA	TMA	Whole section	
	PD-L1 primary antibody	R&D 130021	DAKO 22C3	R&D 130021	AM26531AF-N Acris	DAKO 22C3	Cell Signalling E1L3N	Ventana SP263	Cell Signalling E1L3N	NR	Spring BioScience M4420	Cell Signalling E1L3N	Spring BioScience SP142	
	PD-L1 positivity definition	Score >1 on semi- quantitative 0- 12 scale	>1% tumour cells	>5% tumour cells	Any staining	Score >2 on semi- quantitative 0- 5 scale	>1% tumour cells	>1% tumour cells	>1% tumour cells	>1% tumour cells	>1% tumour cells	>10% tumour cells	>5% tumour cells	
Results	% PD-L1 positive	LMS	70%	0%	32%	11%	59%	22%	11%	10%	32%	NA	NA	NA
		UPS	82%	50%	70%	50%	80%	15%	40%	67%	NA	NA	NA	NA
		DDLPS	67%	0%	82%	0%	17%	0%*	NA	24%*	NA	NA	NA	NA
		SS	75%	0%	25%	25%	53%	5%	7%	NA	NA	NA	0%	NA
		MPNST	50%	0%	67%	25%	NA	11%	NA	NA	NA	17%	NA	NA
		AS	60%	0%	57%	NA	NA	20%	35%	NA	NA	NA	NA	32%
		MLPS	30%	NA	100%	0%	73%	NA	NA	NA	NA	NA	NA	NA
	Others	RMS 75% Other: 43%	GIST: 29% Other: 13%	ChondroS: 75% Other: 63%	OsS: 20% EFT: 13% Other: 10%		FS: 7% ASPS: 20% Other: 25%	Other: 20%	Other: 0%			RMS: 12% EFT: 5% SS: 0%		
	Prognostic association of tumour PD-L1 positivity	Worse OS	Nil	NR	NR	Worse DFS, OS	Worse OS	Better OS in UPS subgroup	Nil	Nil	Nil	Better MFS, OS in aRMS subgroup	Nil	
	Correlates with tumour PD- L1 positivity	Tumour stage and grade	CD8 TIL density	NR	NR	Tumour grade T cell clonality	Tumour size, grade, FOXP3 TIL density	CD3 and CD8 TIL density	No correlation with stage or grade	Tumour grade	No difference between primary and mets	Male gender No correlation with CD8 TIL	No association with tumour stage	

**Table 1.6: Summary of histopathology-based studies profiling tumour PD-L1 expression in STS**

\* Liposarcoma subtypes not specified within included liposarcoma subgroup. RMS=rhabdomyosarcoma, ChondroS=chondrosarcoma, OsS=Osteosarcoma, FS=fibrosarcoma

minimised and where transparent and rational technical approaches for quantifying PLD1 expression are employed.

#### *1.5.2.2 IHC-based assessment of TILs and other immune factors in STS*

In addition to PD-L1 expression, a smaller number of studies have reported data on the extent of T lymphocyte infiltration of the STS microenvironment (**Table 1.7**). As is the case in PD-L1-focussed studies, significant inconsistencies in terms of the composition of cohorts studied and TIL assessment methodologies have likely contributed to inconsistent findings relating to the frequency of heavy TIL infiltration, correlation with clinico-pathological or other immune factors, and any association with clinical outcome.

Data on IDO expression in STS is limited. In a meeting presentation in 2016, Toulmonde *et al* reported results of IHC-based immune profiling of 371 archival STS tumours, finding that tumour cell expression of PD-L1 or IDO was not significantly associated with differential survival outcomes, although the presence of kynurenine (a tryptophan metabolite produced by IDO enzymatic activity) in the tumour was an independent marker of favourable OS<sup>214</sup>. Examination of pre-treatment tumour tissue from a subset of patients treated in a prospective phase II immunotherapy study performed by the same collaboration demonstrated IDO1 expression was present in 69%, 73%, 29% and 63% of LMS, UPS, GIST and other subtypes respectively, and was largely restricted to infiltrating macrophages<sup>215</sup>. Meanwhile, the expression and potential biological relevance of other T cell inhibitory receptors such as TIM3, LAG3 and VTCN1 or T cell costimulatory proteins such as CD137 in STS has yet to be explored. As is the case with IHC-based assessment of PD-L1 in STS, further studies are required in order to establish a consistent picture of the role played by TIL and other immune factors in different STS subtypes. The success of such studies will depend on the use of rationalised methodologies applied to sufficiently powered, subtype-specific cohorts that are controlled for heterogeneity in variables including treatment exposure and disease stage.

	Study	D'Angelo 2015 <sup>203</sup>	Shurell 2016 <sup>213</sup>	Sorbye 2011 <sup>216</sup>	Boxberg 2017 <sup>210</sup>	Van Erp 2017 <sup>204</sup>	Kostine 2018 <sup>212</sup>
	N	49	53	249	128	208	100
<b>Cohort factors</b>	<b>% of cohort</b>						
	LMS	8%	0%	27%	6%	0%	100%
	UPS	6%	0%	27%	45%	0%	0%
	DDLPS	6%	0%	14%*	0%	0%	0%
	SS	10%	0%	4%	23%	11%	0%
	MPNST	2%	100%	4%	0%	0%	0%
	AS	8%	0%	5%	18%	0%	0%
	MLPS	0%	0%	NA*	0%	0%	0%
	Others	GIST: 29% Other: 31%		MFS: 8% RMS: 6% Other: 4%	Other: 8%	RMS: 47% EFT: 21% OsS: 22%	
	Lesion	100% Primary	72% Primary	100% Primary	100% Primary	100% Primary	75% primary
	Disease stage	64% localised	Varied	84% localised	93% localised	90% localised	Varied
	Treatment exposure	Naïve	Varied	Naïve	Naïve	Varied	Varied
<b>Technical factors</b>	Material used	Whole section	TMA	TMA	TMA	TMA	Whole section
	T cell markers	CD3, CD4, CD8	CD8	CD4, CD8	CD3, CD8	CD8	CD3
	High/low TIL cutoff	>5% total cell fraction	>5% total cell fraction	>6 TIL per 0.6mm core	>15% total cell fraction	>10% total cell fraction	>5 cells/HPF (x250)
<b>Results</b>	<b>% High TILs</b>						
	LMS	0%	NA	NR	NR	NA	54%
	UPS	100%	NA	NR	33%	NA	NA
	DDLPS	50%	NA	NR	NR	NA	NA
	SS	20%	NA	NR	NR	41%	NA
	MPNST	100%	21%	NR	NR	NA	NA
	AS	100%	NA	NR	NR	NA	NA
MLPS	NA%	NA	NR	NR	NA	NA	
	Others	GIST: 64% Other: 10%		Overall: 20%	NR	RMS: 29% EFT: 42% OsS: 33%	
	Prognostic association of high TILs	Worse OS	Nil	Worse DSS	Better DFS, OS	Worse MFS in SS	Nil
	Correlates with high TILs	Tumour PD-L1 Leucocyte PD-L1 Tumour size Mets present	No correlation with disease stage	NR	Lower disease stage	No correlation with tumour PD-L1 expression	Higher tumour grade

**Table 1.7: Summary of histopathology-based studies profiling lymphocyte infiltration in STS**

\* Liposarcoma subtypes not specified within included liposarcoma subgroup. EFT=Ewing family tumours

### 1.5.2.3 IHC-based assessment of TAM in STS

A more consistent picture regarding the potential clinical relevance of TAMs in the STS immune microenvironment has been provided by IHC-based profiling studies that, in some cases, have focussed on particular STS subtypes (**Table 1.8**). Macrophages are myeloid-derived cells of the innate immune system that play a number of crucial roles in mediating adaptive immune responses, including antigen presentation and influencing immune fate through paracrine and endocrine mechanisms. The biological and clinical relevance of TAMs remains to be definitively characterised in many cancer types, reflecting the complex and dynamic nature of macrophage function. It is recognised that macrophages demonstrate functional plasticity within the tumour micro-environment and, depending on an immune contexture that may be influenced by a range of tumour and host factors, may differentiate into either antitumorigenic, proinflammatory M1 or pro-tumorigenic, anti-inflammatory M2 functional states<sup>217,218</sup>. In a 2008 study, transcriptome-level, microarray-based gene expression analysis of fresh frozen tumour samples from 51 STS representing 7 histological subtypes found that variable overexpression of macrophage-associated genes was seen in LMS but no other included subtype<sup>219</sup>. Immunostaining for CD68 and CD163 (respective putative markers of global and M2 macrophage populations) was then performed on a TMA containing FFPE tumour material from 149 primary LMS and demonstrated moderate (>5 staining cells per 0.6mm TMA core) or dense (>25 cells per core) CD68+ or CD163+ macrophage infiltrates in 67% and 88% of tumours respectively. Analysis of disease-specific survival (DSS) of the cohort when stratified by macrophage density demonstrated significantly worse outcomes in non-gynaecological LMS that were more heavily infiltrated by CD68+ or CD163+ cells. No significant difference in outcomes in association with macrophage density was seen in the gynaecological LMS subgroup. A follow-up study of the same LMS cohort showed that co-ordinate tumour expression of CSF1, a major biological chemoattractant for macrophages, along with expression in the microenvironment of three genes within a CSF1 response gene set, identified LMS with worse DSS regardless of gynaecological or non-gynaecological origin<sup>220</sup>.

Study		D'Angelo 2015 <sup>203</sup>	Ganjoo 2011 <sup>35</sup>	Lee 2008 <sup>219</sup>	Kostine 2018 <sup>212</sup>	Nabeshima 2015 <sup>221</sup>
N		49	52	245	100	78
Cohort factors	% of cohort					
	LMS	8%	100% (36% Gyne)	100% (51% Gyne)	100% (6% Gyne)	0%
	UPS	6%	0%	0%	0%	0%
	DDLPS	6%	0%	0%	0%	0%
	SS	10%	0%	0%	0%	0%
MPNST	2%	0%	0%	0%	0%	
AS	8%	0%	0%	0%	0%	
MLPS	0%	0%	0%	0%	100%	
Others	GIST: 29% Other: 31%	0%	0%	0%	0%	
Lesion	100% Primary	100% Primary	100% Primary	75% Primary	100% Primary	
Disease stage	64% localised,	72% localised	NR	Varied	72% localised	
Treatment exposure	Naïve	Naïve	Naïve	Varied	Naïve	
Technical factors	Material used	Whole section	TMA	TMA	Whole section	Whole section
	TAM markers	Morphology alone	CD163, CD16, CTSL	CD68, CD163	CD163	CD68, CD163
	High/low TAM cutoff	Any TAM present	>45 cells/HPF	>25 cells/0.6mm core	>20% Total cell fraction	>100 cells/10HPF
Results	% High TAMs					
	LMS	75%	51%	26% (Gyn - 19%, Non-Gyn 35%)	61%	NA
	UPS	75%	NA	NA	NA	NA
	DDLPS	50%	NA	NA	NA	NA
	SS	20%	NA	NA	NA	NA
	MPNST	100%	NA	NA	NA	NA
	AS	100%	NA	NA	NA	NA
	MLPS	NA%	NA	NA	NA	19%
	Others	GIST: 93% Other: 94%	NA	NA	NA	NA
	Prognostic association of high TAMs	Nil	Worse OS in Gyn LMS Nil in non-gyn LMS	Nil in Gyn LMS Worse OS in non-gyn LMS	Worse OS and DSS	Worse OS
Correlates with high TAMs	NR	NR	NR	Higher tumour grade	NR	

Table 1.8: Summary of histopathology-based studies profiling macrophage infiltration in STS

These findings were subjected to validation in an independent LMS cohort wherein expression levels of CD163 as well as CD16 and cathepsin L1 proteinase (CTSL) (both of which were in the CSF1 response gene set) were assessed by IHC<sup>35</sup>. Here, increased numbers of CD163+ cells were associated with only a non-significant trend toward worse DSS, while increased levels of CD16 or CTSL were associated with significantly worse outcome in gynaecological LMS only. High levels of all three markers were the strongest identifier of poor DSS in gynaecological LMS. No individual or combination of markers was associated with significantly differential outcome in non-gynaecological LMS – the authors highlighted that the smaller validation cohort was potentially underpowered to detect a macrophage effect that, in earlier studies, had been shown to be smaller in non-gynaecological LMS compared to gynae LMS. The findings of this series of studies are broadly consistent with those from a more recent investigation of immune cell infiltrates in a series of 100LMS of predominantly non-gynaecological origin<sup>212</sup>. Here, as demonstrated by IHC analysis, the authors reported high levels of CD163-positive infiltrates in 61% of cases, with significantly worse OS and DSS (but not DFS) seen in this subgroup.

Taken together, the data from these studies contribute to an emerging picture of TAMs playing an important role in the immune microenvironment of a significant proportion of LMS, wherein the presence of alternatively activated M2 macrophages may reflect an immunosuppressed TME that promotes tumour aggressiveness and immune escape. Accordingly, the therapeutic depletion or manipulation of TAM responses is an area of active clinical investigation in LMS and other STS subtypes. TAM-targeted therapies that are currently under phase I clinical study include PLX3397, a multitargeted kinase inhibitor with selective activity against CSF1R and KIT that, when used to treat mice bearing MPNST xenografts, has been shown to deplete tumour-infiltrating macrophages and suppress tumour growth<sup>222</sup>, anti-CD47 mAbs that have been shown *in vivo* and *in vitro* to promote anti-tumour functional activation of macrophages (NCT02216409)<sup>223</sup> and pharmaceutical agonists of toll-like receptor 4 (TLR4), an activating receptor expressed by innate immune cells including macrophages (NCT02180698). Meanwhile, cytotoxicity against TAMs has been shown to be a key component of trabectedin's antitumor activity when used to treat sarcoma-

bearing mice, while levels of circulating and tumour-infiltrating macrophages have been shown to reduce with trabectedin treatment in patients with LMS<sup>224</sup>. The potential for an immunomodulatory component of trabectedin's activity in LMS has informed currently recruiting studies investigating the combination of trabectedin with immune checkpoint therapy (NCT03085225, NCT03138161, NCT03590210). Further studies that clarify the precise interaction of TAM effect with anatomical origin of LMS while developing more precise markers of TAM numbers and functional state will provide correlative data that may inform the search for biomarkers of effect of TAM-targeting therapies.

Little histology-based data on macrophage infiltrates in other STS subtypes is available. In a study of 49 STS samples, encompassing 21 different subtypes (8% LMS), macrophage infiltrates were assessed by morphology alone, with positivity defined by the presence of any detected TAM<sup>203</sup>. TAMs were present in a high proportion of tumours from most included subtypes, with no association with clinical outcome seen – the low specificity and stringency of TAM positivity used in this study limit the conclusions that can be drawn from this data regarding any biological importance of TAM in STS outside of LMS. Evidence for the potential importance of TAM in MLPS, an LPS subtype characterised by a recurrent gene fusion with a known driver role via epigenetic dysregulation, was provided by a study of a retrospective FFPE tumour cohort of 78 cases<sup>221</sup>. Using a cut-off threshold comparable to studies in LMS, high levels of CD68+ infiltrates were seen in 19% of tumours and were associated with worse OS, as was high levels of infiltrating cells with co-expression of CD68 and CD163 as assessed by double fluorescence IHC. Meanwhile, histological examination for TAM in pre-treatment tissue was performed for a subset of 49 patients treated within a prospective phase II study of pembrolizumab delivered in combination with metronomic low dose oral cyclophosphamide (LDOC), a cytotoxic regimen believed to provoke anti-tumour immune modulation through depletion of Treg<sup>215,225</sup>. In this heterogeneous cohort that included LMS, GIST, UPS and small numbers of several other STS subtypes, an overall predominance of M2 over M1 macrophages was detected, as evidenced by IHC-based ratios of CD163+ and CD68+ cells. The highest rate of raised CD163:CD68 ratio was seen in UPS (73%), compared to 31% of LMS, 38% of GIST and 46% of the mixed 'other' subtypes. Collectively, these studies indicate that instances of macrophage

infiltration are not limited to LMS but rather are seen across multiple STS subtypes and may reflect a similar association with worse clinical outcome. However, the frequency and functional characteristics of TAMs outside of LMS are currently not well established and it has yet to be seen if M2 macrophage-mediated immunosuppression within the TME plays a significant role in shaping the clinical behaviour of different STS subtypes. As is the case for other immune markers in STS, further, well-designed profiling studies are required to address this shortfall in knowledge.

#### *1.5.2.4 Gene expression-based profiling of the STS immune microenvironment*

The challenges in terms of specificity and reproducibility of IHC-based appraisal of immune microenvironment factors has led to the use of alternative methods including assessment of immune gene expression as reflected by mRNA levels. mRNA analysis of narrow, targeted repertoires of genes through use of in-situ hybridisation or qPCR techniques or by multiplexed, transcriptome-level approaches such as cDNA-based microarrays or RNA-Seq allows parallel analysis of up to thousands of genes and produces data that, with appropriate pre-processing, are often more directly comparable between studies than IHC-based protein-level data. The potentially large number of differentially expressed genes that may be identified by such studies can be bioinformatically assessed for ontologies associated with specific functional processes, allowing for interrogation for the presence or absence of specific immune processes. Typically, mRNA is collected through processing of whole tumour sections, leading to loss of spatial resolution in terms of identifying in which areas and cell type of the TME expression is seen. This limitation can be partly overcome through the application of modern computational approaches such as CIBERSORT to interrogate transcriptome-level data derived from complex tissues in order to infer the cell composition, including immune cell subpopulations, within tumour samples<sup>226</sup>.

Complementing and adding to reported IHC-based profiling data, focussed analyses of publicly available STS genomic datasets have consistently reported that PD-L1 gene expression levels are higher in UPS and LMS when compared to LPS or SS, with expression levels shown to correlate with levels of genomic complexity and CINSARC score, as well as co-expression with genes involved in

T cell response<sup>2,4,210,227,228</sup>. *CD274* (the gene encoding PD-L1) copy number gain has been reported in approximately 20% of STS, most frequently in UPS, and has been associated with higher PD-L1 expression at mRNA and protein level<sup>210,227,228</sup>. Both PD-L1 copy number gain and overexpression have been linked with worse clinical outcome in these studies. Meanwhile, in a study reported by Pollack *et al*, the immune microenvironment of FFPE tumour specimen from 81 STS (25% UPS, 23% LMS, 19% SS, 18% WD/DDLPS, 15% MLPS) was assessed using NanoString-based expression analysis of 760 immune-related genes in conjunction with IHC for PD1 and PD-L1 and TCR gene sequencing<sup>208</sup>. Unsupervised clustering analysis using genes shown to be differentially expressed between at least two different subtypes identified that UPS and LMS tumours were enriched for expression of genes belonging to antigen presentation and T cell-related functional ontology groups. WD/DDLPS were also shown to have increased expression of these genes compared to SS or MRCL, both of which showed low levels of immune gene expression. Both UPS and LMS also exhibited greater levels of T cell clonality, a marker of expansion of specific T cell subpopulations in response to TCR recognition of cognate antigen-complexes and costimulatory ligands on the surface of antigen-presenting cells which, in the context of the tumour microenvironment, may indicate the presence of an effective anti-tumour T cell response. TCR clonality score correlated with expression of genes related to T cell function and antigen presentation as well as PD1 and PD-L1 expression as assessed by IHC, further suggesting the presence of a T cell-mediated anti-tumour immune response that may have been abrogated by tumour-mediated induction of immune checkpoint expression. These studies together indicate that PD-L1 expression is present in a substantial minority of STS in a manner that is associated with broader evidence of T lymphocyte-mediated anti-tumour immune response and that may more commonly occur in STS that harbour a greater degree of genomic complexity.

Two recently published studies have provided broader insight into the immune microenvironment of certain STS subtypes through analysis of TCGA RNA-Seq gene expression data derived from 257 patients with either genomically complex STS (UPS/MFS, LMS, DDLPS or MPNST) or SS, a genomically simple STS subtype. In the initial report of multi-omic profiling of this cohort (as discussed in

**section 1.2.3**), immune cell-related gene signature scores were assigned to each sarcoma type<sup>4</sup>. Individual tumours that had high or low immune infiltration scores generally demonstrated co-ordinate increase or decrease in expression of multiple immune cell types, rather than changes in isolated cell types, potentially reflecting a relatively narrow qualitative range in the character of detected immune responses. Unsupervised clustering using expression levels of immune-related genes identified a cluster of tumours that accounted for approximately one third of all cases and in which higher expression levels of multiple immune cell signatures were upregulated. Within this subgroup, all 5 genomically complex subtypes were represented in approximately equal proportion. Meanwhile, all cases of SS exhibited low expression scores for most immune cell subtypes. UPS/MFS and DDLPS had the highest macrophage scores, while DDLPS had the highest CD8 T cell score and soft tissue LMS the highest PD-L1 score. When assessing for associations of immune infiltrations scores with DSS both across and within the studied STS subtypes, the authors reported that only low NKC score was associated with worse outcome across multiple subtypes (uLMS, STLMS and UPS), potentially reflecting the recognised role of NKC-mediated cytotoxicity in tumour immunosurveillance and immunoediting<sup>229</sup>. In UPS/MFS, increased levels of DC were associated with better outcome, suggesting a central role of effective antigen presentation in immune responses against these genomically complex tumours. In LMS, high levels of CD8 immune signature expression was associated with better DSS in uLMS but not STLMS, a finding consistent with IHC-based data that indicate biologically relevant differences in immune responses in LMS originating in different anatomical sites (see **section 1.5.2.3** and **Table 1.8**). In DDLPS, higher Th2 response score was associated with worse DSS. This finding suggests a possible role in DDLPS for Th2-dominant immune responses in promoting tumour growth while inhibiting cell-mediated cytotoxicity, as has been described in a number of other cancer types<sup>230</sup>. Assessment of immune checkpoint expression identified the highest levels of PD-L1 in non-gynaecological LMS followed by MFS/UPS, while expression of TIM3 was highest in UPS and DDLPS, a finding in keeping with studies discussed above that suggest upregulation of immune checkpoints may be a mechanism of immune escape in genomically complex STS that have provoked lymphocyte-mediated immunity. Of note, in this study, the genomically simple subtype SS exhibited low scores across all immune cell counts.

Interestingly, expression of PD1 was highest in this subtype, which, in the context of otherwise low scores for infiltrating lymphocytes, suggest that any present T cells within SS may be functionally attenuated via engagement of immune checkpoint pathways.

In their analysis that identified six distinct gene expression-defined immune phenotypes within 33 different solid tumour types included in TCGA datasets (see section 1.5.1.4), Thorsson et al found that the 257 included cases of STS were assigned across five of the six described immune subtypes (**Table 1.5**)<sup>201</sup>. No STS were assigned to the immunologically quiet subgroup, which accounted for 4.8% of the pan-cancer cohort, a proportion almost entirely consisting of gliomas. 25% of STS were identified in the wound healing subtype that was characterised by a dominant Th2 lymphocyte signal, suggesting that in approximately one quarter of studied STS possess immune microenvironments wherein tumour survival and progression may be supported by a Th2-dominant response. 15% of STS were assigned to the IFN $\gamma$ -dominant subtype, characterised by a high proportion of M1 macrophages, strong CD8 lymphocyte-related signal and low TCR clonality. This finding suggests that, as has been demonstrated by other IHC and gene expression-based immune profiling studies in STS, a non-trivial proportion of STS contain evidence of significant infiltration by cytotoxic T cells and pro-inflammatory, pro-immunity macrophages. However, the heightened degree of TCR diversity in this immune subtype could potentially point toward a generic proinflammatory state wherein there are few of the high avidity TCR-antigen-MHC interactions that provoke T cell clonal expansion and effective antigen-specific anti-tumour response. A further 16% of STS demonstrated the inflammatory phenotype characterised by dominant pro-inflammatory Th17 and Th1 signals and a lower degree of TCR diversity than the IFN $\gamma$ -dominant subtype, potentially indicating that it is this proportion of STS that more effective anti-tumour immune responses may be encountered. The proportion of STS assigned to either IFN $\gamma$ -dominant or inflammatory immune subtypes was approximately half that seen in the pan-cancer cohort, an observation consistent with other data that indicates that STS are not among the most heavily immune infiltrated cancer types. Consistent with this was the finding that STS were comparatively overrepresented in the lymphocyte depleted subtype (23% vs 1.4% in the pan-cancer cohort), typified by a M2-predominant macrophage signal and low

lymphocyte signal that indicate an immunosuppressed and tumour microenvironment. Finally, 7.8% of STS were identified in the TGF- $\beta$ -dominant subgroup that was characterised by a high lymphocytic signal that was balanced between Th1 and Th2 functional subtypes and a prominent TGF- $\beta$  pathway upregulation, a factor that has been associated with a pro-tumorigenic roles including suppression of T-cell mediated anticancer immunity<sup>231,232</sup>.

Among the 30 assessed cancer types, STS demonstrated an intermediate value for median lymphocytic fraction (calculated through computational deconvolution of cell-specific signatures for 22 immune cell types), similar to that of hepatocellular carcinoma and cervical cancer, but approximately 50-66% that of NSCLC, head and neck carcinomas and melanoma, all cancer types associated with favourable response rates to checkpoint inhibitor therapy. However, the STS cohort exhibited one of the broadest ranges of lymphocyte fraction values, suggesting that a proportion of included STS possessed a lymphocytic infiltrate of comparable magnitude to these immune-active cancers.

Thorsson *et al* did not report STS subtype-specific assignment to immune subgroups, nor provided any specific analysis of association of immune subtype with survival in STS. Regardless, this and the earlier analysis of the TCGA-SARC dataset indicate a diversity in the character of immune responses both within and across the 5 studied genomically complex STS subtypes, and that the effect of specific immune phenotype on clinical outcome may vary between different STS subtypes. These findings require validation in independent STS cohorts, wherein any observation of statistically-significant association between immune phenotype with differential clinical outcome would provide further evidence of the biological and clinical relevance of the immune microenvironment in STS. Such observations could potentially guide efforts to identify biomarkers that can identify patients with STS whose pre-existing but attenuated anti-tumour immune responses might feasibly be reinvigorated to therapeutic effect by immune checkpoint inhibitors, while identifying patient subgroups where research might focus on immunomodulation of 'immune-silent' tumours. Translational investigation within prospective trials of immunotherapy in STS patients is required to assess to what extent the observed variation in immune phenotype is associated with differential therapeutic response. Meanwhile, the ready availability of IHC-based assessment within routine practice should motivate

efforts in the pursuit of manageable repertoires of protein markers that can reproducibly resolve and represent more complex gene expression-based signatures.

### **1.5.3 Immune characteristics of LMS, UPS and DDLPS**

#### *LMS*

Immune profiling studies in STS have indicated that LMS is among the subtypes that most commonly exhibit evidence of an active immune response within the TME. Assessment of immune-related gene expression in STS cohorts has demonstrated that LMS have higher expression of PD-L1 and genes related to antigen presentation and T cell response than most other studied STS subtypes<sup>208</sup>. In addition, a biologically-relevant role of TAM in LMS is indicated by consistent reports of an association between high levels of infiltrating M2 macrophages and worse clinical outcome<sup>35,212,219</sup>. It is possible that such data reflect a process wherein the antitumour potency of infiltrating cytotoxic T lymphocytes is attenuated by immunosuppressive macrophage-mediated immune evasion mechanisms.

LMS is among subtypes included in the limited amount of reported clinical trial data on the efficacy of immune checkpoint inhibitor therapy in advanced STS. Among the patients treated in the initial phase I study of the anti-PD1 mAb pembrolizumab was a single case of LMS that exhibited ongoing disease stabilisation at 35 weeks of follow-up and sub-RECIST tumour shrinkage at a number of metastatic sites<sup>233</sup>. Furthermore, in a case study of a single patient with metastatic uLMS treated with pembrolizumab, a dramatic response which endured for over 2 years was seen in all but one disease sites<sup>234</sup>. However, prospective studies that have treated series of patients with LMS have indicated that clear evidence of benefit from checkpoint inhibitor therapy occurs in only a small minority of LMS. A single-arm phase II study of nivolumab, another anti-PD1 mAb, in uLMS was closed at first interim efficacy analysis after none of the first 12 patients showed evidence of tumour response or stabilisation with treatment<sup>235</sup>. Similarly, in 15 patients with LMS treated in a single-arm phase III study of pembrolizumab combined with low-dose cyclophosphamide in advanced STS, no incidences of tumour shrinkage and a median PFS of 1.4 months were seen<sup>215</sup>. In the SARC028 single-arm phase II study of pembrolizumab in

advanced STS, a total of 10 patients with LMS were evaluable for treatment response<sup>236</sup>. Best objective response was stable disease and progression in 6/10 and 4/10 of patients respectively. Similarly, in a single centre case series of patients with advanced STS treated with various immunotherapy modalities at MD Anderson, a best response of stable disease was seen in 2/12 (17%) of patients with LMS treated with immune checkpoint inhibitors<sup>237</sup>. Marginally more encouraging are the results from a randomised phase II where 85 patients with advanced STS, including 29 with LMS, were treated with nivolumab alone or in combination with the anti-CTLA4 mAb ipilimumab<sup>238</sup>. Objective response was seen in 8/85 patients across the two treatment arms, of which 3/8 had LMS (LMS ORR 10%) – one of these patients received nivolumab monotherapy with the other two receiving combination nivolumab-ipilimumab.

### *UPS*

In immune profiling studies, UPS has been shown with some consistency to be the STS subtype that most frequently exhibits evidence of an immune response within the TME (**Table 1.6 and 1.7**). Expression of PD-L1 as evidenced by IHC or gene expression studies has typically been higher in UPS than other subtypes, with greater levels of lymphocyte infiltration, T cell oligoclonality and pro-inflammatory gene signatures also shown<sup>4,201,208</sup>. Consistent with this evidence of spontaneous immune responses, UPS is the STS subtype currently associated with the most encouraging results in reported trial data for immune checkpoint inhibitors. In the SARC028 trial, objective tumour response to pembrolizumab was seen in 4/10 UPS patients<sup>239</sup>. In this study, tumour expression of PD-L1 (defined as positive staining in >1% tumour cells) was seen in only 3 of 70 evaluable patients (total number enrolled =86), with only 2/3 evaluable for treatment response – both of these tumours were UPS that responded to anti-PD1 therapy. In a randomised study of nivolumab with or without ipilimumab combination in advanced STS, objective tumour response was seen in 3/11 UPS patients, all of whom had received combination therapy<sup>238</sup>. Tumour expression of PD-L1 has not been reported for this study. In contrast, combined pembrolizumab and LDOC demonstrated little evidence of activity in UPS in a phase II study<sup>215</sup>. Best response in 12 evaluable patients with UPS was stable disease in 5 (42%) and progressive in 7 (58%), with associated median PFS and OS of 1.4 months

and 5.6 months respectively. PD-L1 expression in >1% of tumour cells was detected in only 1 case of UPS.

### *DDLPS*

DDLPS has had limited representation in reported immune profiling studies in STS, with several such studies having not discriminated between the biologically distinct LPS subtypes. In the small number of DDLPS studied, high TIL numbers have been reported in a proportion of cases. In a small cohort of fresh surgical resections of eight retroperitoneal LPS, flow cytometric assessment identified substantial populations of TIL in all studied cases, with CD4+ populations predominant<sup>240</sup>. Assessment of FFPE sections identified intratumoral tertiary lymphoid structures in 5 out of 10 retroperitoneal DDLPS – presence of TILS was associated with worse OS. IHC-based immune profiling studies have reported widely varying expression levels of PD-L1 in DDLPS, likely reflecting methodological variation and small sample numbers (**Table 1.6**).

A limited number of objective responses to immune checkpoint inhibitor therapy have been reported among reported clinical trial data that have included patients with DDLPS. In the SARC028 study, 2/10 DDLPS treated with pembrolizumab met partial disease response criteria<sup>239</sup>. 0/2 patients with DDLPS, neither of which exhibited tumour cell expression of PD-L1, exhibited objective response to combined nivolumab and oral cyclophosphamide in a prospective phase II study<sup>215</sup>. In a review of patients with advanced STS treated with immunotherapies at MD Anderson, 2/5 patients with DDLPS had best response of stable disease to anti-PD1 or anti-PD-L1 therapy, with the remaining 3/5 having progression as best response<sup>237</sup>.

#### ***1.5.4 Clinical investigation of immunotherapy in STS***

Given the urgent unmet need for effective new systemic therapies for STS and the translational evidence of potentially biological meaningful immune infiltrates within the microenvironment of some STS, it has been hoped that the practice-changing success development of immune checkpoint inhibitors seen in other cancer types might be replicated in STS. The earliest reported data of immune checkpoint therapy in STS was from a small pilot study in SS, in which six patients with advanced disease with demonstrated expression of the cancer-testis antigen NY-ESO-1 (see below) were treated with 1-3 cycles of ipilimumab<sup>241</sup>. All 6

patients progressed on treatment, leading to early closure of the study. Drugs that target the PD1/PD-L1 axis are being actively investigated in STS, either as monotherapy or in combination with other immune checkpoint-targeting drugs, other immunomodulatory modalities, chemotherapy or small molecule inhibitors. Reported clinical trial data so far has however indicated rates of objective tumour response to anti-PD1 inhibitor monotherapy is low in general STS populations and may be predominantly limited to subtypes typified by higher levels of genomic complexity, in keeping with evidence of pre-existing immune responses in these subtypes provided by immune profiling studies (**Tables 1.6-1.8**) (see **section 1.5.3** for subtype-specific data of checkpoint inhibitor efficacy in LMS, UPS and DDLPS). However, reports of clinically meaningful tumour shrinkage in individual cases of alveolar soft part tumour, a rare STS subtype characterised by a canonical gene fusion and in which the limited available profiling data indicate an absence of immune infiltrates or PD-L1 expression, suggest that the putative relationship between genomic complexity and effectiveness of immune checkpoint inhibitors may inadequately predict in which STS subtypes such agents may be active<sup>237,242-244</sup>. These available data have so far not provided a clear impression of any potential association between PD-L1 expression in the STS immune microenvironment and response to immune checkpoint inhibitor therapy. Clinical trial evidence specific to three of these more genomically complex subtypes (UPS, LMS and DDLPS) are discussed in greater detail in later chapters. More clinical trial evidence is required to confidently establish the activity of immune checkpoint inhibitor therapy in STS. Meanwhile, ongoing and future translational research in conjunction with clinical investigation is needed to better understand the tumour and immune biology that dictates sensitivity or resistance to immunotherapy and to identify candidate predictive biomarkers.

Current understanding reflects that responses to immune checkpoint inhibitor therapy are mediated by cytotoxic T cell recognition of largely non-recurrent tumour antigens that result stochastically from somatic mutation. In contrast, certain STS subtypes have been shown to frequently express recurrent tumour-specific proteins that could provide the basis for antigen-directed immune responses. Cancer-testis antigens (CTA) are a group of over 40 identified proteins whose physiological expression is limited to embryological tissues but whose aberrant expression has been demonstrated in a range of cancers. NY-

ESO-1 is a CTA that has been shown to be expressed in a large proportion of SS and MLPS and has been the focus of research that aims to generate antigen-directed anti-tumour immunity<sup>245,246</sup>. The production of clinical grade, autologous NY-ESO-1-specific T cells has been shown to be feasible through the ex vivo selection and expansion of antigen-specific populations from PBMC isolated from sarcoma patients<sup>247</sup>. The use of this approach for adoptive T cell therapy is under clinical investigation in phase I studies recruiting patients with SS or MLPS<sup>248,249</sup>. An alternative strategy for adoptive cell therapy involves the genetic modification of autologous T cells to express TCR with enhanced affinity binding to MHC-bound, NY-ESO-1-derived antigens. This approach has been associated with rates of objective tumour response over 50% in the treatment of small, early phase trial cohorts of patients with NY-ESO-1-expressing SS<sup>250,251</sup>. Further efficacy and safety are awaited for this promising therapeutic approach, although wider clinical adoption will be challenging in face of the high technical demands and expense of such therapies. Meanwhile, tumour vaccine studies have variably aimed to target CTA or potentially antigenic peptides derived from tumour-specific gene fusion products<sup>252</sup>. Immunologic correlates examined in these studies have indicated instances of successful antigen-directed engagement of host immunity but have produced little evidence that this has translated into meaningful antitumor activity<sup>253</sup>.

			LMS	UPS	DDLPS
<b>Response rates in anti-PD1 clinical trials</b>			0-10%	0-40%	0-20%
<b>PD-L1</b>	<b>IHC</b>	% with expression	0-70%	15-82%	0-82%
		Prognostic association	?nil	?favourable	Nil reported
	<b>GE</b>	Expression level†	High (STLMS>ULMS)	High	Intermediate
<b>TIL</b>	<b>IHC</b>	% with high infiltration	0-54%	33-100%	50%*
		Prognostic association	?nil ?adverse	?favourable	Nil reported
	<b>GE</b>	T cell fraction†	Intermediate	Highest	Intermediate
		TCR clonal expansion†	Intermediate	Highest	Lowest
		Prognostic association	Favourable (CD8 signature in ULMS)	Nil	Adverse (Th2 signature)
<b>TAM</b>	<b>IHC</b>	% with high infiltration	26-75%	75%*	50%*
		Prognostic association	Adverse	Nil reported	Nil reported
	<b>GE</b>	Expression level†	Intermediate	High	High
<b>Other genomic-based findings</b>		Antigen presentation signature†	Increased expression	Increased expression	Intermediate expression
		Druggable negative immune modulators (B7-H3, TIM3, TGF-B) †	Lower	High	Intermediate
		NKC signature prognostic association	Favourable	Favourable	Nil
		DC signature prognostic association	Favourable	Nil	Nil
		Immune subtypes (as per Thorsson 2018)‡	25% Wound healing (C1) 15% IFN $\gamma$ -dominant (C2) 16% Inflammatory (C3)	23% Lymphocyte-depleted (C4) 0% Immunologically quiet (C5) 8% TGF- $\beta$ dominant (C6)	

**Table 1.9: Summary of immune profiling data in LMS, UPS and DDLPS**

IHC-based data drawn from studies summarised in Tables 1.5-1.7. Gene-expression (GE)-based data drawn from Pollack *et al*, TCGA-SARC, and Thorsson *et al*. STLMS = soft tissue LMS. ULMS= uterine LMS. NKC = natural killer cell. DC = dendritic cell

\*based on small sample in single study †relative to other STS subtypes ‡ percentages represent proportion of tumours across 6 STS subtypes assigned to each immune subtype

#### **1.5.4 Summary**

Gene expression-based studies examining the immune component of several STS subtypes have indicated that a non-trivial proportion of tumours demonstrate features suggestive of intra-tumoural immune activity. This has especially been the case in genomically complex subtypes such as UPS, while in STS characterised by few genomic alterations such as SS, profiling data indicate that an immune-suppressed microenvironment is typical. Such data are consistent with the limited amount of clinical trial data for the use of immune checkpoint inhibitors in STS, which have indicated that objective tumour response is seen most commonly, and is potentially largely limited to, a minority proportion of patients with genomically complex STS. It is however unclear as to how gene expression-based immune phenotypes may relate to or predict response to immunotherapy in STS. Meanwhile, the current body of reported IHC-based immune profiling evidence for STS has yet to contribute a clear, consistent picture of the extent of lymphocyte infiltration or immune checkpoint protein expression within these diseases, although studies that have used IHC-approaches to specifically focus on TAM in LMS have produced compelling results that point toward a potentially important role in conferring an immune-suppressed, pro-tumorigenic microenvironment in this subtype. The potential utility of IHC as prognostic biomarkers and/or proxy markers of different immune phenotypes that have been described at gene expression level has been subject to limited investigation that has been subject to methodological inconsistency.

As summarised in **Table 1.9**, reported gene expression- and IHC-based immune profiling in LMS, UPS and DDLPS, 3 of the most common genomically complex STS subtypes, have so far indicated that there exists qualitative and quantitative variety in the immune microenvironment of these tumour types. However, the frequency with which evidence of an active immune response is seen in these subtypes has not been reliably established, nor has the prognostic association of such immune responses. The development of immune-based biomarkers that may serve to inform clinical decision making regarding the use of immunotherapy and other treatment modalities will depend upon further and more in-depth investigation and analysis of existing and new cohort datasets.

## **1.6 Cancer biomarkers**

Cancer biomarkers are objectively measurable individual molecules or patterns of molecules that, when detected in the body, indicate the presence of cancer or a cancer-related process and can provide measures on which cancer classification can be based. Biomarkers may act to inform cancer risk assessments, as seen in the detection of germline genetic variants known to predispose to cancer or the assessment of tissue for evidence of premalignant changes – here, the positive detection of a biomarker predicts for an increased risk of cancer developing. Biomarkers also play a central role in cancer diagnosis and may involve the assessment of histological appearance, IHC phenotype, radiological appearance and molecular traits – as discussed above, subtype-specific diagnosis in STS increasingly calls upon a combination of such markers to be assessed. Beyond these, cancer biomarkers can prospectively inform an individual patient's likely prognosis or predict response to particular therapy – it is these prognostic and predictive biomarkers that play a central role in the modern concept of personalised or precision medicine.

### **1.6.1 Prognostic biomarkers**

Prognostic biomarkers can be of direct usefulness to patients and their doctors in terms of setting expectations, but also provide a basis for stratification of clinical trial cohorts and for investigation for underlying biology that dictates differential clinical outcome. Commonly assessed tumour properties such as histological grade or clinical stage, while varying in terms of disease-specific definitions, generically provide prognostic information in the majority of cancer types. Increasingly, cancer-specific ancillary tests are performed to provide information to explain the heterogeneity in outcomes between patients with cancers of apparently equivalent type, stage and grade. This is well illustrated by HER2 overexpression in breast cancer, which is associated with an aggressive phenotype, poor prognosis and sensitivity to HER2-targeting therapies irrespective to tumour stage or grade. A wide range of single gene alterations (commonly activating mutation/ amplification of oncogenes or inactivating mutation/ deletion of tumour suppressor genes) have been associated with better or worse outcomes in many retrospective studies of many different cancer types but few such discoveries have been developed into validated and clinically useful biomarkers<sup>254,255</sup>. Notable exceptions to this include amplification and

overexpression of *HER2* in breast cancers, serving as a negative prognostic marker but positive predictive marker for HER2-directed therapies, and loss-of-function alterations in *IDH1* or *IDH2* that predict for more favourable prognosis in glioblastoma multiforme and other forms of brain tumour<sup>256,257</sup>.

The introduction of cDNA microarray and, more recently, NGS has potentiated the development of multigene prognostic signatures, wherein transcriptome-level gene expression data is resolved into subsets of 10s to 100s of genes that describe biologically-defined tumour subsets that are then assessed for differential clinical phenotype. Particular success has been seen with this approach in early stage breast cancer, where a number of expression profile-based classifications have been able to consistently identify intrinsic biological subgroups that outperform conventional clinico-histological subtype classification in predicting risk disease relapse<sup>258</sup>. Companion laboratory diagnostic tests (LDT) or in vitro diagnostic devices (IVD) based on these gene expression signatures are now commercially available and provide an avenue for the robust and routine clinical application of multigene prognostic signatures. These biomarker results are often also used to inform choice of adjuvant treatment strategy, although for all but one of these panels, this is based the assumption that proven prognostic value of the biomarker can also extend to providing predictive information in terms of benefit of chemotherapy.

Conventional clinic-pathological parameters such as histological subtype, grade and stage remain the predominant source of prognostic information in the current standard management of most STS. A number of risk nomograms variably based on variables including tumour size, grade, vascular invasion, depth and anatomical position have been derived from retrospective assessment of large patient cohorts with varying extent of validation – the clinical utility of such measures is largely limited to setting expectations for clinical outcome. In early stage GIST, risk classification scores based on clinic-pathological variables have been used in the prospective stratification of trials of adjuvant Imatinib and are now routinely inform clinical decision making regarding the use and duration of adjuvant therapy<sup>259</sup>. None of these GIST risk scores currently incorporate KIT or PDGFRA mutation status – given that it is increasingly recognised that specific KIT mutations are associated with a more aggressive clinical phenotype, future refinement to GIST risk models will likely incorporate such genomic

variables<sup>260,261</sup>. As in most other cancer types, a large number of retrospective studies of STS cohorts have identified various circulating or tumour-based factors with associations with clinical outcome, but the likely high rate of false positive findings within such studies and lack of independent validation have contributed to the near-total attrition of such findings in translating to impact on standard practice. The CINSARC score, as discussed above, represents a promising pan-STS prognostic score that has been subject to successful validation in a number of independent patient cohorts. Ultimately, the clinical impact of this and other gene expression-based scores will be dictated by the success of investigation of the predictive value of these technologies.

### **1.6.2 Predictive Biomarkers**

Predictive biomarkers are central to the notion of precision/personalised oncology, wherein patients are matched to the treatments that are identified as most likely to be of benefit by a biomarker that has been shown to be capable of prospectively characterising a tumour as being relatively sensitive or resistant to a given therapy. Such biomarkers are of particular relevance to the large repertoire of modern cancer drugs that target discrete molecular aberrations. By enabling a focus of the use of expensive novel agents on only those patients with a high likelihood of benefit while reducing unnecessary treatment and adverse effects in those unlikely to respond, predictive biomarkers can deliver dramatic improvements in both the clinical and cost-effectiveness of cancer therapies.

It remains the case that the large majority of predictive biomarkers in standard clinical use are centred on the detection of monogenic cancer drivers as predictors of effect of drugs that target related aspects of tumour biology. The effectiveness of inhibitors of EGFR is predicted by the presence of activating mutations of the RTK in NSCLC, or the absence of RAS or RAF mutations in colorectal cancer. Activating mutations of BRAF predict the effectiveness of BRAF and MEK inhibitors in melanoma, while the clinical activity of Her2-targeting drugs in breast and upper GI cancers is predicted by Her2 overexpression and/or amplification. The clinical usefulness of such biomarkers may often complement (as is the case with Her2 expression in breast cancer) or even supplant (as with KIT mutation in GIST) conventional clinico-pathological classification and, increasingly, have come to define new disease sub-

classifications that in turn have directed the co-evolution of biomarkers and their respective targeted therapies – this is exemplified by the development of successive generations of EGFR inhibitors that variably exhibit selective inhibition of originator or acquired resistance-associated mutations.

The targeting of activated oncogenes has been associated with major clinical advances that heralded a new era of targeted cancer medicine that is now entering its third decade. However, extensive investigation has revealed that only a minority of cancers have single oncogene drivers and that even in cases where effective therapies are now established, the eventual emergence of acquired resistance through a variety of mechanisms is near-ubiquitous. Meanwhile, the use of a range of molecularly targeted drugs that inhibit multiple cancer-related proteins is now standard in a number of cancers without identified monogenic drivers and for which predictive biomarkers have not been established. In these cases, the frequency and degree of disease response to drug treatment is generally limited when compared to the specific targeting of monogenic drivers, and, in those who do initially respond, duration of disease control is generally modest prior to development of acquired resistance.

The use of biomarker panels based on more complex mutational or gene expression signatures has begun to enter standard clinical practice, often through engagement of commercial third-party providers. For example, in 2017, the FDA approved the use of the Foundation One diagnostic panel for use in any solid tumour. This panel utilises FFPE-derived tumour DNA for targeted NGS of 324 genes for which actionable alterations, including MSI, have been clinically validated in at least one cancer<sup>262</sup>. Numerous similar panels are at varying stages of clinical development, with the intended benefit identifying actionable alterations that can be used to select patients for either the licensed use of molecularly-targeted therapy, off-label use of the same agents outside of the tumour types in which definitive clinical benefit has been demonstrated or molecularly-stratified clinical trials.

There is currently a near-complete lack of predictive biomarkers in routine use for the management of STS. The one notable example is seen in GIST, where the presence of activating mutations of *KIT* or *PDGFRA* predict for benefit of imatinib and other TKIs, with so-called wildtype GIST, wherein no *KIT* or *PDGFRA*

mutations are detected, showing no response. Furthermore, specific mutations have been associated with differential Imatinib sensitivity – GIST with exon 9 mutations of *KIT* are less sensitive to imatinib than those with exon 11 mutations, while D842V mutations of *PDGFRA* are associated with low rates of Imatinib response. Beyond this, the absence of other known, targetable monogenic drivers in STS has meant further examples of molecularly-targeted, biomarker-stratified treatment have not been forthcoming. As is the case in other cancers, the development of robust predictive biomarkers for specific cytotoxic drugs or multi-targeted small molecule inhibitors in STS has been limited by poor understanding of molecular mechanisms of tumour sensitivity and resistance. For the most part, the choice of systemic therapies for advanced STS are guided by an understanding of histotype-specific therapeutic sensitivity that is based on a variable and often limited level of trial evidence and patient-specific factors such as co-morbidity, level of fitness and preference.

### **1.7 Conclusions, Hypothesis and Aims**

Current, largely histological methods of classification of STS inadequately account for the heterogeneity in clinical behaviour that is observed both between and within subtypes. There is an urgent unmet clinical need for the development of prognostic and predictive biomarkers that provide novel means of classifying STS into groups of shared biological traits that are in turn reflected by common phenotypic characteristics such as likelihood of disease relapse and mortality, or sensitivity or resistance to currently available therapies such as pazopanib. The development of candidate biomarkers would provide a platform for investigation for optimised use of existing therapies, while enhancing the likelihood of successful development of novel agents.

The clinical- and cost-effectiveness of pazopanib is currently limited by a lack of predictive biomarkers. So far, research that has aimed to address this has largely focussed on attempts to identify clinico-pathological or circulating angiogenic factors that identify patient subgroups in which pazopanib benefit is enriched – of the few putative candidates identified here, none have progressed beyond discovery stage. Meanwhile, very few studies have investigated the potential for tumour tissue-derived biomarkers for pazopanib, although preclinical evidence

indicates that specific molecular traits within tumour cells may indicate differential drug sensitivity.

Evidence in multiple cancer types has demonstrated recurrent immune microenvironment features that may serve as prognostic biomarkers and/or inform the likelihood of response to currently available immunotherapies. Available profiling data indicate that, as is seen in other cancer types, variation in terms of the frequency and character of immune responses exists within STS, with reported research suggesting that certain immune traits may either be restricted to or transcend the boundaries of conventional histological classifications. However, results from IHC-based profiling studies have produced inconsistent reports of the proportion and type of STS in which evidence of an active immune microenvironment can be found. While analysis of transcriptomic data has shown with some consistency that certain genomically complex STS subtypes exhibit evidence of inflammatory infiltrates that exhibit the hallmarks of an active anti-tumour response, these too have yet to translate into the development of clinically useful biomarkers that can identify subgroups with distinct clinical phenotype.

The overarching hypothesis of my thesis project is that histological and molecular characterisation of STS clinical tumour samples can identify shared biological characteristics that define subgroups with distinct clinical phenotype. In addressing this hypothesis, my project aims to identify means of biomarker-based classification that accounts for clinical heterogeneity within STS:

### **Aims**

1. Characterise the immune microenvironment of LMS, UPS and DDLPS
2. Assess for association between immune phenotype and clinical outcome in LMS, UPS and DDLPS
3. Investigate for molecularly-defined subgroups with association with differential treatment outcome in a cohort of pazopanib-treated STS.

## **Chapter 2: Materials and Methods**

### **2.1 Validation of TMAs for immune profiling**

Methods detailed in this section refer to experiments for which results are discussed in chapter 3

#### ***2.1.1 Tumour sample selection and processing***

Surgical resection specimens of primary LMS (n=47) and accompanying annotation of baseline clinico-pathological variables were identified and retrieved through retrospective review of departmental database and medical notes at a single specialist cancer centre. Histological diagnosis was confirmed by contemporaneous assessment by a specialist sarcoma histopathologist. Where available, five FFPE blocks containing viable tumour from spatially distinct areas (at least 2 blocks each from tumour margins and core) of the same primary tumour were selected. Newly prepared haematoxylin and eosin (H&E) slides from each block were assessed to confirm presence of viable tumour material. IHC staining of T lymphocyte markers (CD3, CD4 and CD8) was performed on consecutive 4µm sections from each block. IHC staining for B lymphocytes (CD20) was performed on all blocks from an initial set of 19 tumours – this was not expanded to all tumours due to uniformly low numbers of infiltrating B cells in this initial set. Details of IHC conditions as per below table:

<b>Antigen</b>	<b>Clone/Ref (Manufacturer)</b>	<b>Antigen Retrieval</b>	<b>Primary antibody dilution</b>
CD3	M0452 (DAKO)	Pressure cooking 2 min in citrate, pH6	1:600
CD4	4B12 (DAKO)	PTM buffer 20min at 97c, pH9	1:80
CD8	C8/144B (DAKO)	PTM buffer 20min at 97c, pH9	1:100
CD20	L26 (DAKO)	Microwave for 18min, pH6	1:400

DAKO link automated stainer was used for all IHC processing. Deparaffinisation was with xylene followed by graded ethanol rehydration. Antigen retrieval performed using DAKO FlexEnvision kit (K8002) under stated conditions. Incubation with primary antibody was for 60 minutes at room temperature. Secondary antibody staining and visualisation was performed using DAKO FlexEnvision (Rabbit/Mouse) Kit, followed by application of DAB and haematoxylin counterstaining.

### **2.1.2 IHC scoring**

#### *Full tissue sections*

The number of CD3, CD4, CD8 and CD20 IHC-positive lymphocytes in ten non-adjacent, tumour-containing high-power fields (HPF) (x400 magnification, approx. area per HPF 0.31mm<sup>2</sup>) was manually counted by direct brightfield microscopy for each stained slide.

#### *Virtual TMA (vTMA)*

Digital microscopy images for slides stained for H&E, CD3 and CD8 from a single block from each of 47 cases were captured at x40 resolution using Nanozoomer-XR (Hamamatsu Photonics). 20 x 1mm diameter circular areas were randomly selected from viable-tumour areas on each H&E image. The corresponding areas were then selected on CD3 and CD8 digital slide images. Images of these areas at x10 magnification were exported as .tif files that were cropped to uniform 0.785mm<sup>2</sup> circular areas in Image J<sup>263</sup>. Positive-staining TIL in these images were counted using 'Particle analysis' function of image J following optimization of pixel intensity, particle size and circularity thresholds – the selected configuration was associated with a bias of -0.52 cells, with 95% limits of agreement at -17 to +16 cells, as assessed by Bland-Altman analysis. Due to the presence of pleomorphic, CD4-staining histiocytes, we were unable to use this approach for counting of CD4+ TIL, and so this marker was not included in the vTMA experiment.

#### *Physical TMA (pTMA)*

Triplicate 1mm diameter cores were sampled from areas of viable tumour within donor blocks from 44/47 LMS and re-embedded in an arrayed recipient paraffin block. Consecutive 4µm sections from the arrayed block were stained for H&E, CD3 and CD8. After assessment of H&E slides to confirm viable tumour content, all CD3- and CD8-positive staining TIL were counted under direct brightfield microscopy. Average TIL number per 1mm core (referred to herein as 'TIL/core') was calculated from triplicate cores for each tumour.

### **2.1.3 Statistical analysis**

#### *Degree of infiltrating lymphocyte burden across LMS cohort*

To assess the extent of TIL burden in each of 47 LMS cases, an average number of infiltrating CD3+, CD4+ and CD8+ TIL per HPF (referred to herein as 'TIL/HPF') was calculated from 50 HPF per tumour (10 HPF from each of 5 related tumour blocks). Comparison of TIL burden of tumours from different anatomical sites of origin was performed using 1-way ANOVA of Log2-transformed average TIL/HPF values with Prism v7.0 (GraphPad Software Inc).

#### *Inter- vs intra-tumour variance in TILs*

To assess the variability in TIL burden between different blocks from the same surgical specimen, we assessed the relative contribution of inter-block variation (block effect) and inter-tumour variation (tumour effect) on the total amount of variance in TIL numbers within the 47 LMS cohort by (i) Log2 transformation of all raw TIL/HPF count values (ii) calculation of average TIL/HPF with 95% confidence interval for each tumour block (average of 10 HPF) and across all 5 related blocks from each primary tumour (average of 50 HPF), and (iii) Ordinary 2 way ANOVA (Prism v7.0) to assess the percentage of total variability attributable to block effect, tumour effect, interaction between the two effects and residual variation. Agreement of average TIL/HPF between blocks from the same tumour was assessed using single measures intraclass correlation (R package 'ICC')<sup>264</sup>, taking each of five related blocks to be an 'observer' of that tumour's average TIL/HPF.

#### *Virtual TMA assessment of optimal core number*

Automated counts of infiltrating CD3+ and CD8+ TIL in all 20 x 1mm vTMA cores for each tumour were used to calculate average TIL/core – this value was taken as representing the 'true' TIL burden of each tumour. Estimates of these true TIL burdens were then derived from the average TIL/core from all possible combinations of between 2 and 19 randomly selected cores. The percentage of estimates generated from  $n$  cores that fell within the following prescribed boundaries were then calculated: a) within +/- 20% of true TIL burden; b) within correct (i.e. same as true TIL burden) side of dichotomised 'high/low' boundary set at median of true TIL burdens from 47 LMS cohort; c) within correct quartile of 47 LMS cohort.

#### *Assessment of accuracy of triplicate cores within a physical TMA*

The differences between Log<sub>2</sub>-transformed values of the estimated average TIL/core values derived from the pTMA and the true TIL burdens derived from the vTMA were calculated and plotted against the average of the two values in a Bland Altman plot along with 95% levels of agreement (Prism v7.0).

Average of TIL/core values derived from triplicate cores within pTMA were used to identify each included LMS as having a 'high' or 'low' TIL burden, relative to the cohort median of true TIL burdens, as defined in the vTMA experiment. This high/low identification was then compared to a 'gold standard' high/low allocation, defined as the 'true' TIL burden of that tumour as derived from all 20 vTMA cores. Accuracy (%) of pTMA was defined as  $100 \times (\text{True Positive} + \text{True Negative}) / (\text{True Positive} + \text{False Positive} + \text{True Negative} + \text{False Negative})$

#### **2.1.4 Research ethics**

Use of archival FFPE tumour samples and linked anonymised patient was approved by Institutional Review Board as part of the PROSPECTUS study, a Royal Marsden Marsden-sponsored non-interventional translational protocol (CCR 4371, REC 16/EE/0213).

## **2.2 Profiling the immune microenvironment in 3 genomically-complex histological subtypes of STS**

Methods detailed in this section refer to experiments for which results are discussed in chapters 4 and 5

### ***2.2.1 Patient selection and treatment***

Collection and analysis of anonymised archival FFPE tissue and associated clinical data was approved as part of the Royal Marsden-sponsored PROSPECTUS (PROgnoStic and PrEdiCTive ImmUnoprofiling of Sarcomas) study, an observational retrospective cohort study of patients treated for STS at the Royal Marsden Hospital in London (RMH Committee for Clinical Research reference 4371, NHS Research Ethic Committee reference 16/EE/0213). Patients were selected for inclusion by the following criteria: received definitive management for primary tumours at the Royal Marsden within a 5 year period; age >18 years at point of study commencement; histologically confirmed diagnosis of LMS, UPS or DDLPS; FFPE tumour material available from surgical resection specimen; details of clinical follow-up available; naïve to pre-operative chemotherapy and radiotherapy at time of surgical resection. Perioperative radiotherapy has an established role in the management of high grade, deep-seated early stage STS occurring in the limbs – exclusion of irradiated tumours that received pre-operative radiotherapy from the study cohort could thus be a potential source of bias for certain STS subtypes. However, the adoption of pre-operative over post-operative irradiation in routine practice at The Royal Marsden (RMH) occurred c.2014-2015, and so cases prior to this will be free from potential selection bias.

Eligible patients were identified by retrospective search of hospital medical and histopathology records and departmental database. Baseline clinico-pathological characteristics and survival data were collected on retrospective review of contemporaneous electronic medical records. In view of the retrospective and anonymised use of patient-derived material and data, a consent waiver was approved by the Research Ethics Committee, in keeping with Human Tissue Authority Code of Practice and Research E: Research.

### **2.2.2 Tumour sample selection and processing**

FFPE tumour blocks and H&E slides of surgical specimens taken from identified patients were retrieved from the institutional diagnostic archive. With reference to contemporaneous diagnostic histopathology reports and archival H&E slides, a single block containing representative and adequate tumour material was selected from each tumour for use. New H&E slides were cut and reviewed from each block to ensure tumour content and for TMA mark-up. TMAs of included tumours were constructed using 3 replicate 1mm core biopsies from representative areas of viable tumour. For DDLPS, only tumour areas containing dedifferentiated, rather than well-differentiated, LPS were sampled. After sampling for TMA, 4x10µm sections were cut and, where necessary, macrodissected to enrich for >75% viable tumour content, prior to extraction of tumour total RNA using All Prep DNA/RNA FFPE kit (Qiagen, Hilden, Germany) following vendor's standard protocol. RNA concentrations were measured using Qubit fluorometric quantitation (Thermo Fisher Scientific, Waltham, MA, USA). RNA Integrity Number and percentage of total RNA <300bp in size was measured using 2100 Bioanalyzer system (Agilent, CA, USA). RNA samples were stored at -80°C until use in downstream analyses.

### **2.2.3 IHC staining and scoring**

Serial 4µm sections were cut from TMA, mounted on slides and used for IHC. DAKO link automated stainer was used for all IHC processing. Details of IHC conditions as per below table:

<b>Antigen</b>	<b>Clone/Ref (Manufacturer)</b>	<b>Antigen Retrieval</b>	<b>Primary antibody dilution</b>
CD3	M0452 (DAKO)	Pressure cooking 2 min in citrate, pH6	1:600
CD4	4B12 (DAKO)	PTM buffer 20min at 97c, pH9	1:80
CD8	C8/144B (DAKO)	PTM buffer 20min at 97c, pH9	1:100
CD68	M0814 (DAKO)	Pressure cooking 2 min in citrate, pH6	1:200
PD-L1	E1L3N (Cell Signalling)	Pressure cooking 2 min in citrate, pH6	1:150

Deparaffinisation was with xylene followed by graded ethanol rehydration. Antigen retrieval performed using DAKO FlexEnvision kit (K8002) under stated conditions. Incubation with primary antibody was for 60 minutes at room

temperature. Secondary antibody staining and visualisation was performed using DAKO FlexEnvision (Rabbit/Mouse) Kit, followed by application of DAB and haematoxylin counterstaining. Positive staining controls were human tonsil (CD3, CD4, CD8, CD68) and placenta (PD-L1). Negative control was through omission of primary antibody.

Digital microscopy images for all stained TMA slides were captured at x40 resolution using Nanozoomer-XR (Hamamatsu Photonics). These images were used to assess tumour staining was by researchers blinded to associated outcome data.

For CD3, CD4 and CD8, the number of individual positive-staining lymphocytes within each TMA core were counted at x400 magnification. When, due to sectioning artefact, a non-trivial proportion of the 1mm core section was missing, the percentage of core present was evaluated. For sections with  $\geq 50\%$  of complete section present, cell counts were corrected to 100% area. Sections with  $< 50\%$  complete section present were not included in the analysis. For each tumour, the lymphocyte counts from associated replicate TMA core were averaged then multiplied by 1.274 to produce an average TIL/mm<sup>2</sup> for each tumour for each of the three T lymphocyte stains.

To assess the extent of infiltration by CD68-staining macrophages, each TMA core was also scored on a semi-quantitative scale of 1-3. An average score for each included tumour was calculated from the individual scores across associated replicate cores (average CD68 score).

To investigate the degree of tumour-cell expression of PD-L1, we assessed each TMA core for tumour cell membranous and/or cytosolic PD-L1 staining according to a semi-qualitative scale based on frequency (0= $< 1\%$  of cells, 1=1-10%, 2=11-50%, 3= $> 50\%$ ) and intensity (0=absent, 1=weak, 2=moderate, 3=strong) or tumour cell staining. These were combined to provide a range of possible scores from 0 to 6 for each TMA core. The maximum score among associated replicate cores was used to represent each tumour (max tPD-L1 score). The presence or absence of PD-L1 expression by any tumour-infiltrating leucocytes (lymphocytes and/or histiocytes) was recorded as a binary variable (IcPD-L1 present or absent).

#### **2.2.4 Gene expression analysis**

Tumour expression of a custom panel of 21 immune-related genes and 3 housekeeper genes was assessed using the nCounter PlexSet-96 platform (NanoString Technologies, Seattle, WA, USA). Given the generally high level of nucleic acid degradation in extracted RNA and the frequently low levels of target gene expression expected within the originating tissues, pilot investigation of optimal RNA loading amounts was performed using the nCounter PlexSet-96 titration kit. Based on this, RNA loading amounts of 150-450ng total RNA (adjusted to account for variable degree of RNA degradation) was used as input for hybridisation and digital analysis as per manufacturer's instructions using nCounter Dx analysis system (NanoString Technologies). Raw expression data from all analysed tumours were subject to an initial QC step, with tumours with any housekeeper gene value  $<3$  standard deviations above mean negative control probe values being excluded from analysis based on insufficient signal: noise ratio. Expression data from 266 tumours that passed this QC step were then normalised by a positive control factor calculated as geometric mean of the three positive control probes with highest values followed by normalisation by a factor determined by the geometric mean of the three housekeeper genes. Expression values were then Log<sub>2</sub> transformed and subjected to gene-level Z standardisation. Processed expression data was then subjected to unsupervised two-way agglomerative clustering using Wards minimum distance linkage and Euclidean distance clustering.

#### **2.2.5 Statistical analysis**

For descriptive statistics, average TIL/mm<sup>2</sup> values were treated as continuous variables, with comparative and correlative statistics performed on Log<sub>2</sub>-transformed values to conform to assumptions of normal distribution. Average CD68 and max tPD-L1 scores were treated as ordinal categorical variables, and lcPD-L1 as a binary categorical variable.

The primary endpoint for survival analyses was OS, defined as time from date of sample collection (i.e. date of surgery) to date of death from any cause. The secondary endpoint was advanced disease-free survival (adDFS), defined as time from date of sample collection to date of development of radiologically-confirmed relapse with advanced disease (defined as distant metastasis and/or

inoperable locally advanced disease). Patients who had not experienced survival event were censored at point of last follow-up or, where specified, death. The Kaplan–Meier method was used to estimate PFS and OS, and the log-rank test to compare survival between different subgroups as stated in results text. In view of the exploratory nature of this study, no adjustments of P values to account for multiple significance testing were applied. Multivariable Cox proportional hazards regression models were used to estimate statistical significance adjusted for the standard clinico-pathological variables (R studio). The proportional hazard assumption was tested using Schoenfeld residuals and found to hold for all results.

## **2.3 Molecular risk classification and investigation of resistance mechanisms in advanced STS treated with pazopanib**

Methods detailed in this section refer to experiments for which results are discussed in chapters 6 and 7

### ***2.3.1 Patient selection and treatment***

Collection and analysis of anonymised archival FFPE tissue and associated clinical data was approved as part of the Royal Marsden-sponsored Elucidation of a Molecular signature of Pazopanib Response in Advanced soft tissue Sarcoma including Solitary fibrous tumours (EMPRASS) study (RMH Committee for Clinical Research reference 4107, NHS Research Ethic Committee reference 14/WA/0164). This cohort is referred to as RMH-SARC.

Patients were retrospectively identified for inclusion by search of institutional database and electronic patient records compiled during routine clinical practice. Eligibility criteria for inclusion were: i) histopathological diagnosis of STS as confirmed by specialist sarcoma histopathologist; ii) received at least one dose of pazopanib for treatment of unresectable or advanced STS; iii) available FFPE tumour specimen, obtained from patient prior to first dose of pazopanib. Treatment and response monitoring were as per standard institutional practice, with pazopanib at 800mg once daily until disease progression, intolerable toxicity or significant clinical deterioration. Dose interruption and/or reduction were instigated based on standard institutional guidelines and the discretion of the treating physician. Baseline clinico-pathological characteristics and survival data were collected on retrospective review of contemporaneous electronic medical records. All related radiological imaging was retrospectively reviewed and disease response assessed on computerised tomography (CT) images according to RECIST 1.1. For a single patient (RMH001) who exhibited durable pazopanib response, a full series of MRI performed throughout the patient's entire clinical course was reviewed and two axes measurements taken for all tumour areas. Estimated ellipsoid tumour volumes were calculated by the equation  $V = \frac{4}{3}\pi * a * b * c$ , where  $a$  and  $b$  are the two axial dimensions and  $c$  is their mean.

### **2.3.2 Tissue selection and processing**

Available pre-pazopanib FFPE tumour specimens were retrieved from an institutional diagnostic archive. From a single patient (RMH001) who exhibited good pazopanib response, both pre-pazopanib and post-progression FFPE tumour specimens were obtained. A tissue microarray of included tumours was constructed using 3x1mm core biopsies from representative areas of adequate tumour blocks; tumours whose blocks contained smaller biopsy specimen underwent full sections rather than incorporation into TMA. After sampling for TMA, 4x10µm sections were cut and, where necessary, macrodissected to enrich for >75% viable tumour content., prior to extraction of tumour DNA and total RNA using All Prep DNA/RNA FFPE kit (Qiagen, Hilden, Germany) following vendor's standard protocol. DNA and RNA concentrations were measured using Qubit fluorometric quantitation (Thermo Fisher Scientific, Waltham, MA, USA). RNA Integrity Number and percentage of total RNA <300bp in size was measured using 2100 Bioanalyzer system (Agilent, CA, USA). RNA and DNA samples were stored at -80°C until use in downstream analyses.

### **2.3.3 IHC**

Serial 4µm sections were cut from TMA and tumour blocks not included in the TMA. All IHC was performed using the DAKO Link Autostainer. Tissue sections were deparaffinised with xylene then rehydrated with graded ethanol (100%, 95% 70%) to water. Antigen retrieval was performed in DAKO low pH Antigen Retrieval buffer (K8005) using either microwave pretreatment (PDGFRA) or the MenPath Access Retrieval Unit (FGFR1). Slides were incubated with primary antibodies (FRFR1 – Epitomics 2144-1, 1:50 dilution; PDGFRA – Cell Signalling clone D1E1E, 1:250) for 60 minutes at room temperature and visualised using DAKO FlexEnvision (Rabbit/Mouse) kit (K8010), followed by application of DAB, resulting in visible brown colouration reaction at site of target antigen. Finally, nuclear counterstaining with haematoxylin was performed prior to coverslipping. Positive controls were normal breast (PDGFRA) and appendix (FGFR1). Negative control was through omission of primary antibody. Tumour cell staining for PDGFRA (Cell Signalling, clone D1E1E) and FGFR1 (Epitomics, 2144-1) was assessed IHC by researchers blinded to associated outcome data.

IHC expression was scored in terms of intensity (0=absent, 1=weak, 2=moderate, 3=strong) and proportion of positive tumour cells (0=absent, 1 = 1-10%, 2: = 11-50%, 3: >50%). The summation of the two scores gave values ranging from 0 to 6. Staining score  $\geq 3$  was classified as high expression and scores  $< 3$  as low expression. In cases of discrepancy between related TMA cores, an average score was calculated and used to categorise the parent tumour as having high or low expression.

### **2.3.4 TP53 exon sequencing**

Extracted tumour DNA was used as a template for amplification and Sanger sequencing of exons 2-11 of *TP53* as per International Agency for Research on Cancer (IARC) protocol<sup>265</sup>. *TP53* exon primers and PCR conditions are as below:

TP53 exon(s)	Forward primer	Reverse Primer	PCR program
2-3	tctcatgctggatccccact	agtcagaggaccagggtcctc	A
4	tgaggacctggcctctgac	agaggaatcccaaagttcca	A
5-6	tgttcacttgccctgact	ttaaccctcctcccagaga	A
7	aggcgcactggcctcatctt	tgtgcagggtggcaagtggc	A
8-9	ttgggagtagatggagcct	agtgttagactggaaacttt	A
10	caattgtaactgaaccatc	ggatgagaatggaatcctat	B
11	agaccctctcactcatgtga	tgacgcacacctattgcaag	A

#### **PCR program A:**

94°C for 2 min

(94°C for 30 sec, 63°C\* for 45 sec, 72°C for 60 sec) x20 \*=-0.5°C every 3 cycles

(94°C for 30 sec, 60°C for 45 sec, 72°C for 60 sec) x30

72°C for 10 min

#### **PCR program B**

94°C for 2 min

(94°C for 30 sec, 58.5°C\* for 45 sec, 72°C for 60 sec) x20 \*=-0.5°C every 3 cycles

(94°C for 30 sec, 55°C for 45 sec, 72°C for 60 sec) x30

72°C for 10 min

PCR products were Sanger sequenced (Eurofins Genomics, Ebersberg, Germany). Sequences were aligned to reference human *TP53* sequence (GrCH38.p7) and manually analysed for variants using CLC Sequence Viewer v7.7 (Qiagen).

Detected missense SNV of *TP53* was assessed using four functional prediction algorithms (SIFT, PROVEAN, PolyPHEN-2, and FATHMM-MKL –accessed 19/09/2017)<sup>266–269</sup>. Annotation of dominant negative effect of SNV was derived from the IARC *TP53* database<sup>270</sup>, which summarises reported evidence of the ability of specific missense mutations to suppress transactivation of p53 response elements (RE) by wildtype p53. Missense variants at predicted splice sites were assessed using Human Splicing Finder (HSF\_V3.0 – accessed 19/09/2017)<sup>271</sup>. Reported incidences of detected variants were assessed through search of COSMIC and IARC *TP53* databases and through assessment of genomic sequencing data from the TCGA-SARC cohort (all accessed 19/09/2017).

### **2.3.5 Gene expression analysis**

Expression of 730 genes, representing 13 major cancer pathways including key driver genes was assessed using nCounter PanCancer Pathways panel (NanoString Technologies, Seattle, WA, USA). 150ng total RNA was used as input for hybridisation and digital analysis as per manufacturer's instructions using nCounter Dx analysis system (NanoString Technologies). In cases with high RNA degradation, loading adjustments of up to 300ng were made. Expression data from RMH-SARC (n=38) was processed together as follows: a) background correction was done by subtracting the geometric mean of the negative control probes, b) normalised by positive control normalization factor calculated as geometric mean of the positive controls followed by normalisation with the housekeeping genes. Expression values were then Log2 transformed and subjected to gene-based centring. When processing the expression profile of the paired pre- and post-treatment samples from a single patient, data was normalised with the list of genes showing the lowest variance across RMH-SARC.

Large average submatrices (LAS) bi-clustering algorithm<sup>272</sup> was applied on the log<sub>2</sub> transformed, median-centred gene expression data of the RMH-SARC cohort samples (n=38), with the following parameters: (a) at the Data Normalization step column standardization was applied, (b) the biclustering algorithm was stopped after finding 10 large positive and 10 large negative average sub-matrices (bi-clusters) (c) 1000 iterations were performed. Briefly, the biclustering model measures coherence within the subset of genes and conditions/phenotypes, and thus is particularly useful in revealing the involvement of a gene or a condition in multiple pathways.

In order to identify biological subgroups within a subset of RMH-SARC, consensus clustering (CC) was used to objectively separate the tumours into stable biological subgroups<sup>273</sup>. The goal of CC was to search for a partition of the 22 tumours into at least 2 or, at most, 8 groups using expression of the 730 cancer pathway-associated genes. CC using 1-Pearson's correlation coefficient as distance metric was used to identify robust unsupervised clusters by performing 200 iterations subsampling 80% of the samples each round. Having identified initially five clusters that were consolidated into three clearly separated subgroups, Multiclass Significance Analysis of Microarrays (SAM)<sup>274</sup> was used to identify a subset of genes with significant differential expression (false discovery rate  $\leq 10\%$ ) among the three subgroups. Reference (training) gene expression profiles datasets for each of the three subgroups were built using gene subsets identified by SAM analysis. Functional enrichment analysis of these gene subsets was performed using the Database for Annotation, Visualization and Integrated Discovery (DAVID), using the 730 genes included in the nCounter PanCancer Pathways panel as background.<sup>275,276</sup> These gene subsets were also used to calculate a standardised centroid representing each of the three subgroups based on the Prediction Analysis of Microarray (PAM) algorithm<sup>277,278</sup>. Each centroid was the average expression value for each gene in each subtype divided by the within-class standard deviation for that gene. Nearest centroid single sample classification could then be applied to the gene expression profile of a new sample, comparing it to each defined subgroup centroid and assigning the sample to a subtype based on the highest Spearman's correlation coefficient to the centroid.

To identify genes putatively associated with pazopanib resistance, SAM analysis was performed on gene expression data from RMH-SARC to identify key differentially expressed genes in the subgroup of patients with F-Lo/P-Hi IHC status versus IHCneg cases at q-value  $\leq 10\%$ . For the single patient case study (RMH001), genes whose expression were increased by at least 1.5 fold in post-pazopanib tumour compared to pre-pazopanib tumour were identified.

### **2.3.6 Independent evaluation of the biological subgroups on Stanford-LMS dataset**

Normalised gene expression profile data by 3'End RNA-sequencing (3SEQ) from a cohort of 99 cases of LMS (GSE45510; accessed 09/03/2017) was obtained<sup>32</sup>, referred to here as Stanford-LMS. When comparing data from multiple analyses (e.g. comparing expression profiles for one or more test samples to centroids constructed from samples collected and analysed in an independent cohort), it is necessary to normalise data across these datasets. Distance-Weighted Discrimination (DWD)<sup>279</sup> was used to combine Stanford-LMS and RMH-SARC datasets together to adjust for systematic biases between these two separate datasets. Each case was assigned to one of three subgroups on the basis of distance from centroids defined within our RMH-SARC cohort. Descriptive statistics was done to compare the frequency of our subgroups within each of the molecular LMS subgroups as described by Guo *et al*<sup>82</sup>. Hierarchical clustering of Stanford-LMS using our list of significant differential genes identified in RMH-SARC was used to illustrate the gene expression pattern.

### **2.3.7 Independent Evaluation of identified biomarkers in TCGA-SARC dataset**

RNA sequencing (RNA-Seq) and accompanying clinical data for 257 cases of mixed STS were downloaded from TCGA (TCGA-SARC; accessed 27/02/2017). The abundance of transcripts was estimated using an Expectation-Maximization algorithm implemented in the software package RSEM8 v1.1.13. Quality control of RNA-Seq data was performed as described in TCGA, and RSEM data was upper quartile normalized and Log2 transformed.

High and low expression levels of *FGFR1* and *PDGFRA* were defined using a cutoff at the first tertile of normalized gene expression values. Associated *TP53*

mutational status (defined as exonic non-synonymous single nucleotide variant or small indel) from DNA sequencing data for the cohort was downloaded from cBioPortal (accessed 22/04/2017). OS outcomes were available for 204 of these cases and were stratified by presence or absence of F-Lo/P-Hi expression pattern and *TP53* mutation. 144/204 cases were identified as having neither FGFR1-low/PDGFR4-high expression pattern nor *TP53* mutation – the expression data of these cases were normalized and standardised to the expression data of IHCneg*TP53*wt cases within RMH-SARC in order to remove batch effect between the two gene expression analysis platforms. Subsequently, each of the 144 cases were assigned to one of three subgroups on the basis of correlation with centroids defined within the RMH-SARC cohort. This subgroup assignment was used alongside F-Lo/P-Hi expression pattern and *TP53* mutation to recapitulate PARSARC groups when stratifying OS in the cohort.

### **2.3.8 Statistical analysis**

The stepwise primary objectives were to assess whether a surrogate of two IHC markers (FGFR1 and PDGFR4) and *TP53* mutation status had statistical significant prognostic information for advanced STS. In this event, the two biomarkers panel were tested to determine if there was added statistically significant prognostic information to standard clinico-pathological variables in multivariable comparisons. The secondary analyses included identification of biological subgroups based on gene expression profiles, and evaluation of the significance of these biological subgroups association with patient outcome. PFS (defined as time in months from first dose of pazopanib to radiological disease progression or death from any cause) was the primary outcome endpoint, with OS (defined as a time in months from first dose of pazopanib to death from any cause) as the secondary outcome endpoint. Data cut-off for survival follow-up was 30<sup>th</sup> November 2016. Statistical analyses were performed independently by two statisticians. The Kaplan–Meier method was used to estimate PFS and OS, and the log-rank test to compare survival between different strata. Multivariable Cox proportional hazards regression models were used to estimate statistical significance adjusted for the standard clinico-pathological variables (including age, tumour grade, performance status and histological subtype). The proportional hazard assumption was tested using Schoenfeld residuals and found to hold for all results. Interaction tests between FGFR1 and PDGFR4 expression

to predict for survival were evaluated for PFS and OS respectively. Likelihood ratio tests based on proportional hazards regression were used to test the prognostic information of all biomarkers. The quantification of the amount of prognostic information provided by one biomarker was assessed by the likelihood ratio  $\chi^2$  value ( $LR\chi^2$ ), and the additional information of one biomarker to biomarker score was measured by the increase of the likelihood ratio  $\chi^2$  value ( $\Delta LR\chi^2$ ) obtained from the proportional hazards model.

## **Chapter 3: Validation of TMAs for immune profiling**

### **3.1 Background and Objectives**

TMA are useful diagnostic and research tools that permit high-throughput histological and molecular studies of up to several hundred tissue specimens simultaneously by arraying them into a paraffin block<sup>280</sup>. This approach offers several advantages over conventional examination of full tissue sections by minimising consumption of often limited tissue resources, ensuring identical experimental conditions are applied across all included samples while providing various efficiencies in downstream sample processing and analysis steps. However, an inherent limitation to the use of TMAs is that, for each included specimen, only a small amount of tissue is sampled and arrayed, meaning that sampling error may lead to a distorted representation of the full tissue section. This limitation is of particular relevance in the study of tumour specimens, where intra-tumour spatial heterogeneity in terms of morphology and underlying molecular pathology is now well established in many cancer types<sup>281</sup>. Multiple studies have been undertaken to validate the TMA methodology in the assessment of various cancer biomarkers, with the aim of demonstrating that biomarker levels reported by TMAs are representative of results obtained when full sections are assessed. In this manner, it has been shown that expression levels of a diverse repertoire of tumour biomarkers are accurately reported through the assessment of TMAs, typically with the provision that between 1 and 3 replicate cores from each included tumour are assessed and aggregated<sup>282–285</sup>.

TMAs continue to be frequently employed in studies that seek to investigate the immune microenvironment factors as a source of prognostic and predictive biomarkers<sup>174,286–290</sup>. The success of such studies is dependent on the ability of the TMA approach to capture a sufficiently representative picture of the immune phenotypes present within the wider tumour. Observations of quantitative and qualitative spatial heterogeneity in the immune microenvironment of individual tumours call into question how well TMAs can provide such representation and whether the scope for sampling error renders them inappropriate for studies of tumour immunity<sup>291–295</sup>. There is currently little published evidence that addresses this question<sup>296–298</sup>.

To assess the suitability of the use of TMAs for the profiling of the immune microenvironment in genomically-complex STS, we evaluated a pilot cohort of LMS tumour specimens to investigate the extent of inter- and intra-tumoral heterogeneity of TIL burden and how accurately TIL burden is represented by the TMA methodology, compared to full tumour sections. As with other STS subtypes, the immune microenvironment and its potential prognostic value is not well characterised in LMS (**see chapter 1.5.3**). Meanwhile, there is accumulating evidence that LMS is a disease that harbours extensive inter- and intra-tumoural genetic and morphological heterogeneity. For instance, recent genomic profiling analyses demonstrate that LMS is characterised by inter-tumour variability in SCNA, a molecular characteristic found to have negative correlation with active anti-tumour immune response in a number of other cancers<sup>4,299</sup>. Meanwhile, given that LMS often present with large primary tumours that exhibit intra-tumoural morphological heterogeneity of tumour cells and tumour-associated stroma, it is possible that spatial variation in immune microenvironment may also be present in this disease<sup>1</sup>. To assess the suitability of TMAs for profiling TIL burden in LMS, we sought to address two questions in this study: 1) What is the extent of inter- and intra-tumour heterogeneity of TIL burden in LMS, by comparing related tumour blocks from spatially distinct areas of primary tumours and 2) how many TMA cores are required to provide sufficient representation of the TIL burden of the full tissue section?

### ***Contributions***

Study conception and design; identification, collection and curation of archival histological material and associated clinic data; digital microscopy image capture; figure generation; data analysis were the work of the candidate

TMA mark up and construction was performed by the candidate under the supervision of Dr Khin Thway and with the assistance of Dr Cornelia Szecsei, histopathology fellow, Frank McCarthy and Nafia Guljar, Scientific Officers.

Direct light and digital histological analysis and scoring was performed by the candidate under the supervision and training of Dr Khin Thway, consultant histopathologist, The Royal Marsden.

IHC optimisation, FFPE slide cutting and staining was performed by staff of the ICR Histopathology Core Facility.

## 3.2 Results

### 3.2.1 Patient and tumour characteristics

Adequate tumour material was identified for 47 patients with a confirmed diagnosis of LMS who had undergone radical resection of primary tumour (baseline clinico-pathological variables are summarised in **Table 3.1**). Tumours tended to be large, with a large majority >5cm in maximal dimension, and 44% >10cm, and were mostly intermediate or high grade.

	Overall	Intra-cavity (exc. Uterine)	Uterine	Extremity/ Trunk
<b>N (%)</b>	47	27 (57%)	8 (17%)	12 (26%)
<b>Anatomical position</b>	-	RP - 20 (74%) AP- 7 (26%)	-	Lower limb - 6 (50%) Upper limb - 3 (25%) Trunk - 3 (25%)
<b>Average age/years (range)</b>	61.5 (29.4 - 87.5)	62.2 (30.6-87.0)	46.4 (29.4-73.4)	69.8 (53.2-87.5)
<b>% M:F</b>	51:49	48:52	0:100	83:17
<b>Max tumour dimension:</b>				
<5cm	5 (11%)	2 (7%)	1 (13%)	1 (8%)
5-10cm	21 (45%)	12 (44%)	3 (38%)	6 (50%)
10-15cm	10 (21%)	6 (22%)	1 (13%)	3 (25%)
>15cm	11 (23%)	7 (26%)	3 (38%)	1 (8%)
<b>Histological grade:</b>				
1	6 (13%)	6 (22%)	0	0
2	25 (53%)	16 (59%)	3 (38%)	6 (50%)
3	16 (34%)	5 (19%)	5 (62%)	6 (50%)

**Table 3.1: Baseline clinico-pathological status of 47 patients with primary LMS.**

RP=retroperitoneal. AP = abdominopelvic.

### **3.2.2 LMS are variably infiltrated by T lymphocytes**

For each case in the cohort, 5 tissue blocks that sampled spatially distinct tumour areas were assessed for TIL burden (outlined in workflow in **Figure 3.1A**). IHC staining for CD3 was used as a global T lymphocyte marker, with staining of consecutive slides for CD8 and CD4 used as markers for cytotoxic and helper T cell subpopulations respectively. CD20 staining was used as a global marker for B lymphocytes. Positive-staining TILs in 10 non-adjacent HPF were counted in sections from each of 5 blocks per tumour, with the average of all 50 related HPF (equating to a total area of 15.5mm<sup>2</sup> of assessed tumour) taken to represent the overall tumour TIL burden. Exemplar IHC images showing different degrees of CD3+ lymphocyte infiltration are shown in **Figure 3.1B**. The distribution of overall tumour TIL burdens for each lymphocyte marker across the cohort is shown in **Figure 3.1C**. The cohort medians of average TIL/HPF were CD3: 16.5 (IQR 11.3-30.9), CD4: 10.5 (IQR 5.5-18.9), CD8: 16.1 (IQR 7.2-23.0). It should be noted that these median values are below the 'low infiltration' thresholds currently used in studies of TILs in other well-studied cancer types such as melanoma, NSCLC and colorectal cancer<sup>175,176,300-302</sup>. Meanwhile, a median CD20+ TIL/HPF of 0.3 (0.1 – 1.5), indicated the near-absence of infiltrating B cells in a subset of 19 tumours. Across the different T lymphocyte markers, a dynamic range of 2-3 orders of magnitude (e.g. CD3 range 1-124 TIL/HPF) was seen in the extent of TIL burden between individual tumours (**Figure 3.1B**). No significant differences in T lymphocyte burden was seen when comparing LMS from different anatomical sites of origin (**Figure 3.1D**). These data indicate that markedly varying levels of infiltrating T lymphocyte burden are seen among individual LMS cases in a manner that was not associated with anatomical site of origin, and that LMS generally have a lower TIL burden than other, well-studied epithelial tumour types.

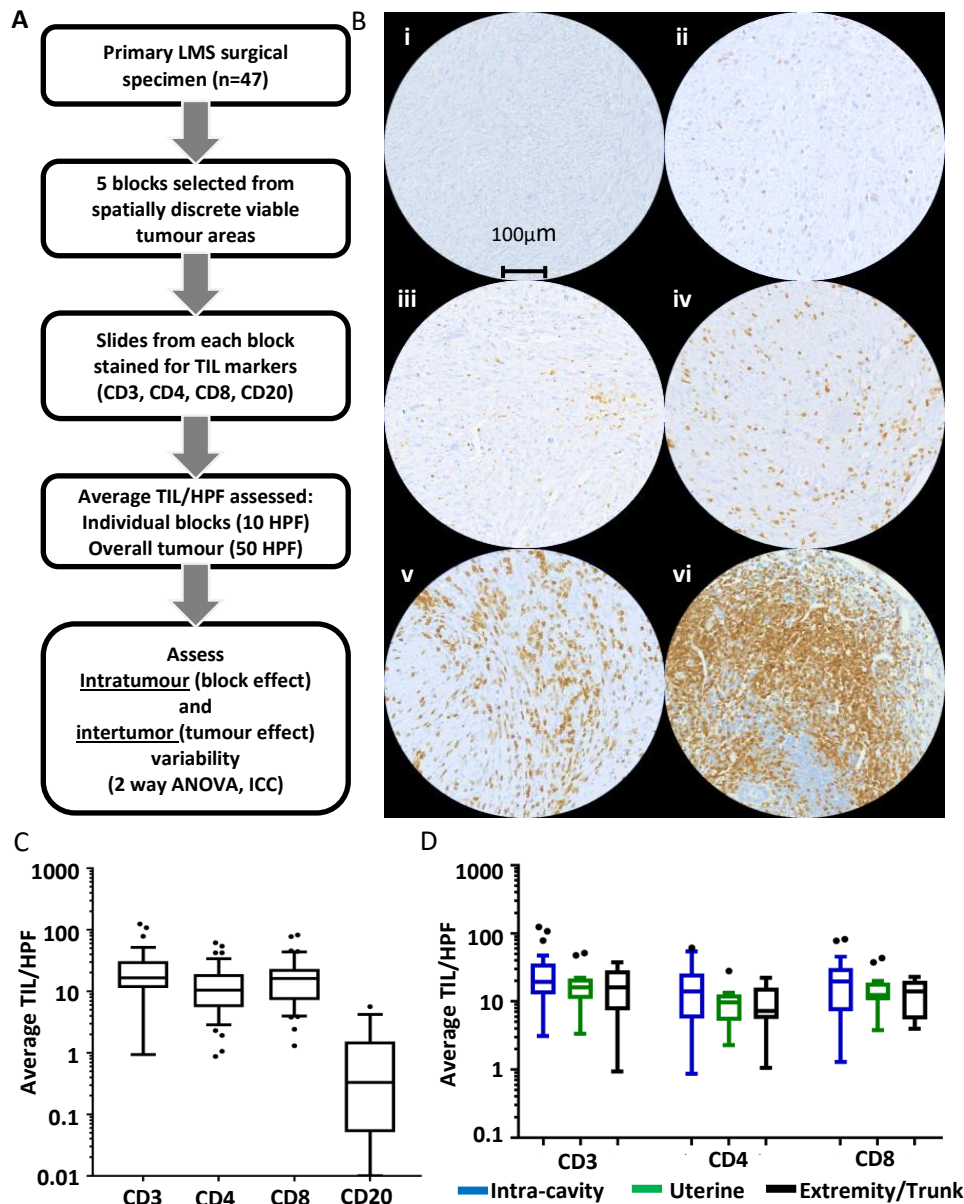


**Figure 3.1: Evaluation of infiltrating T and B lymphocyte burden in LMS**

**A.** Workflow of experimental approach. **B.** Representative areas from different CD3-stained LMS demonstrating range of infiltrating CD3+ T lymphocyte burdens. Densities are (i) 1, (ii) 35, (iii) 100, (iv) 250 and (v) 800 TIL/HPF (vi) positive control tissue (appendix) with 1400 TIL/HPF. **C.** Tukey box and tail plots showing overall lymphocyte burdens (average number of tumour-infiltrating lymphocytes (TIL) per x400 high-powered fields (HPF), calculated from 50 HPF) in LMS cohort based on IHC staining for CD3, CD4, CD8 (n=47) and CD20 (n=19) of LMS. **D.** Tukey box and tail plots showing distribution of CD3+, CD4+ and CD8+ TIL burdens within 47 LMS cohort when stratified by site of tumour origin. 1-way ANOVA of Log<sub>2</sub>-transformed values demonstrates no significant differences in T lymphocyte counts between tumours of different site of origin.

### ***3.3.3 Inter-tumour heterogeneity in TIL burden of LMS greatly outweighs intra-tumour heterogeneity***

It is currently not known to what extent TIL burden varies between different regions within individual LMS tumours. Intra-tumoral heterogeneity of TIL burden may introduce sampling error in immune profiling studies where only a single, potentially non-representative tumour area is sampled for assessment. Having established that overall TIL burdens can vary between individual LMS tumours, we assessed the extent of heterogeneity in average TIL/HPF between different blocks taken from the same LMS specimen (**Figure 3.1A**).

Block average TIL/HPF of each of the 5 sampled blocks across the 47 cases are shown along with tumour average TIL/HPF for CD3, CD4 and CD8 staining in **Figure 3.2A**. These data indicate that there is a variable extent of heterogeneity of TIL burden between related blocks, with some tumours showing very similar TIL/HPF values for all constituent blocks, while other tumours showed much wider variation between related blocks. The different extent of variation in CD3+ TIL burden between the most and least heavily infiltrated blocks are exemplified and illustrated in **Figure 3.2B**. The tumours with the largest variation between constituent blocks (as assessed by the maximum difference in TIL/HPF of any block from the overall tumour average) tended to be among those with the heaviest lymphocyte infiltrations (**Figure 3.2A**), suggesting that the cases with the most dense infiltrates were also more likely to harbour higher levels of intra-tumoural heterogeneity in TIL burden.

Objective assessment of the contribution of block effect (i.e. intra-tumour variability) to total variation in TIL counts by 2 way ANOVA indicated that while block effect significantly contributed to the overall amount of variance in the datasets for all 3 IHC markers, this was much smaller than the contribution of tumour effect between cases within the cohort (i.e. inter-tumour variability) (**Figure 3.2C**). Tumour effect accounted for 54.1%, 53.7% and 55.5% of total variance in lymphocyte counts for CD3, CD4 and CD8 respectively, while block effect contributed to only 0.3%, 0.5% and 0.7% total variance for the same respective markers. Significant interaction between tumour and block effect was detected for all three T lymphocyte measurements, in keeping with the pattern of greater degree of intra-tumour variance in tumours with higher overall

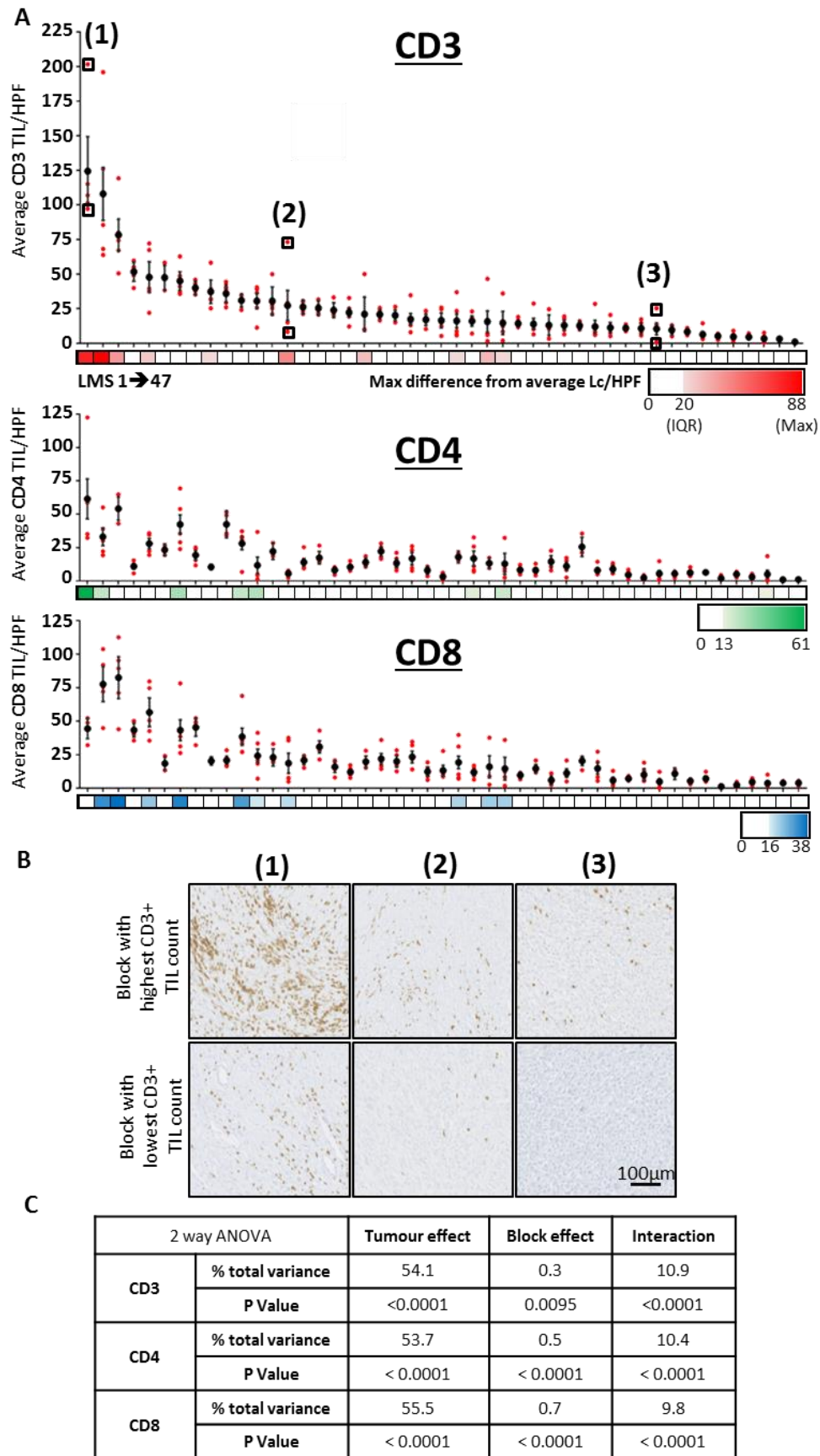


**Figure 3.2: Assessment of inter- and intra-tumour heterogeneity of TIL burden in LMS**  
(legend overleaf)

**A.** Dot plot shows average CD3+, CD4+ and CD8+ TIL/HPF values for each of 47 LMS tumours (vertically aligned), with overall tumour value (+/-95% confidence interval) and individual constituent blocks values shown with in black and red respectively. Colour bars demonstrate maximum difference of any related tumour block from overall tumour average, with zero, cohort interquartile range (IQR), and maximum difference values shown on colour key for each lymphocyte marker. **B.** Representative IHC images at x40 magnification demonstrate CD3+ TIL burden between the most and least densely infiltrated blocks from three tumours as indicated in **(A)**. **C.** Table summarising results from three separate 2-way ANOVA analyses that identifies the contribution of intra-tumour (block effect) and inter-tumour (tumour effect) variance to the overall total amount of variance in lymphocyte counts for CD3, CD4 and CD8 within the 47 LMS cohort.

average lymphocyte counts. Single measures intraclass correlation values of 0.73 (95% CI 0.63-0.82), 0.70 (0.60-0.80), and 0.76 (0.66-0.84) were seen for CD3, CD4 and CD8 respectively, indicating good levels of inter-block agreement for all three markers<sup>264</sup>.

Collectively, these results indicate that different blocks from the same tumour contained similar TIL burdens, and that intra-tumoural heterogeneity in TIL burden within the same tumour is notably outweighed by inter-tumoural heterogeneity. This suggests that different areas from the same tumour are more similar in terms of TIL burden than any given area in a different tumour, demonstrating that in LMS immune profiling studies, the potential for intra-tumoural heterogeneity to introduce sampling error is limited.

#### **3.2.4 Optimal number of cores to ensure representativeness of tissue microarrays depends on required degree of accuracy**

To address the question of how many TMA cores must be sampled from a tumour to provide adequate representation of the tumour's overall TIL burden, we devised an *in silico* 'virtual TMA' (vTMA) that would allow for the iterative sampling of a number of cores that would be impractical for a physical TMA. We then assessed how many cores were required to produce an estimate of TIL burden that either (i) accurately recapitulated that tumour's true TIL burden, or (ii) was sufficiently accurate to identify whether a tumour had high or low TIL burden, relative to the cohort's median or quartile TIL values – this second approach was based on the observation that, in many published studies that have demonstrated clinical relevance of TIL numbers, similar rank-based categorisation was used, often based on dichotomisation around cohort median value<sup>302</sup>.

For each of 47 LMS cases, digital microscopy images were taken of slides cut from a single tumour block and stained for H&E, CD3 and CD8. 20 x 1mm circular 'core' areas (total area. 15.7mm<sup>2</sup> - equivalent to approximately 50 HPF) were selected on H&E images, with the number of lymphocytes within the corresponding areas (TIL/core) on CD3- and CD8-stained slides digitally counted (**Figure 3.33A**). For each tumour, the average lymphocyte counts from each of every possible combination of 2 out of 20 cores, 3 out of 20 cores, and so on, were calculated (**Figure 3.3B**). The average lymphocyte count of all 20 cores was taken to represent the 'true' overall TIL burden of each tumour. For each of the

47 tumours, we assessed how many cores needed to be sampled in order for >80% of possible combinations to produce an estimated TIL burden that fell within each of three different thresholds: (i) +/-20% of true TIL burden, (ii) same side of cohort median or (iii) in same cohort quartile as true TIL burden across the entire cohort (**Figure 3.3C**).

A median of 11 cores (CD3 range 4-16, CD8 range 4-17) was required for >80% of estimated TIL burdens to fall within 20% of the corresponding tumour's true CD3+ or CD8+ TIL burden (**Figure 3.3D**). However, a median of only 1 core was required for >80% of estimated CD3+ or CD8+ TIL burdens to fall the same side of cohort median as the tumour's true TIL burden. Similarly, a lower number of cores (median of 5 and 3 cores for CD3 and CD8 respectively) were required for >80% of estimated TIL burdens to fall in the same cohort quartile as the corresponding true TIL burden. A minority of tumours required a greater number of cores for >80% of estimated TIL burdens to fall on the correct side of cohort median (8/47 and 6/47 requiring  $\geq 8$  cores for CD3 and CD8 respectively), primarily due to these tumours having true TIL burdens that lay close to median cut-off values (**Figure 3.3D**).

Taken together, these data indicate that a large and likely impractical number of TMA cores (11 cores) must be sampled in order to accurately recapitulate the true burden of infiltrating T lymphocytes in LMS. However, many studies that have described association between TILs and clinical outcome ultimately reduced continuous data on TIL numbers into ordinal categories that reflect relative rather than absolute degree of infiltration e.g. 'high' or 'low' infiltration<sup>302</sup>. We found that sampling only 1 core was sufficient to correctly identify a majority of tumours as having a 'high' or 'low' degree of infiltration, while 2-5 cores was adequate to correctly identify a majority of tumours as having 'very low', 'low', 'high' or 'very high' degree of TIL infiltration, based on categorical cut-offs at cohort quartiles. These data demonstrate that TMAs that employ a conventional number of cores (i.e. 1-3) would be sufficiently representative for studies where ordinal categorisation of TIL burden is planned. However, should precise quantification of absolute TIL burden be desired, a conventional TMA approach is not likely to be representative.

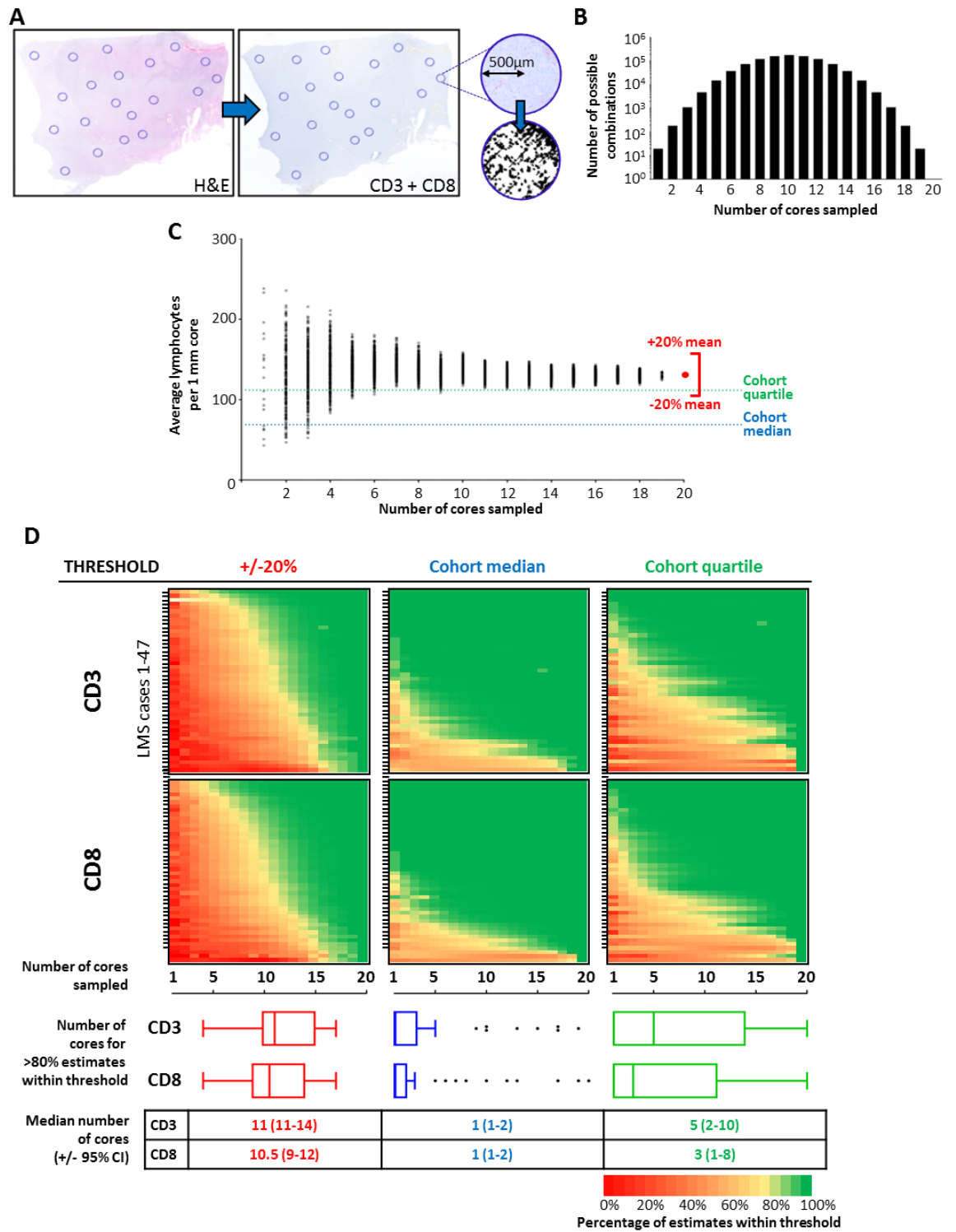


**Figure 3.3: Optimal number of TMA cores relates to required degree of accuracy for assessment of lymphocyte infiltration**

*(legend overleaf)*

**A.** Overview diagram of process for selection of 'virtual TMA cores' and T lymphocyte counting. For each of 47 LMS, a digital H&E slide from a representative block was marked for 20 x 1mm diameter areas, encompassing spatial and any morphological heterogeneity with section. Selected core areas were mapped on to corresponding CD3 and CD8-stained sections. Core areas were isolated as individual digital images. Number of IHC-positive lymphocytes in each core area was digitally counted.

**B.** Bar chart showing number of possible combination of cores when between 2-20 cores are assessed. Average lymphocyte counts per core (TIL/core) were calculated for all possible combinations for each tumour.

**C.** Dot plot showing all possible average lymphocyte counts (number indicated in **B**) for a single exemplar tumour when 1-20 cores are selected. Average of all 20 cores (red dot) taken to be represent overall TIL burden for that tumour. For each tumour, the number of cores that needed to be sampled in order for >80% calculated averages to fall within either (i) +/-20% of 'true TIL burden' for corresponding tumour, (ii) correct side of cohort median TIL value (CD3 median = 69 TIL/core; CD8 median = 59 TIL/core) , or (iii) within correct cohort quartile (CD3 IQR = 18-110 TIL/core; CD8 IQR = 19-121 TIL/core). In this illustrated exemplar case, overall CD3+ TIL burden is above 3rd quartile (Q75 = 110).

**D.** Colour plots indicating percentage of systematically calculated average lymphocyte counts from all possible combinations of between 1-20 cores to fall within stated threshold (+/-20%, cohort median or cohort quartile) Tukey box and tail plots indicate cohort distribution of number of cores required for >80% of estimates to fall within stated threshold. Table summarises cohort median number of cores required >80% of estimates to fall within stated threshold (+/- approx. 95% confidence interval).

### **3.2.5 Triplicate TMA cores provide adequate sampling for the classification of LMS as containing high or low TIL burden.**

To validate our finding from the vTMA experiment that a conventional number of TMA cores was sufficient for categorising tumours as having high or low TIL burden, we constructed a physical TMA (pTMA) that included triplicate 1mm cores from sampled tumours. 44/47 LMS were included in this TMA. In 11/44 tumours, the same block was used for pTMA construction as was used for the vTMA model. In 33/44 tumours, due to insufficient tissue depth remaining in blocks used for the vTMA, a different tumour block from the same specimen was used for core sampling for the pTMA.

We first assessed if triplicate cores in the pTMA produced inaccurate estimates of true TIL burden of the tumour specimen (defined as average of all 20 cores from the vTMA experiment) (**Figure 3.4A-C**). When comparing pTMA-derived estimates TIL burden to the associated true TIL burden, an overall positive bias (+46% for CD3, +9% for CD8) indicated that pTMAs produced a modest overestimate of true TIL burden. However, consistent with the results from the vTMA analysis, 95% limits of agreement (LOA - an estimate of the size of sampling error) across all 44 LMS were wide, meaning that, for any pTMA-derived estimated TIL burden, there was 95% confidence that the true TIL burden was anything from 6-8 times less or 9-14 times more than the estimate. These levels of agreement were improved when analysis was limited to the 11 tumours where pTMA and vTMA were taken from the same tumour blocks), but still reflected that estimates were associated with 95% confidence of true TIL burden falling between 2 times less or 3 times more the estimated value.

In the vTMA experiment, a median of 1 core was needed to correctly identify a LMS tumour has having a high or low CD3+ or CD8+ TIL burden, as defined by position above or below cohort median value. When triplicate cores within the pTMA were used to similarly assign tumours as having 'high' or 'low' TIL burdens (as per cohort median values, shown in **Figure 3.3C**), we found good levels of agreement with assignment versus the true TIL burden (**Figure 3.4D-E**). Across all 44 tumours represented in the pTMA, accuracy (i.e. percentage of tumours that were correctly identified as having high or low true TIL burden) was 70.5% and 90.9% for CD3 and CD8 respectively. When limited to the 11 cases where

the same block was used for both vTMA and pTMA, accuracy for correct identification of CD3+ or CD8+ TIL burden was improved to 72.7% and 100% respectively. Accuracy for the 36 cases where different blocks were used between vTMA and pTMA was 70.0% and 87.9%. These results demonstrate that, for a large majority of tumours in the cohort, triplicate TMA cores were adequate for correctly identifying whether the tumour had a high or low TIL burden. The accuracy of the pTMA was only modestly improved in tumours where the same tumour block was sampled for vTMA and pTMA, again indicating that there is only a minor contribution of intra-tumoural heterogeneity between related blocks to sampling error.

Consistent with the conclusions of the vTMA experiment (Figure 3D), these findings show that the inclusion of a conventional number of replicate cores from the same tumour (i.e. 3 cores) in a pTMA provides sufficient representation of overall tumour TIL burden to accurately categorise tumours as having 'high' or 'low' TIL numbers, and that this accuracy is maintained between different blocks from the same tumour. However, this conventional number of cores can produce significant inaccuracy in estimating the absolute TIL burden within a tumour.

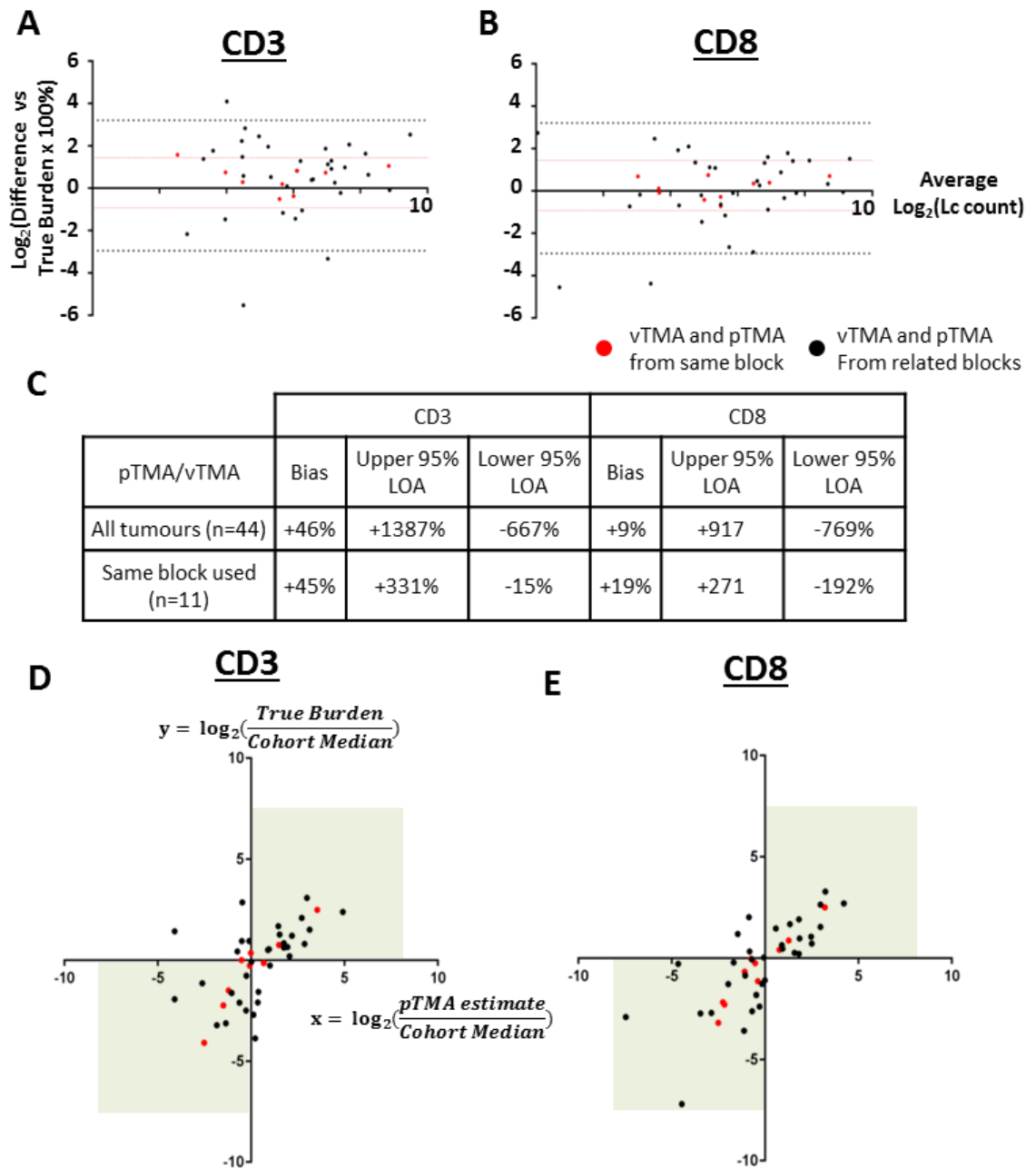


**Figure 3.4: Triplicate TMA cores can identify tumours as having a high or low TIL burden, but do not accurately estimate precise TIL numbers**

*(legend overleaf)*

Bland Altman plots show percentage difference of pTMA-derived estimated TIL burdens compared to true TIL burdens for **(A)** CD3 and **(B)** CD8. 95% limits of agreement (LOA) for all 44 tumours shown by black dotted lines, 95% LOA for 11 tumours with pTMA and vTMA from same block shown by red dotted lines. LOA and biases from these plots are summarised in **(C)**. Dot plots show ratio of pTMA-derived estimated TIL burden:cohort median value (x axis) plotted against ratio of true TIL burden:cohort median value (y axis) for **(D)** CD3+ and **(E)** CD8+ TILs. Ratio >0 indicates tumour identified as 'High TIL burden' (i.e above cohort median). Ratio <0 indicated tumour identified as 'Low TIL burden'. Values in top right or bottom left quadrant (green boxes) indicate consistent TIL categorisation based on pTMA-derived estimate and true TIL burden. Red dots represent tumours where pTMA and vTMA sampled from same tumour block, black dots represent tumours where pTMA and vTMA were sampled from different blocks from same tumour specimen.

### 3.3 Discussion

In this pilot study, we characterised the TIL burden in a cohort of primary LMS tumours and demonstrated that there is evidence for both inter- and intra-tumoral heterogeneity in this STS subtype. We found that the TIL burden in LMS is generally low compared to immune-active cancer types, but that a subset of LMS exhibit heavier lymphocytic infiltration. Limited reported data on TIL burden are available in LMS and other STS subtypes to which this finding can be compared<sup>203,216</sup> (**see Chapter 1.5.2 and 1.5.3**), although inferential cell fraction results from the TCGA gene expression data set indicate that STS overall, and LMS specifically, contain a lower lymphocyte cell fraction than many other solid cancer types<sup>201</sup>. Large intra-tumoural variation in TIL burden was observed in a minority of cases, particularly in tumours with a greater overall degree of TIL burden. However, across the whole cohort, the degree of intra-tumoural heterogeneity was small relative to the inter-tumoural differences in overall TIL burden between cases within the cohort. Additionally, our investigation of both a virtual and physical TMA indicates that a conventional and practical number of 1mm cores (between 1-3) provide sufficient representation for ordinal categorisation of tumours as having either a high or low degree of lymphocyte infiltration. These data indicate that intra-tumour heterogeneity of TIL burden may not be a great source of confounding sampling error and that TMAs represent a feasible and appropriate research tool for immune profiling studies in LMS.

The applicability of these findings to other STS or epithelial cancers remains to be determined. Intra-tumoural heterogeneity in the immune microenvironment has been described in numerous epithelial cancer types, both within primary lesions and between different metastatic sites<sup>174,286–288,290</sup>. In breast cancer, a virtual TMA methodology was used to demonstrate that agreement between TMA and whole tumour assessment of TIL burden plateaued when sampling any more than four 0.6mm cores<sup>298</sup>. Interestingly, the degree of this correlation varied depending upon breast cancer subtype – Her2+ breast cancers had generally worse correlation, indicating greater spatial heterogeneity in TIL distribution – and that a greater degree of TIL ‘skewness’ (i.e. greater spatial heterogeneity) was itself independently associated with worse prognosis. This suggests that spatial uniformity of TIL burden may vary between different cancer types and within different molecular and histological subtypes, and that spatial distribution itself

may provide clinically relevant information – both findings that warrant caution when adopting TMA methods for assessing TIL burden.

Our data indicate that TMAs can provide a degree of representation of overall tumour TIL burden which is adequate for ordinal categorisation into high or low subgroups. These findings informed my experimental design to investigate the immune microenvironments of larger cohorts of LMS and two other genomically-complex STS subtypes (UPS and DDLPS). Firstly, when constructing TMAs for use in IHC-based immune profiling, we employed 1mm TMA cores sampled in quadruplicate from randomly selected areas of viable tumour within single tumour blocks in order to provide a sampling accuracy that would be at least sufficient to identify high or low TIL burdens. Secondly, we employed immune-related gene expression analysis as an orthogonal profiling technique wherein mRNA collected from full tissue sections was used for analysis, thus avoiding the potential for sampling bias related to core sampling when constructing and analysing TMAs.

## **Chapter 4: Characterising the immune microenvironment in genomically-complex STS subtypes**

### **4.1 Objectives**

In order to substantively add to available data on the character and potential clinical relevance of the immune microenvironment in LMS, UPS and DDLPS (**see Chapter 1.5.3**), retrospective, clinically-annotated cohorts of tumours controlled for clinical stage and treatment exposure were subjected to IHC-based assessment of TILs, PD-L1 expression and TAM (**see Chapter 2.2 for methods**). RNA extracted from these tumours was also used for expression analysis of a targeted panel of immune-related genes. Descriptive statistics were used to explore the inter-tumour variation in immune microenvironment characteristics and to assess for associations between immune and clinico-pathological characteristics. Unsupervised clustering analysis of gene expression data was used to discover immune-based tumour subgroupings in an unbiased fashion. These subgroups were then assessed for qualitative differences in integrated gene expression and IHC-based immune characteristics and associated clinico-pathological features.

### ***Contributions***

Study conception and design was the work of the candidate in conjunction with his supervisory team and the co-authors of the PROSPECTUS study protocol (**see Appendix 1**).

Identification, collection and curation of archival histological material and associated clinic data; digital microscopy image capture; NanoString PlexSet assay and data analysis; IHC and clinic data analysis; analysis of gene set functional annotation; figure generation were the work of the candidate.

TMA mark up and construction was performed by the candidate under the supervision of Dr Khin Thway, consultant histopathologist, The Royal Marsden, and with the assistance of Dr Cornelia Szecei, histopathology fellow, Frank McCarthy and Nafia Guljar, Scientific Officers.

Tumour RNA extraction and quality assessment was performed by the candidate with the assistance of Dr Cornelia Szecsei, Frank McCarthy, Nafia Guljar and Martina Millighetti, masters student.

Direct light and digital histological analysis and scoring was performed by the candidate and Dr Connie Szecsei, histopathology fellow, under the supervision and training of Dr Khin Thway.

IHC optimisation, FFPE slide cutting and staining was performed by staff of the ICR Histopathology Core Facility.

## 4.2 Results

### 4.2.1 Cohort identification

Retrospective search of a prospectively curated departmental database was used to identify patients with LMS or UPS referred to the Royal Marsden STS multidisciplinary team meeting (MDT) for definitive management of primary tumours. As histological subtype information for patients with LPS was not consistently recorded in this database, retrospective search of institutional histopathology specimen database was performed using SNOMED terms for DDLPS. Consolidated Standards of Reporting Trials (CONSORT) figures for identification of sub-cohorts for each histological subtype are shown in **Figure 4.1**.

244 patients with LMS were identified as having been referred to STS MDT between 01/01/2010 and 31/12/2015. 194 with UPS were identified within the same time period. Histological specimen for 372 unique patients with DDLPS were registered between 01/01/2009 and 31/12/2014 – of these, only the first 163 patients to be registered with the hospital were taken forward due to time constraints.

Medical notes and histopathology records were reviewed to identify patients for whom FFPE tumour blocks from resection specimen of primary tumours could be retrieved – for DDLPS, resection specimen of locally recurrent tumours were also included. Such material was not available for approximately 1 in 3 initially-identified patients. This attrition reflects the referral practice to the Royal Marsden STS MDT, where patients may have had initial treatment of primary disease at other centres. A proportion of cases were not retrievable from the specimen archive for unidentified reasons.

The adequacy of viable tumour content of all retrieved blocks was assessed through review of freshly cut H&E slides - tumours with insufficient viable tissue were excluded from the cohort. The remaining specimens were processed for IHC and gene expression analysis. Tumours that produced gene expression data that did not pass initial QC assessment were excluded from the cohort for analysis. This resulted in a final cohort of 266 tumours, consisting of sub-cohorts of 124, 72 and 70 patients with LMS, UPS and DDLPS respectively.

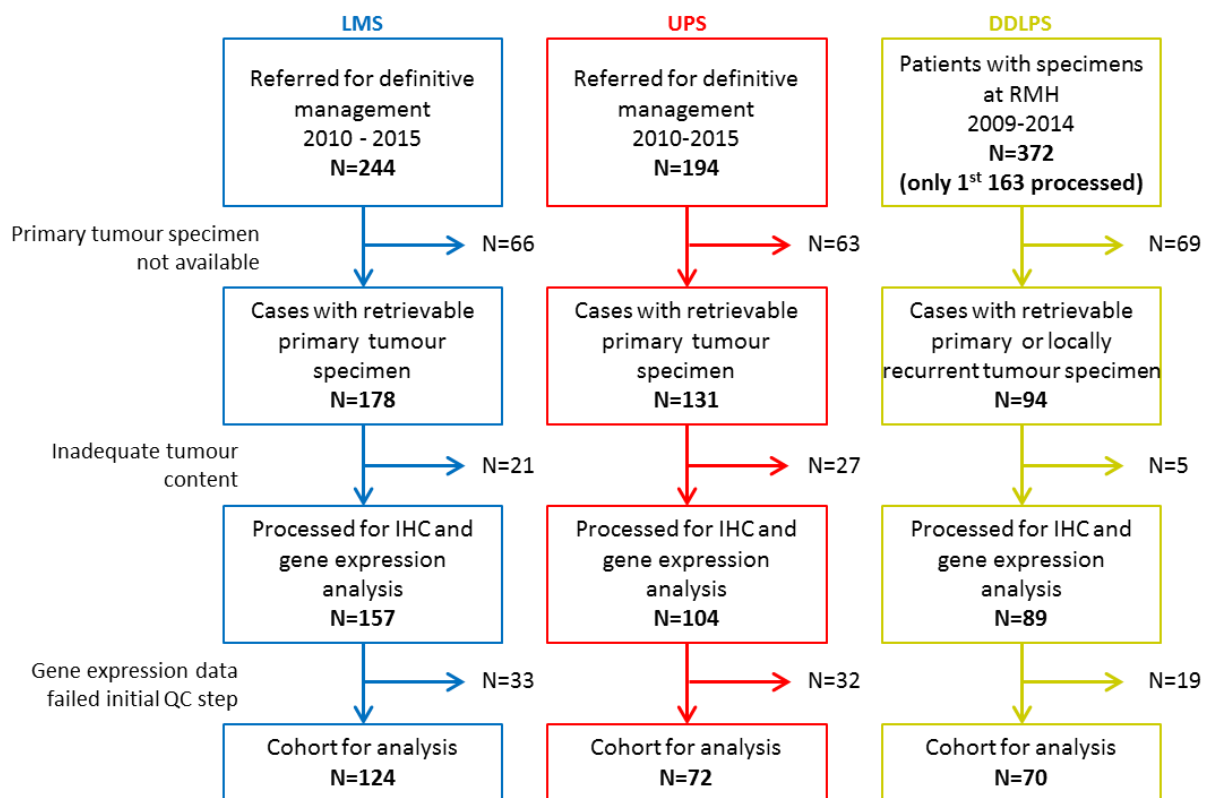


**Figure 4.1: CONSORT diagram of LMS, UPS and DDLPS sub-cohorts**

#### **4.2.2 Baseline Characteristics**

Baseline clinico-pathological characteristics of the LMS, UPS and DDLPS sub-cohorts are summarised in **Table 4.1**. A female preponderance in the LMS sub-cohort was consistent with previous reports of higher incidence of non-cutaneous LMS in woman and also reflected the inclusion of uLMS<sup>14</sup>. An overrepresentation of men in the DDLPS sub-cohort may have been due to chance, given roughly equivalent incidence by gender reported in the literature<sup>303</sup>. Patients with UPS were significantly older than those with LMS or DDLPS (**Supplemental Figure 4.1A**), with an average age 10 years older (71 years in UPS vs. 61 years in both LMS and DDLPS). This finding is consistent with literature that indicates a later age of onset in UPS compared to the other subtypes<sup>14,18,19</sup>. The LMS sub-cohort was evenly split between extremity and intracavity site of origin, reflecting the range of presentation of the disease. The preponderance for higher grade tumours and underrepresentation of uLMS in the cohort likely reflects referral patterns to the Royal Marsden. As expected, primary UPS and DDLPS showed preponderance for the extremities and retroperitoneum. The DDLPS sub-cohort had significantly larger maximum tumour dimensions (encompassing both WD and DD components) than UPS and LMS (**Supplemental Figure 4.1B**), reflecting the frequent pattern of presentation with large retroperitoneal WD/DDLPS tumours. Across the three histological subtypes, intracavity/RP tumours were significantly larger than extremity tumours (average maximum dimension 17.8cm (95% CI 15.8-19.8) vs. 8.9cm (95% CI 8.0-9.8),  $p < 0.0001$ ) (**Supplemental Figure 4.1C**). As per selection criteria, the large majority of LMS and UPS were localised tumours. In the DDLPS, 28% of tumours were locally recurrent, reflecting the proportion of patients that had undergone prior resection for WD and/or DD disease). Reflecting standard practice to use adjuvant radiotherapy for the treatment of high grade, large STS arising in the extremities, a majority of patients were UPS received post-operative radiotherapy, while a smaller proportion of patients with LMS (which were more likely to be of lower grade, smaller and less likely to arise in the extremities) and DDLPS (which were intracavity in the large majority of patients) received adjuvant therapy. In the DDLPS sub-cohort, 69% of tumours contained a predominant dedifferentiated component, whereas in 31%, the dedifferentiated component accounted for the minority of tumour bulk.

		LMS N=124	UPS N=72	DDLPS N=70
<b>Gender</b>	Male	45 (36.3%)	38 (52.8%)	44 (62.9%)
	Female	79 (63.7%)	34 (47.2%)	26 (37.1%)
<b>Age (years)</b>	Average (range)	61 (29 - 87)	71 (26-89)	61 (34 - 86)
	<50	27 (22.3%)	5 (6.9%)	13 (18.6%)
	50-70	56 (44.6%)	21 (29.2%)	40 (57.1%)
	>70	41 (33.1%)	46 (63.9%)	17 (24.3%)
<b>Site of origin</b>	Extremity,trunk,head	56 (45.2%)	67 (93.1%)	11 (15.7%)
	Intracavity/RP	68 (54.8%)	5 (6.9%)	59 (84.3%)
	- uterine	-12 (17.6%)	NA	NA
	- non-uterine	-56 (82.4%)	NA	NA
<b>FNLCC Grade</b>	1	16 (12.9%)	0	6 (8.6%)
	2	58 (46.8%)	6 (8.3%)	37 (52.9%)
	3	50 (40.3%)	66 (91.7%)	27 (38.6%)
<b>Stage at surgery</b>	Localised	115 (92.7%)	69 (95.8%)	46 (65.7%)
	Locally recurrent	2 (1.6%)	1 (1.4%)	20 (28.6%)
	Metastatic	7 (5.6%)	2 (2.8%)	4 (5.7%)
<b>Max tumour dimension (cm)</b>	Average (range)	9.4 (0.7-29.0)	10.4 (1.5-45.0)	23.2 (3.0-57.0)
	<5cm	23 (18.5%)	10 (13.9%)	1 (1.4%)
	>=5-<10cm	58 (46.8%)	32 (44.4%)	7 (10.0%)
	>=10-<15cm	19 (15.3%)	14 (19.4%)	12 (17.1%)
	>=15cm	24 (19.4%)	16 (22.2%)	50 (71.4%)
<b>Post-op Rx</b>	Yes	22 (17.7%)	41 (56.9%)	7 (10.0%)
	No	102 (82.3%)	31 (43.1%)	63 (90.0%)
<b>Histology:</b>	Predominant DD	NA	NA	48 (68.6%)
	Predominant WD			22 (31.4%)
<b>Prior surgery:</b>	Any	NA	NA	24 (34.3%)
	For WD disease			20 (28.6%)
	For DD disease			16 (22.9%)

**Table 4.1: Baseline characteristics of LMS, UPS and DDLPS sub-cohorts**

### 4.2.3 Summary of cohort survival

Median duration of follow-up and OS and adDFS event rates for LMS, UPS and DDLPS sub-cohorts are summarised in **Table 4.2**. An overview of patient follow-up and survival is shown in **Figure 4.2**. While there was no significant difference in overall and adDFS between sub-cohorts, a trend toward worse OS in UPS was observed, consistent with widely-reported poor prognosis of these higher grade, undifferentiated tumours<sup>18</sup> (**Supplemental Figure 4.2**). In keeping with reported relapse rates for resected early stage STS, approximately half of all patients across all subtypes developed advanced disease<sup>3</sup>. As expected, tumour grade and stage were significantly associated with adDFS and OS, while higher age at time of surgery was a significant adverse factor for OS but not adDFS (**Supplemental Figure 4.3**). There was no significant association between gender and survival.

	LMS	UPS	DDLPS
Median follow-up (years)	5.2	5.0	6.3
Overall survival event rate	50.8%	59.7%	60.0%
Median overall survival (years)	5.3	2.8	4.0
Advanced disease-free survival event rate	57.3%	48.6%	51.4%
Median advanced disease-free survival (years)	2.8	2.5	4.6

**Table 4.2: Summary of follow-up and event rate in 3 sub-cohorts**

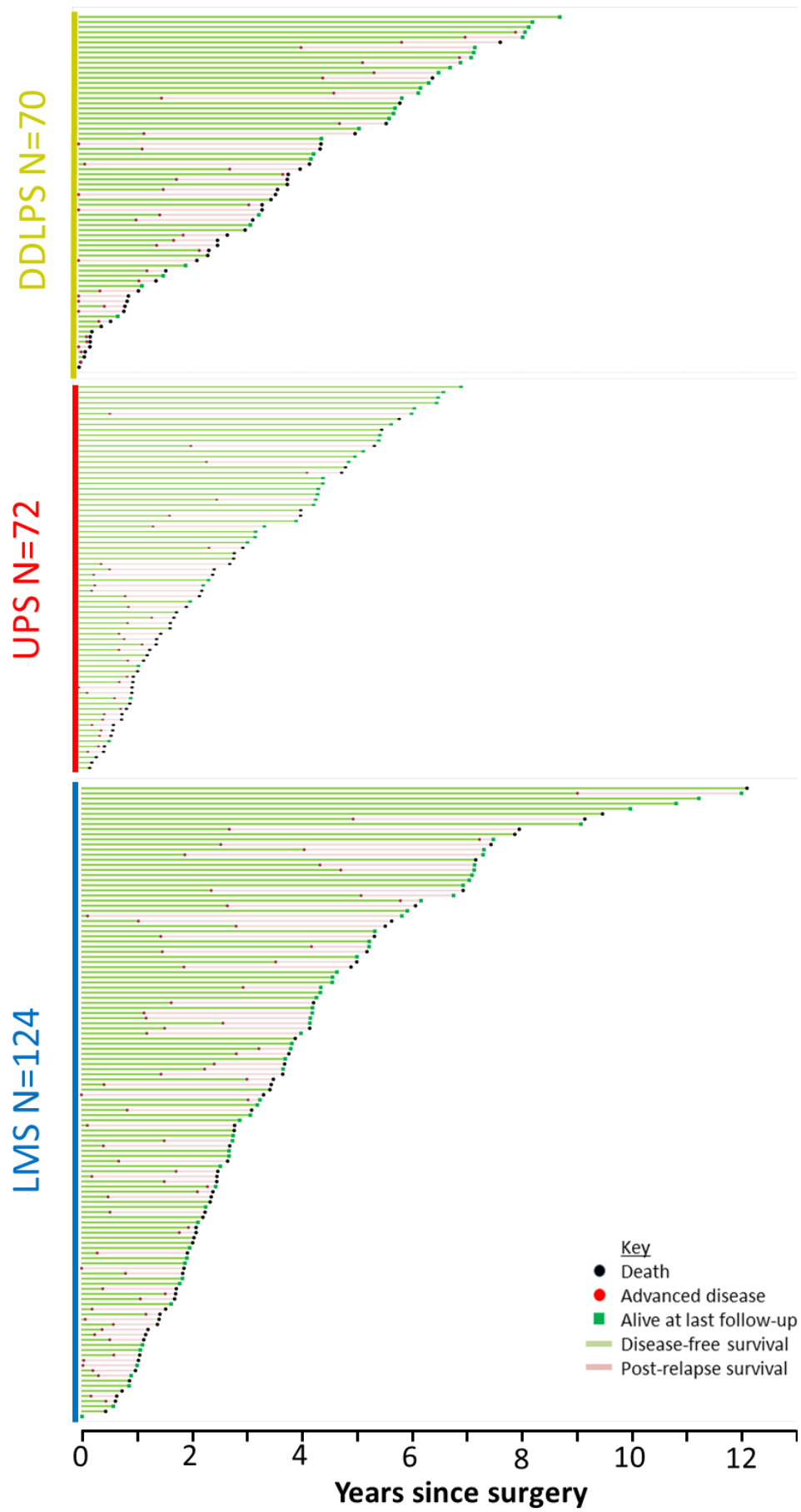


Figure 4.2: Swimmer's plots of LMS, UPS and DDLPS sub-cohorts

#### **4.2.4 IHC-based analysis of immune microenvironment**

##### **4.2.4.1 TIL**

To quantify the amount of T lymphocyte infiltration in LMS, UPS and DDLPS, we used antibodies against three commonly expressed, T-lymphocyte specific antigens. CD3 is a ubiquitously-expressed component of the TCR complex and serves as a specific and global marker of T lymphocytes. CD4 is a co-receptor of within the TCR whose expression in lymphocytes is specific to T helper cells. CD8 is a co-receptor of the TCR whose expression in lymphocytes is specific to cytotoxic T cells. The number of TIL with positive membranous staining was counted in TMA sections, with the average value across replicate TMA cores from the same tumour calculated and stated in terms of average TIL/mm<sup>2</sup>. This number was taken to represent the degree of tumour infiltration by global (CD3), helper (CD4) and cytotoxic (CD8) T cells.

As demonstrated in **Figure 4.3**, there was wide variation in the extent of T lymphocyte infiltration between individual tumours in the 3 sub-cohorts. In many tumours, a total or near-total absence of infiltrating T cells was seen, while in others, average TIL/mm<sup>2</sup> values of hundreds to thousands were seen. The distribution of TIL values showed positive skew, indicating that relatively fewer cases in each sub-cohort demonstrated these higher TIL values. Positive skew was least pronounced for all TIL markers in the UPS sub-cohort, indicating that that proportionately more UPS had higher TIL values than in the LMS or DDLPS populations. Representative microscopy images of different degrees of lymphocyte infiltration are shown in **Supplemental Figure 4.4**.

Values for CD3 TILs were expectedly higher than those for CD4 or CD8 TILs, reflecting the hierarchical relationship between CD3-positive and CD4- or CD8-positive lymphocytes. This relationship was also seen in the fact that median values for average CD3 TILs were approximately the sum of corresponding CD4 and CD8 TILs. A strong correlation between matched CD3, CD4 and CD8 TIL values was seen (CD3 v CD4 R=0.84; CD3 v CD8 R=0.92; CD4 v CD8 R=0.76; All p<0.0001 – **Supplemental Figure 4.5**). CD8 TIL values were significantly higher in all 3 sub-cohorts than CD4 TILs (unpaired t tests p<0.0001 for each sub-cohort) (**Supplemental Table 4.1**).

When comparing average TIL/mm<sup>2</sup> values between LMS, UPS and DDLPS sub-cohorts, the only significant difference was seen in CD4 TIL values (1-way ANOVA p=0.039) – on post-hoc multiple comparison testing, this was related to a significant difference in CD4 values between LMS and DDLPS sub-cohorts (adjusted p=0.0302). There were otherwise no significant differences in TIL counts between LMS, UPS or DDLPS when Log2-transformed values were compared by 1-way ANOVA (**Supplemental Table 4.2**).

These data demonstrate that LMS, UPS and DDLPS are variably infiltrated by T lymphocytes, with cytotoxic T lymphocytes more prevalent than T helper lymphocytes. Low T cell infiltrates were more commonly seen than heavy infiltrations in all 3 tumour types.

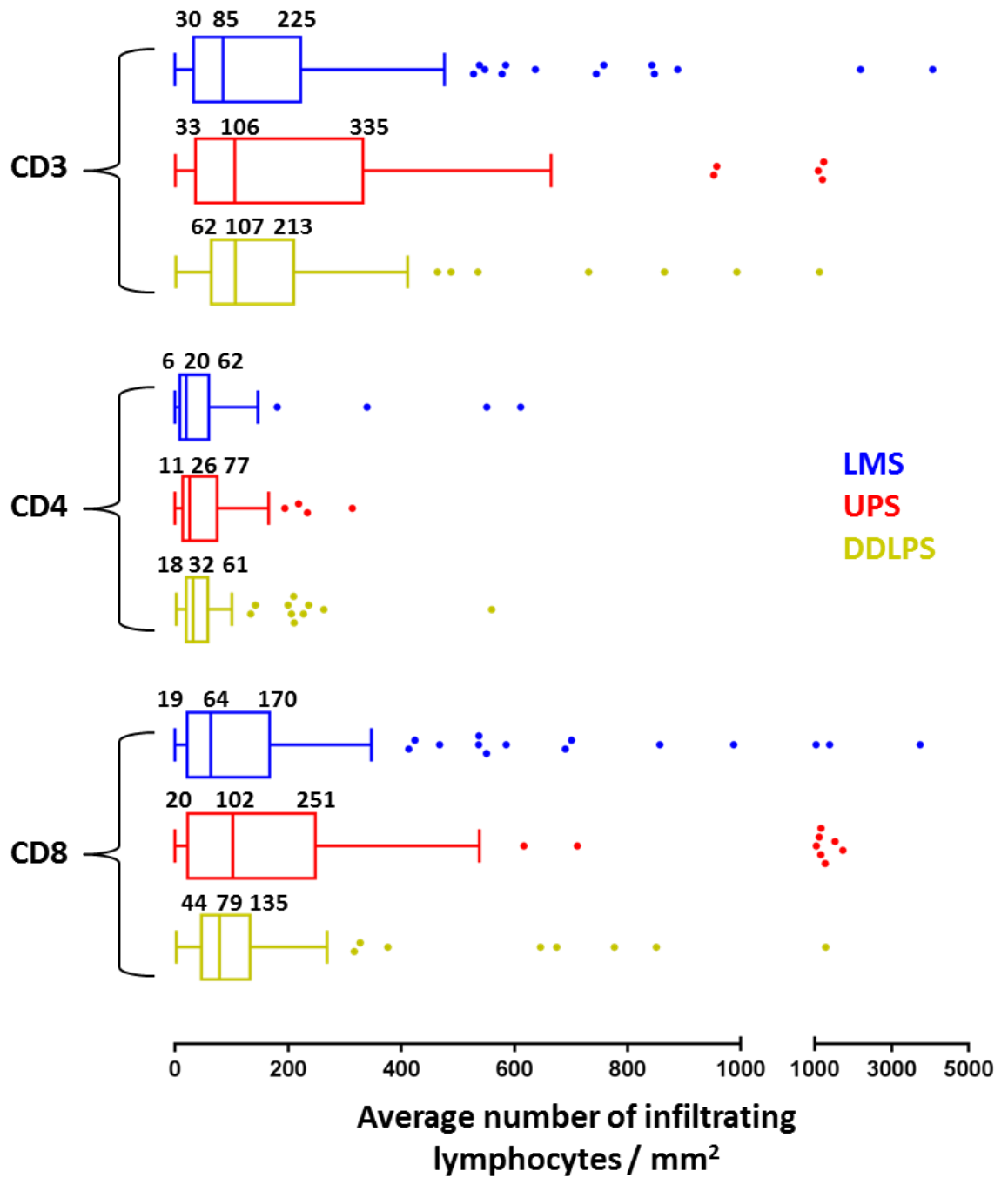


**Figure 4.3: Distribution of TIL densities within STS cohorts.**

Tukey box plots demonstrate average density (TIL/mm<sup>2</sup>) of CD3, CD4 and CD8-staining lymphocytes in LMS, UPS and DDLPS cohorts. 1<sup>st</sup>, 2<sup>nd</sup> and 3<sup>rd</sup> quartile average TIL/mm<sup>2</sup> values stated.

#### 4.2.4.2 Macrophages

To quantify the degree of infiltration by TAM in LMS, UPS and DDLPS, we performed IHC of TMA slides using an antibody against CD68, a scavenger receptor family protein that is highly expressed by tissue macrophages within the cytoplasm and cell membrane. Accurate and reproducible counting of individual TAM was challenging due to the morphological heterogeneity of individual TAM, and so a semi-quantitative scale described by Lee *et al*<sup>19</sup> was used to assess the degree of macrophage infiltration. Each stained TMA core was assigned a score between 0 and 3, with the average score across replicate TMA cores from the same tumour calculated (**Supplemental Figure 4.6**).

The distribution of these scores within LMS, UPS and DDLPS sub-cohorts are illustrated in **Figure 4.4**. Almost all tumours demonstrated at least some infiltration by CD68-positive macrophages. Total concordance in CD68 score between replicate TMA cores was seen in 66% of tumours, with a single core discordant by 1 point (e.g. 1 core scored 2, with all other related cores scoring 3) in 25%, and a greater than 2 point discordance (i.e. some areas scored 1 and others scored 3) seen in 9%. This suggests that, in a majority of tumours, there was intratumoural homogeneity in density of infiltrating macrophages.

Uniformly dense intra-tumoral macrophage infiltration (average CD68 score 3) was seen in 38%, 69% and 64% of LMS, UPS and DDLPS respectively. Non-dense infiltration (average CD68 score <2.0) was seen in 26%, 10% and 6% of LMS, UPS and DDLPS respectively. Average CD68 scores were significantly lower than in the LMS sub-cohort than those in the UPS (Kruskal-Wallis test  $p < 0.0001$ ) and DDLPS (Kruskal-Wallis test  $p = 0.0001$ ) sub-cohorts.

CD68 score was significantly associated with T cell infiltration, with tumours with dense CD68-positive macrophage infiltration also demonstrating the higher TIL counts than tumours with less dense CD68-positive infiltrates (**Supplemental Figure 4.7**)

These data indicate that a large majority of UPS and DDLPS have dense infiltration by CD68-positive macrophages. Dense infiltration is also seen in LMS, but a larger proportion of tumours in this sub-cohort had non-dense infiltration.

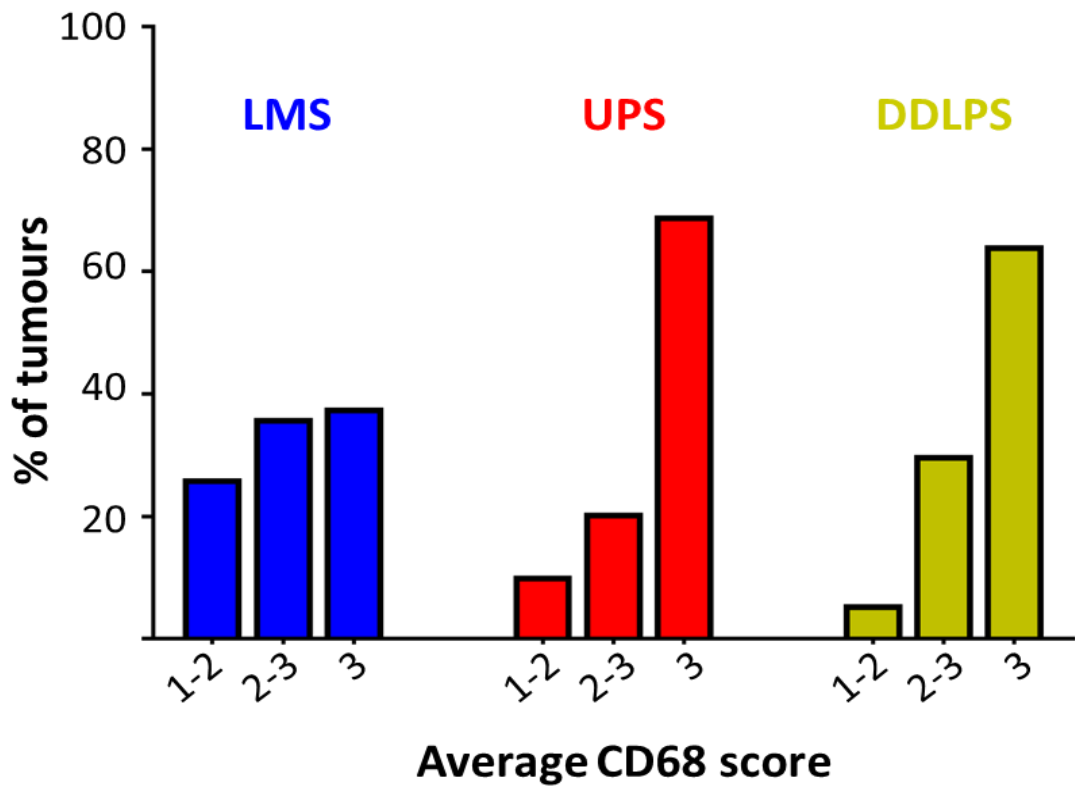


Figure 4.4: Distribution of average CD68 scores in LMS, UPS and DDLPS sub-cohorts

#### 4.2.4.3 Tumour expression of PD-L1

To quantify the expression of the immune checkpoint protein PD-L1 by tumour cells within LMS, UPS and DDLPS, we assessed the extent of tumour cell membranous and/or cytosolic staining of TMA cores by an anti-PD-L1 antibody. Each TMA core was scored on a semi-quantitative scale that account for frequency and intensity of tumour cell staining. Given generally scanty presence of staining within the studied cohort, we took the maximum score of any of the studied replicate TMA cores to represent the staining score for that tumour. Example images of different degrees of tumour PD-L1 staining are shown in **Supplemental Figure 4.8**.

The distribution of tPD-L1 scores within LMS, UPS and DDLPS sub-cohorts are illustrated in **Figure 4.5**. A high proportion of tumours in each sub-cohort showed no evidence of tumour cell expression of PD-L1 (56%, 42% and 54% with maximum tPD-L1 score of 0 in LMS, UPS and DDLPS sub-cohorts respectively). Of the tumours with any evidence of tPD-L1 positivity, a majority showed only very limited staining (staining score 1-2: <1% cells with weak or moderate staining, or 1-10% of cells with weak staining – 30%, 39% and 33% in LMS, UPS and DDLPS sub-cohorts respectively). 15%, 19% and 13% of LMS, UPS and DDLPS respectively showed higher levels of tPD-L1 expression (staining score of 3 or more). Strong expression of PD-L1 (staining score 5-6) was seen 3%, 6% and 6% of LMS, UPS and DDLPS respectively. No significant difference was detected in maximum tPD-L1 scores between LMS, UPS and DDLPS (Kruskal-Wallis test  $p=0.16$ ).

Of the 129 of tumours across all 3 sub-cohorts that had a maximum tPD-L1 score > 0, only 10 (8%) had full concordance of max tPD-L1 score across all replicate TMA cores. Of the 42 tumours with a maximum staining score of 3 or more, 19 (45%) had at least one replicate TMA core in which tumour PD-L1 staining was absent.

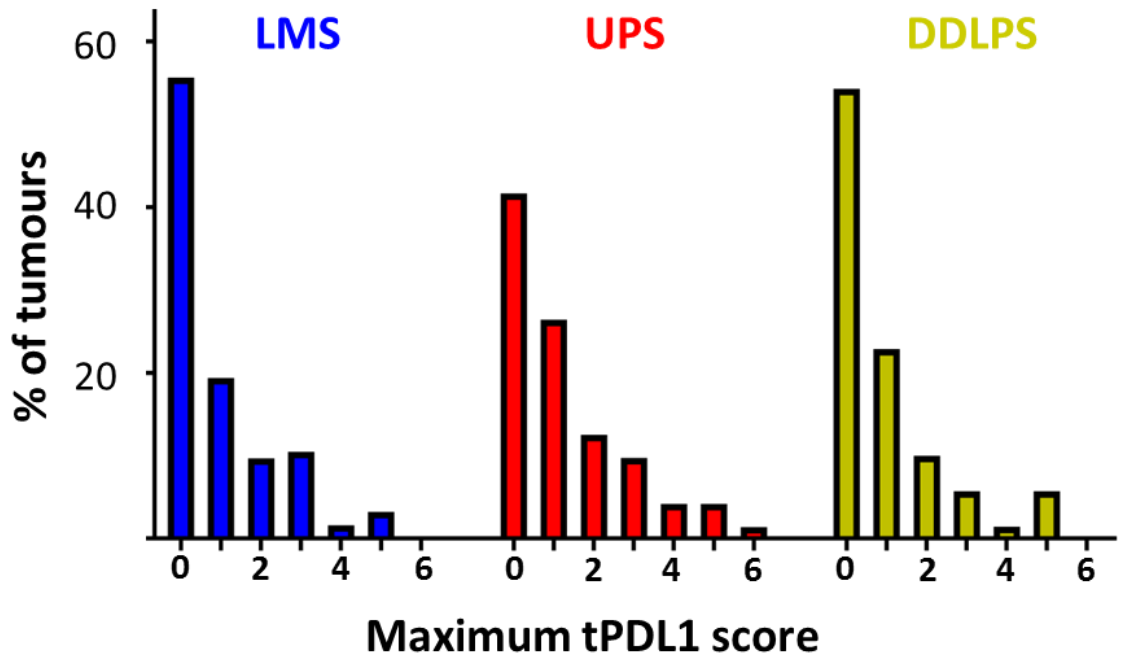


Figure 4.5: Distribution of maximum tumour PD-L1 scores in LMS, UPS and DDLPS sub-cohorts

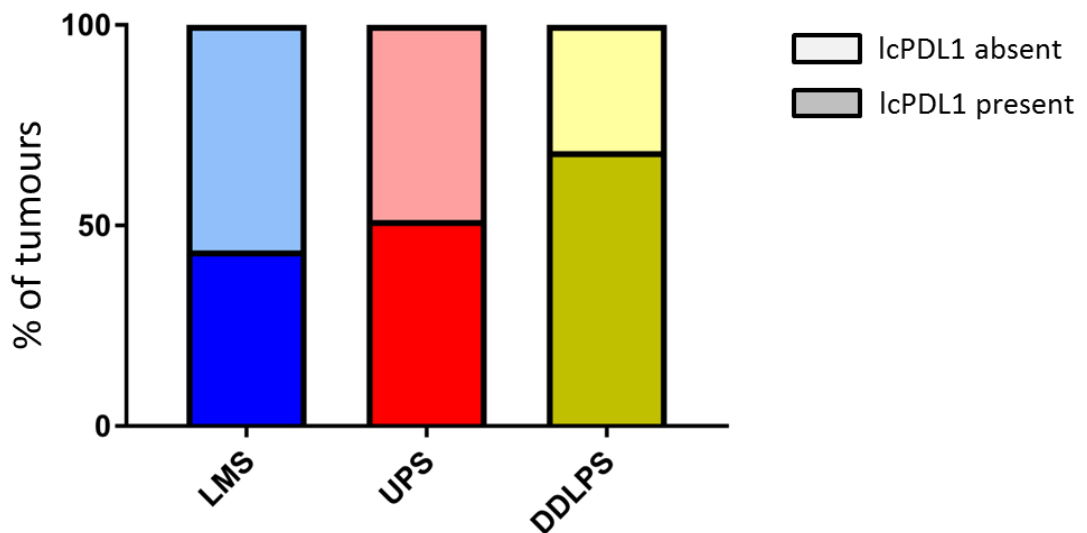


Figure 4.6: Proportion of tumours with presence or absence of PD-L1-staining leucocytes in LMS, UPS and DDLPS sub-cohorts.

Tumour PD-L1 score was significantly associated with T cell infiltration. Tumours with max tPD-L1 score of 0 had significantly lower average TIL/mm<sup>2</sup> than tumours with tPD-L1 positivity (**Supplemental Figure 4.9A**). Average CD68 score was also associated with max tPD-L1 score – tumours with dense CD68 infiltrates were more likely to be positive for PD-L1 expression (**Supplemental Figure 4.9B**)

These data indicate that a majority of LMS, UPS and DDLPS exhibit no or very limited tumour expression of PD-L1. A greater proportion of UPS showed some evidence of PD-L1 expression compared to LMS and DDLPS. Strong tumour expression of PD-L1 was rare and more frequently seen in UPS and DDLPS compared to LMS. When tumour PD-L1 staining was present, degree of positivity was often variable between related TMA cores, indicating spatial heterogeneity in tumour

#### *4.2.4.4 PD-L1 expression by tumour-infiltrating leucocytes*

In parallel to assessment for tumour cell expression of PD-L1, we assessed for the presence of leucocytes exhibiting membranous and/or cytosolic expression of PD-L1. Given the quantitative and qualitative variation in leucocyte infiltration between individual tumours and the associated challenges in counting individual PD-L1-staining cells, we assigned a binary categorisation to each TMA core as having PD-L1 staining leucocytes present or absent.

PD-L1-staining leucocytes were present in 44%, 51% and 69% of LMS, UPS and DDLPS respectively (**Figure 4.6**). The presence of PD-L1-positive leucocytes was associated with higher numbers of TILs, higher density infiltration by CD68-positive macrophages, and tumour expression of PD-L1 (**Supplemental Figure 4.10A-C**).

#### *4.2.4.5 Association of immune markers with baseline clinic-pathological characteristics*

Across the 3 sub-cohorts, tumour grade was significantly associated with average C68 score and maximum tPD-L1 score, with higher grade tumours more likely to have dense CD68-positive macrophage infiltration and to exhibit evidence of tumour cell expression of PD-L1 (**Supplemental Figure 4.11A-B**). Low grade

tumours had significantly lower numbers of CD3- and CD4-positive TILs than intermediate or high grade tumours (**Supplemental Figure 4.11C**).

Tumours originating from the extremities were significantly more likely to have dense CD68-positive macrophage infiltration compared to intra-cavity tumours, although this may reflect the preponderance of UPS tumours, the subtype with highest rate of dense CD68+ infiltrates, for the extremities (**Supplemental Figure 4.12A**). In the LMS sub-cohort, there was no significant difference in CD68 infiltration between extremity or intra-cavity tumours (**Supplemental Figure 4.12B**). There was no association between tumour site of origin and tPD-L1 or TIL values (**Supplemental Figure 4.12C-D**).

There was no significant association of any immune microenvironment component with patient age or gender (**Supplemental Figure 4.13 and 4.14**). AJCC stage III tumours were more likely to have dense CD68 infiltrates and tumour expression of PD-L1 than stage I-II or IV tumour (**Supplemental Figure 4.15**) - this finding likely reflects the marked imbalance in stage distribution, with a large majority of cases stage III.

In the DDLPS sub-cohort, tumours with a predominant dedifferentiated component were significantly more likely to exhibit tumour PD-L1 expression than those with a predominant well-differentiated component (**Supplemental Figure 4.16A**). There was no significant difference between DD and WD predominant tumours in terms of CD68-positive or T cell infiltrates (**Supplemental Figure 4.16B-C**). There was no significant difference in any immune component between DDLPS that had undergone prior resection compared to no prior resection (**Supplemental Figure 4.17**).

Collectively, these results indicate that the presence of an immune-active microenvironment (i.e higher numbers of TILs and infiltrating macrophages, and presence of PD-L1-expressing cells) was more commonly seen in higher grade, less differentiated sarcomas.

#### ***4.2.5 Targeted gene expression-based profiling of the immune microenvironment***

In addition to IHC-based analysis of infiltrating immune cells and checkpoint protein expression, we performed targeted expression analysis of immune-related genes to provide orthogonal assessment of the immune microenvironment in STS subtypes with complex karyotypes. Total RNA was extracted from full tumour sections taken from the same samples as used in TMA construction for IHC analysis. This tumour RNA was then used as input for expression analysis of 21 target and 3 housekeeper genes using a customised NanoString PlexSet Codeset (**Table 4.3**). Target genes were selected on the basis of either corresponding to the proteins examined by IHC, providing further information relating to functional sub-classification of immune cells studied in the IHC experiment, or immune checkpoint proteins or lymphocyte co-stimulatory receptors that are under active research interest as immune-therapeutic targets but for which expression data in STS are limited<sup>304</sup>. Housekeeper genes were selected from the list of 40 that are included in the PanCancer Pathways codeset, with 3 genes selected on the basis of housekeeper performance in the RMH-SARC cohort and LMS cases within TCGA-SARC (**Supplemental Figure 4.18**).

<b>21 gene panel assessed using NanoString PlexSet</b>	
<b>Gene</b>	<b>Annotation</b>
CD3G	T cell receptor
CD4	Helper T cell receptor
CD8A	Cytotoxic T cell receptor
FOXP3	Regulatory T cell-related transcription factor
CD68	Macrophage surface marker
CD163	'Alternatively activated' M2 macrophage marker
NCAM1 (CD56)	NK cell marker
KIR3DL1	NK cell surface receptor
LAMP3	Activated dendritic cell marker
HLA-A	MHC class I molecule – antigen presentation
STAT6	Th2-related transcription factor
TBX21	Th1-related transcription factor
PRF1	Perforin – cytotoxic T cell effector enzyme
CTLA4 (CD152)	Inhibitory T cell immune checkpoint receptor
CD274 (PDL1)	Ligand for inhibitory T cell immune checkpoint receptor
PDCD1LG2 (PDL2)	Ligand for inhibitory T cell immune checkpoint receptor
VTCN1 (B7.H4)	Ligand for co-stimulatory T cell receptor
PDCD1 (PD1)	Inhibitory T cell immune checkpoint receptor
IDO1	Immune-modulating enzyme – induces T cell exhaustion
LAG3 (CD223)	Inhibitory T cell immune checkpoint receptor
TNFRSF9 (4-1BB/CD137)	Co-stimulatory T cell receptor

**Table 4.3: 21 immune-related gene panel**

#### *4.2.5.1 Expression of immune-related genes correlates with IHC-based immune microenvironment characteristics*

Gene expression data was collected for 350 tumours across the 3 included STS subtypes (**Figure 4.1**). 84 tumours produced expression data that did not pass an initial QC assessment (HK gene values <3 standard deviations above mean negative control values), likely reflecting excessively degraded RNA. Gene expression data for 266 tumours passed this initial QC stage and were taken forward for analysis.

Raw gene counts were processed by positive control normalisation, housekeeper normalisation then Log<sub>2</sub> transformation. There was a high degree of correlation between many of the genes analysed, indicating analytical redundancy between the selected panel of target genes (**Figure 4.7**). There was significant correlation between IHC-derived average lymphocyte count values and associated gene expression values (**Supplemental Figure 4.19A-C**). The correlation coefficient for CD4 (Pearson R=0.35) was lower than that for CD3G (R=0.43) and CD8A (R=0.67), possibly reflecting that, while CD3 and CD8 expression is limited to lymphocytes, CD4 is also expressed by other leucocytes that were not included in IHC-based counting of CD4<sup>+</sup> lymphocytes. CD68 and CD274 (PD-L1) normalised gene values were significantly higher in tumours with higher average CD68 and maximum PD-L1 IHC scores respectively (**Supplemental Figure 4.19D-E**). These findings indicate that our data reflect an expected, albeit imperfect, association between paired transcript and protein levels, providing cross-validation of IHC and gene expression methods used.

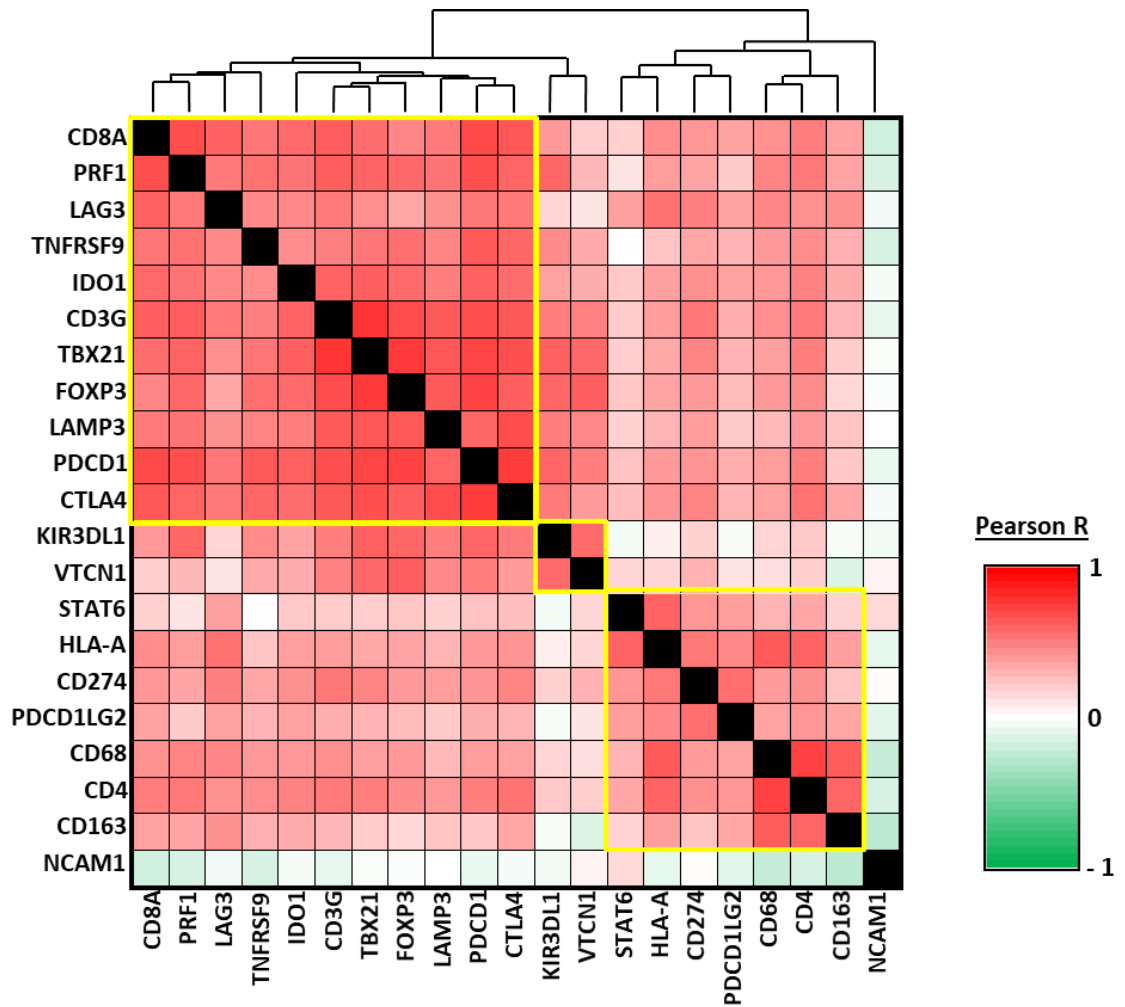


**Figure 4.7: Correlation of expression of 21 immune-related genes in STS cohort**  
 Matrix indicates Pearson R correlation coefficients derived from correlation analysis of normalised, Log<sub>2</sub>-transformed expression values for all pairs of 21 immune-related genes within 266 STS cohort. Dendrogram shows clustering of genes as per Figure 4.8, with main gene clusters highlighted within yellow boxes.

#### *4.2.5.2 Unsupervised clustering of immune gene expression data reveals distinct tumour subgroups*

Following gene-level Z standardisation of normalised, Log2-transformed gene expression values, unsupervised two-way agglomerative clustering using Wards minimum distance linkage and Euclidean distance was used to identify subgroups within the 266 tumour cohort that clustered together on the basis of similar levels of expression of immune-related genes (**Figure 4.8**).

Visual inspection of the sample dendrogram identified 3 main groups of tumours. Cluster 1 was characterised by significantly lower levels of expression of nearly all analysed genes, Cluster 3 had significantly higher levels of expression of the majority of included genes, and Cluster 2 had an intermediate expression level of most genes – significantly higher than Cluster 1 but significantly lower than Cluster 3 (**Supplemental Figure 4.20**).

Further inspection of the heatmap indicated that Cluster 3 could be subdivided into 2 groups – cluster 3a and 3b (**Figure 4.8**). Compared to Cluster 3b, tumours in Cluster 3a had significantly increased expression of CD4, CD68, CD163, HLA-A, PDCD1LG2, LAG3, IDO1 and CD8A (**Supplemental Figure 4.21**), several of which are genes involved in antigen presentation/ recognition by macrophages and T cells respectively. Compared to Cluster 3a, Cluster 3b had significantly higher expression of KIR3DL1 and VTCN1, cell surface molecules with inhibitory function against NKC- and T-cell-mediated immune responses. Compared to cluster 2, tumours in cluster 3b had significantly higher expression of 11 genes – among these were several proteins with recognised inhibitory or stimulatory immune checkpoint function (**Supplemental Figure 4.22**). Meanwhile, compared to cluster 2, cluster 3a had upregulation of almost all (19/21) genes, including the immune checkpoint-related genes that were upregulated in cluster 3b, and also the antigen presentation/recognition genes that were comparatively downregulated in cluster 3b (**Supplemental Figure 4.23**).

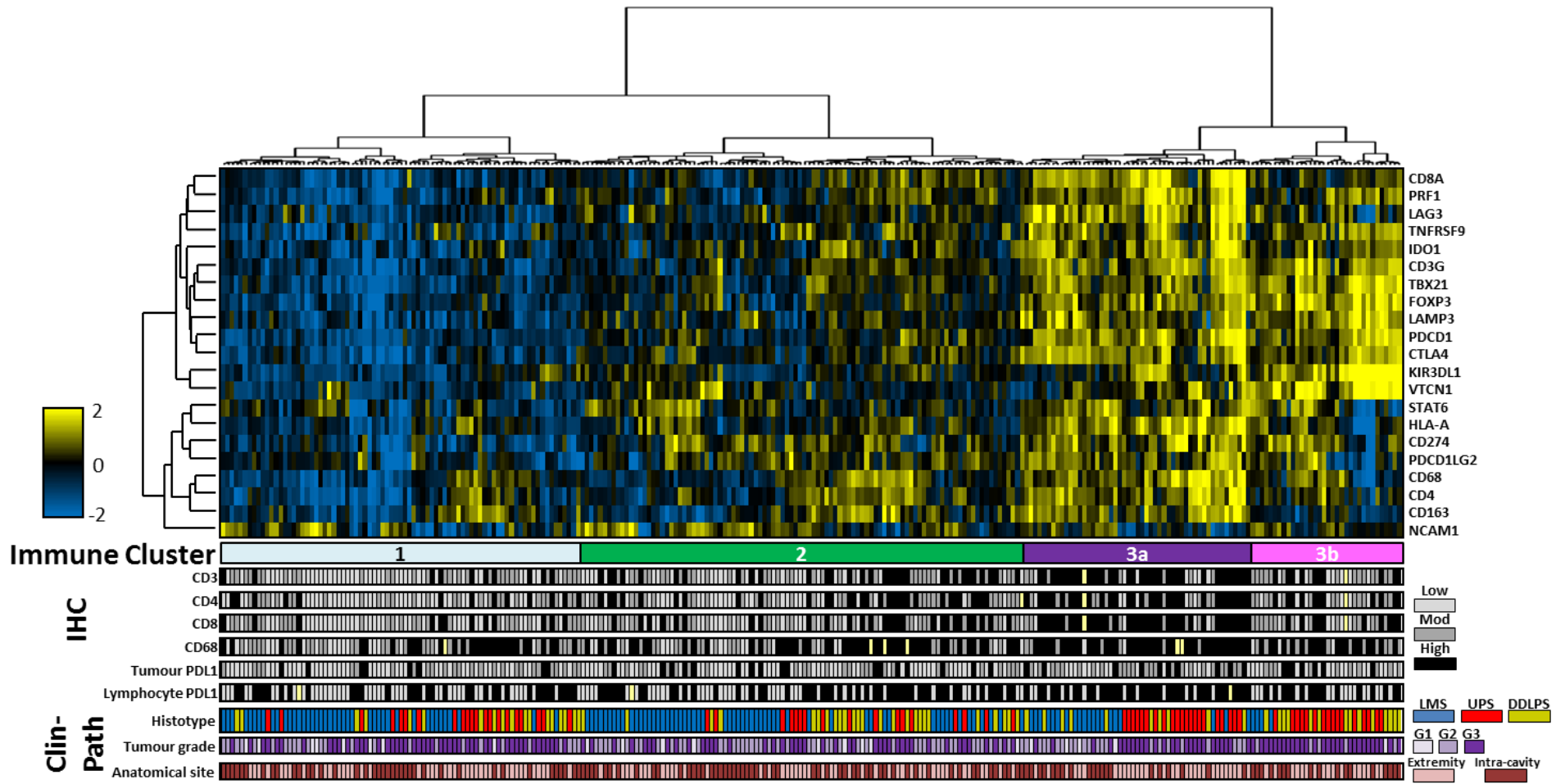


**Figure 4.8: Unsupervised clustering of immune gene expression data identifies 4 pan-subtype clusters.**

Normalised,  $\text{Log}_2$  transformed expression data for 21 immune-related genes from 266 STS were subjected to unsupervised clustering using Wards minimum distance linkage and Euclidean distance. Shown is a clustered heatmap with associated IHC values and clinico-pathological characteristics vertically aligned in colour bars. Immune clusters 1,2,3a and 3b were identified by manual inspection of sample dendrogram. For CD3/CD4/CD8 TIL, population tertile TIL/mm<sup>2</sup> values were used for low/medium/ high cutoff. For CD68, low/medium/ high cutoff corresponded to average CD68 score <2, 2-3 and 3. For tumour PD-L1, low/medium/high cutoff corresponds to maximum tPLD1 values of 0, 0-2 and 3+. For leucocyte PD-L1, low/high corresponds to absence or presence of lcPD-L1 expression.

#### *4.2.5.2 Distribution of baseline clinico-pathological characteristics across immune gene-based clusters*

We examined the distribution of tumour baseline clinico-pathological characteristics between the four identified clusters.

A majority of both Cluster 1 (characterised by uniformly low expression of immune-related genes), and Cluster 2 (characterised by low to intermediate gene expression) were LMS (52 and 57% respectively), with the remainder consisting of an approximately equal proportion of UPS and DDLPS (**Figure 4.9A**). Cluster 3a, characterised by higher levels of expression of genes involved in antigen presentation/recognition and immune checkpoints, consisted of 39% LMS, 40% UPS and 21% DDLPS, while Cluster 3b, characterised by higher levels of immune checkpoint genes but not antigen presentation/recognition, consisted of 15% LMS, 41% UPS and 44% UPS.

42/124 (34%) of tumours in the LMS sub-cohort were in the Cluster 1, while 56/124 (45%) were in Cluster 2, leaving a minority of LMS in Clusters 3a and 3b (16% and 4% respectively) (**Figure 4.9B**). UPS and DDLPS cases were more equally distributed across the 4 identified clusters.

The distribution of tumour histological grade was similar between Clusters 1,2 and 3a (**Figure 4.9C-D**). However, grade 3 tumours were significantly overrepresented in Cluster 3b, accounting for 82% of all tumours in this cluster. There was no significant imbalance in the distribution of tumours originating from the extremities or intracavity areas between the four clusters (**Figure 4.9E**).

These findings indicate that the gene expression-defined clusters transcended histological subtype, grade and anatomical site of tumour origin. There was some preponderance for LMS in the clusters associated with low or intermediate immune gene expression, with higher grade tumours and UPS and DDLPS enriched in the clusters with higher levels of immune gene expression.

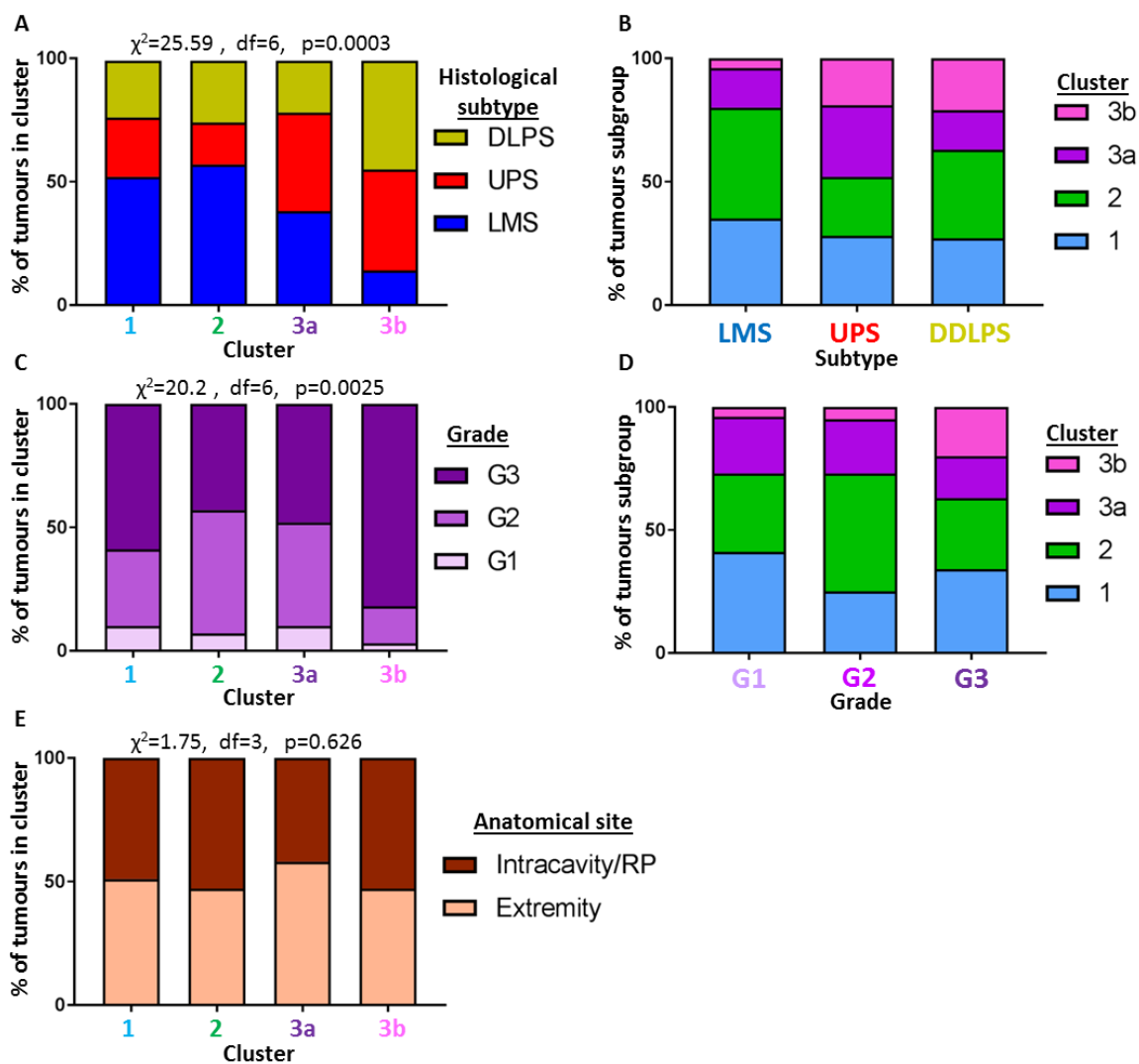


**Figure 4.9: Distribution of baseline clinico-pathological characteristics within 4 immune clusters**

Bar charts show distribution of baseline tumour characteristics across each of 4 immune clusters. **A** Distribution of histological subtypes within immune clusters **B**. Distribution of immune clusters within sub-cohorts. **C**. Distribution of histological grade within immune clusters. **D**. Distribution of immune clusters across tumours of same histological grade. **E**. Distribution of anatomical site of tumour origin within immune clusters. Stated are chi-squared values with associated degrees of freedom (d.f) and p values.

#### *4.2.5.3 Distribution of IHC-based immune microenvironment characteristics across immune gene-based clusters*

Comparison of IHC-derived average TIL/mm<sup>2</sup> values between tumours in each cluster showed that Cluster 3a had significantly higher numbers of infiltrating CD3, CD4 and CD8 lymphocytes than all other clusters (**Figure 4.10A**). Cluster 1 had significantly lower TIL values for CD3 and CD4 than all other clusters.. Cluster 2 and 3b had similar average TIL/mm<sup>2</sup> values across all three markers – this contrasted to related gene expression data, where expression of CD3G (although not CD4 or CD8) were significantly higher in cluster 3b compared to cluster 2.

There were significant differences in the IHC-based average CD68 scores between tumours in different clusters (**Figure 4.10B**). Cluster 3A contained the highest proportion of tumours with uniformly dense CD68+ macrophage infiltrations (average score 3) and the lowest proportion of intermediate (average score  $\geq 2$ ,  $< 3$ ) or low (average score  $< 2$ ) density infiltrates. Cluster 1 had the highest proportion of tumours with non-dense infiltrates. The distribution of average CD68+ scores in Clusters 2 and 3b were similar.

There was no significant difference in the IHC-based maximum tPD-L1 scores between tumours in different clusters (**Figure 4.10C**) – Cluster 3b had the smallest proportion of tPD-L1 negative tumours (34% vs 50-58% in other clusters). There were significant differences in the proportions of tumours with IHC-based LcPD-L1 positivity between different clusters, with 72% of tumours in Cluster 3b containing PD-L1-staining leucocytes, compared to 41%, 52% and 47% of tumours in Cluster 1, 2, and 3b respectively (**Figure 4.10D**).

These data indicate that associated IHC-based immune microenvironment characteristics provide further distinction between expression-based clusters. The low expression Cluster 1 had similarly low levels of immune cell infiltration. The intermediate expression Cluster 2 and higher expression Cluster 3b had similar and intermediate levels of immune cell infiltration, while the higher levels of immune cell infiltration distinguished Cluster 3a.

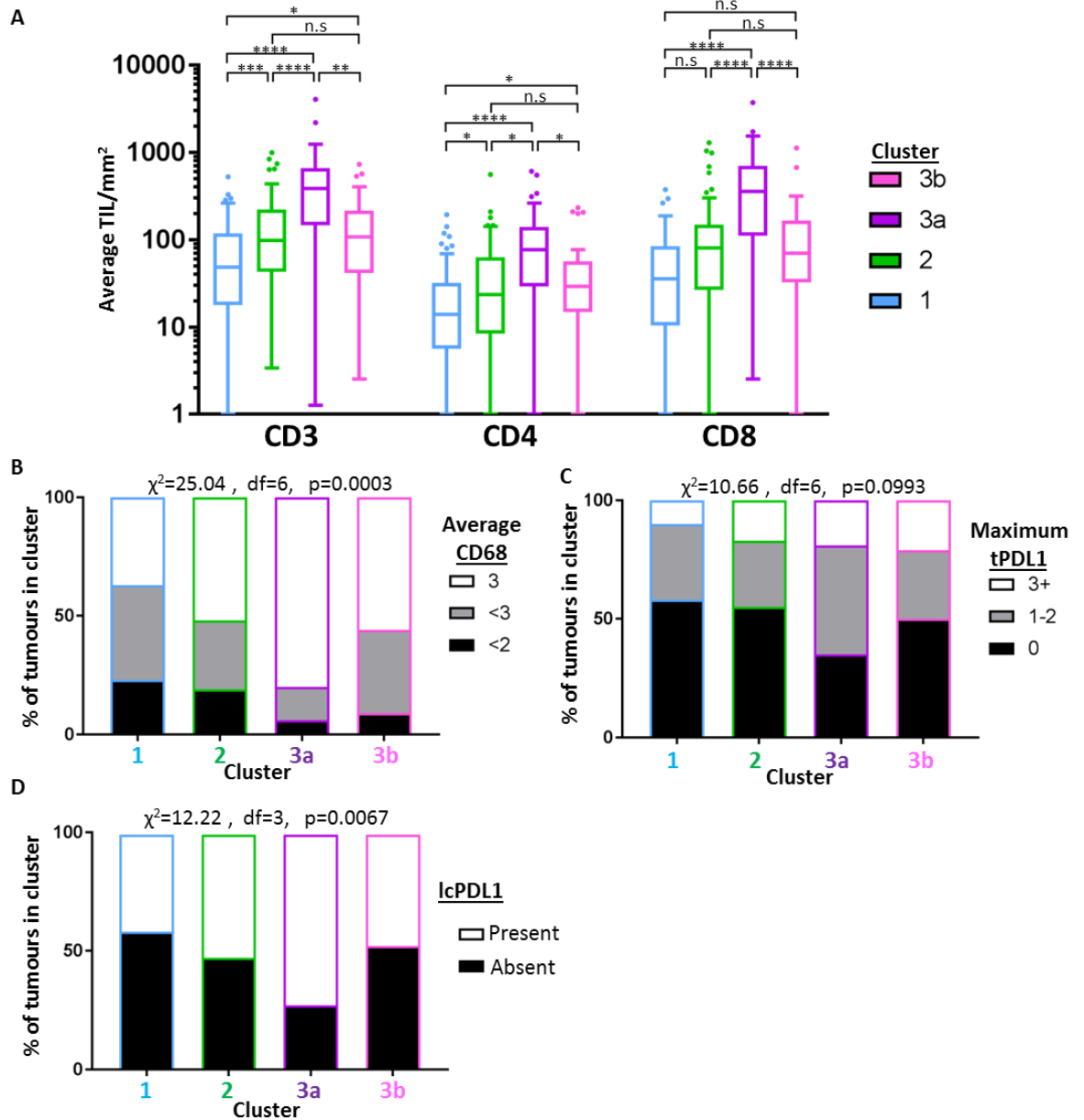


**Figure 4.10: Association of gene expression-derived immune clusters with IHC-based immune microenvironment parameters**

**A.** Tukey box and tail plots show distributions of average TIL/mm<sup>2</sup> values for CD3, CD4 and CD8 for 266 STS when stratified by 4 immune clusters. Adjusted P values derive from post-hoc Tukey's multiple comparisons testing after 1-way ANOVA as indicated. N.S. =  $p > 0.05$ , \* $p < 0.05$ , \*\* $p < 0.01$ , \*\*\* $p < 0.001$ , \*\*\*\* $p < 0.0001$ . Bar charts show distribution of **(B)** average CD68, **(C)** maximum tPD-L1 and **(D)** lcpD-L1 values for 266 STS across 4 immune clusters. Stated are chi-squared values with associated degrees of freedom (d.f) and p values.

#### *4.2.5.4 IHC- and gene expression-based immune microenvironment characteristics identify distinct STS subgroups*

Unsupervised clustering analysis of a targeted gene expression data from the 266 STS cohort identified 4 clusters with contrasting immune microenvironment characteristics (**Table 4.4**).

Cluster 1 was characterised by low expression of immune-related genes, lower numbers of infiltrating T lymphocytes and CD68+ macrophages, and low levels of tumour PD-L1 expression – we labelled this the **Immune cold** cluster.

Cluster 2, labelled the **Immune intermediate** cluster, was characterised by intermediate expression levels of most of the examined genes in combination with an intermediate degree of infiltration by T lymphocytes and CD68+ macrophages. LMS were proportionally overrepresented in both the immune-cold and immune-intermediate clusters.

A third cluster, which had higher expression of many of the targeted genes compared to the immune-cold or immune-intermediate clusters, was further subdivided on the basis of separation within the clustering dendrogram. These two clusters (3a and 3b) were distinct from one another in terms of expression levels of a subset of genes, including genes associated with antigen-presenting cells and antigen processing.

The cluster with the higher expression of these genes (cluster 3a) was also characterised by the highest levels of infiltration by lymphocytes and CD68+ macrophages and also the highest degree of tumour and leucocyte PD-L1 expression – on the basis of these observations, we named this the **high infiltration** cluster. This cluster consisted of an equal proportion of LMS and UPS, and a lower proportion of DDLPS.

As opposed to this high infiltration cluster, cluster 3b had increased expression of fewer genes compared to the intermediate cluster, among which were a number of targetable immune checkpoint proteins. This cluster was also associated with an intermediate degree of infiltration by T lymphocytes and CD68+ macrophages and low tumour PD-L1 expression. Compared to the high infiltration cluster, cluster 3b had higher expression of two immune inhibitory genes and lower expression of antigen processing and presentation genes.

Based on this finding of increased expression of only some immune-related genes, which were largely associated with immune response inhibition, and the lower degree of immune cell infiltration compared to the high infiltration cluster, we named cluster 3b the **immune checkpoint-dominant** cluster. This cluster consisted of equal proportions of UPS and DDLPS, and a lower proportion of LMS.

	Immune Gene Expression	IHC				STS subtype			Grade		
		TILs	CD68 Mc	tPDL1	LcPDL1 Positive (%)	LMS	UPS	DDLPS	1	2	3
<b>Cluster 1</b> N=82 Immune cold	Low expression	Low	Low	Low	41%	52%	24%	23%	11%	31%	58%
<b>Cluster 2</b> N=98 Immune intermediate	Intermediate expression	Intermediate	Intermediate	Low	52%	57%	17%	26%	7%	50%	43%
<b>Cluster 3a</b> N=52 High Infiltration	High expression, including antigen presentation/recognition gene cluster	High	High	Intermediate	72%	39%	40%	21%	10%	42%	48%
<b>Cluster 3b</b> N=34 Immune checkpoint-dominant	<ul style="list-style-type: none"> <li>• High expression of immune checkpoint proteins</li> <li>• Intermediate expression of antigen presentation/recognition gene cluster</li> </ul>	Intermediate	Intermediate	Low	47%	15%	41%	44%	3%	15%	82%

**Table 4.4: Summary of gene expression, IHC and histological characteristics of 4 immune clusters**

### 4.3 Discussion

This study provides an integrated IHC- and gene expression-based description of the immune microenvironment of clinically-annotated tumour sub-cohorts of LMS, UPS and DLDPS. We have demonstrated that there is broad variation in a number of immune microenvironment components within each of the 3 studied STS subtypes and that contrasting immune phenotypes can be identified in a manner that is independent of conventional histological classification. These findings provide a platform for the identification of candidate prognostic biomarkers within the immune microenvironment of STS subtypes with complex karyotypes.

The cohort included in our study is larger compared to many previously reported studies that have described the immune microenvironment of in LMS, UPS or DDLPS (**See Chapters 1.5.3 and 1.5.4**). By design, our cohort was homogenous in terms of tumour stage, prior treatment exposure and treatment setting, limiting the scope for confounding of immune-based observations and possible association with clinical behaviour. Expected associations between patient survival and baseline characteristics such as tumour grade and stage were observed, indicating that the cohort reflected an expected range of clinical behaviour and prognosis. This set of biological and linked clinical data thus represents a valuable resource for the investigation for immune-based prognostic biomarkers in STS.

The broader applicability of the findings within our study is dependent upon how representative the included sample is of the broader STS patient population. The included patients were all seen within a single high-volume specialist centre that has contact with approximately 1000 new patients per year (i.e approximately 1 quarter to 1 third of all STS diagnoses within the UK). However, given the availability of dedicated subspecialist services, there is a chance that the patients seen at this centre are selected for greater complexity and/or aggression of disease, and may receive different treatments to a broader STS population. Comprehensive national statistics on STS incidence and survival outcome are collected in the UK by the National Cancer Registration and Analysis Service (NCRAS) and in the US by the Surveillance, Epidemiology and End Results (SEER) program – however, these have only been reported with high level data that offers little granularity regarding specific STS diagnoses. While 5 year

survival rates of 76%, 90% and 51% have been reported by SEER for localised LMS, LPS and UPS respectively, the lack of detailed information regarding grade, disease site and, in the case of LPS, histological subclassification make comparison of such population-level data to our sample cohort challenging. Within our cohort, a prognostic association with tumour grade and stage was seen, consistent with population-level prognostic risk factors. Meanwhile, comparison to the TCGA-SARC dataset can be performed to assess the similarity of baseline characteristics of our cohort with that of an independent STS cohort, albeit one that was also collected in subspecialist centres under research conditions and thus is vulnerable to similar confounders (**Supplemental table 4.3**). This comparison indicates broad similarities in terms of gender distribution, age of diagnosis, grade and anatomical sites between our 266 patients and the 164 patients with LMS, UPS or DDLPS within the TCGA-SARC cohort – key differences include the greater representation of uterine LMS and lower proportion of grade 3 UPS. Similar median overall survival was seen between corresponding LMS and DDLPS cohorts, while the better survival of UPS in TCGA (median OS not reached after median after median 3.25 years f/u in TCGA-SARC) may reflect the lower rate of high grade tumours. This comparison does however support the representativeness of our cohort. This would be further assessed within the validation of our findings in independent STS cohorts.

We chose to use IHC-based tissue profiling as this represented a readily-available, tractable and reproducible approach that is well suited to use in archival clinical samples and that is widely used in clinical practice for quantitative and qualitative assessment of protein expression in tissue. A large proportion of currently used diagnostic, prognostic and predictive biomarkers either originally developed as IHC-based assays or otherwise subsequently developed from an alternative molecular analysis into a surrogate IHC assay. To accurately and reliably reflect protein expression in tissue, IHC requires the availability of specific and sensitive antibodies against the intended target, that have been optimised and validated for use. For this study, we used a number of antibodies (i.e anti-CD3, CD4, CD8 and CD68) that are highly validated, as reflected by their use in routine clinical diagnostic practice and were readily available for use within our histopathology core facility laboratory. As research interest into PD-L1 expression as a biomarker has grown in the wake of the clinical approval of PD1- and PD-

L1-targeting therapeutic mAb, the assessment of tissue expression of PD-L1 by IHC has become a source of contention<sup>194</sup>. With a range of anti-PD-L1 antibodies marketed for use in IHC assays now commercially available, questions regarding the specificity and reproducibility of many of these products persist. For our study, we made use of the Cell Signalling E1L3N rabbit mAb, for which validation data is available from both the manufacturer and several independent researchers and has been used in over 100 reported studies. Subsequent to the start of our study, a number of clinically validated, quantitative PD-L1 IHC-based assays using different antibodies have become established as companion biomarkers that are used in the treatment of NSCLC and other cancers (see **Chapter 1.5.1.4**)<sup>305</sup>. There is significant variability between these clinically-approved assays in terms of reagents used, cellular compartment assessed (tumour vs immune cell, membranous vs cytoplasmic), and positive/negative cutoffs that do not provide a consistent picture of what is a clinically meaningful level of PD-L1 expression within the tumour microenvironment. In my study, I aimed to address this issue by producing semi-quantitative scoring of PD-L1 on tumour cells. Because of technical challenges, I was unable to produce corresponding quantitation of PD-L1 expression on infiltrating immune cells, representing a limitation of my study given that levels of PD-L1 expression have been shown to have predictive value in the use of anti-PD-L1 mAbs in the treatment of urothelial, lung and head and neck cancers. A further potential limitation to my study is the inclusion of cytosolic as well as membranous staining for PD-L1 expression in tumour cells. Given that clinically validated assays for tumour cell expression of PD-L1 score membranous staining only, it is possible that my study includes false positive PD-L1 staining – further review of IHC specimen in my series would allow for distinguishing between membranous and cytosolic PD-L1 staining.

In **Chapter 3**, we described how a practical number of replica TMA cores were sufficiently representative of a larger tumour area, to allow for accurate ordinal categorisation of tumours based on the degree of T lymphocyte infiltration. Taking this finding forward, and extrapolating this conclusion to apply to other, non-TIL immune microenvironment components, we used a TMA approach, wherein each tumour within the cohort was represented by 3 x 1mm cores, for the IHC-based immune profiling experiment. The time and resource efficiencies of this approach potentiated the inclusion of several hundred tumours in the study and ensured a

consistency in upstream processing. However, as explored in **Chapter 3**, a TMA-based approach is likely to have introduced sampling error into this study, which could have a confounding effect on its conclusions. The extent of sampling error could be investigated in future work that compares TMA-derived results to values derived from the inspection of matched full section mounts.

IHC-based biomarkers are typically reliant on resolving protein expression data to ordinal categories of expression (i.e. present/absent or low/medium/high) – such categorisation is dependent upon the establishment of cut-off values that reproducibly separate independent cohorts into groups of consistently contrasting outcomes. At present, no such categories or related cut-off values have been established for immune microenvironment components in STS, i.e. it is not yet known as to what would constitute a clinically-meaningful ‘high’ and ‘low’ degree of lymphocyte infiltration. With this in mind, we aimed to collect IHC-based data that was as granular as possible, so as to allow for later establishment of data categories. The consistent morphology of lymphocytes coupled with T lymphocyte-restricted expression of CD3 and CD8 and the high specificity of the antibodies for these proteins allowed for counting of individual T lymphocytes that could be expressed as a value normalised for area of tumour tissue inspected. The specificity of CD4 as a marker for helper T lymphocytes is reduced by the fact that CD4 expression is also found on certain myeloid cell types, but, again, distinct morphology allowed for counting of individual CD4+ lymphocytes. The heterogeneous morphology of CD68+ macrophages posed a challenge to counting individual positive-staining histiocytes – in the face of this, we resorted to ordinal categorisation of tumour infiltration by these cells, based on a system previously described by Lee *et al*<sup>19</sup>. Expression of PD-L1 by tumour cells demonstrated wide variation in terms of both staining intensity and frequency, posing further challenges in defining positive staining and counting the number of often morphologically heterogeneous tumour cells. In order to capture granular data, we devised a semi-quantitative ordinal scoring system based on staining intensity and percentage of tumour cells exhibiting staining, similar to that used by other authors<sup>194</sup>. We chose to report the presence or absence of PD-L1 expression on any tumour-infiltrating leucocytes as a binary variable as a response to the challenges posed by the morphological and quantitative heterogeneity of tumour infiltrating leucocytes.

We used expression analysis of a targeted panel of immune-related genes in this study to provide orthogonal validation for our TMA/IHC-based sampling and quantification, and to provide assessment of a broader panel of immune-related targets than could be practically assessed using IHC. The gene panel was chosen in a manner that selected either gene analogues of the proteins being examined with IHC, genes whose expression indicate functional sub-classification of T lymphocytes, or genes with recognised stimulatory or inhibitory immune checkpoint function that are current therapeutic targets of clinical interest. Given that the selected genes were all chosen on the basis of involvement in immune processes, it was unsurprising to find a high level of correlation between many of the genes – this likely limited the study's ability to identify tumour subgroups with biologically-meaningful qualitative differences in immune response.

The relatively narrow and superficial focus of the IHC and gene panel used in my immune-profiling study means there is a strong possibility that there are important components and nuances of the immune microenvironment in STS that we failed to record. The IHC panel used provides high level information regarding the degree of T lymphocyte infiltration and basic functional subtyping (i.e CD4 vs CD8), but does not account for the broad and dynamic variation in T lymphocyte functional, activation and exhaustion states described within the microenvironment of a range of solid tumour types<sup>171</sup>. Markers of T cell cytotoxic activation (e.g. granzymes, perforins, CD45) and exhaustion (PD-1, LAG3, CD160) would provide additional information regarding the functional state of the CD8<sup>+</sup> T cells present within STS. Meanwhile, interrogating for important functional subsets of CD4<sup>+</sup> T lymphocytes, including T<sub>H</sub>1 (typified by TBX1 and STAT4 expression and release of IFN $\gamma$ ), T<sub>H</sub>2 (typified by GATA-3 and STAT6 expression and release of IL-4, IL-5 and IL-13) and immunosuppressive T<sub>reg</sub> cells (CD4<sup>+</sup>CD25<sup>+</sup>FOXP3<sup>+</sup>, release of IL-10 and TGF- $\beta$ ), would provide greater detail as to the potential pro- or anti-tumour effect of helper T cells present in these tumours. In my study, TAMs were identified by expression of CD68, a global macrophage marker that provides no information regarding the functional activation status of the infiltrating cells. Delineating where upon the dynamic spectrum between pro-inflammatory, anti-tumour M1 and anti-inflammatory, pro-tumorigenic M2 activation status can be abetted by assessment for macrophage

expression of the M2 markers CD163 and the presence or absence of MHC-II expression, and by consideration of the broader cytokine/chemokine milieu within the microenvironment. While the gene expression panel used in our study provides some insight into the level of expression of markers of T cell and macrophage subset, activation and exhaustion status, the loss of spatial resolution associated with this methodology limits the resolution by which the nuance of immune cell activation state can be assessed. The use of multiplexed IHC/immunofluorescence allows for the assessment of as many as eight markers of immune cell type and state while retaining spatial resolution – such an approach has been shown to outperform monoplex IHC, gene expression profiling and assessment of tumour mutational burden when assessing for predictive biomarkers for immune checkpoint therapy<sup>306</sup>.

The degree of T cell infiltration seen in individual tumours within the studied cohort varied widely, with average TIL/mm<sup>2</sup> values ranging from fewer than 10 to several thousand, while there was generally no difference in the degree of lymphocyte infiltration between the 3 sub-cohorts. Within our STS cohort, TIL values for a majority of tumours were below thresholds that have been reported as identifying clinically-meaningful lymphocyte infiltration in cancer types where immunotherapy responses are commonplace, such as melanoma and NSCLC<sup>175,176,300–302</sup>. If such thresholds hold cross-cancer relevance, which is by no means a certainty, then our findings may indicate that most STS with these 3 subtypes typified by complex karyotypes do not contain meaningful lymphoid reactions. Conversely, a minority of tumours across all 3 studied subtypes demonstrate what would be a meaningful degree of T cell infiltration, with UPS proportionately overrepresented. These findings are largely consistent with the limited amount of previously reported data on the extent of lymphocyte infiltration in LMS, UPS and DDLPS (**see Tables 1.6 and 1.8**).

We found that a large proportion of tumours of all three subtypes contained dense infiltration by CD68+ macrophages. Greater inter-tumour heterogeneity in macrophage infiltration was seen in LMS, with a majority of tumours showing either moderate or scanty infiltration. This is consistent with a study reported by Lee *et al* which assessed macrophage infiltration in 149 primary LMS specimens using the ordinal scoring system employed by our study<sup>219</sup>. Here, sparse, moderate and dense infiltrates were seen in 33%, 41% and 26% of tumours

respectively. When limited to the 73 non-gynaecological LMS included, sparse, moderate and dense infiltrates were seen 31%, 34% and 35% respectively, proportions that are closely reflected within our study's primarily non-gynaecological LMS sub-cohort. In contrast to LMS, most UPS and DDLPS in our study contained uniformly dense infiltrates. This finding is consistent with data from CIBERSORT analysis of TCGA-SARC gene expression data set which shows that cell type propensity scores for macrophages was significantly greater in UPS and DDLPS compared to LMS<sup>201</sup>.

Tumour cell expression of PD-L1 was absent or low in most tumours from all 3 sub-cohorts. In tumours where some degree of PD-L1 positivity was detected, there was frequently non-concordance between related TMA cores from the same tumour, indicating spatial heterogeneity in tumour cell PD-L1 expression, thus suggesting that our study may have underestimated the degree of PD-L1 expression due to sampling error. A small minority of tumours demonstrated high levels of tumour PD-L1 expression, with this proportion greater in UPS and DDLPS sub-cohorts compared to LMS. Consistent with this finding, previously reported studies have indicated with that PD-L1 expression is more common in UPS, although reported rates of PD-L1 positivity in DDLPS have been more varied and often significantly lower than included UPS (**see Chapter 1.5.3**). This may, in part, reflect inconsistency in the LPS subtype included in these studies, and whether profiling was strictly limited to dedifferentiated tumour areas, as was the case in our study.

Consistent with matched gene expression data, which showed positive correlation between many of the examined immune-related genes, there was strong correlation between all the examined IHC-based immune microenvironment components. This covariance of immune markers again indicates the likely limited ability of our study to identify qualitatively distinct immune phenotypes within the examined cohort. Further analysis of this study's dataset may include assessment of the intersection of different immune markers e.g. the combination of high TIL but lower CD68 density. Other studies of the immune microenvironment in cancer have reported potential clinical or biological significance in the ratio of CD8:CD4 T cells, reflecting the relative dominance of cytotoxic or helper T lymphocytes within immune infiltrates – this is an avenue to explore within our dataset.

In our cohort, tumours with higher histological grade tended to have a higher degree of lymphocyte and macrophage infiltration as well as higher rates of tumour PD-L1 expression, an important observation to consider when assessing for any independent prognostic association of immune microenvironment components. No other associations between baseline clinico-pathological characteristics and IHC-based immune component were seen – importantly, in the DDLPS sub-cohort, there was no association between any immune factor and whether the tumour was primary disease or a recurrence following previous resection.

Through the integration of unsupervised clustering analysis of gene expression data with IHC data, we identified four tumour subgroups on the basis of distinct immune microenvironment characteristics and that were independent of baseline clinico-pathological characteristics. These subgroups consisted of one with the lowest degree of immune gene expression and immune cell infiltration, one with intermediate gene expression and infiltration and two groups identified as having higher levels of gene expression but were distinct from one another in terms of differential expression of genes related to antigen presentation and recognition and a greater degree of leucocytic infiltration. Through this analysis, we have discovered subgroups of STS tumours that have qualitative differences in immune microenvironment and could feasibly reflect clinically meaningful differences in tumour biology that is independent of conventional means of histological classification. It is plausible that these subgroups may at least partially align with the cancer immune subtypes within TCGA datasets as described by Thorsson *et al*<sup>201</sup> (**see Table 1.4**). For example, our ‘Immune cold’ subgroup shares characteristics with the M2 macrophage predominant, intermediate grade, lymphocyte deplete (C4) group, while our ‘High infiltration’ subgroup has superficial similarities with the CD8 and M1-macrophage predominant IFN $\gamma$  dominant (C2) immune subtype. Consistent with our study’s findings, and supporting the relevance of these immune subtypes in STS, is the observation that within the TCGA-SARC cohort, the C4 lymphocyte depleted subtype is overrepresented in STS compared to other cancer types, suggesting that a significant proportion of STS have minimal intratumoral immune responses. Meanwhile, the IFN $\gamma$ -dominant subtype (C2) was more commonly seen in UPS compared to LMS or DDLPS within the TCGA-SARC cohort (**Supplemental**

**Figure 4.24).** Given that Thorssen *et al* based their observations on genome-wide multiomic profiling of thousands of tumours, further work is required to investigate whether these clinically relevant immune subtypes have been recapitulated in our study.

## **4.4 Supplementary material**

### ***4.4.1 Supplemental Tables***

**Supplemental Table 4.1:** Comparison of CD4 and CD8 TIL values

**Supplemental Table 4.2:** Comparison of TIL values between STS subtype cohorts

**Supplemental table 4.3:** Comparison of baseline clinicopathological characteristics in TCGA-SARC and RMH immunoprofiling STS cohort

	LMS	UPS	DDLPS
<b>Paired values from individual tumours</b>			
Mean of differences CD8 v CD4 (95%CI)	+126 (66.75-185.2)	+201 (10.8-282.8)	+84 (48.16-120.6)
Paired T test P value	<0.0001	<0.0001	<0.0001
Correlation coefficient (P)	0.78 (<0.0001)	0.67 (<0.0001)	0.85 (<0.0001)

**Supplemental Table 4.1. Comparison of CD4 and CD8 TIL values**

Matched, log<sub>2</sub>-transformed average TIL/mm<sup>2</sup> values from individual tumours were used for paired T tests to assess the mean of differences and associated 95% confidence intervals (stated as back-transformed values) between CD4 and CD8 TIL values across the 3 STS subtype cohorts. Pearson correlation coefficients for matched CD4 vs. CD8 values stated with associated p values.

	<b>LMS v. UPS. DDLPS</b>		
<b>ANOVA summary</b>	<b>CD3</b>	<b>CD4</b>	<b>CD8</b>
<b>F</b>	1.315	3.285	1.687
<b>P</b>	0.2703	0.0390	0.187
<b>R<sup>2</sup></b>	0.009974	0.02465	0.01277

**Supplemental Table 4.2. Comparison of TIL values between STS subtype cohorts**  
 1 way ANOVA analysis of Log2-transformed average TIL/mm<sup>2</sup> values for each of CD3, CD4 and CD8 derived from LMS, UPS and DDLPS cohorts was performed to assess for differences in degree of T lymphocyte infiltration. Stated are F, p and R<sup>2</sup> values derived from these 1 way ANOVA.

	LMS		UPS		DDLPS	
	TCGA	RMH	TCGA	RMH	TCGA	RMH
<b>n</b>	80	124	44	72	50	70
<b>M:F (%)</b>	31:69	36:63	55:45	53:47	66:34	63:37
<b>FNLCC Grade</b>						
<b>1</b>	15%	13%	-	-	2%	9%
<b>2</b>	64%	47%	30%	8%	74%	53%
<b>3</b>	21%	40%	70%	92%	24%	39%
<b>Average age (range)</b>	57.4 (33-84)	61 (29-87)	66.5 (29-90)	71 (26-89)	63.0 (34-86)	61 (34-86)
<b>Site</b>						
<b>Extremity</b>	20%	45%	80%	93%	10%	16%
<b>Intracavity</b>	51%	45%	20%	7%	90%	84%
<b>Uterine</b>	29%	10%	-	-	-	-
<b>Median OS</b>	6.7y	5.3y	Not reached	2.8y	4.5y	4.0y

**Supplemental table 4,3 Comparison of baseline clinicopathological characteristics in TCGA-SARC and RMH immunoprofiling STS cohorts**

#### **4.4.2 Supplemental Figures**

**Supplemental figure 4.1.** Comparison of baseline characteristics between STS subtype cohorts

**Supplemental figure 4.2.** Overall and advanced-disease free survival in STS cohort stratified by histological subtype.

**Supplemental figure 4.3.** Overall and advanced-disease free survival in STS cohort stratified by baseline clinico-pathological parameters

**Supplemental figure 4.4.** TMA cores demonstrating variable degree of lymphocyte infiltration

**Supplemental figure 4.5.** Correlation between average CD3, CD4 and CD8 TIL values

**Supplemental figure 4.6.** TMA cores demonstrating variable degree of CD68+ macrophage infiltration.

**Supplemental figure 4.7.** Association between average TIL/mm<sup>2</sup> and average CD68 score

**Supplemental figure 4.8.** TMA cores demonstrating variable degree of tumour cell PD-L1 staining

**Supplemental figure 4.9.** Association of maximum tumour PD-L1 scores with average TIL values and CD68 scores

**Supplemental figure 4.10.** Association of the presence of infiltrating leucocyte PD-L1 expression with average TIL values, average CD68 scores and maximum tumour PD-L1 scores

**Supplemental figure 4.11.** Association of tumour grade with average TIL values, average CD68 scores and maximum tumour PD-L1 scores

**Supplemental figure 4.12.** Association of anatomical site of tumour origin with average CD68 scores, maximum tumour PD-L1 scores and average TIL values.

**Supplemental figure 4.13.** Association of patient age at time of surgery with average TIL values, average CD68 scores and maximum tumour PD-L1 scores

**Supplemental figure 4.14.** Association of patient gender with average TIL values, average CD68 scores and maximum tumour PD-L1 scores.

**Supplemental figure 4.15.** Association of tumour stage with average TIL values, average CD68 scores and maximum tumour PD-L1 scores.

**Supplemental figure 4.16.** Association of predominant histological subtype with average CD68 scores, maximum tumour PD-L1 scores and average TIL values in DDLSP cohort.

**Supplemental figure 4.17.** Association of prior resection status with average TIL values, average CD68 scores and maximum tumour PD-L1 scores in DDLPS cohort.

**Supplemental figure 4.18.** Analysis of housekeeper gene performance in RMH-SARC and TCGA-S

**Supplemental figure 4.19.** Association of IHC-based scoring of immune microenvironment components with expression values of corresponding genes.

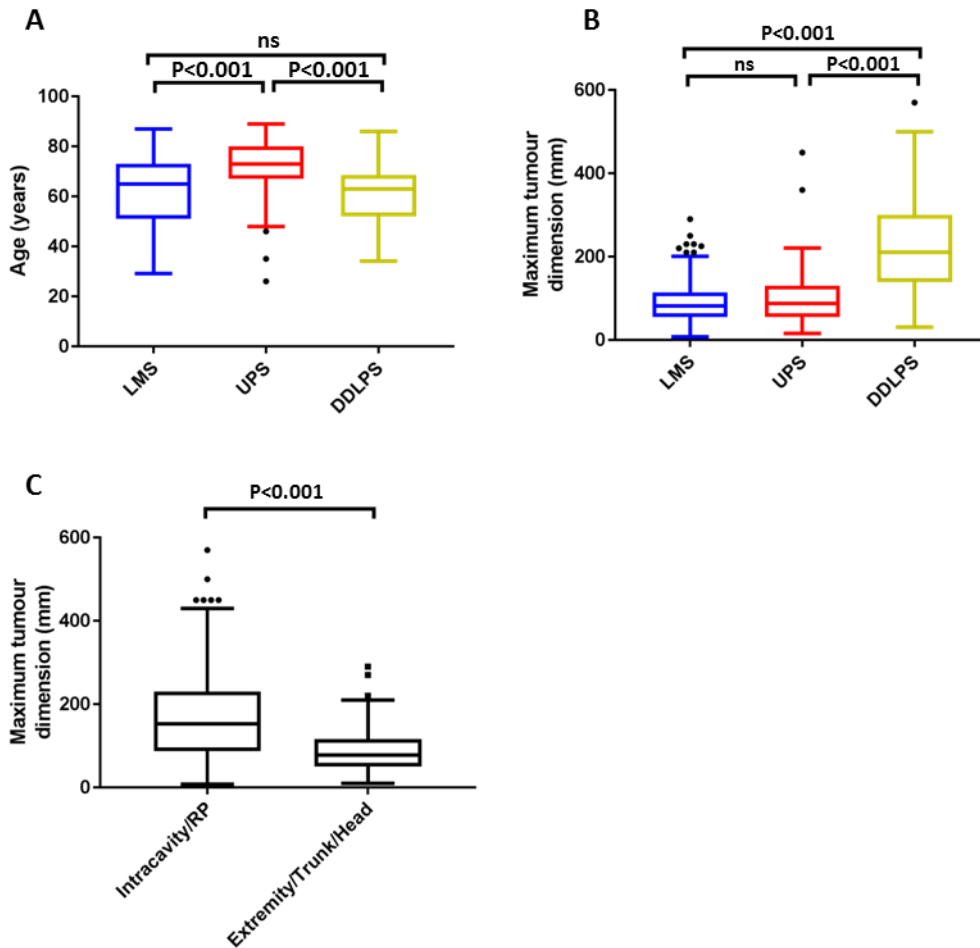
**Supplemental figure 4.20.** Differences in expression of 21 immune-related genes between 3 identified clusters

**Supplemental figure 4.21.** Differences in expression of 21 immune-related genes clusters 3a and 3b

**Supplemental figure 4.22.** Differences in expression of 21 immune-related genes clusters 2 and 3b

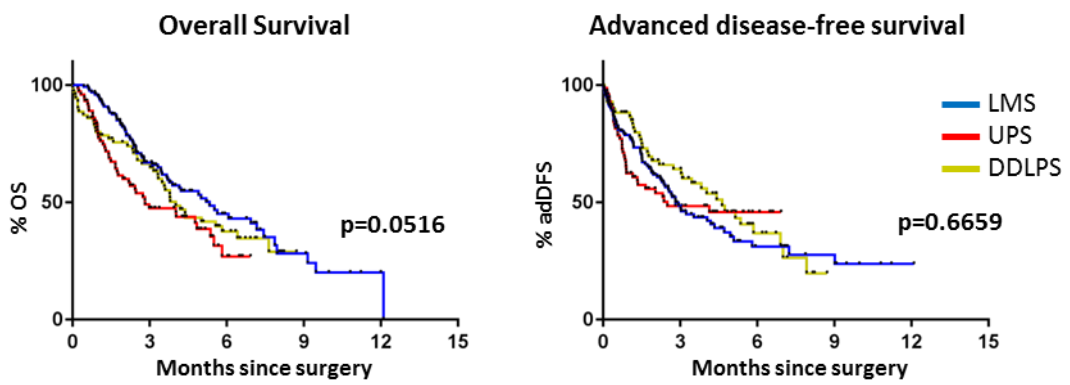
**Supplemental figure 4.23.** Differences in expression of 21 immune-related genes clusters 2 and 3a

**Supplemental figure 4.24.** Distribution of immune subtypes within TCGA-SARC dataset

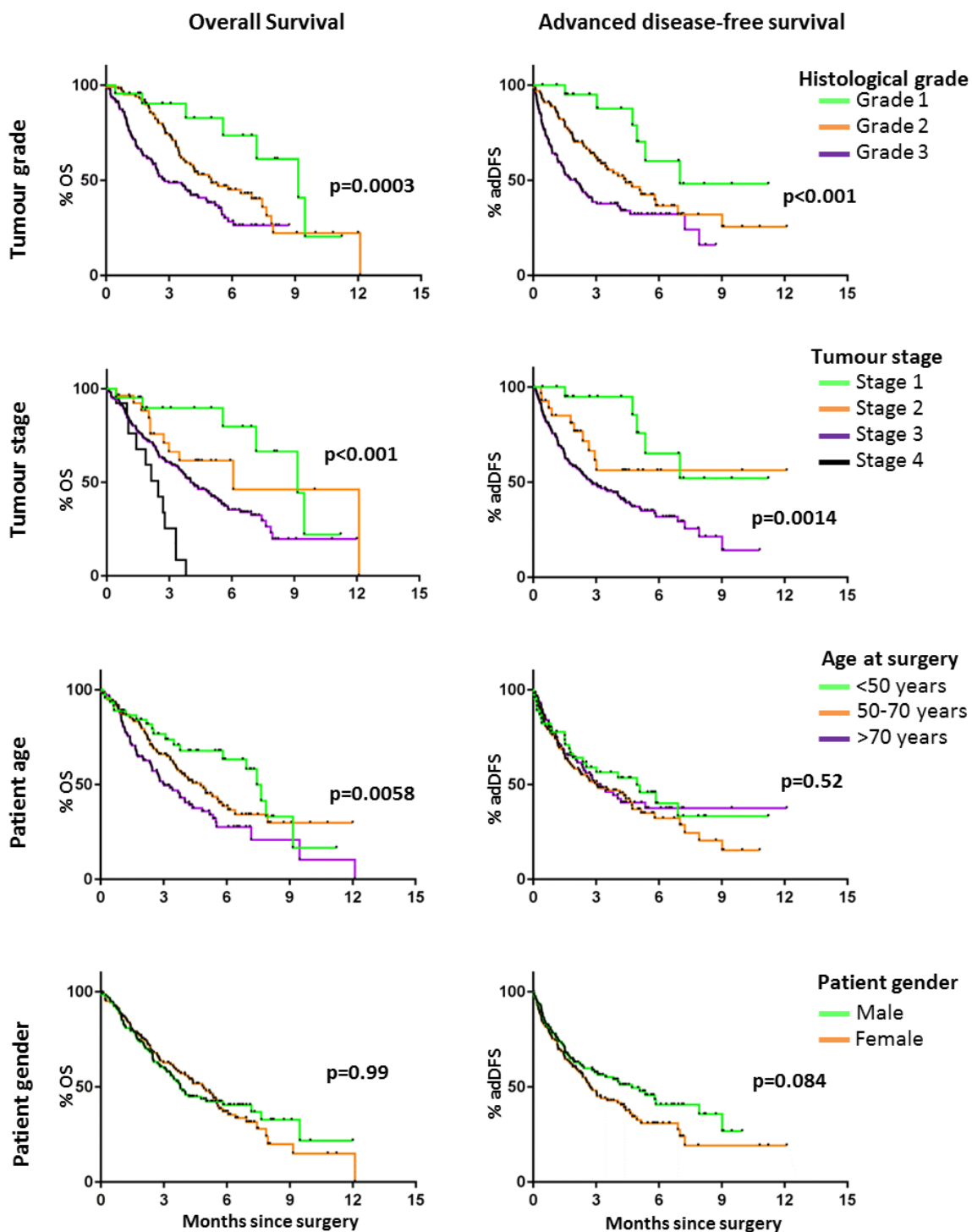


**Supplemental figure 4.1. Comparison of baseline characteristics between STS subtype cohorts.**

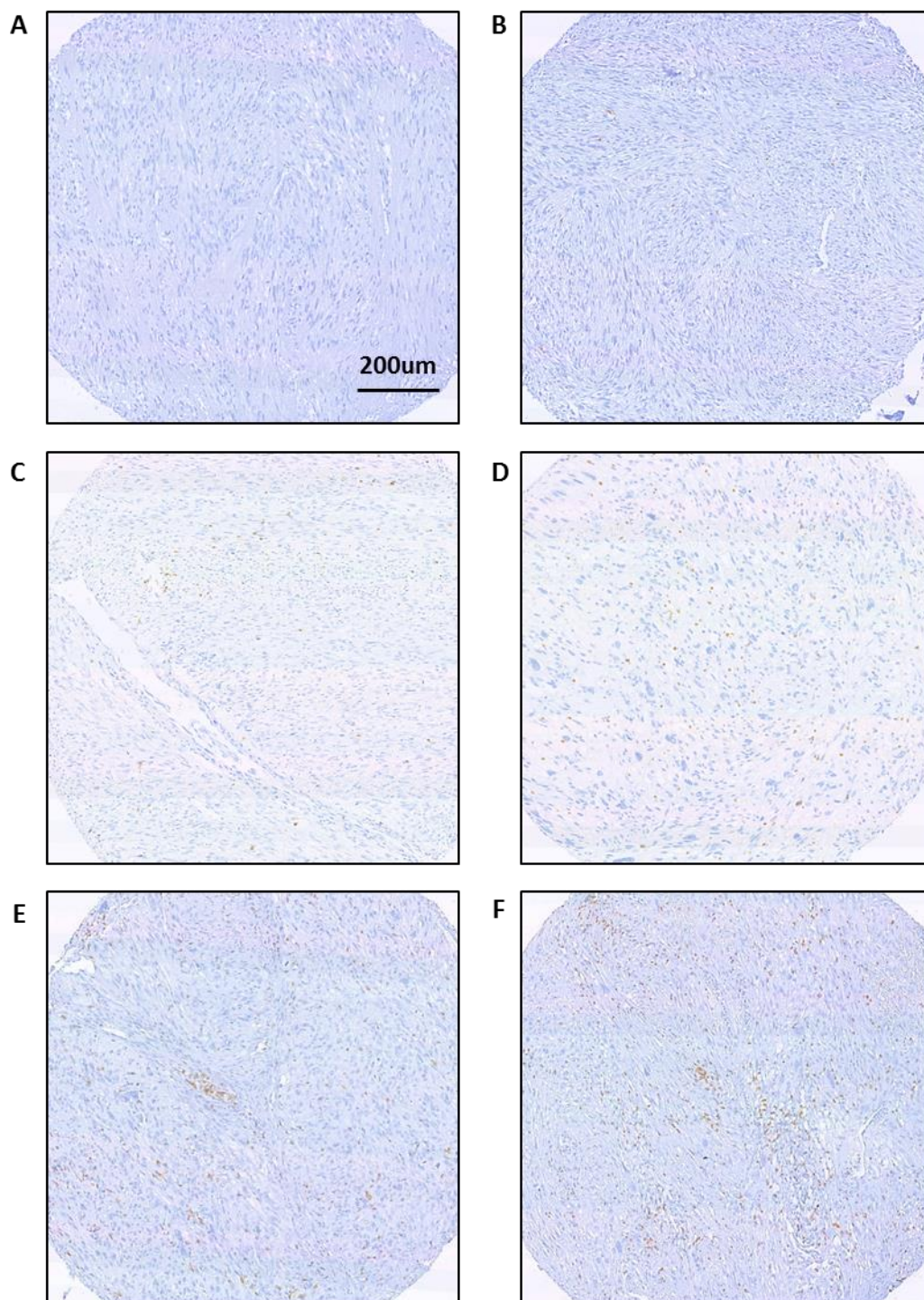
Tukey box and tail plots show comparative distributions of baseline characteristics in STS patient/ tumour cohort. **A.** Patient age at surgery, stratified by STS subtype. **B.** Maximum tumour dimension, stratified by STS subtype. **C.** Maximum tumour dimension, stratified by anatomical site of tumour origin. All P values derive from Dunn's multiple comparisons test following Kruskal Wallis test.



Supplemental figure 4.2. Overall and advanced-disease free survival in STS cohort stratified by histological subtype P values from logrank test

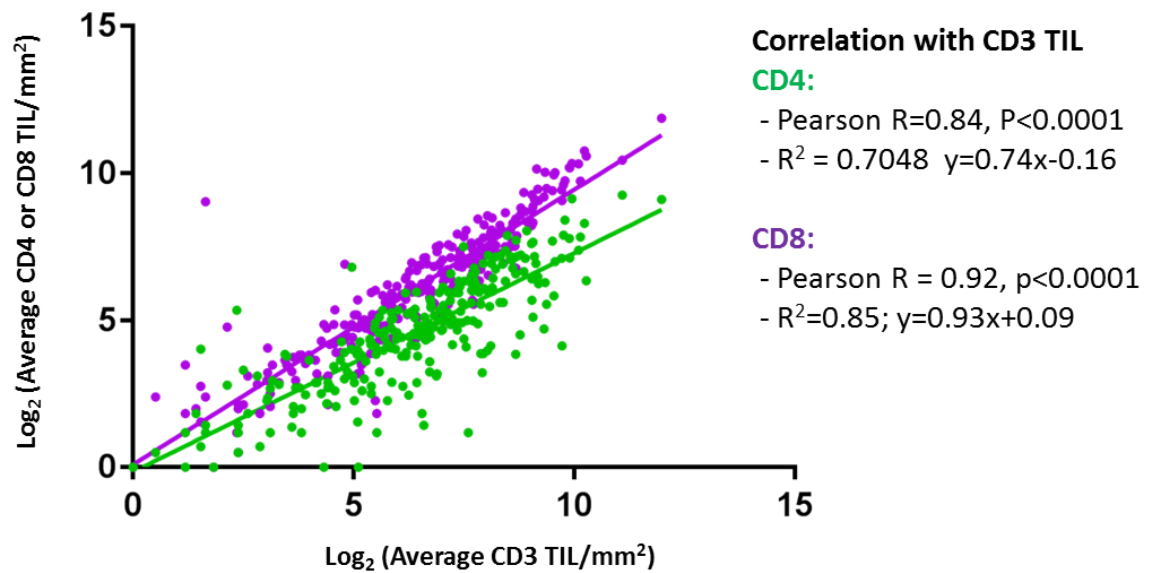


Supplemental figure 4.3. Overall and advanced-disease free survival in STS cohort stratified by baseline clinico-pathological parameters P values from logrank test



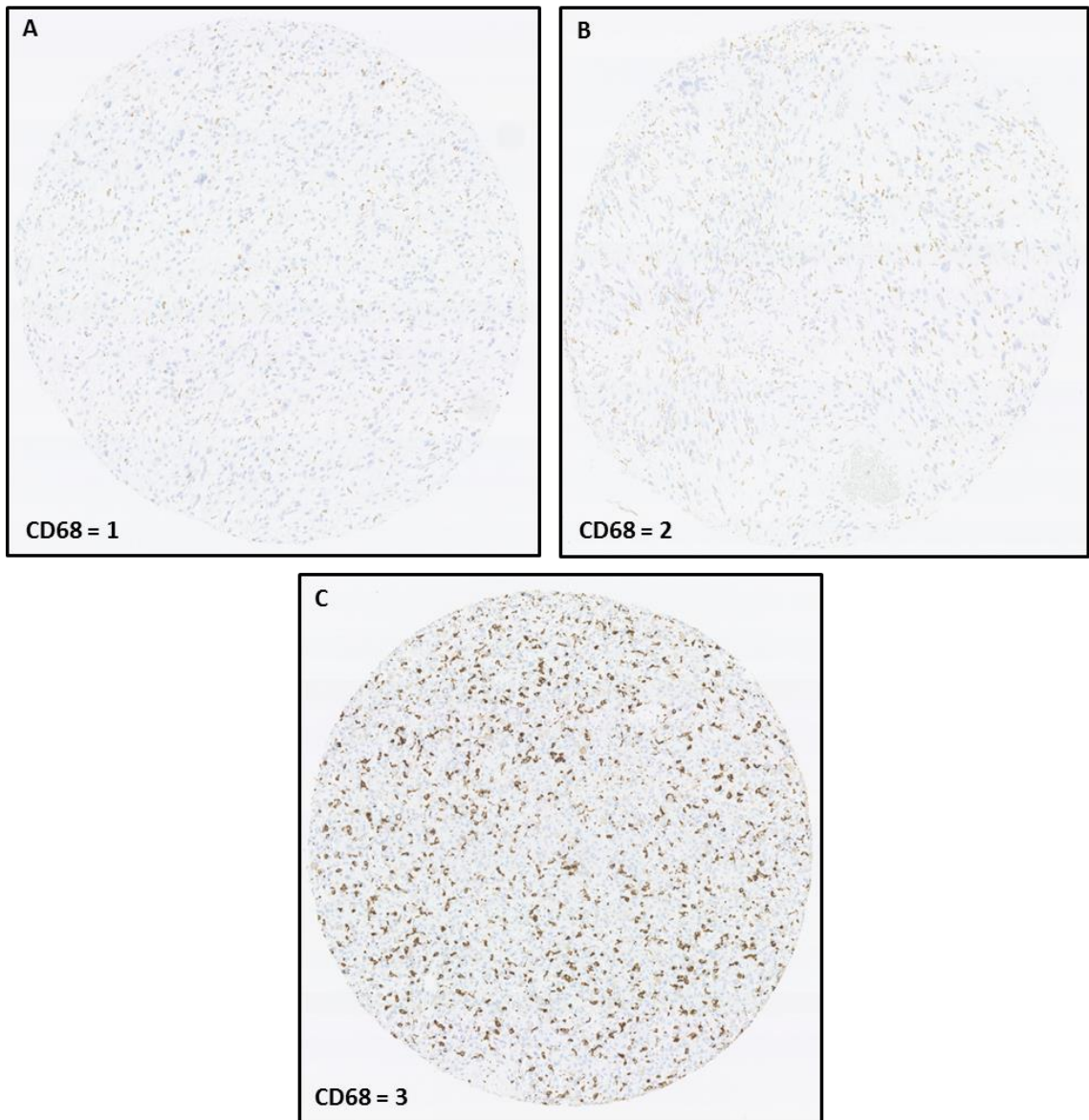
**Supplemental figure 4.4. TMA cores demonstrating variable degree of lymphocyte infiltration**

Images at x50 magnification of TMA cores of LMS immunostained for CD3, demonstrating different degrees of T lymphocyte infiltration. Shown are TIL burdens of (A) 0, (B) 30, (C) 100, (D) 200 (E) 500, and (F) 1000 TIL/mm<sup>2</sup>

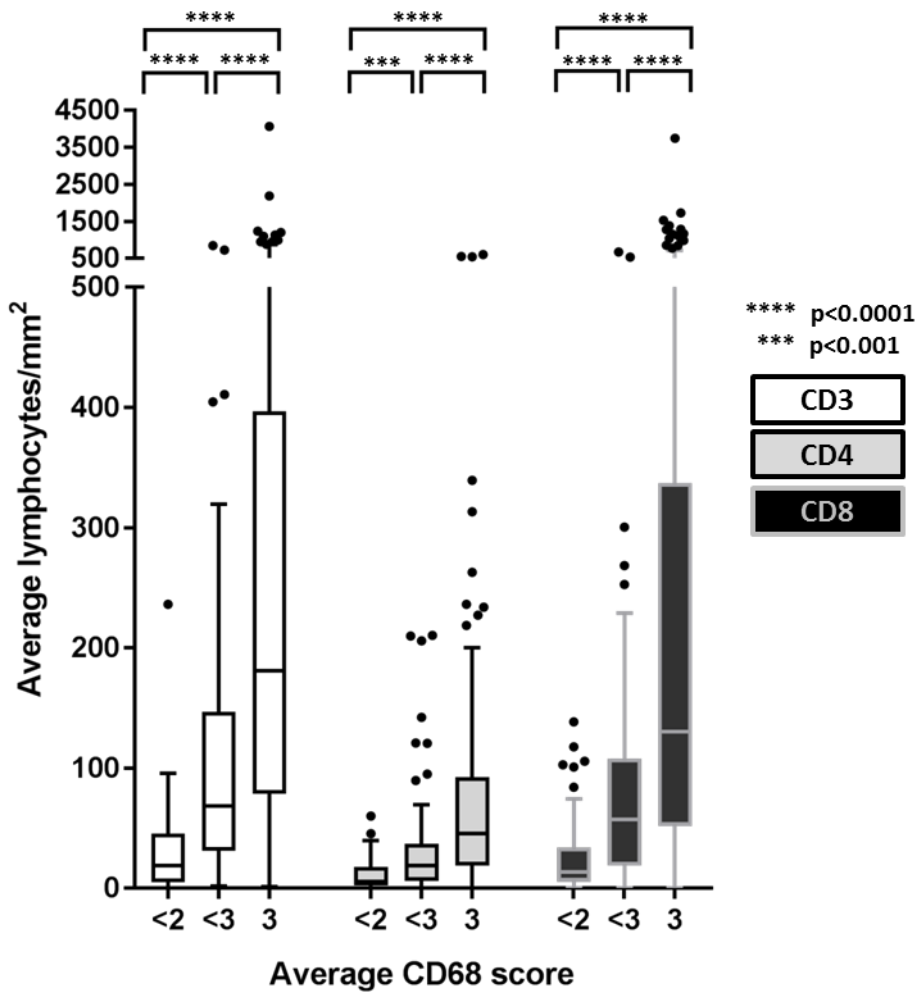


**Supplemental figure 4.5. Correlation between average CD3, CD4 and CD8 TIL values**

Scatter plot demonstrates relationship between Log<sub>2</sub>-transformed average CD3 TIL/mm<sup>2</sup> values with matched CD4 and CD8 TIL values from same tumour. Shown are Pearson R correlation coefficients with associated p values and regression coefficient and equations for lines of best fit

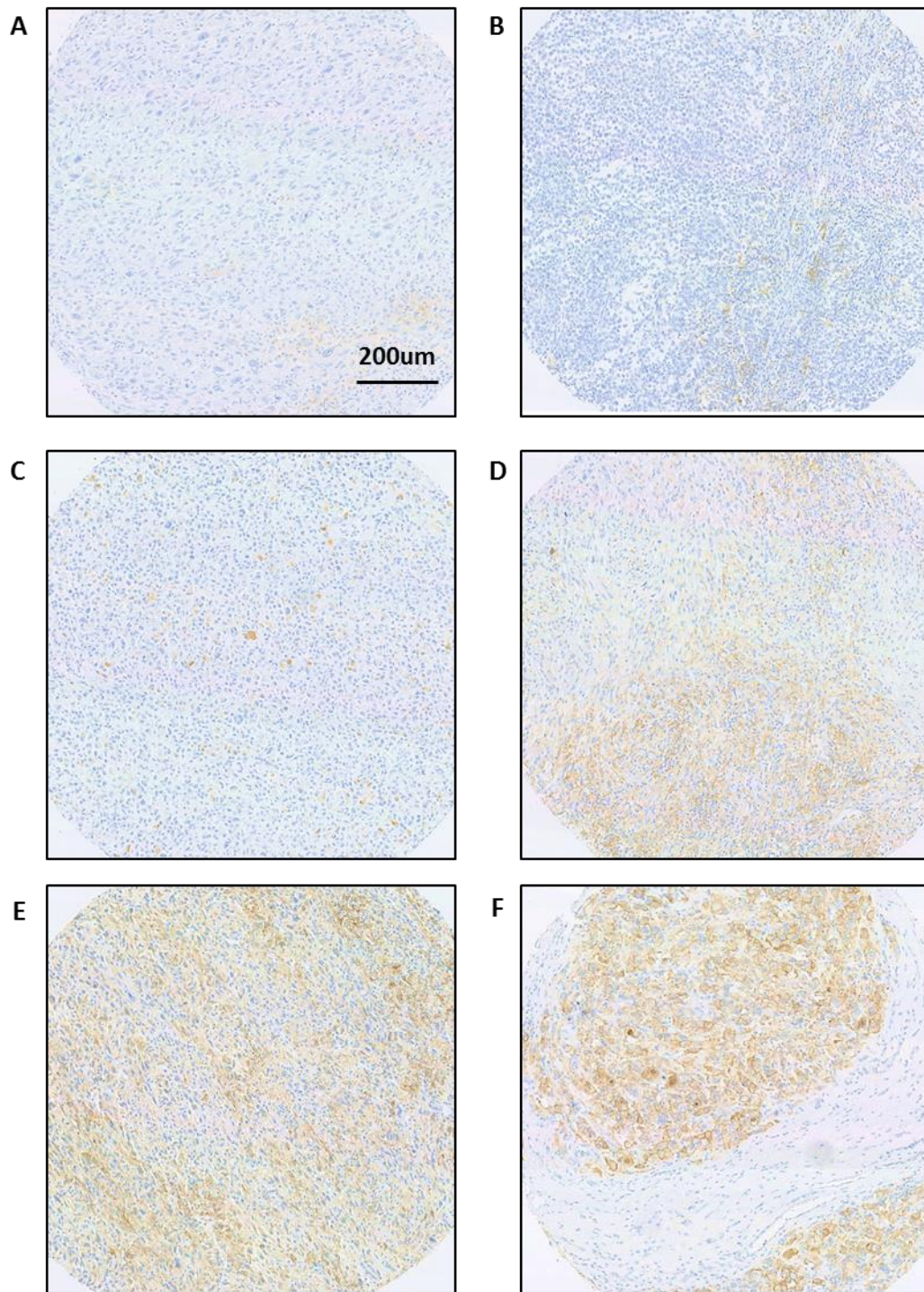


**Supplemental figure 4.6. TMA cores demonstrating variable degree of CD68+ macrophage infiltration.** Representative e TMA cores imaged at x100 magnification demonstrating degree of tumour infiltration by CD68+ macrophages scored as **(A)** 0, **(B)** 2 and **(C)** 3.



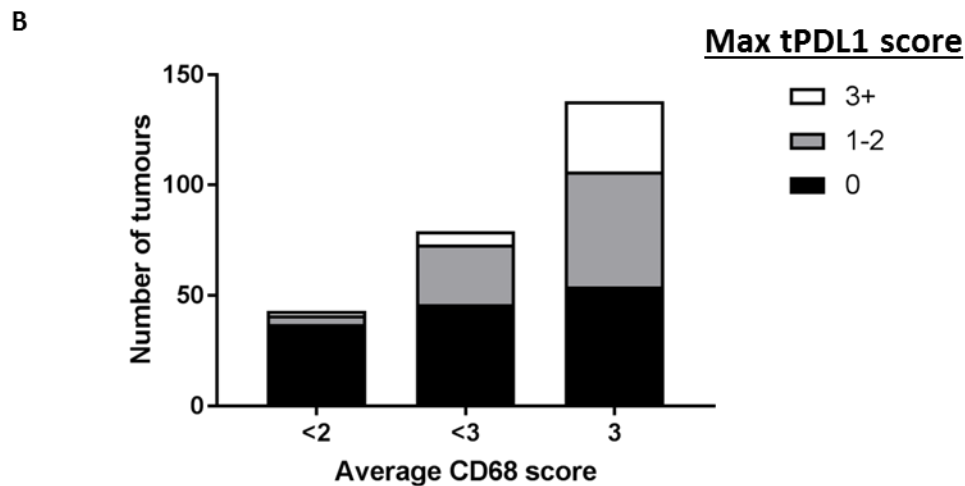
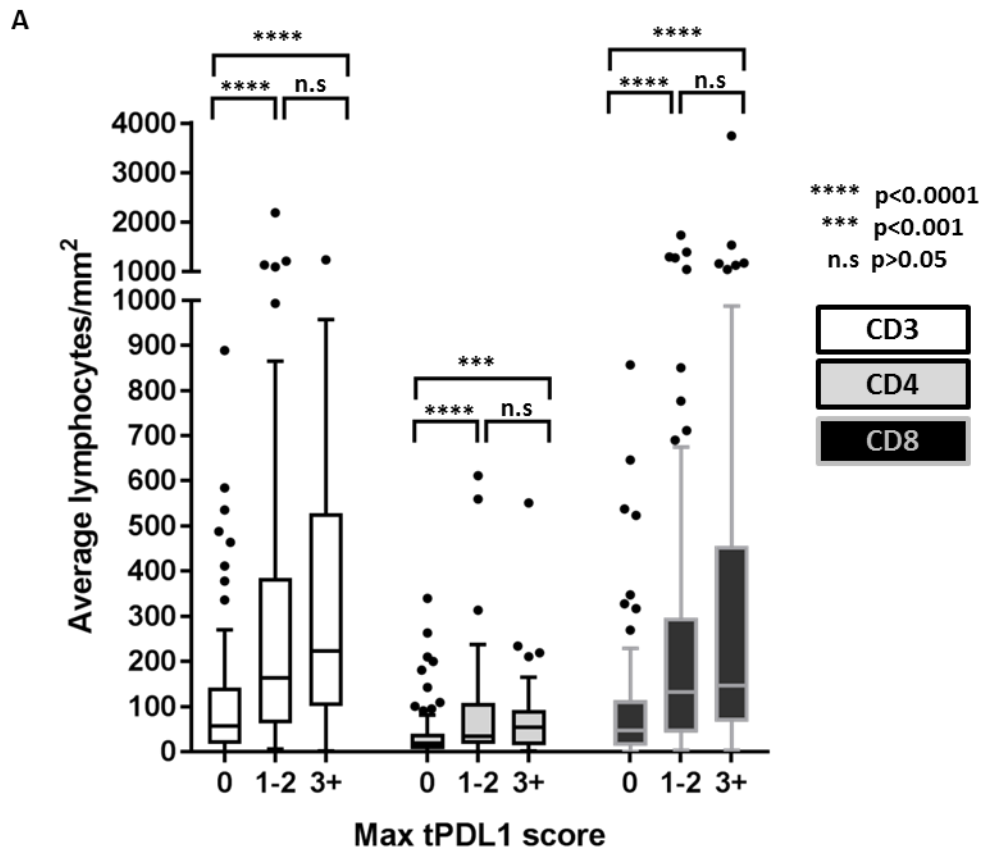
**Supplemental figure 4.7. Association between average TIL/mm<sup>2</sup> and average CD68 score**

Tukey box and tail plots show distributions of average TIL/mm<sup>2</sup> values for CD3, CD4 and CD8 from 266 STS when stratified by associated average CD68 scores. Adjusted P values derive from post-hoc Tukey's multiple comparisons testing after 1 way ANOVA of log<sub>2</sub>-transformed average TIL values



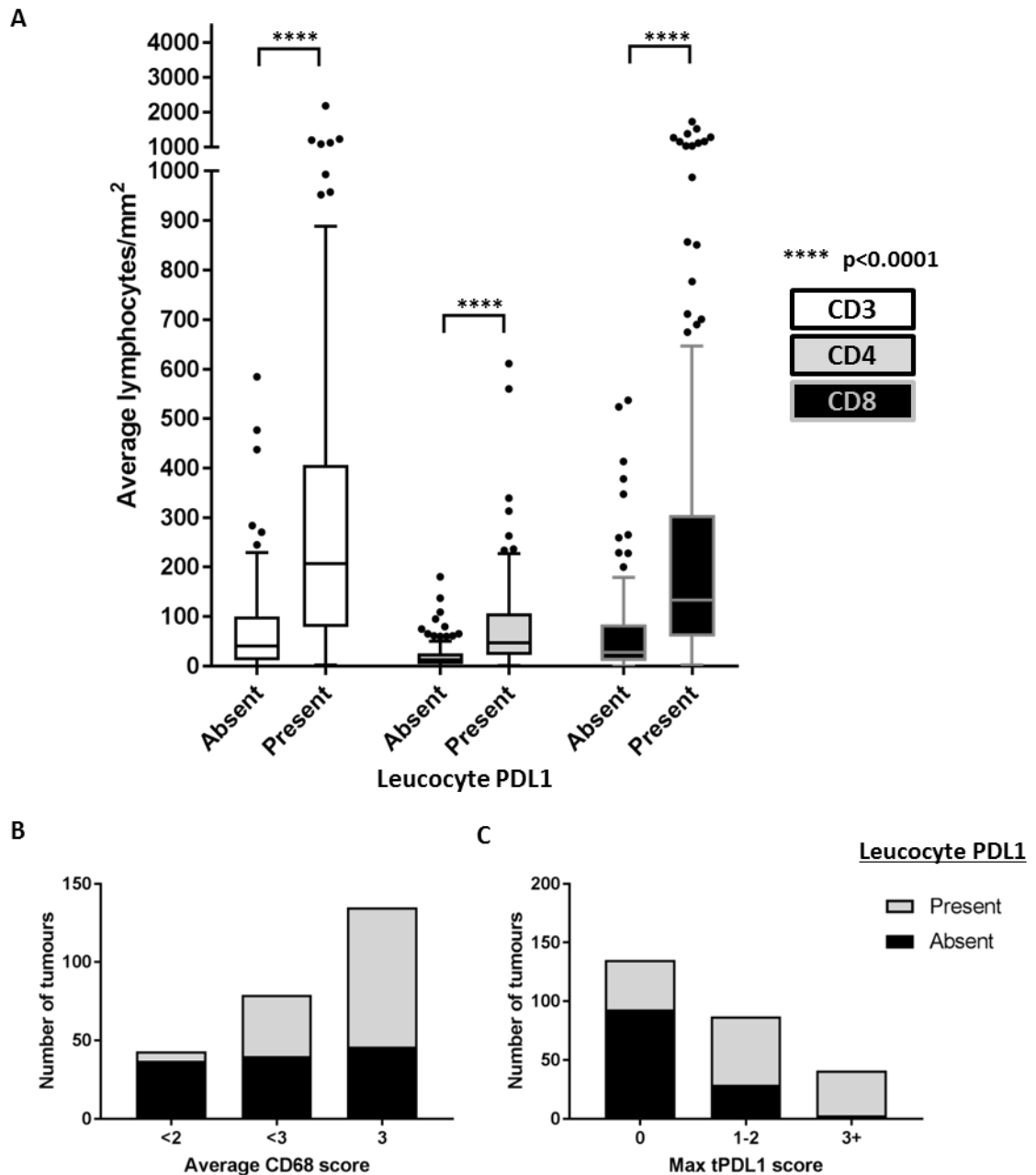
**Supplemental figure 4.8. TMA cores demonstrating variable degree of tumour cell PD-L1 staining**

Images at x50 magnification of TMA cores of UPS immunostained for PD-L1, demonstrating different degrees of T lymphocyte infiltration. Shown are tumours with PD-L1 scores of **(A) 1**, **(B) 2**, **(C) 3**, **(D) 4** **(E) 5**, and **(F) 6**



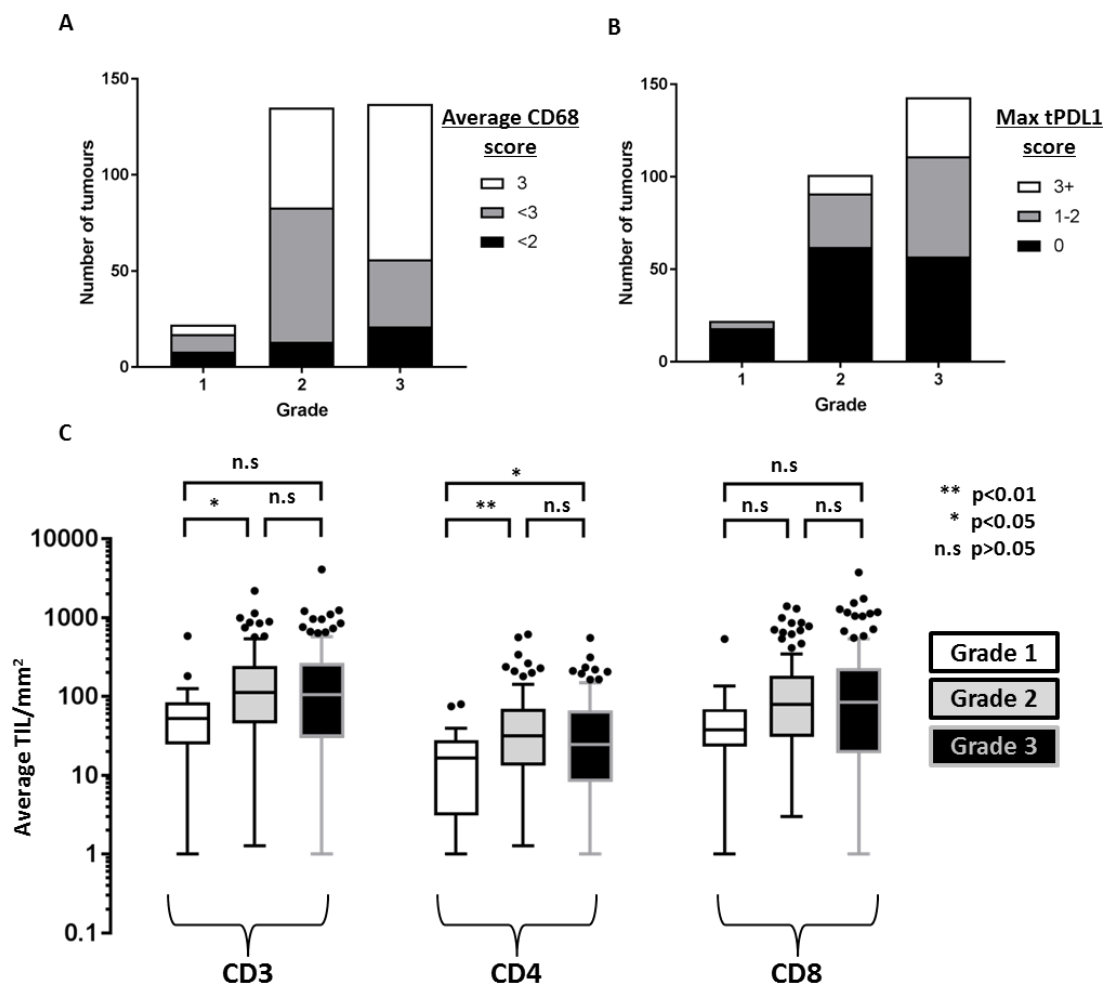
**Supplemental figure 4.9. Association of maximum tumour PD-L1 scores with average TIL values and CD68 scores**

**A.** Tukey box and tail plots show distributions of average TIL/mm<sup>2</sup> values for CD3, CD4 and CD8 from 266 STS when stratified by associated maximum tumour PD-L1 scores. Adjusted P values derive from post-hoc Tukey's multiple comparisons testing after 1 way ANOVA of log<sub>2</sub>-transformed average TIL values. **B.** Bar chart shows association between matched average CD68 and maximum tumour PD-L1 scores.  $\chi^2=34.61$ , df=4, p<0.0001



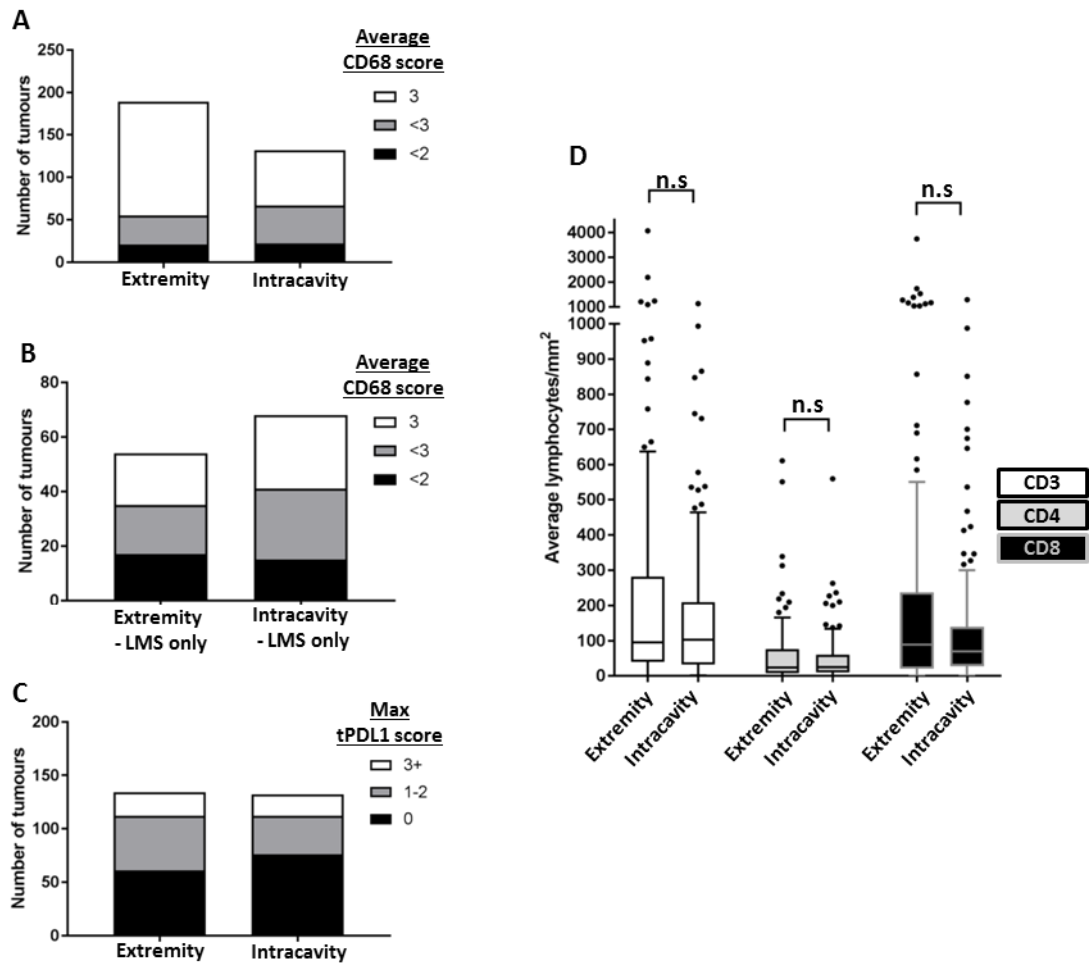
**Supplemental figure 4.10. Association of the presence of infiltrating leucocyte PD-L1 expression with average TIL values, average CD68 scores and maximum tumour PD-L1 scores**

**A.** Tukey box and tail plots show distributions of average TIL/mm<sup>2</sup> values for CD3, CD4 and CD8 from 266 STS when stratified by the presence or absence of infiltrating leucocytes with PD-L1 expression. Adjusted P values derive from post-hoc Tukey's multiple comparisons testing after 1 way ANOVA of log<sub>2</sub>-transformed average TIL values. **B.** Bar chart shows association between presence or absence of leucocyte PD-L1 expression and matched average CD68 score and maximum tumour PD-L1 scores.  $\chi^2=35.65$ , df=2, p<0.0001. **C.** Bar chart shows association between presence or absence of leucocyte PD-L1 expression and matched maximum tumour PD-L1 scores.  $\chi^2=58.31$ , df=2, p<0.0001



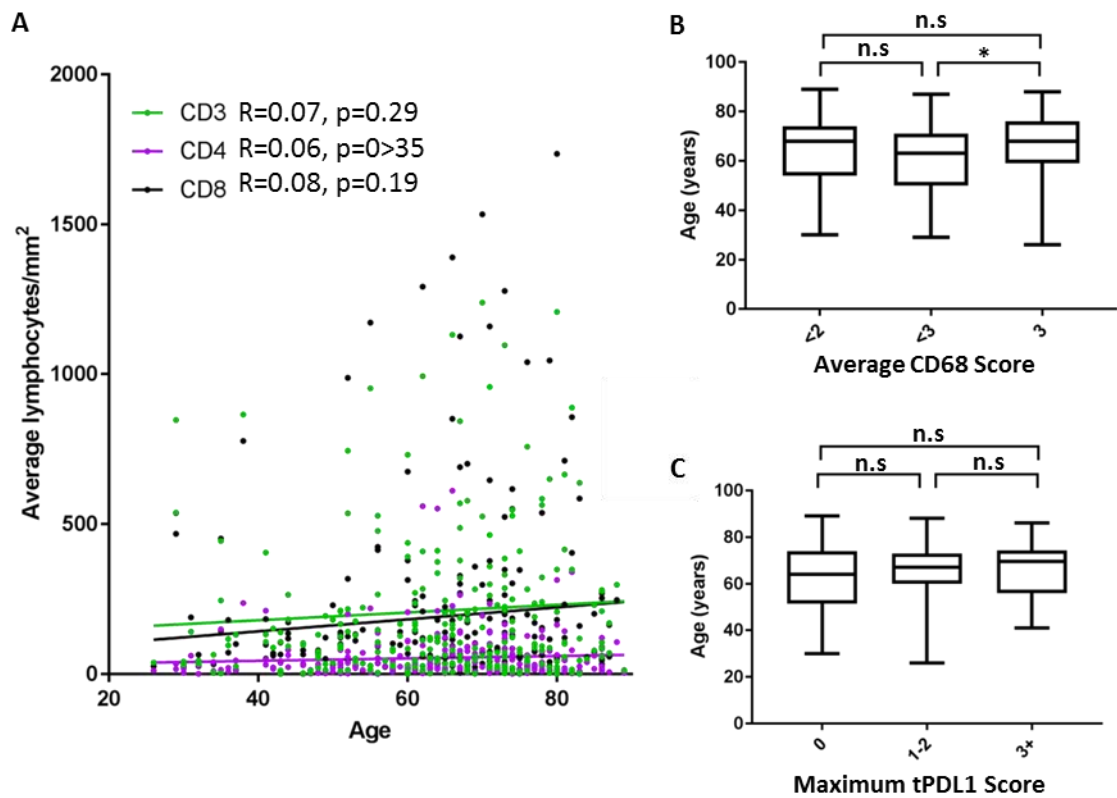
**Supplemental figure 4.11. Association of tumour grade with average TIL values, average CD68 scores and maximum tumour PD-L1 scores**

**A.** Bar chart shows association between tumour histological grade and matched average CD68 score and maximum tumour PD-L1 scores.  $\chi^2=30.94$ ,  $df=4$ ,  $p<0.0001$ . **B.** Bar chart shows association between tumour histological grade and matched maximum tumour PD-L1 scores.  $\chi^2=22.26$ ,  $df=4$ ,  $p=0.0002$ . **C.** Tukey box and tail plots show distributions of average TIL/mm<sup>2</sup> values for CD3, CD4 and CD8 from 266 STS when stratified by tumour histological grade. Adjusted P values derive from post-hoc Tukey's multiple comparisons testing after 1 way ANOVA of log<sub>2</sub>-transformed average TIL values.



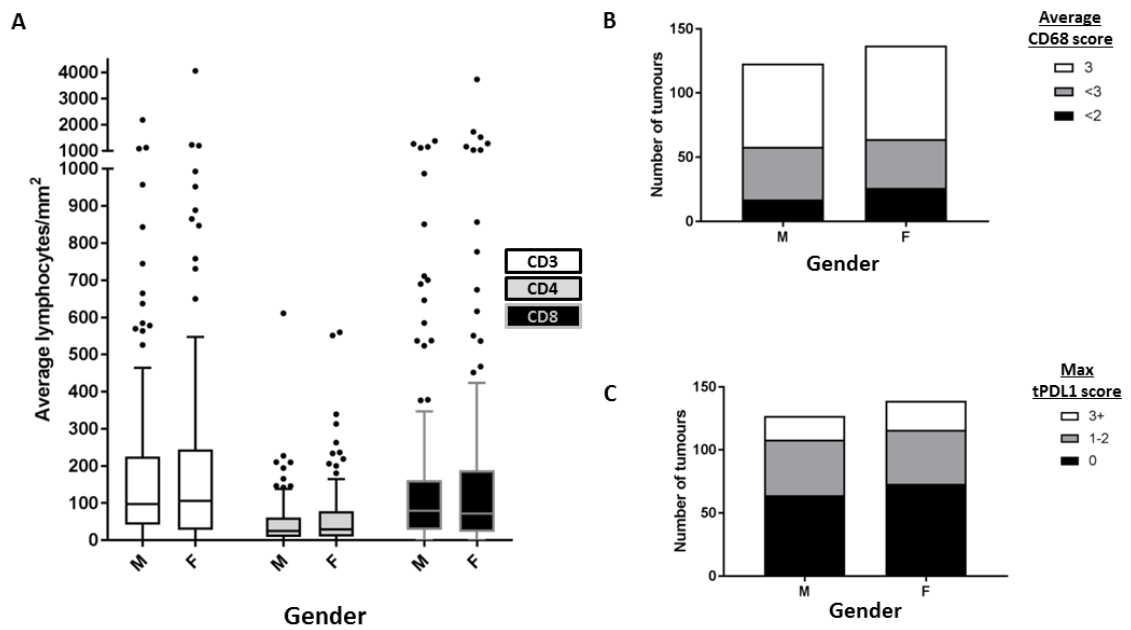
**Supplemental figure 4.12. Association of anatomical site of tumour origin with average CD68 scores, maximum tumour PD-L1 scores and average TIL values.**

Bar chart shows association between anatomical site of tumour origin and tumour matched **(A)** average CD68 score across all tumours ( $\chi^2=15.86$ ,  $df=2$ ,  $p=0.0004$ ), **(B)** average CD68 score in LMS cohort only ( $\chi^2=1.382$ ,  $df=2$ ,  $p=0.501$ ) and **(C)** maximum tumour PD-L1 scores. ( $\chi^2=4.309$ ,  $df=2$ ,  $p=0.116$ ). **D.** Tukey box and tail plots show distributions of average TIL/mm<sup>2</sup> values for CD3, CD4 and CD8 from 266 STS when stratified by anatomical site of tumour origin. Adjusted P values derive from post-hoc Tukey's multiple comparisons testing after 1 way ANOVA of log<sub>2</sub>-transformed average TIL values.



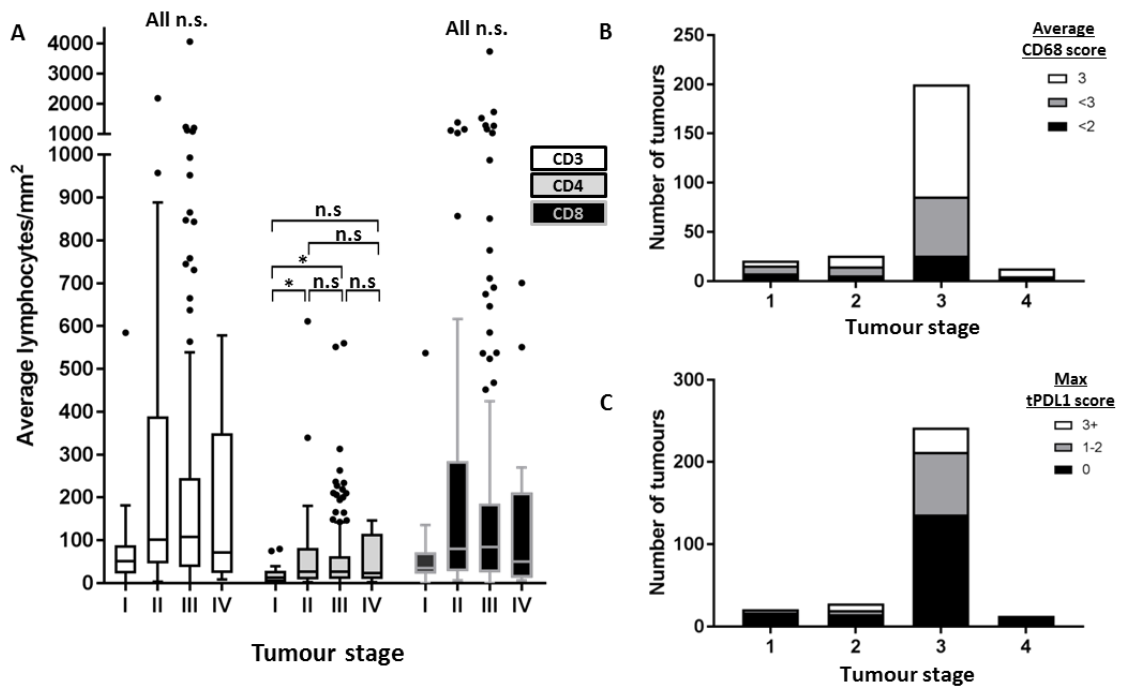
**Supplemental figure 4.13. Association of patient age at time of surgery with average TIL values, average CD68 scores and maximum tumour PD-L1 scores**

**A.** Scatter plot shows association between patient age and time of surgery and average TIL/mm<sup>2</sup>. Spearman correlation coefficients and associated P values shown. Tukey box and tail plots show distributions of patients' age at surgery when stratified by **(B)** average CD68 and **(C)** maximum tumour PD-L1 values. Adjusted P values derive from post-hoc Tukey's multiple comparisons testing after 1 way ANOVA .n.s. = p>0.05, \*p=0.01 - 0.05



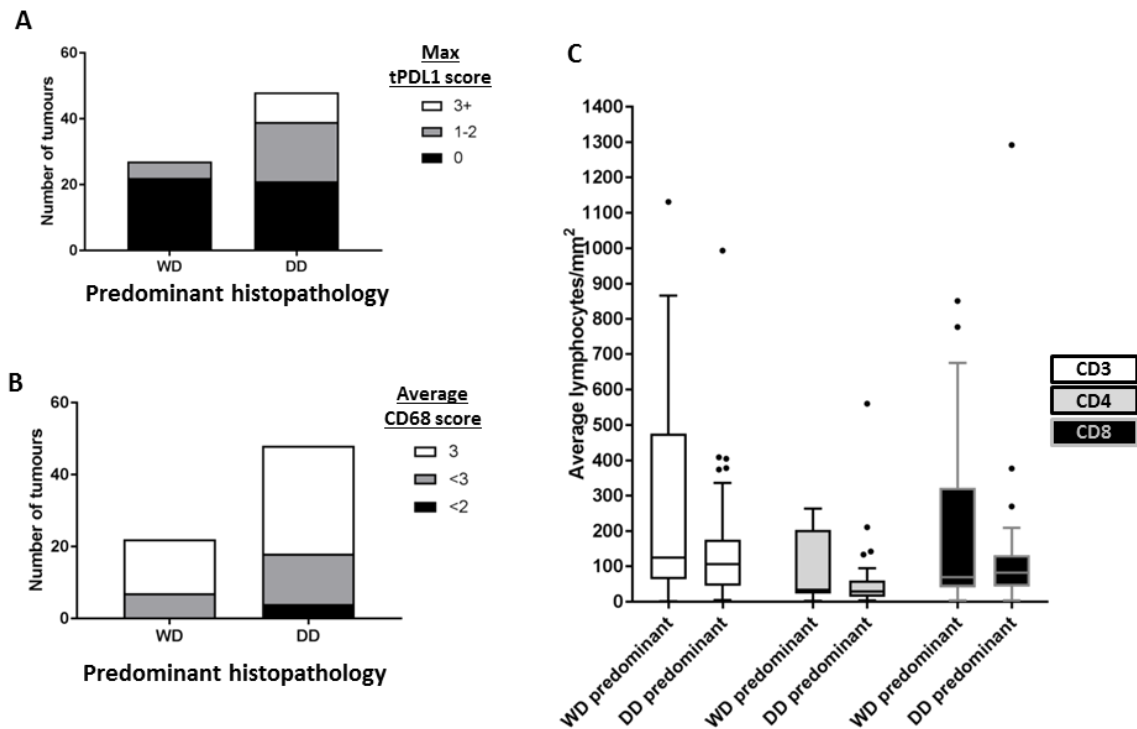
**Supplemental figure 4.14. Association of patient gender with average TIL values, average CD68 scores and maximum tumour PD-L1 scores.**

**A.** Tukey box and tail plots show distributions of average TIL/mm<sup>2</sup> values for CD3, CD4 and CD8 from 266 STS when stratified by patient gender. Comparison of log<sub>2</sub>-transformed average TIL values between gender groups by unpaired T tests all non-significant. Bar charts show association between patient gender and **(B)** average CD68 score across all tumours ( $\chi^2=1.713$ , df=2, p=0.425), or **(C)** maximum tumour PD-L1 scores. ( $\chi^2=0.443$ , df=2 p=0.801).



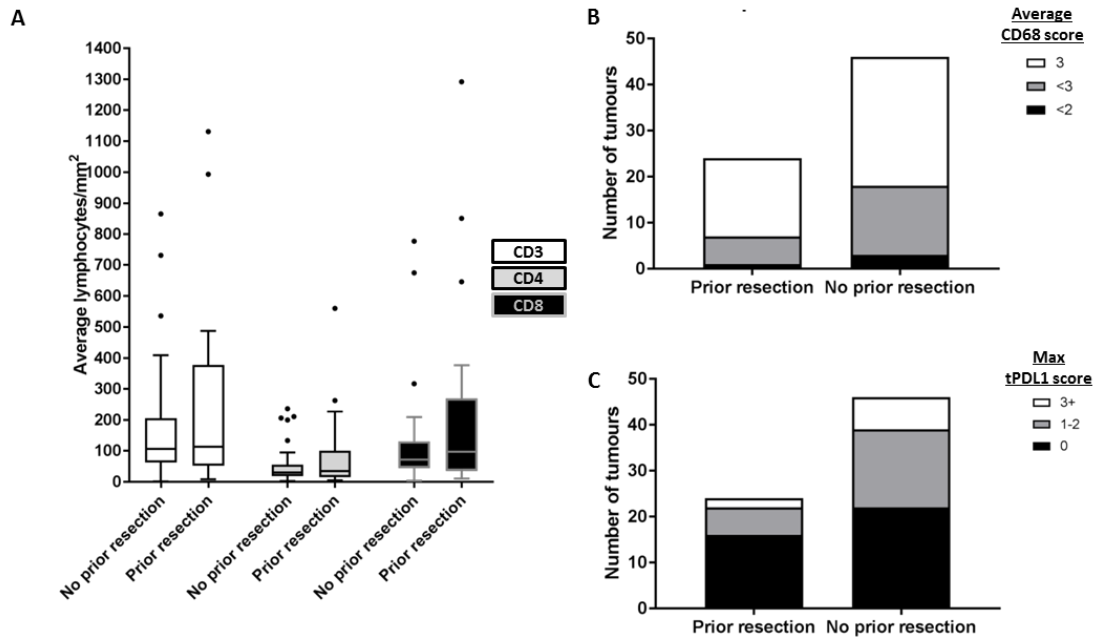
**Supplemental figure 4.15. Association of tumour stage with average TIL values, average CD68 scores and maximum tumour PD-L1 scores.**

**A.** Tukey box and tail plots show distributions of average TIL/mm<sup>2</sup> values for CD3, CD4 and CD8 from 266 STS when stratified by tumour stage. Adjusted P values derive from post-hoc Tukey's multiple comparisons testing after 1 way ANOVA .n.s. = p>0.05, \*p=0.01 - 0.05. Bar charts show association between patient gender and **(B)** average CD68 score across all tumours ( $\chi^2=1.713$ , df=2, p=0.425), or **(C)** maximum tumour PD-L1 scores. ( $\chi^2=0.443$ , df=2 p=0.801).



**Supplemental figure 4.16. Association of predominant histological subtype with average CD68 scores, maximum tumour PD-L1 scores and average TIL values in DDLPS cohort.**

Bar chart shows association within 70 DDLPS between predominant histological subtype and **(A)** maximum tPD-L1 score ( $\chi^2=11.38$ ,  $df=2$ ,  $p=0.0034$ ) and **(B)** average CD68 score ( $\chi^2=1.94$ ,  $df=2$ ,  $p=0.378$ ). **C.** Tukey box and tail plots show distributions of average TIL/mm<sup>2</sup> values for CD3, CD4 and CD8 from 70 DDLPS when stratified by predominant histological subtype. Comparison of log<sub>2</sub>-transformed average TIL values between gender groups by unpaired T tests all non-significant. WD = well-differentiated liposarcoma. DD = dedifferentiated liposarcoma.

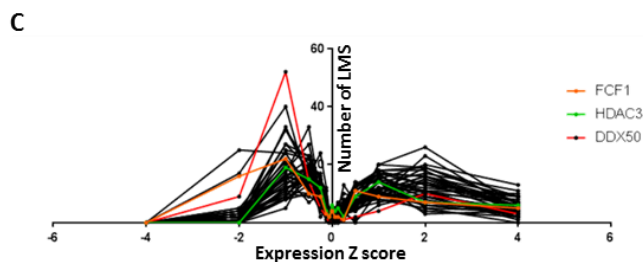


**Supplemental figure 4.17. Association of prior resection status with average TIL values, average CD68 scores and maximum tumour PD-L1 scores in DDLPS cohort.**

**A.** Tukey box and tail plots show distributions of average TIL/mm<sup>2</sup> values for CD3, CD4 and CD8 from 70 DDLPS when stratified by patient gender. Comparison of log<sub>2</sub>-transformed average TIL values between gender groups by unpaired T tests all non-significant. Bar charts show association between prior resection status in DDLPS cohort and **(B)** average CD68 score across all tumours ( $\chi^2=0.701$ ,  $df=2$ ,  $p=0.704$ ), or **(C)** maximum tumour PD-L1 scores. ( $\chi^2=2.30$ ,  $df=2$   $p=0.317$ ).

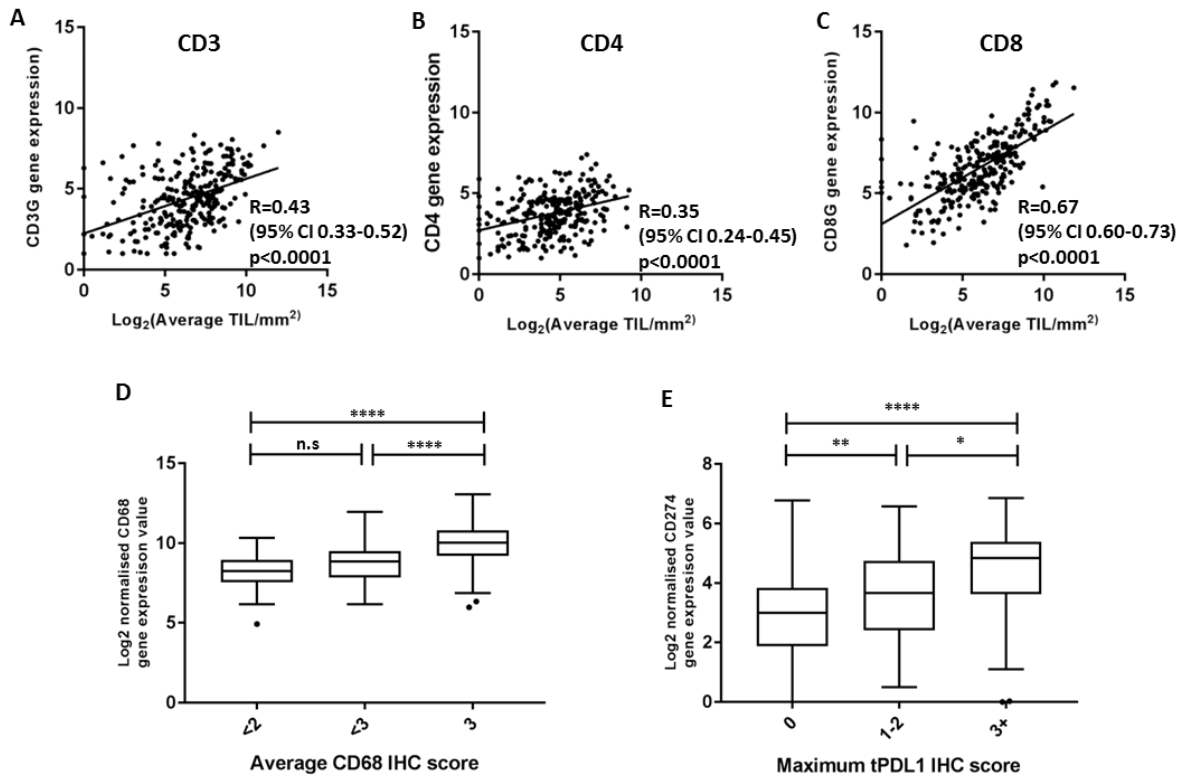
Gene Name	Order selected by geNorm	SD after normalization
FCF1	1	0.334
CNOT4	2	0.421
ACAD9	3	0.366
HDAC3	4	0.406
PIK3R4	5	0.363
EIF2B4	6	0.395
SLC4A1AP	7	0.396
FTSJ2	8	0.4
PIAS1	9	0.435
TTC31	10	0.467
ERCC3	11	0.446
PRPF38A	12	0.441
ZNF143	13	0.447
COG7	14	0.436
EDC3	15	0.464
DHX16	16	0.455
ZNF384	17	0.472
DDX50	18	0.497
TRIM39	19	0.51
AMMECR1L	20	0.493
RBM45	21	0.522
AGK	22	0.499
USP39	23	0.508
MRPS5	24	0.517
TLK2	25	0.514
SAP130	26	0.564
NUBP1	27	0.542
TMUB2	28	0.563
NOL7	29	0.569
ZKSCAN5	30	0.581
MTMR14	31	0.6
CNOT10	32	0.603
DNAJC14	discarded	0.728
C10orf76	discarded	0.837
SF3A3	discarded	0.699
ZC3H14	discarded	0.709
ZNF346	discarded	0.78
VPS33B	discarded	0.664
CC2D1B	discarded	1.05
GPATCH3	discarded	0.995

	R (95% CI)	P (two-tailed)
MTMR14	0.86 (0.75-0.92)	<0.0001
TLK2	0.83 (0.71-0.91)	<0.0001
FCF1	0.82 (0.69-0.90)	<0.0001
HDAC3	0.81 (0.68-0.90)	<0.0001
SAP130	0.80 (0.66-0.89)	<0.0001
TMUB2	0.80 (0.66-0.89)	<0.0001
DDX50	0.80 (0.65-0.88)	<0.0001
AMMECR1L	0.79 (0.64-0.88)	<0.0001
FTSJ2	0.78 (0.63-0.88)	<0.0001
MRPS5	0.78 (0.62-0.87)	<0.0001
ERCC3	0.78 (0.62-0.87)	<0.0001
SF3A3	0.77 (0.61-0.87)	<0.0001
CNOT4	0.77 (0.61-0.87)	<0.0001
PIK3R4	0.76 (0.59-0.86)	<0.0001
PRPF38A	0.75 (0.58-0.86)	<0.0001
EIF2B4	0.75 (0.58-0.86)	<0.0001
USP39	0.75 (0.57-0.86)	<0.0001
DHX16	0.74 (0.56-0.85)	<0.0001
ZNF143	0.73 (0.55-0.84)	<0.0001
SLC4A1AP	0.72 (0.54-0.84)	<0.0001
PIAS1	0.72 (0.54-0.84)	<0.0001
ACAD9	0.72 (0.53-0.84)	<0.0001
AGK	0.72 (0.53-0.84)	<0.0001
NOL7	0.70 (0.50-0.82)	<0.0001
COG7	0.69 (0.50-0.82)	<0.0001
C10orf76	0.68 (0.48-0.82)	<0.0001
VPS33B	0.68 (0.48-0.82)	<0.0001
RBM45	0.66 (0.44-0.80)	<0.0001
ZNF384	0.65 (0.44-0.80)	<0.0001
TTC31	0.64 (0.41-0.79)	<0.0001
TRIM39	0.64 (0.42-0.79)	<0.0001
GPATCH3	0.63 (0.41-0.78)	<0.0001
EDC3	0.61 (0.39-0.77)	<0.0001
CC2D1B	0.61 (0.38-0.77)	<0.0001
ZKSCAN5	0.59 (0.35-0.76)	<0.0001
NUBP1	0.55 (0.30-0.73)	0.0001
DNAJC14	0.55 (0.30-0.73)	0.0001
ZC3H14	0.51 (0.25-0.70)	0.0004
CNOT10	0.34 (0.04-0.58)	0.0275
ZNF346	0.31 (0.01-0.56)	0.0447



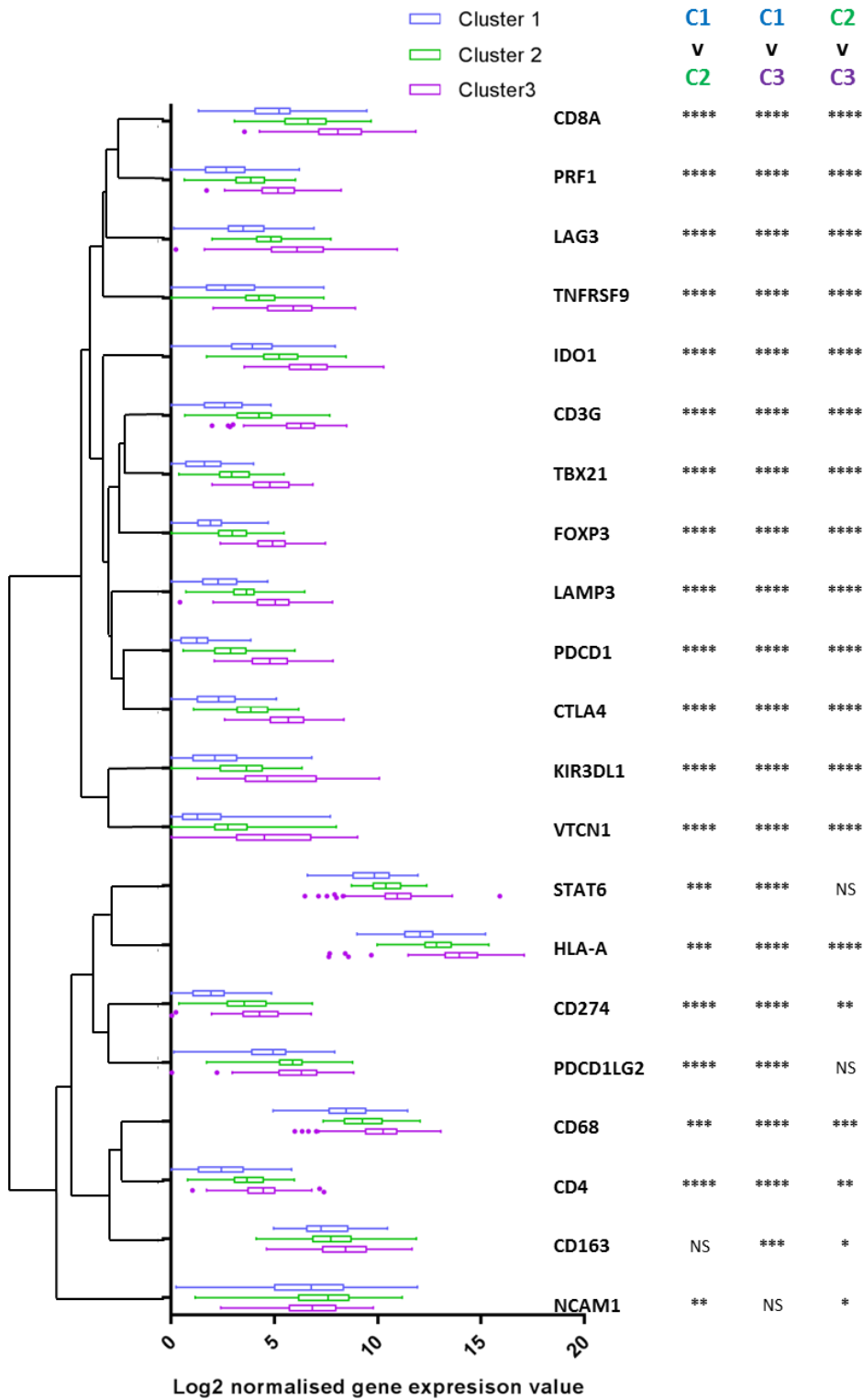
**Supplemental figure 4.18. Analysis of housekeeper gene performance in RMH-SARC and TCGA-SARC cohorts.**

**A.** Table showing results of geNorm (ref) analysis of performance of 40 housekeeper genes included in nCounter PanCancer Pathways codeset when applied to RMH-SARC gene expression dataset. **B.** Table shows Spearman correlation coefficient and associated confidence interval and P values when individual normalised expression values for 40 housekeeper genes compared to matched sum of all expression values for 40 housekeeper genes within RMH-SARC dataset. **C.** Frequency plot of expression Z scores for 40 candidate housekeeper genes in LMS (n=80) included within TCGA-SARC cohort.



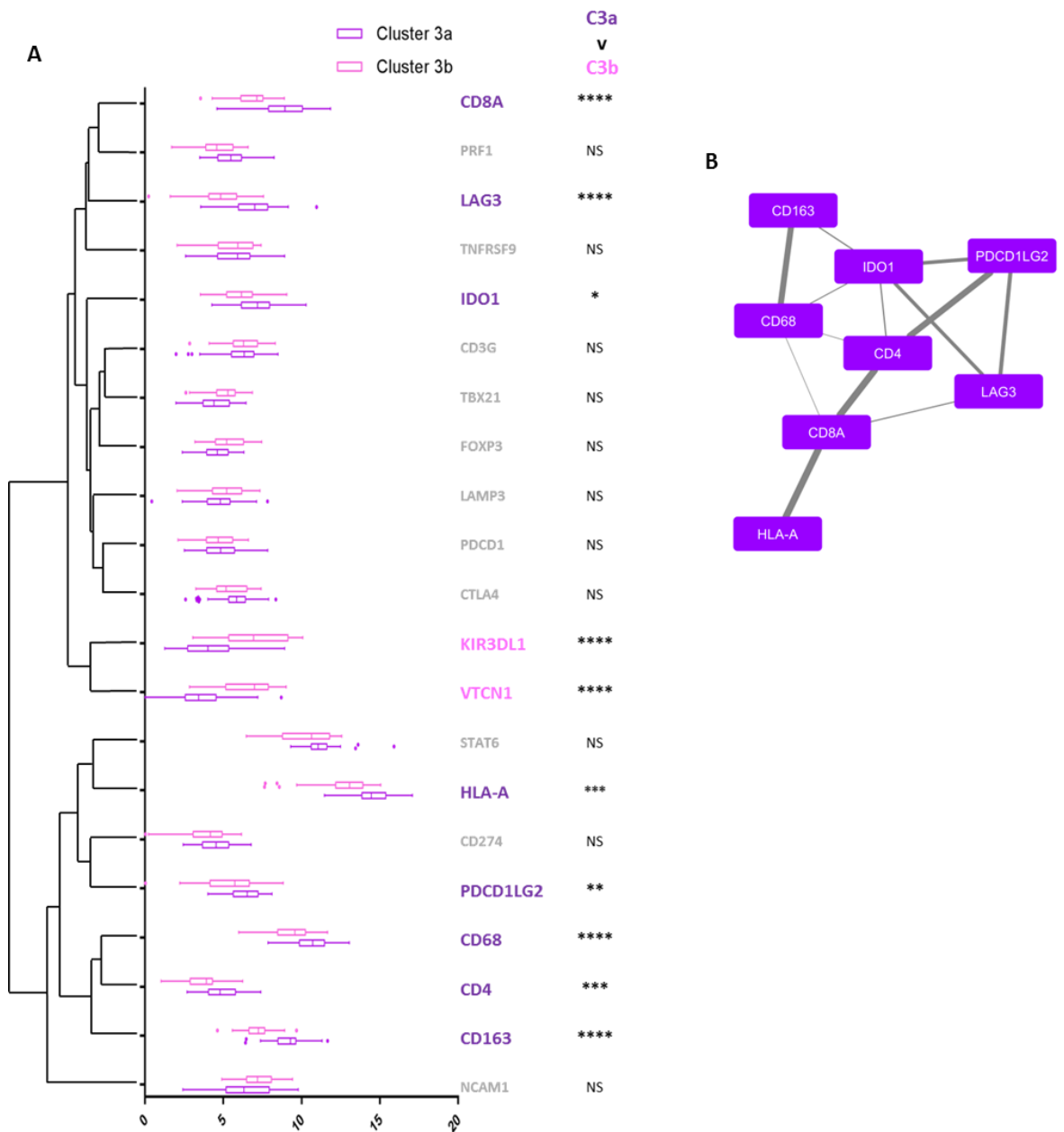
**Supplemental figure 4.19. Association of IHC-based scoring of immune microenvironment components with expression values of corresponding genes.**

Scatter plots show matched Log<sub>2</sub>-transformed average TIL/mm<sub>2</sub> values and normalised, Log<sub>2</sub>-transformed expression values for **(A)** CD3/CD3G, **(B)** CD4/CD4 and **(C)** CD8/CD8A. Pearson R correlation coefficient with 95% confidence intervals and associated P values shown. Tukey box and tail plots show distributions of associated Log<sub>2</sub>-transformed, normalised gene expression values for **(D)** CD68 and **(E)** CD274 y when stratified by average CD68 and maximum tumour PD-L1 values respectively. Adjusted P values derive from post-hoc Tukey's multiple comparisons testing after 1 way ANOVA .n.s. =  $p>0.05$ , \* $p<0.05$ , \*\*  $p<0.01$ , \*\*\* $p<0.001$ , \*\*\*\* $p<0.0001$



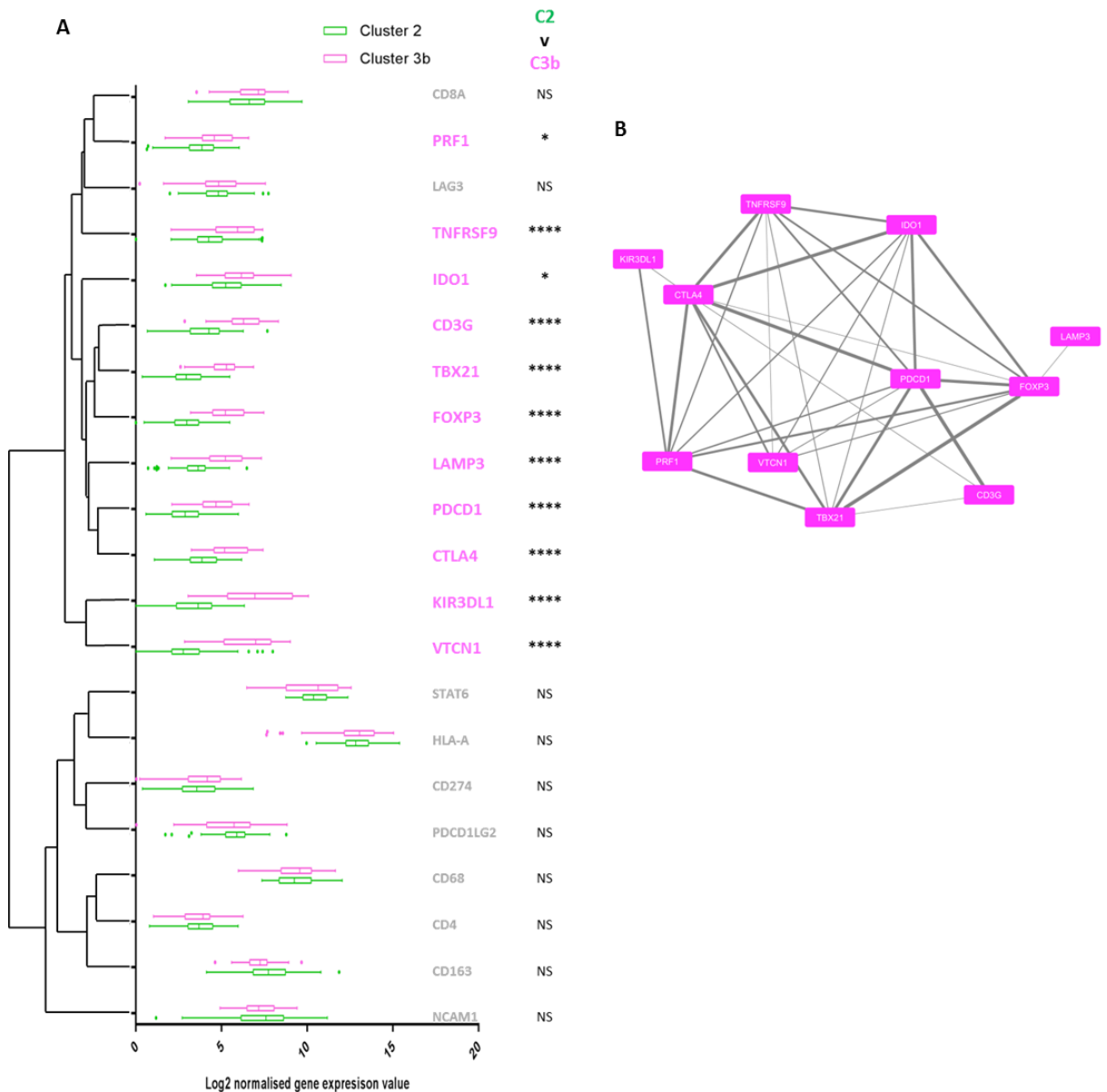
**Supplemental figure 4.20. Differences in expression of 21 immune-related genes between 3 identified clusters**

Tukey box and tail plots demonstrate distribution of expression values for each of 21 genes within 3 identified tumour clusters. Gene dendrogram derived from unsupervised clustering of dataset (see Figure 4.7). Adjusted P values derive from post-hoc Tukey's multiple comparisons testing after 1 way ANOVA as indicated. N.S. =  $p > 0.05$ , \* $p < 0.05$ , \*\*  $p < 0.01$ , \*\*\* $p < 0.001$ , \*\*\*\* $p < 0.0001$



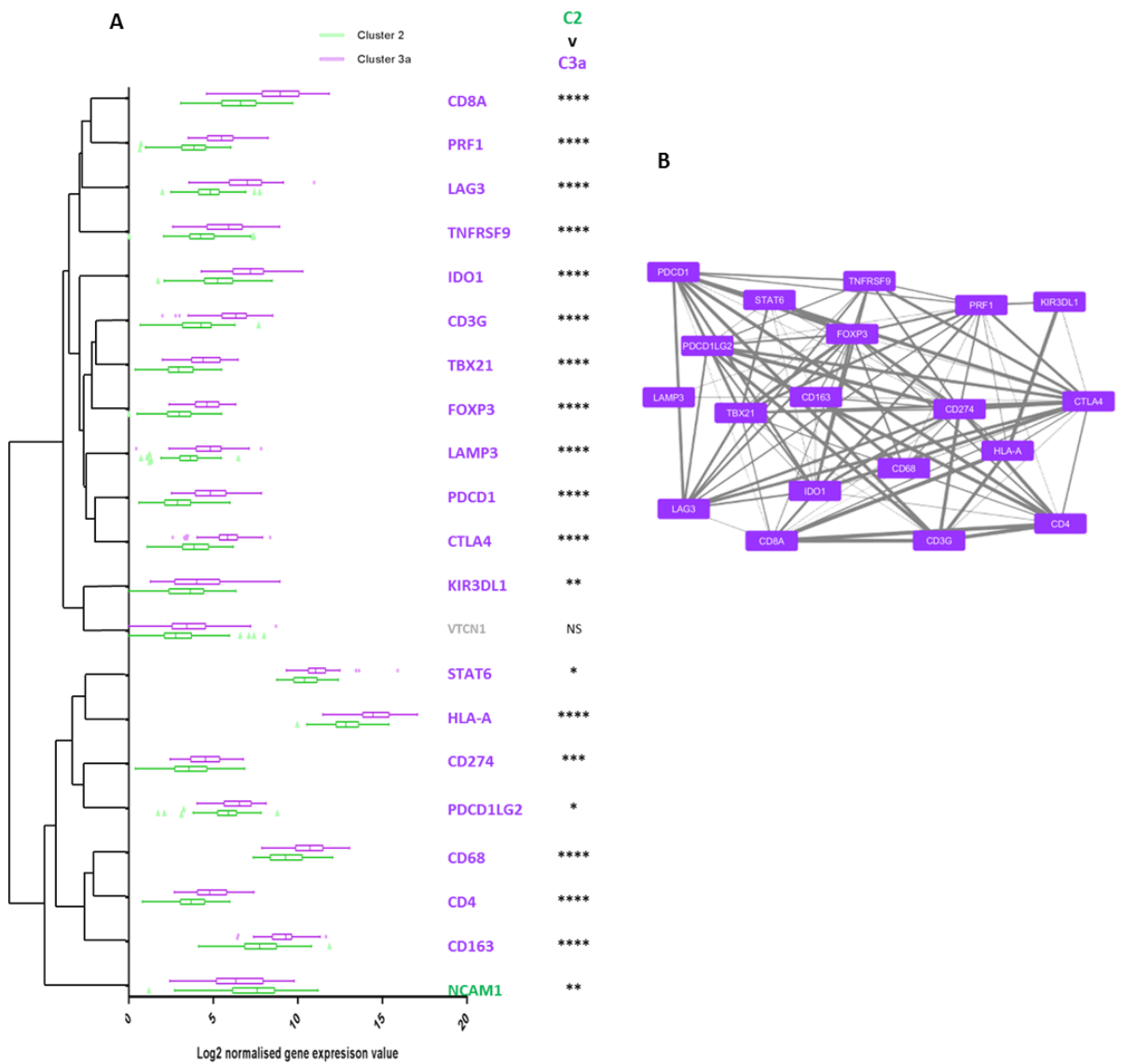
**Supplemental figure 4.21. Differences in expression of 21 immune-related genes clusters 3a and 3b**

**A.** Tukey box and tale plots demonstrate distribution of expression values for each of 21 genes within clusters 3a and 3b. Genes with significantly different expression highlighted in purple (higher in cluster 3a) or pink (higher in cluster 3b). Gene dendrogram derived from unsupervised clustering of dataset (see Figure 4.7). Adjusted P values derive from post-hoc Tukey's multiple comparisons testing after 1 way ANOVA as indicated. N.S. =  $p > 0.05$ , \* $p < 0.05$ , \*\* $p < 0.01$ , \*\*\* $p < 0.001$ , \*\*\*\* $p < 0.0001$ . **B.** Association network of 8 genes identified as upregulated in Cluster 3a compared to Cluster 3b, produced using the STRING application. Line thickness portrays the STRING calculated association confidence.



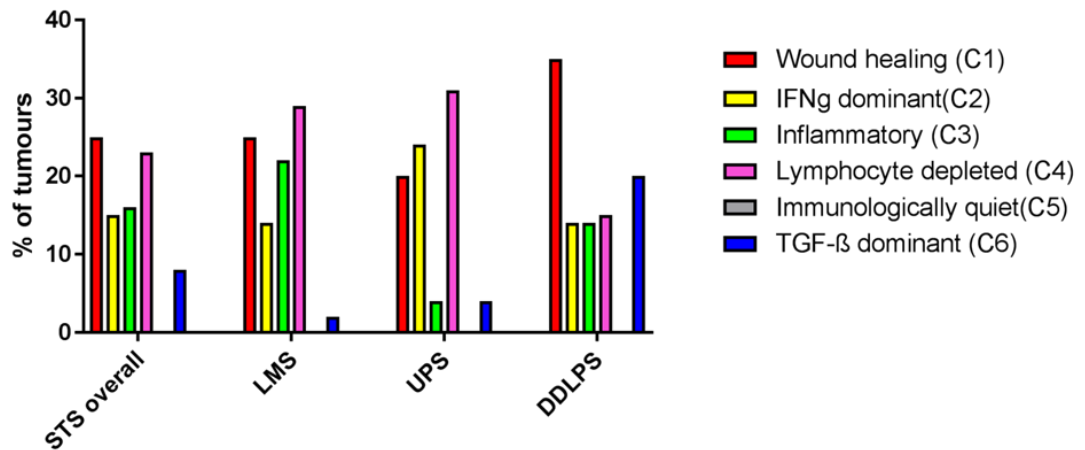
**Supplemental figure 4.22. Differences in expression of 21 immune-related genes clusters 2 and 3b**

Tukey box and tale plots demonstrate distribution of expression values for each of 21 genes within clusters 3a and 3b. Genes with significantly different expression highlighted in pink (higher in cluster 3b). Gene dendrogram derived from unsupervised clustering of dataset (see Figure 4.7). Adjusted P values derive from post-hoc Tukey's multiple comparisons testing after 1 way ANOVA as indicated. N.S. =  $p > 0.05$ , \* $p < 0.05$ , \*\*  $p < 0.01$ , \*\*\* $p < 0.001$ , \*\*\*\* $p < 0.0001$ . **B.** Association network of 11 genes identified as upregulated in Cluster 3a compared to Cluster 3b, produced using the STRING application. Line thickness portrays the STRING calculated association confidence.



**Supplemental figure 4.23. Differences in expression of 21 immune-related genes clusters 2 and 3a**

Tukey box and tale plots demonstrate distribution of expression values for each of 21 genes within clusters 2 and 3a. Genes with significantly different expression highlighted in pink (higher in cluster 3b). Gene dendrogram derived from unsupervised clustering of dataset (see Figure 4.7). Adjusted P values derive from post-hoc Tukey’s multiple comparisons testing after 1 way ANOVA as indicated. N.S. =  $p > 0.05$ , \* $p < 0.05$ , \*\* $p < 0.01$ , \*\*\* $p < 0.001$ , \*\*\*\* $p < 0.0001$ . **B.** Association network of 19 genes identified as upregulated in Cluster 3a compared to Cluster 2, produced using the STRING application. Line thickness portrays the STRING calculated association confidence.



**Supplemental figure 4.24. Distribution of immune subtypes within TCGA-SARC dataset**

Bar charts demonstrate the proportion of tumours within TCGA-SARC dataset allocated to each of 6 cancer immune subtypes, as described by Thorsson *et al.* Shown are data for all 257 STS across 6 STS subtypes, as well as immune subtype allocations within LMS, UPS and DDLPS subgroups. Figure derived by supplemental data reported by Thorsson *et al.*

## **Chapter 5 - Prognostic associations of the immune microenvironment in STS subtypes with complex karyotypes**

### **5.1 Background and Objectives**

As discussed in **Chapter 1.5.1**, an association between immune microenvironment characteristics and clinical phenotype in terms of prognosis and/or therapeutic response have been described across many different solid tumour types. As summarised in **Chapter 1.5.2 and 1.5.3**, the limited amount of reported translational data in STS provides some indication that an association between immune microenvironment and prognosis may exist, particularly in subtypes typified by complex karyotypes. In **Chapter 4**, we described the quantitative and qualitative variation observed in the immune microenvironment of a cohort of 266 early stage STS tumours, representing 3 histological subtypes with complex karyotypes. In this chapter, we investigated for associations between immune microenvironment characteristics and patient survival outcomes as a means of identifying candidate prognostic biomarkers.

#### ***Contributions***

Univariate survival analyses; cut-off analyses; TCGA-SARC data access, curation and analysis; figure generation were performed by the candidate. Multivariate Cox proportional hazard analyses were performed by Martina Millighetti, masters student.

## 5.2 Results

### ***5.2.1 T lymphocyte infiltration is associated with survival in UPS but not LMS or DDLPS***

To assess whether there was an association between the degree of T lymphocyte infiltration (as assessed by IHC) and overall and/or adDFS, we stratified the 266 STS cohort and also the subtype-specific sub-cohorts into subgroups with either high, moderate or low T lymphocyte infiltration based on cohort/sub-cohort-specific tertile values for tumour average TIL/mm<sup>2</sup>. There was no significant difference in OS across the 266 STS cohort when stratified into tumours with high, moderate or low infiltration by CD3, CD4 or CD8 lymphocytes (**Supplemental Figure 5.1**). However, when the subsub-cohorts were analysed in the same way, significant associations were seen between OS and lymphocyte infiltration in UPS (**Figure 5.1A-C**). UPS with high CD3, CD4 and CD8 TIL values (i.e. those with TIL values above upper tertile) had

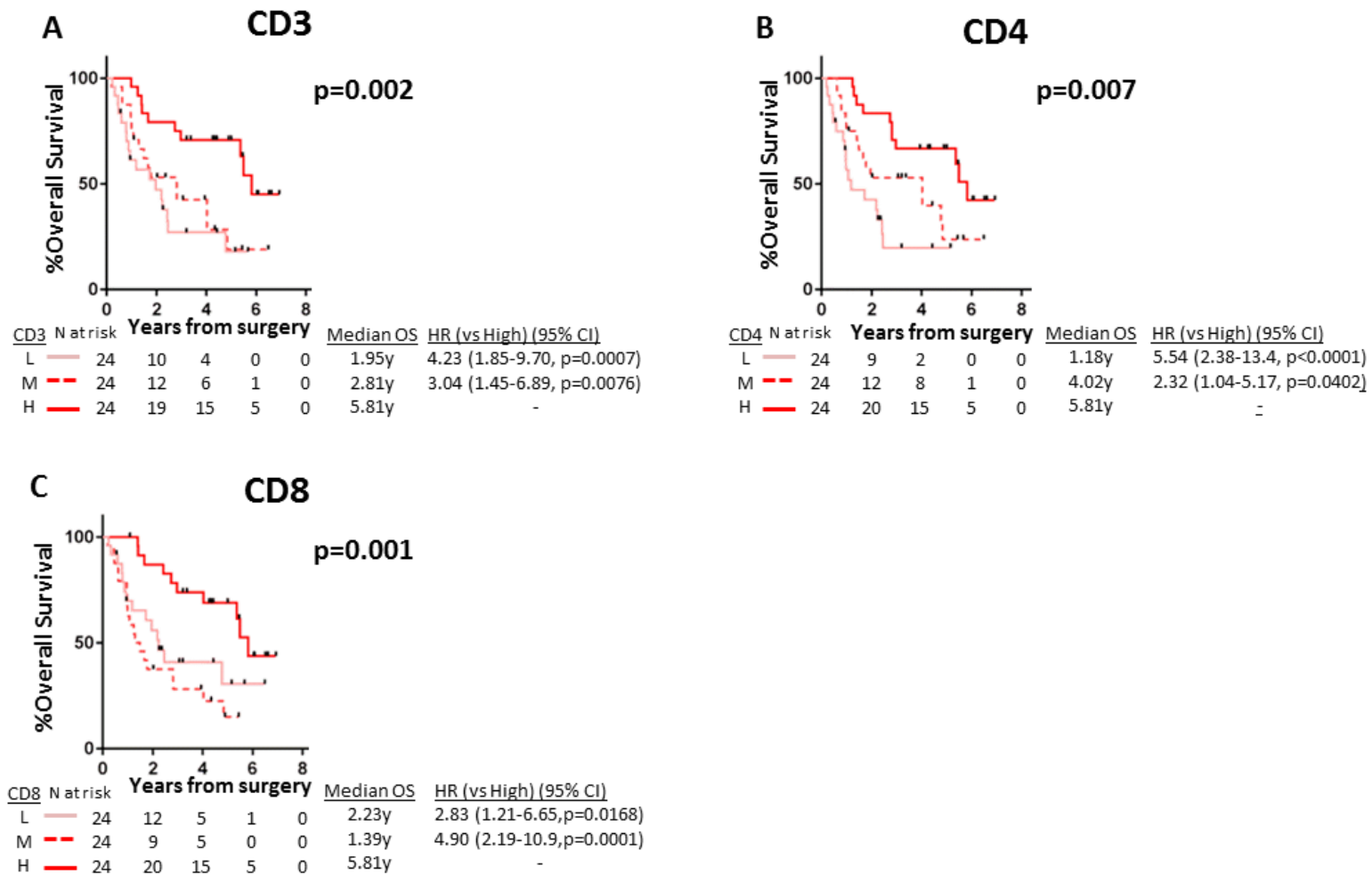


**Figure 5.1: Overall survival in UPS stratified by T lymphocyte infiltration**

Kaplan Meier survival curves show overall survival in 72 UPS when stratified into high, moderate or low T lymphocyte infiltration subgroups according to sub-cohort-specific tertile values for CD3, CD4 and CD8 average TIL/mm<sup>2</sup> values. Tertile cutpoints (average TIL/mm<sup>2</sup>) for CD3 48.2/235.9; CD4 15.4/54.7; CD8 40.0/216.1. HR, 95% CI (confidence interval) and P values derived from log rank test.

significantly longer OS from time of surgery compared to tumours with moderate or low TIL values. A similar relationship between adDFS and TIL level using the same tertile cutoffs was also seen, with tumours with high TIL levels associated with significantly longest adDFS (**Supplemental Figure 5.2A-C**). Assessment of the effect on using different average TIL/mm<sup>2</sup> values as cutpoints to dichotomise the UPS sub-cohort into 'high' and 'low' TIL tumours demonstrated a consistent relationship with higher TIL values and significantly improved OS across a large proportion of possible cutpoint values, indicating that the relationship between higher T lymphocyte infiltration and improved survival in the UPS sub-cohort was unlikely to be a false-positive finding resulting from overfitting of our dataset (**Supplemental Figure 5.3**). When the UPS sub-cohort was divided randomly in half, an association between higher CD3 TIL and improved OS was retained in both halves of the sub-cohort, albeit to a lesser degree of statistical significance, again suggesting that the observed association between TILs and prognosis was unlikely to be a false positive finding (**Supplemental Figure 5.4**).

In contrast to the UPS sub-cohort, no significant difference was seen in OS when the LMS and DDLPS sub-cohorts were stratified into high, moderate and low TIL tumours based on subtype-specific tertile values (**Supplemental Figure 5.5**).

### ***5.2.2 CD68+ macrophage infiltration is associated with survival in UPS but not LMS or DDLPS***

To assess for any association between patient survival and the degree of tumour infiltration by CD68+ macrophages, we stratified the 266 STS cohort and also the LMS, UPS and DDLPS sub-cohorts into subgroups based on averaged CD68+ scores. As was the case with TIL burden, there was no significant difference in survival within the entire cohort or LMS sub-cohort when stratified into tumours with uniformly dense, intermediate or non-dense CD68+ infiltrates (**Figure 5.2A-B**). However, as was seen with TIL burden, when sub-cohorts were assessed individually, a significant association between average CD68 score and OS was seen in UPS patients (**Figure 5.2C**). In 7/72 (9.7%) of patients with UPS with non-dense CD68 infiltrates (average CD68 score <2), significantly shorter OS was seen compared to patients with average CD68 scores ≥2 (CD68 score <2 vs. score ≥2: OS HR 5.79; 95% 1.51-22.3; p=0.0105). Meanwhile, no significant difference in OS was seen in DDLPS sub-cohorts when stratified by average

CD68 score (**Figure 5.2D**). These data indicate that, as was the case with TIL burden, an association between survival and degree of tumour infiltration by CD68+ve macrophages was detectable in the UPS sub-cohort only.

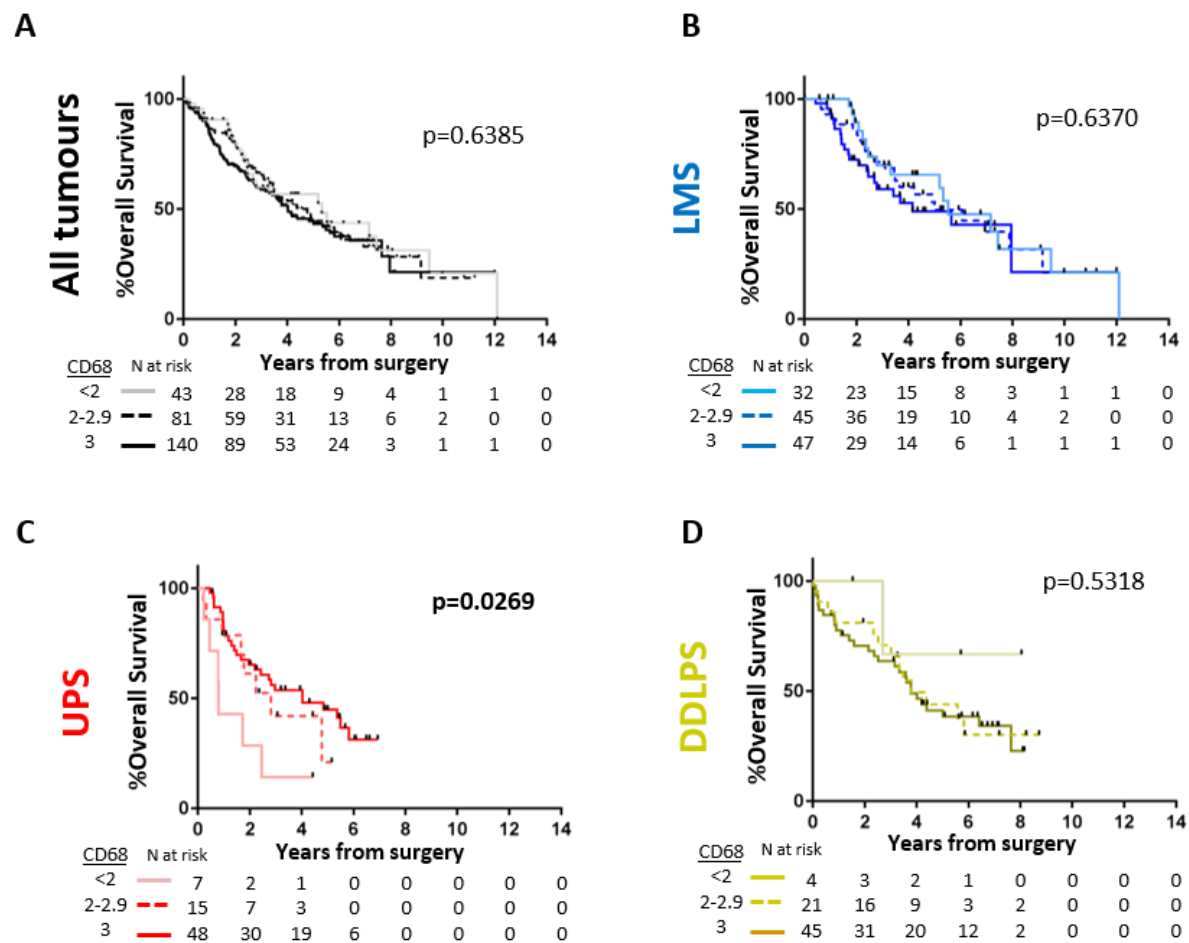


**Figure 5.2: Overall survival in karyotypically-complex STS when stratified by infiltration by CD68+ macrophages**

Kaplan Meier survival curves show overall survival in (A) entire 266 STS cohort, (B) 124 LMS, (C) 72 UPS and (D) 70 DDLPS sub-cohorts when stratified by degree of CD68+ macrophage infiltration. Tumours were stratified as having either uniformly dense (average CD68 score of 3), intermediate (average CD68 score 2-2.9) or non-dense (average CD68 score <2) infiltrates. P values derived from log rank test.

### ***5.2.3 Tumour and leucocyte PD-L1 expression has contrasting associations with survival depending on STS histological subtype***

To assess for any association between patient survival and the extent of tumour cell expression of PD-L1, we stratified the entire STS cohort (n=266) and the LMS, UPS and DDLPS sub-cohorts by maximum tPD-L1 score. In the entire cohort, there was no significant difference in OS between tumour subgroups defined by either absent, limited or higher expression of PD-L1 (defined by max tPD-L1 scores of 0,1-2 and 3-6, respectively) (**Figure 5.3A**). Similarly, stratification of the LMS sub-cohort by max tPD-L1 score revealed no association between OS and tumor cell expression PD-L1 in this subtype (**Figure 5.3B**). A significant association of OS with max tPD-L1 score was seen in both the UPS and DDLPS sub-cohorts, although the direction of association differed between the two subtypes (**Figure 5.3C-D**). In the UPS sub-cohort, a significant difference in OS was detected between tumours with absent, limited or higher PD-L1 expression (p=0.027), with the 30/72 (43%) of tumours with absent tumour PD-L1 expression associated with the worst outcomes (tPD-L1 0 vs >1: median OS 1.7 vs 5.4 years, HR 2.64, 95% CI 1.34-5.20, p=0.0006) (**Figure 5.3C**). In contrast, in the DDLPS sub-cohort, it was the small proportion of tumours with higher levels of PD-L1 expression that were associated with worse prognosis (**Figure 5.3D**). In the 9/70 (13%) of DDLPS with max tPD-L1 score of 3 or higher, OS was dramatically worse than in tumours with lower tPD-L1 scores (Median OS 0.2 vs 4.4 years, HR 4.53, 95% CI 1.12-18.3, p<0.0001).

The patterns of association of PD-L1-expressing tumour-infiltrating leucocytes with OS were like that seen with tPD-L1. In the entire cohort, OS curves were superimposed between the similarly-sized lcPD-L1 absent and present subgroups (**Figure 5.4A**). Likewise, no difference in OS was seen in the LMS sub-cohort when stratified by lcPD-L1 Status (**Figure 5.5B**). As was the case with tPD-L1, inverse associations of lcPD-L1 status with OS were seen between the UPS and DDLPS sub-cohorts. In the UPS sub-cohort, the presence of PD-L1-expressing leucocytes was associated with significantly longer OS than in tumours where infiltrating PD-L1-expressing leucocytes were absent (median OS 5.4 v 1.7, HR 1.92, 95% CI 1.04-3.56, p=0.0280) (**Figure 5.4C**). In contrast, in the DDLPS sub-cohort, the presence of PD-L1-expressing leucocytes was associated with shorter OS, but this was not

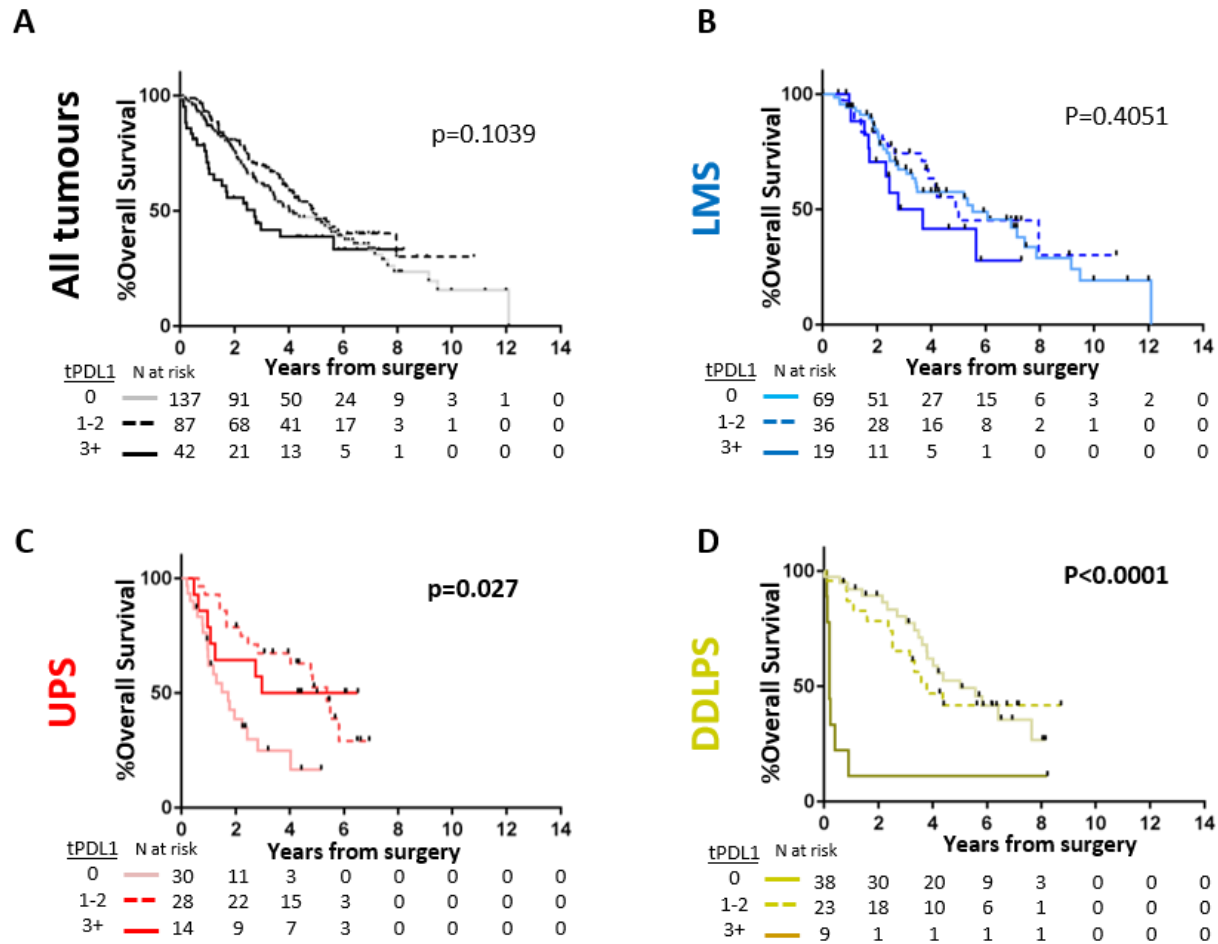


**Figure 5.3: Overall survival in karyotypically-complex STS when stratified by tumour expression of PD-L1**

Kaplan Meier survival curves show overall survival in **(A)** entire 266 STS cohort, **(B)** 72 UPS, **(C)** 124 LMS and **(D)** 70 DDLPS sub-cohorts when stratified by tumour cell expression of PD-L1. Tumours were stratified as having either absent (max tPD-L1 score = 0), limited (max tPD-L1 score 1-2) or higher (max tPD-L1 score 3-6) levels of tumour cell PD-L1 expression. P values derived from log rank test.

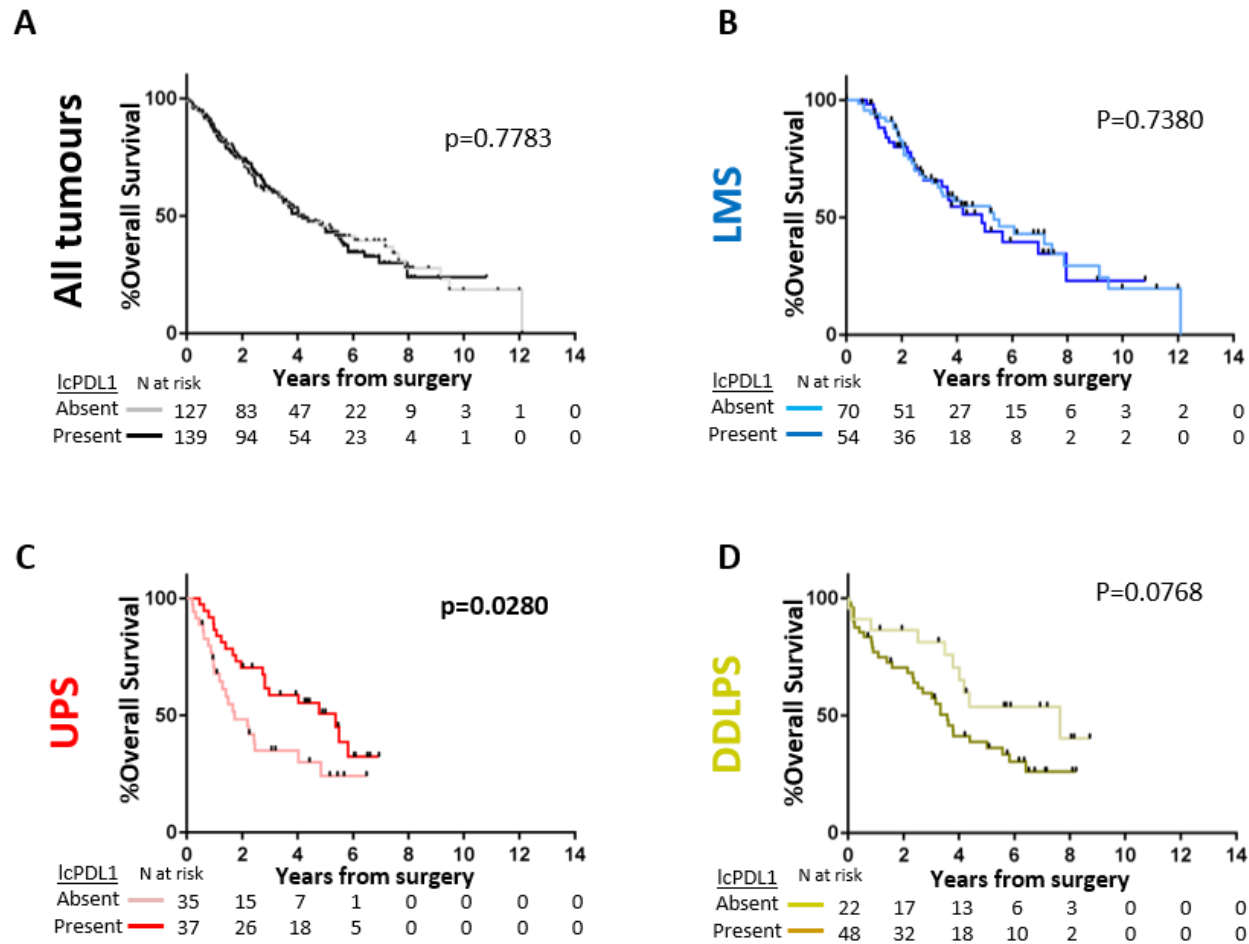


**Figure 5.4: Overall survival in karyotypically-complex STS when stratified by PD-L1 expression on tumour-infiltrating leucocytes**

Kaplan Meier survival curves show overall survival in (A) entire 266 STS cohort, (B) 72 UPS, (C) 124 LMS and (D) 70 DDLPS sub-cohorts when stratified by presence or absence of PD-L1-expressing tumour-infiltrating leucocytes (lcPD-L1). P values derived from log rank test.

statistically significant. (median OS 7.6 vs 3.6 years, HR 0.54, 95% CI 0.29-1.00,  $p=0.0768$ ) (**Figure 5.4D**).

Taken together, these data reinforce a pattern wherein any association of patient survival with tumour immune microenvironment components, as assessed by IHC, is qualitatively distinct between different STS subtypes. In the UPS sub-cohort, higher TIL burdens, greater density of infiltrating CD68+ macrophages and PD-L1 expression in tumour cells and infiltrating leucocytes were all associated with improved OS. In contrast, in the LMS sub-cohort, there was no association between any immune factor and survival, while in the DDLPS sub-cohort, tPD-L1 and lcPD-L1 demonstrated a negative association with survival – the inverse of the association seen in the UPS sub-cohort. In view of these contrasting, subtype-specific associations, it is unsurprising that there were no observed associations between survival and any immune component in the entire cohort.

#### ***5.2.4 The High Infiltration Immune Cluster is associated with improved overall survival across STS subtypes***

In **Chapter 4.2.5**, we described 4 distinct subgroups within the 266 STS cohort identified through unsupervised clustering of immune-related gene expression data and superimposition of related IHC-based immune microenvironment profiling results. We found that these immune clusters were associated with significantly different prognosis (**Figure 5.5A**). The Immune Cold (cluster 1) and the immune checkpoint-dominant response (cluster 3b) clusters were associated with worse prognosis (median OS 3.3 years and 2.7 years, respectively), while the Highly Infiltrated cluster (3a) was associated with longest OS (median OS 5.8 years). (cluster 3a vs. all others: HR 1.60, 95% CI 1.08-2.38,  $p=0.0197$ ) (**Figure 5.5B**).

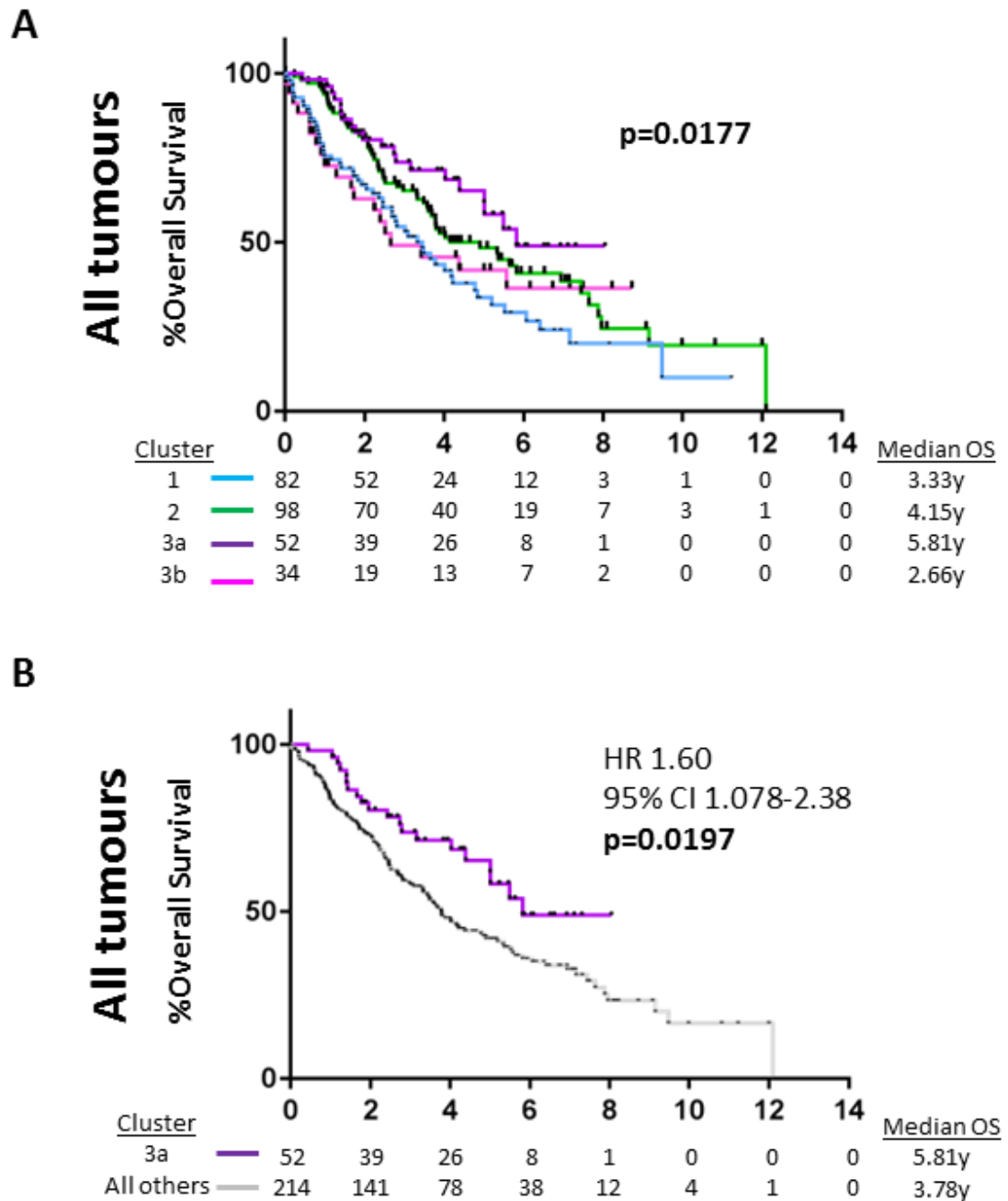


**Figure 5.5: Overall survival in karyotypically-complex STS when stratified by immune-based clusters**

Kaplan Meier survival curves show OS in 266 STS cohort when (A) stratified into 4 immune clusters or (B) stratified into High Infiltration (3a) vs all other immune clusters. Hazard ratios (HR), 95% confidence intervals (CI) and P values derived from log rank test.

These findings indicate that a subgroup of tumours that is characterised by the highest levels of immune cell infiltration and immune-related gene expression, and is independent of histological subtype, is associated with more favourable prognosis compared to all other tumours.

### ***5.2.5 Immune microenvironment characteristics are independent prognostic factors in STS with complex karyotypes***

Using Cox proportionate hazards modelling, we performed univariate and multivariate analysis to assess whether the prognostic association of the Highly Infiltrated cluster was independent of other recognised prognostic factors in the entire cohort. As previously observed in **Chapter 4.2.3**, higher age, tumour grade and stage were all adverse prognostic factors on univariate analysis, while histological subtype was not (**Table 5.1**). When the High Infiltration immune cluster was included in a Cox Proportional Hazards model alongside these baseline clinico-pathological factors, only High Infiltration cluster and tumour stage retained significant association with survival. In this multivariate analysis, tumours in the High Infiltration cluster were associated with significantly better OS than tumours not in this cluster (HR 0.56, 95% 0.34-0.91,  $p=0.0205$ ), while higher stage tumours were associated with significantly worse survival. This indicates that the immune cluster profile provides prognostic information that is independent of histological subtype or other baseline clinico-pathological prognostic factors.

As discussed in Chapters 4.2.4 and 5.2.1-3, average TIL values and average CD68 and max tPD-L1 scores were all positively correlated and associated with favourable prognosis in the UPS sub-cohort. Based on the covariance of IHC-based markers, we included only average CD3 TIL value (1<sup>st</sup> vs 2<sup>nd</sup>/3<sup>rd</sup> tertile), along with High Infiltration cluster status, age, grade and stage in a further Cox Proportional Hazard model to assess for prognostic factors in the UPS sub-cohort (**Table 5.2**). Here, only high CD3 values were shown to be independently associated with OS in the UPS sub-cohort (1<sup>st</sup> vs 2<sup>nd</sup>/3<sup>rd</sup> tertile HR 3.16, 95% CI 1.47-6.79,  $p=0.0033$ ). High infiltration cluster status did not exhibit independent prognostic association in the UPS sub-cohort. This finding indicates that high TIL level is an independent prognostic factor in UPS,

	Univariate			Multivariate		
	HR	95% CI	P	HR	95% CI	P
<b>Cluster 3a vs others</b>	0.57	0.36-0.92	<b>0.0213</b>	0.56	0.34-0.91	<b>0.0205</b>
<b>Histology (v DDLPS)</b>						
LMS	0.81	0.55-1.20	0.299	0.87	0.58-1.29	0.4775
UPS	1.32	0.86-2.03	0.204	1.07	0.66-1.75	0.7816
<b>Age (vs &lt;50y)</b>						
50-70y	1.47	0.88-2.47	0.1400	1.32	0.79-2.21	0.2951
70+	2.15	1.29-3.60	<b>0.0035</b>	1.82	1.06-3.13	<b>0.0304</b>
<b>Grade (1/2 v 3)</b>	0.53	0.38-0.74	<b>0.0002</b>	0.71	0.49-1.03	0.0727
<b>Stage (1/2 v 3/4)</b>	1.94	1.40-2.70	0.0001	1.82	1.28-2.57	0.0008

**Table 5.1: Univariate and multivariate survival analysis in 266 STS cohort**

	Univariate			Multivariate		
	HR	95% CI	P	HR	95% CI	P
<b>CD3 High vs Mod/Low</b>	<b>3.38</b>	<b>1.70-6.73</b>	<b>0.0005</b>	<b>3.16</b>	<b>1.47-6.79</b>	<b>0.0033</b>
<b>Cluster 3a vs others</b>	0.53	0.26-1.06	0.0719	0.90	0.42-1.92	0.7770
<b>Age (vs &lt;50y)</b>						
50-70y	0.66	0.18-2.39	0.5280	0.79	0.22-2.90	0.7247
70+	0.78	0.24-2.57	0.6800	0.94	0.28-3.15	0.9189
<b>Grade (1/2 v 3)</b>	0.60	0.18-1.94	0.3918	0.50	0.15-1.65	0.2517
<b>Stage (1/2 v 3/4)</b>	2.08	0.77-5.57	0.1453	1.46	0.54-3.95	0.4589

**Table 5.2: Univariate and multivariate survival analysis in 72 UPS sub-cohort**

while gene expression-based subgrouping does not provide additional prognostic information in this subtype when analysed in isolation.

### 5.3 Discussion

Using both IHC- and gene expression-based measures as described in **Chapter 4**, we have shown that immune microenvironment factors are able to identify STS tumour subgroups with contrasting survival in both a histology-specific and histology-agnostic fashion within a single retrospective cohort. While these findings are hypothesis-generating, they present a platform for future validation studies that could form the basis for novel prognostic and/or predictive biomarkers in STS with complex karyotypes.

While no IHC-based immune microenvironment marker was found to have a prognostic association within the STS cohort, a histology-subtype specific effect was seen. Within the 72UPS, a statistically significant, positive association between OS and higher levels of TIL infiltration, CD68+ macrophage infiltration and PD-L1 expression within the TME was demonstrated. CD3+ TIL were shown to provide prognostic information that was independent of other baseline clinico-pathological factors when included in a Cox PH model. No such associations were seen in the LMS and DDLPS sub-cohorts. This study represents the largest reported IHC-based study of TILs in UPS and provides evidence for the prognostic relevance of immune microenvironment factors in this STS subtype. The absence of such a signal in previously reported studies may relate to the small numbers of UPS (ranging from 3-62) included in heterogeneous cohorts wherein subtype-specific survival analyses were not performed (**see Table 1.6 and Chapter 1.5.2.2**)<sup>203,204,210,212,213,216</sup>. Likewise, our study demonstrated a subtype-specific association between IHC-based iTME factors and outcome may offer explanation of the inconsistent results reported by previous studies, wherein STS cohorts that consisted of a heterogeneous mix of histological subtypes were analysed for associations between iTME and outcome (see **Tables 1.5-1.7 and Chapter 1.5.2**)<sup>35,202-213,216,219,221</sup>. Many of these studies also included tumours that were of variable stage and treatment exposure, introducing further uncontrolled variation into analysis for survival association. This study addressed this issue by including treatment-naïve, largely primary tumour material– this control of non-iTME factors may have contributed to the successful identification

of prognostic associations. This study is based on a solitary, single-centre cohort and requires validation in independent tumour cohorts to improve confidence that the observed association between iTME and prognosis in UPS is not a chance false-positive finding.

In our study, a significant association between heavier CD68+ macrophage infiltration and prognosis was only observed in the UPS sub-cohort. While previous data on such an association in UPS were lacking, several studies have previously identified a significant association between greater macrophage infiltration and worse prognosis in LMS (**see Table 1.7 and Chapter 1.5.2.3**)<sup>35,203,212,219,221</sup>. In the LMS sub-cohort in our study, no such association was seen between extent of CD68+ macrophage infiltration and OS, a finding that is inconsistent with these earlier reports. This inconsistency may reflect a number of differences between studies. In our study, uLMS accounted for only 12/124 (9.6%) of included tumours, reflecting local referral practices that see few patients with uLMS undergoing surgery at our centre, relative to those with LMS at other sites. In contrast, uLMS accounted for up to 51% of previously reported LMS cohorts, giving rise to the possibility that the prognostic significance of TAM may be related to anatomical site of LMS origin. Furthermore, differential prognostic associations between uterine and non-uterine LMS were reported in these earlier studies<sup>35,219</sup>. In our study, CD68 was used as a sole immunophenotypic marker and does not in isolation provide further information regarding functional polarisation between M1 and M2 status. In contrast, the study reported by Lee *et al* recorded macrophage expression of both CD68 and CD163, a putative marker of M2 functional polarisation, while the studies reported by Ganjoo *et al* and Kostine *et al* used CD163 but not CD68<sup>35,212,219</sup>. While, in the study by Lee *et al*, assessment of macrophages by CD68 or CD163 identified similar prognostic associations. It is possible that, in our study, the use of a high-level, low-detail macrophage marker resulted in the loss of important information relating to a possible association of only certain macrophage functional subsets with outcome. Assessment of our STS cohort using further IHC-based markers of macrophage functional subclassification would allow for more detailed analysis of possible associations of TAMs with prognosis in the LMS and other sub-cohorts.

In our study, tumour expression of PD-L1 was associated with better prognosis in UPS and worse prognosis in DDLPS, with no prognostic association seen in

the LMS sub-cohort. This again indicates qualitative differences in the potential clinical relevance of iTME factors between different STS subtypes. Relative to data on TIL or TAMs, a greater number of studies investigating PD-L1 expression in STS have been reported (see Table 1.5 and Chapter 1.5.2.1)<sup>202–204,206–213</sup>. These have encompassed a more exaggerated degree of methodological and cohort heterogeneity that has likely contributed to inconsistency in the detection of prognostic associations. In our study, we adopted a semi-quantitative scoring method to assess PD-L1 expression, as demonstrated by staining with a frequently used anti-PD-L1 antibody, in a cohort controlled for stage and treatment exposure. Our finding that UPS with any degree of tumour PD-L1 expression had significantly better outcome than those with absent PD-L1 expression is consistent with the findings of Boxberg *et al*, who found that improved OS was associated with PD-L1 positivity (defined as expression in >1% tumour cells) in the 58 UPS included in their study<sup>210</sup>. The lack of association with PD-L1 expression and outcome in our LMS sub-cohort is consistent with the findings of Kostine *et al*, who found that, in a cohort of 100 LMS, there was no difference in outcome between the 32% of tumours with PD-L1 positivity (again defined as expression >1% of tumour cells) and the 68% without PD-L1 staining<sup>212</sup>. Contrastingly, in our DDLPS sub-cohort, strong tumour PD-L1 expression was associated with worse outcome. Previously reported studies have included only small numbers of LPS and so provide little guidance as to the potential validity of our finding. In our study, the optimal tPD-L1 score cut-off to detect a significant survival difference was different in the UPS and DDLPS sub-cohorts (0 vs >0, <3 vs ≥3 respectively). This may reflect that at least one of these results was a false positive, although it is not implausible that there may be true qualitative and quantitative differences in the association of PD-L1 expression with prognosis in UPS and DDLPS.

Having identified a subgroup of STS that consisted of tumours from each of the LMS, UPS and DDLPS cohort that were characterised by high levels of immune-related gene expression and immune cell infiltration, we have shown that the Highly Infiltrated cluster is associated with favourable OS in a manner that is independent of other recognised prognostic factors. While our IHC-based analysis found prognostic association of iTME components in only the UPS sub-cohort, the identification of the Highly Infiltrated cluster indicates that gene

expression analysis provides prognostically-relevant characterisation of the iTME in a manner that is supplemental to IHC-based data.. This is in line with STS-specific data accompanying the report by Thorssen *et al* of the application of 6 immune phenotypes to the TCGA dataset<sup>201</sup> (**Supplemental Figure 5.6**). Here, LMS, UPS and DDLPS are distributed across the 6 immune phenotypes, with tumours allocated to the C3 (Inflammatory) subgroup demonstrating a trend toward longer progression-free interval, and those in the C3 or C2 (IFN $\gamma$ -dominant) subgroups showing some evidence of improved OS. In combination, these data suggest the existence of a subtype-agnostic subgroup of STS, whose iTME are quantitatively and qualitatively distinct from other tumours and that are associated with more favourable clinical outcomes following surgery. More detailed investigation of our study cohort that broadens analysis to other immune-related genes is needed to further assess for the existence of clinically-significant immune-defined subgroups. Meanwhile, validation of prognostic associations in other independent STS cohorts that are similarly controlled in terms of baseline characteristics are required to provide more robust evidence of the prognostic value of such classification. However, our findings significantly add to a nascent literature that indicates that, in a subgroup of karyotypically-complex STS, the immune microenvironment is a promising source of biomarkers and that could yet play a meaningful role in terms of risk stratification for early stage disease and that could prove to be of relevance in selecting optimal candidates for immunotherapy.

## **5.4 Supplementary Material**

### **5.4.1 Supplemental Figures**

**Supplemental figure 5.1** Overall survival in genomically-complex STS stratified by T lymphocyte infiltration

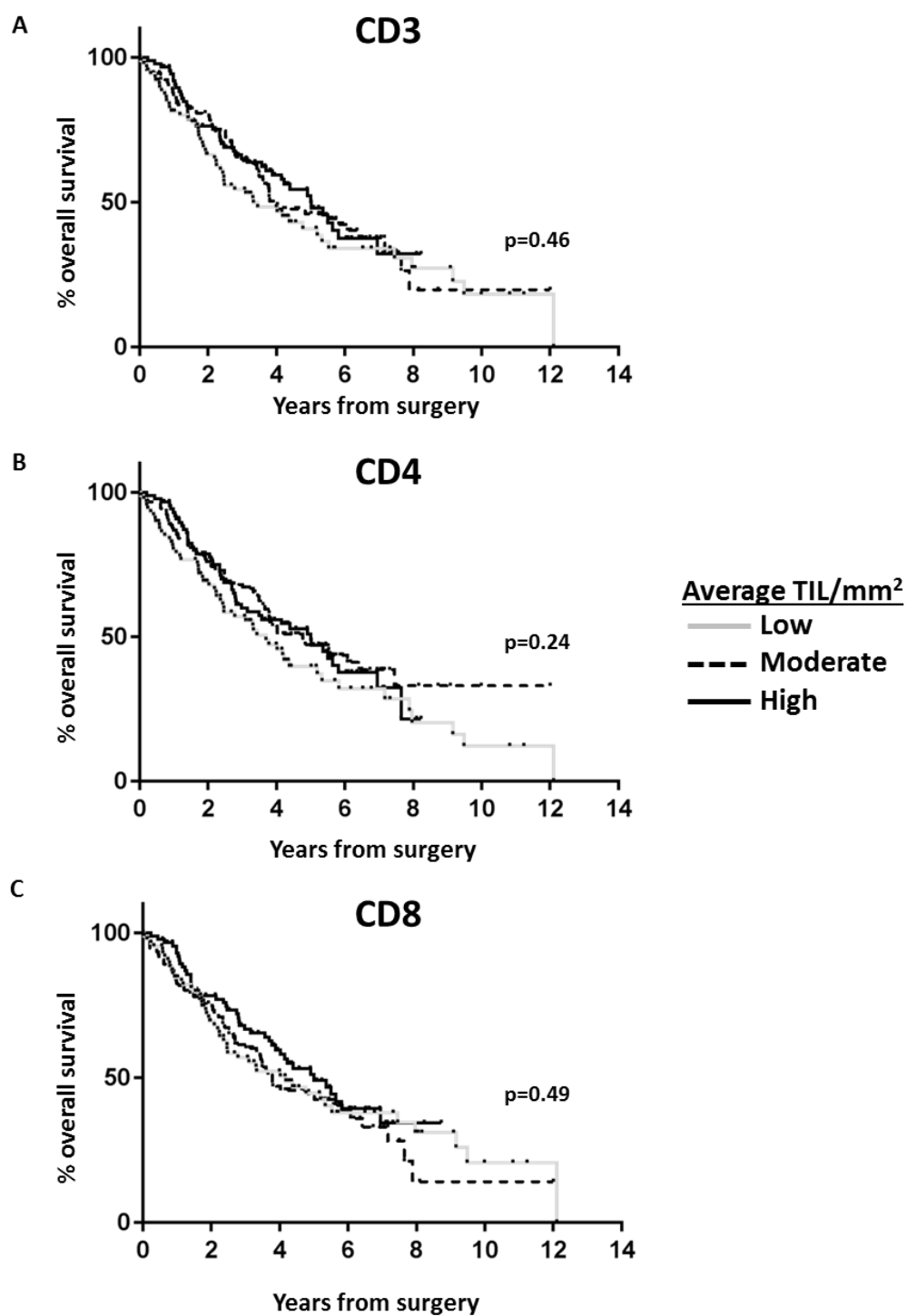
**Supplemental figure 5.2** Advanced disease-free survival in undifferentiated pleomorphic sarcoma stratified by T lymphocyte infiltration

**Supplemental Figure 5.3** Difference in overall survival between UPS with 'high' and 'low' TIL values across all high/low cutpoints

**Supplemental Figure 5.4** Association of CD3 TIL value and overall survival in randomly allocated subgroups of USP cohort

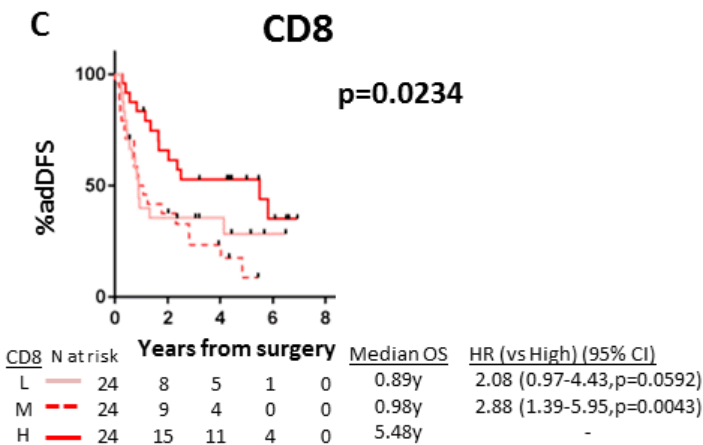
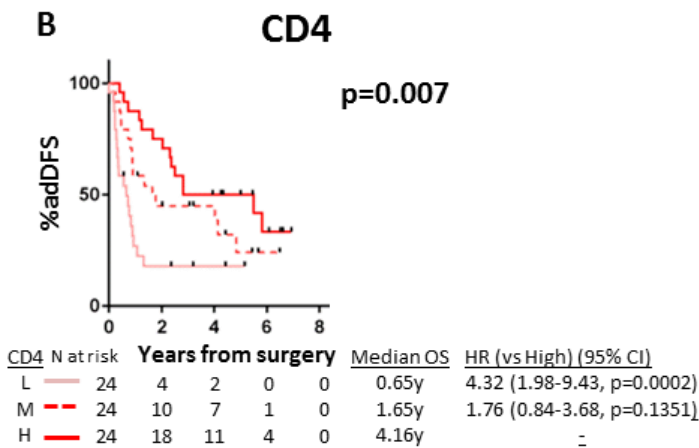
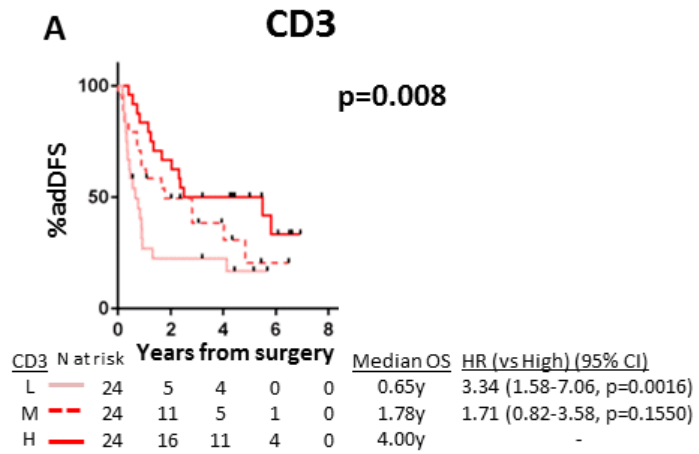
**Supplemental figure 5.5** Overall survival in LMS and DDLPS stratified by T lymphocyte infiltration

**Supplemental Figure 5.6:** Immune Phenotypes in TCGA-SARC



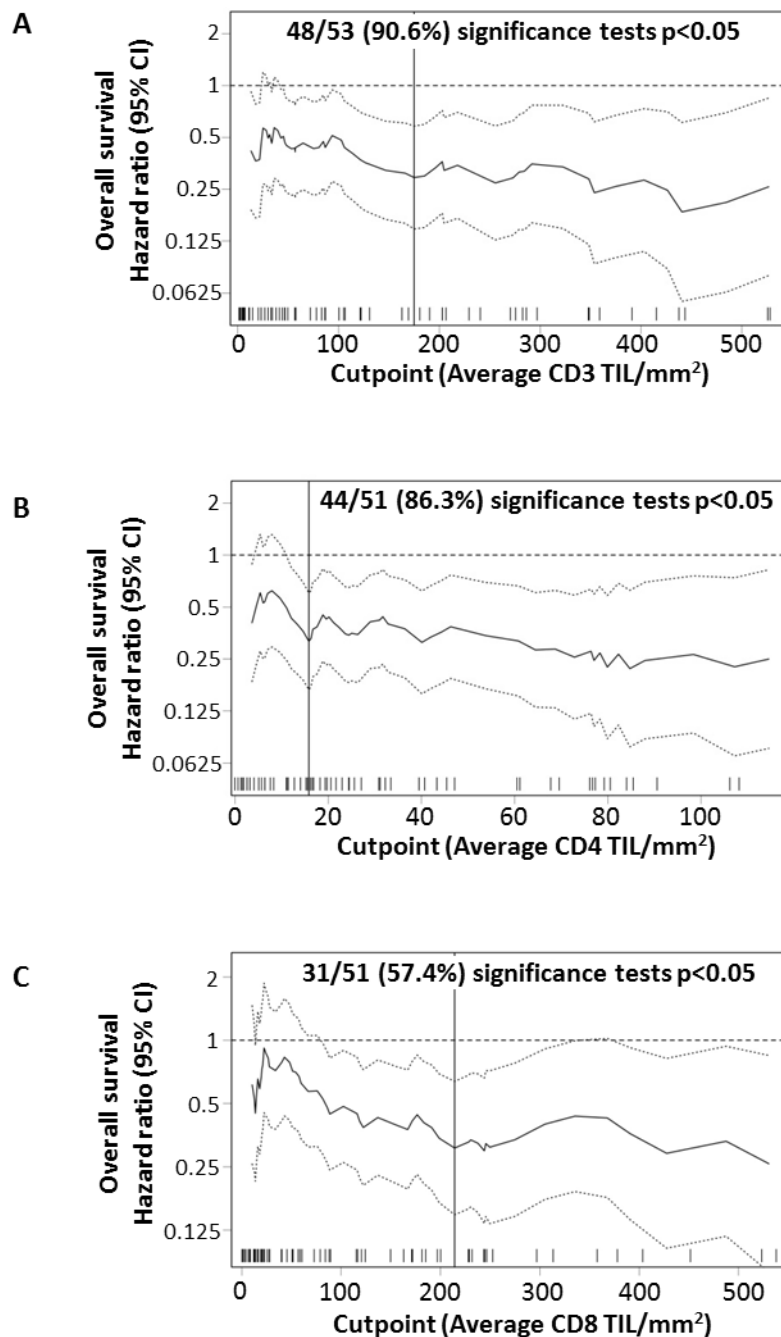
**Supplemental figure 5.1 Overall survival in genomically-complex STS stratified by T lymphocyte infiltration**

Kaplan Meier survival curves show overall survival in 266 STS cohort when stratified into high, moderate or low T lymphocyte infiltration subgroups according to tertile values for **(A)** CD3 (tertile cut-offs 51.8 and 182.5), **(B)** CD4 (tertile cut-offs 14.3 and 45.7), and **(C)** CD8 (tertile cut-offs 35.7 and 135.7), average TIL/mm<sup>2</sup> values. P values derived from log rank test.



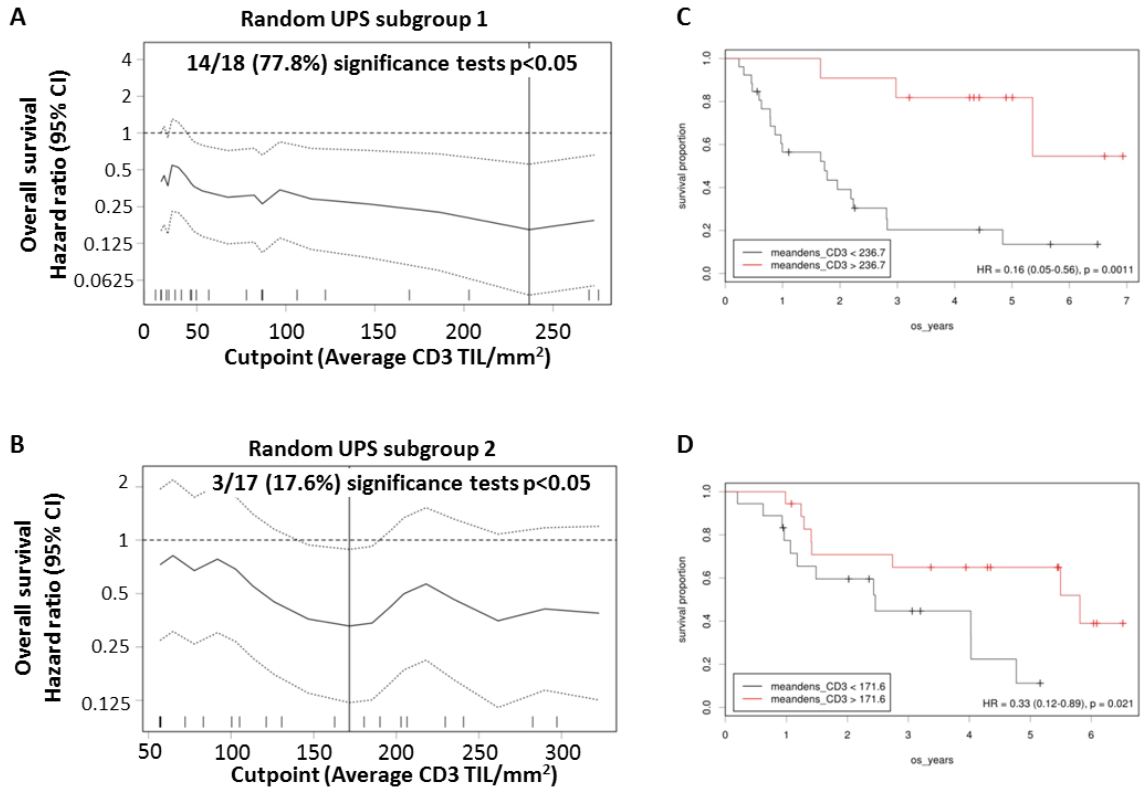
**Supplemental figure 5.2 Advanced disease-free survival in undifferentiated pleomorphic sarcoma stratified by T lymphocyte infiltration**

Kaplan Meier survival curves show adDFS in 72 UPS when stratified into high, moderate or low T lymphocyte infiltration subgroups according to subcohort-specific tertile values for CD3, CD4 and CD8 average TIL/mm<sup>2</sup> values. Tertile cutpoints (average TIL/mm<sup>2</sup>) for CD3 48.2/235.9 ; CD4 15.4/54.7 ; CD8 40.0/216.1



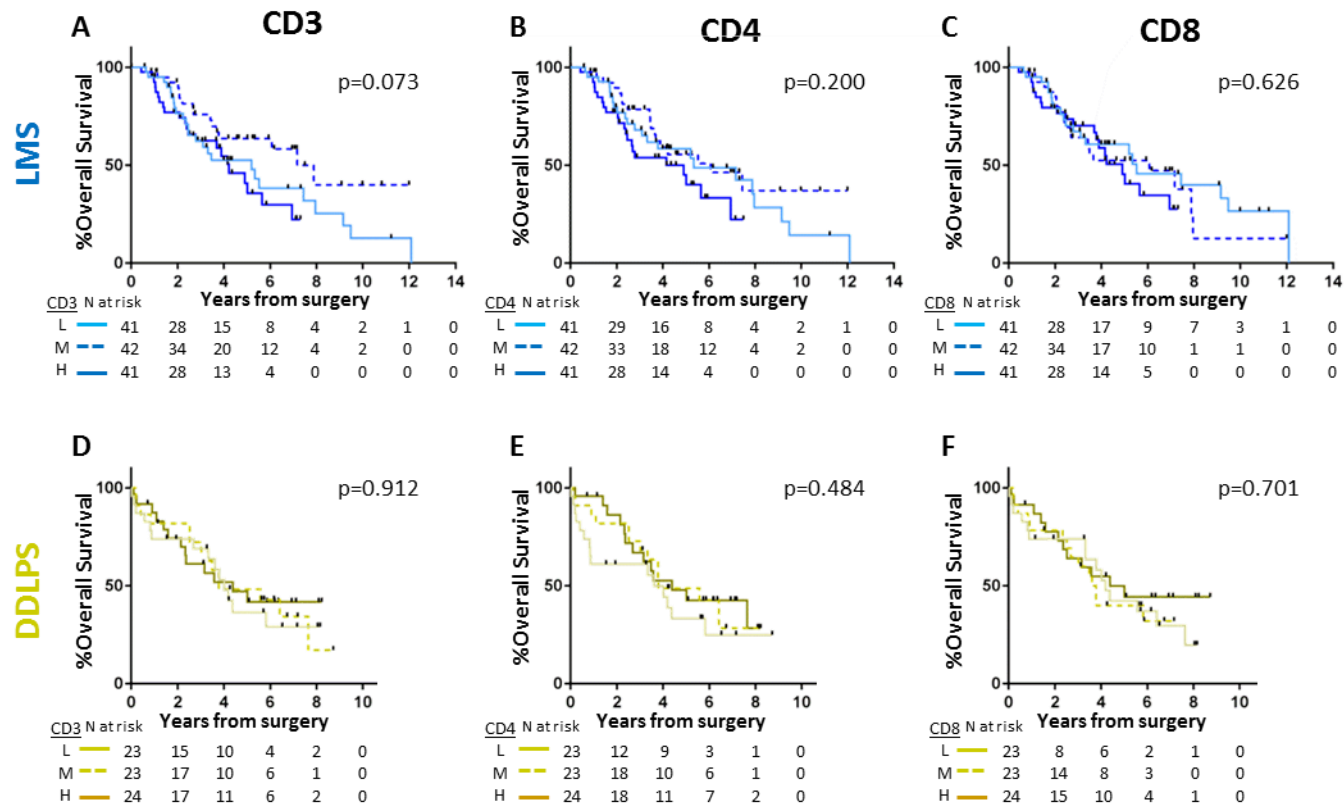
**Supplemental Figure 5.3 Difference in overall survival between UPS with ‘high’ and ‘low’ TIL values across all high/low cutpoints**

Plots demonstrate hazard ratios (solid curve) and associated 95% confidence interval boundaries (dashed curve) derived from multiple log rank tests (y axis) that use varying high/low cutpoint values for average TIL/mm<sup>2</sup> (x axis) for **(A)** CD3, **(B)** CD4 and **(C)** CD8 within 72 UPS cohort. Vertical line highlights cutpoint that provides most significant difference in OS between high and low groups. Plots generated using Cutoff Finder<sup>307</sup>



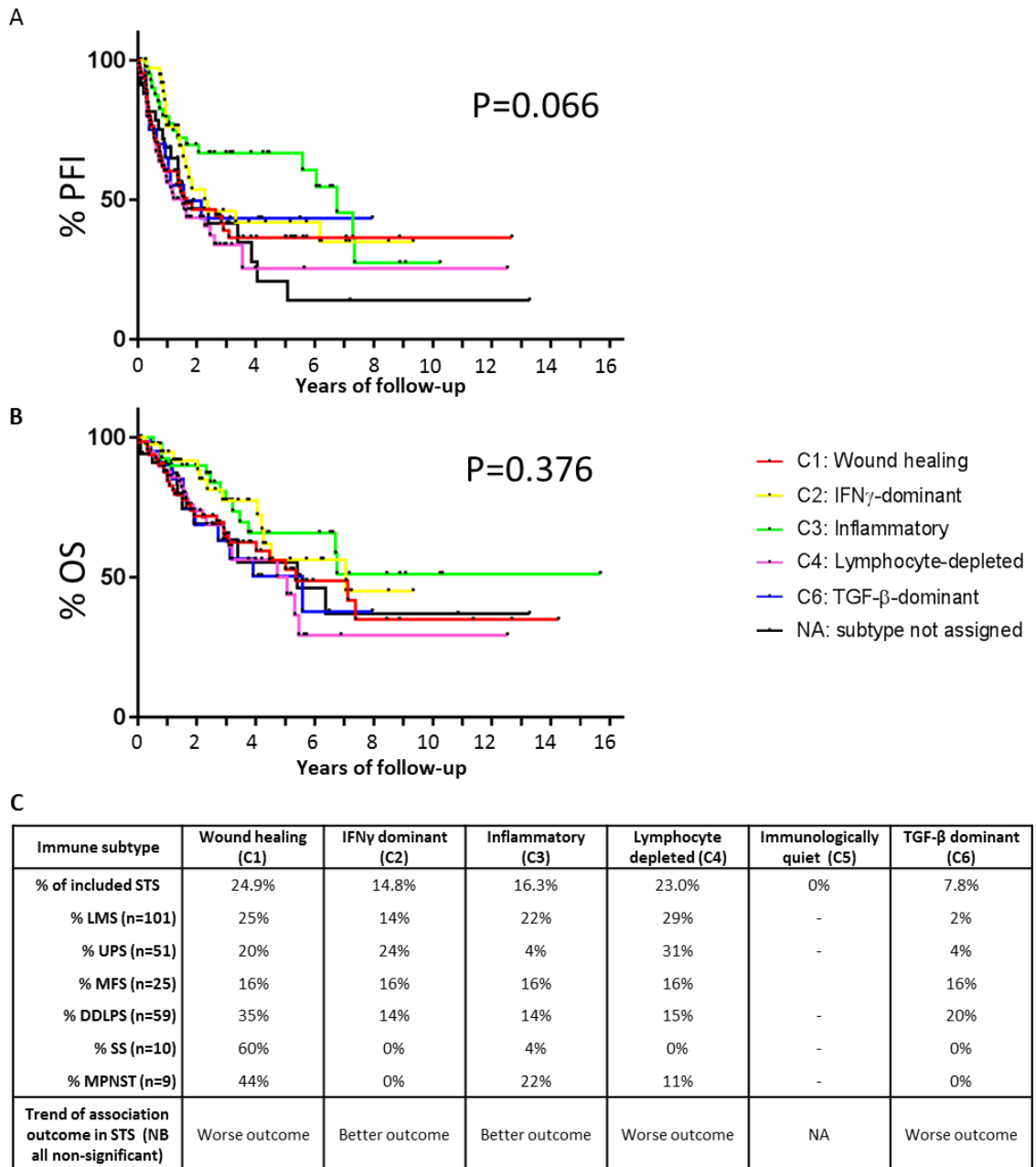
**Supplemental Figure 5.4 Association of CD3 TIL value and overall survival in randomly allocated subgroups of USP cohort**

UPS cohort of 72 patients was randomly allocated into 2 equally sized subgroups (each  $n=36$ ). Plots demonstrate hazard ratios (solid curve) and associated 95% confidence interval boundaries (dashed curve) derived from multiple log rank tests (y axis) that use varying high/low cutpoint values for average CD3 TIL/mm<sup>2</sup> (x axis) for (A) 1<sup>st</sup> and (B) 2<sup>nd</sup> random UPS subgroups. Vertical line highlights cutpoint that provides most significant difference in OS between high and low groups. Kaplan Meier plots demonstrate OS difference between 'high' and 'low' CD3 TIL tumours within (C) 1<sup>st</sup> and (D) 2<sup>nd</sup> random UPS subgroup, with associated high/low cutpoints as determined in (A) and (B). CD8 within 72 UPS cohort. Vertical line highlights cutpoint that provides most significant difference in OS between high and low groups. Plots generated using Cutoff Finder<sup>307</sup>. Hazard ratios (HR), 95% confidence intervals (CI) and p values derive from log rank tests.



**Supplemental figure 5.5 Overall survival in LMS and DDLPS stratified by T lymphocyte infiltration**

Kaplan Meier survival curves show overall survival in (A-C) 124 LMS and (D-F) 70 DDLPS when stratified into high, moderate or low T lymphocyte infiltration subgroups according to subcohort-specific tertile values for CD3, CD4 and CD8 average TIL/mm<sup>2</sup> values. Tertile cutpoints (average TIL/mm<sup>2</sup>) for **LMS**: CD3 42.5/176.5; CD4 11.8/37.3; CD8 27.4/123.0, **DDLPS**: CD3 80.6/166.8 ; CD4 23.0/47.5 ; CD8 52.4/120.2. P values derived from log rank test.



**Supplemental Figure 5.6: Immune Phenotypes in TCGA-SARC**

Thorsen *et al* assigned each of 257 tumours from TCGA-SARC dataset to one of 6 immune subtypes as demonstrated<sup>201</sup>. Kaplan Meier curves demonstrate **(A)** progression-free interval and **(B)** OS within TCGA-SARC when stratified by immune phenotype. P value derived from log rank test. **(C)** Table details allocation of 257 TCGA-SARC cohort, and constitutive histological subtype-specific sub-cohorts, to each of 6 immune phenotypes.

## **Chapter 6: Molecular risk classification for pazopanib in STS**

### **6.1 Background and Objectives**

As discussed in **Chapter 1.4**, pazopanib is an approved treatment for advanced STS with phase III evidence of clinical benefit in terms of prolongation of PFS in a trial cohort consisting of multiple STS histotypes. However, cost-effectiveness of the drug is limited by a lack of proven OS benefit and the absence of validated predictive biomarkers capable of prospectively identifying patients most likely to benefit from treatment.

To address the hypothesis that within STS there are shared tumour molecular characteristics capable of identifying subgroups of patients with differential pazopanib response, and that these features can form the basis for clinically useful predictive biomarkers, we sought to retrospectively identify and analyse pre-treatment tumour tissue from a cohort of patients with advanced STS treated with pazopanib at the Royal Marsden Hospital. The analyses performed were informed by results reported by Koehler *et al* that indicated an association between tumour TP53 mutation and better pazopanib outcome in STS, and also those reported by Wong *et al* that demonstrate that pathway signalling mediated by PDGFRA and FGFR1, both kinase targets of pazopanib, are able to modulate basal sensitivity and acquired resistance to pazopanib in MRT cell line models<sup>165,166</sup>. Incorporating and extending these observations, two stages of tissue analysis were performed:

1. Characterisation tumour expression of FGFR1 and PDGFRA and TP53 mutational status
2. Identification of intrinsic, biology-defined STS subgroups through profiling expression of genes involved in key oncogenic signalling pathways

Having identified an integrated molecular classifier that describes subgroups of distinct pazopanib outcome within our cohort, we used an independent, clinically-annotated, pazopanib-naïve STS molecular dataset from TCGA to determine the prognostic role of our identified signature.

## ***Contributions***

Study conception and design was the work of the candidate in conjunction with his supervisory team.

TMA mark-up and construction, tumour DNA and RNA extraction and quality assessment was performed by the candidate with the assistance of Frank McCarthy, higher scientific officer.

IHC optimisation, FFPE slide cutting and staining was performed by staff of the ICR Histopathology Core Facility.

Identification, collection and curation of archival histological material and associated clinic data; TP53 PCR, sequence analysis, variant calling and annotation; digital microscopy image capture; NanoString nCounter assay; IHC and clinic data analysis; univariate survival analyses within RMH-SARC, TCGA-SARC and Stanford LMS cohorts; figure generation were the work of the candidate.

RECIST tumour measurements were performed by the candidate under the supervision of Dr Christina Messiou, consultant radiologist at The Royal Marsden.

Direct light and digital histological analysis and IHC scoring was performed by the candidate under the supervision and training of Dr Khin Thway. Dr Thway and Dr Ioannis Roxanis, consultant histopathologist, performed independent IHC scoring for assessment of inter- and intra-observer variability.

NanoString data analysis, including biclustering and consensus clustering; multivariate Cox proportional hazard survival analyses; upstream processing of TCGA-SARC and Stanford-LMS datasets were the work of Dr Maggie Cheang and her team in the ICR Clinical Trials and Statistics Unit.

## 6.2 Results

### 6.2.1 Cohort Characteristics

Between October 2009 and September 2016, 46 patients with retrievable pre-treatment tissue were treated with pazopanib for advanced STS at the Royal Marsden Hospital. On examination of FFPE specimen, tissue that was adequate for downstream analysis was available for 38 patients (**Figure 6.1**)

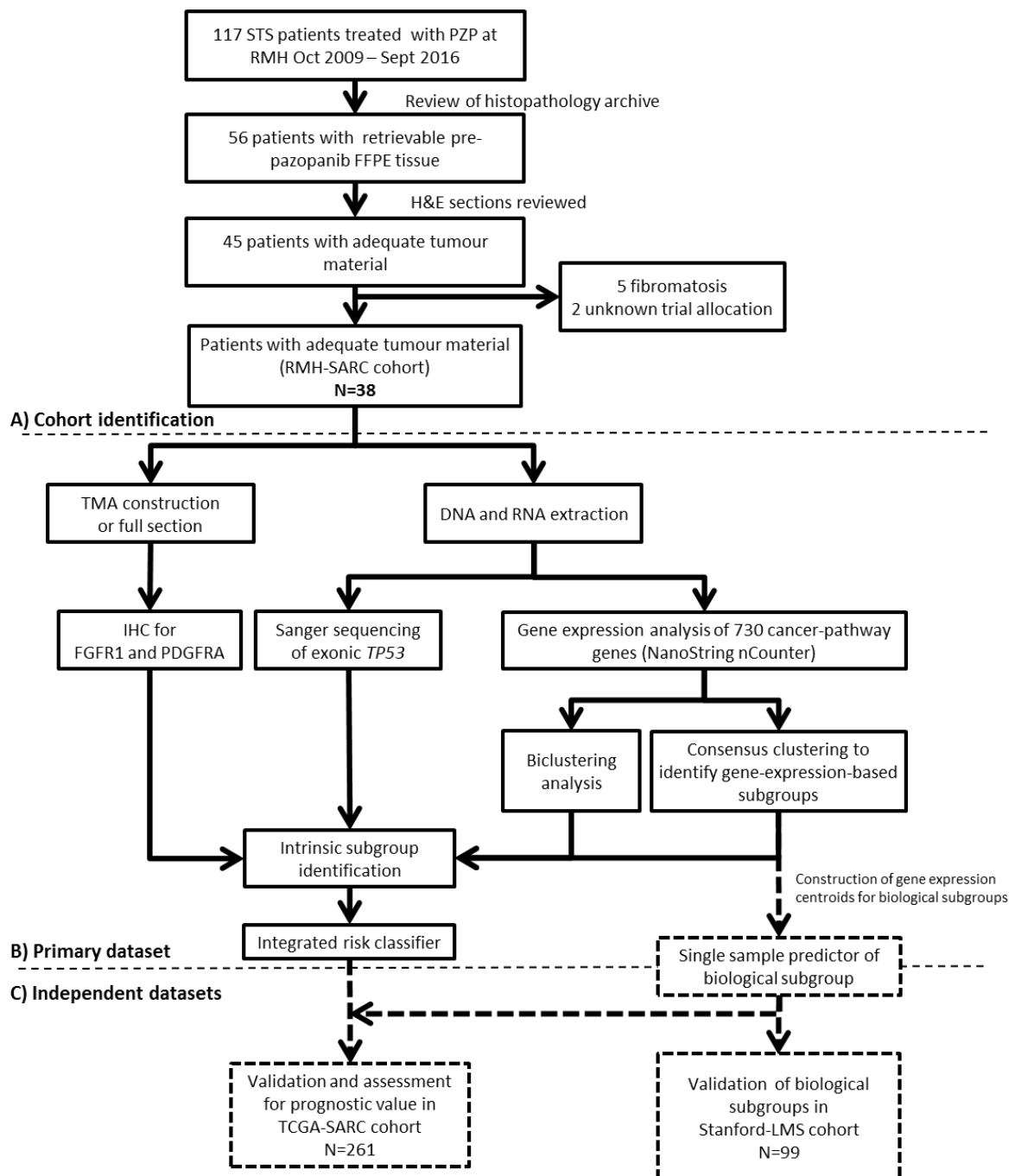


**Figure 6.1: Identification of study cohort and experimental plan**

Baseline clinico-pathological characteristics are summarised in **Table 6.1**. Median age at start of pazopanib therapy was 54.4 years (range 19.8-81.2). Median number of prior lines of therapy was 1.5. All patients with documented performance status were ECOG 0-2. All but one patient had metastatic disease, with a median of 2 organ sites involved by disease. Sixteen distinct STS subtypes were represented within our cohort, with LMS the most common subtype (11 cases). SFT was the second most represented subtype (7 cases) – the over-representation of this rare subtype resulted from the stated focus of the EMPRASS study on SFT and subsequent pursuit of tissue blocks from referring centres. The interval between tumour resection/biopsy and pazopanib start ranged from hours (in cases where prospective pre-pazopanib biopsy was taken within the EMPRASS study) to over 6 years (median 12.1 months), with a variable number of intervening systemic therapies (range 0-3).

At data cut-off (median follow-up in all patients 9.2 months), 35 of 38 patients (92%) had experienced a PFS event and 31 (82%) had died. Median PFS for the cohort was 3.7 months; median OS was 9.5 months. Following retrospective review of imaging series by RECIST 1.1 criteria, 1/38 (2.6%) patient experienced objective partial radiological response, 20/38 (52.6%) had stable disease and 17/38 (44.7%) had progression as best response. For patients with partial response or stable disease, median PFS was 6.4 months.

<b>Baseline clinico-pathological factors</b>	<b>N=38 (%)</b>
<b>Age at pazopanib start:</b>	
<45 years	10(26)
45-65 years	18(48)
>65 years	10(26)
<b>Gender:</b>	
Female	25 (66)
Male	13 (34)
<b>ECOG Performance status:</b>	
0	7 (18)
1	17 (44)
2	7 (18)
NA	7 (18)
<b>Prior lines of systemic therapy:</b>	
0	10 (26)
1-2	19 (50)
3+	9 (24)
<b>Disease stage:</b>	
Unresectable localised	1 (3)
Metastatic	37 (97)
<b>Organs Involved:</b>	
1	11 (29)
2	12 (32)
3	5 (13)
4+	10 (26)
<b>Grade:</b>	
1	2 (5)
2	18 (47)
3	18 (47)
<b>Interval between tumour sampling and start of pazopanib (median, range)</b>	12.1 months (0.0-77.1)
<b>Histopathological subtype:</b>	
Leiomyosarcoma	11 (29)
Solitary fibrous tumour	7 (18)
Spindle cell sarcoma	3 (8)
Myxofibrosarcoma	3 (8)
Undifferentiated pleomorphic sarcoma	2 (5)
Myxoid liposarcoma	2 (5)
Other *	10 (26)
<p>*'Other' subtype groups consisted of single cases of mesenchymal chondrosarcoma, extraskeletal myxoid chondrosarcoma, fibrosarcoma, malignant peripheral nerve sheath tumour, malignant PEComa, granular cell tumour, clear cell sarcoma, alveolar soft part sarcoma, malignant epithelioid haemangioendothelioma, angiosarcoma</p>	

**Table 6.1: Baseline clinico-pathological features of RMH-SARC cohort**

### **6.2.2 FGFR1 and PDGFRA expression**

In view of their reported role in modulating pazopanib sensitivity in a preclinical model, we analysed tumour expression levels of FGFR1 and PDGFRA in the RMH-SARC cohort using IHC (**Figure 6.2, Table 6.2**). 20/38 cases had high FGFR1 expression, 17/38 had high PDGFRA expression. All 7 cases of SFT exhibited high FGFR1 expression, with 5/7 cases also displaying high PDGFRA expression. Two cases each of high grade UPS and MFS had high PDGFRA expression, with three of these also having high FGFR1. There were no other clear patterns of FGFR1 and PDGFRA expression in relation to the other histological subtypes within our dataset – of note, there was no consistent pattern of receptor expression among the 11 LMS cases in the cohort.

To determine the inter- and intra- observer agreement of IHC assessment, two histopathologists scored 18 cases independently, with one repeating scoring of the same tumours on two occasions separated by several months. Both were blinded to the scores from each other. There were good levels of agreement for FGFR1 (weighted  $\kappa$ : inter-observer 0.82, intra-observer 0.90,  $p < 0.0001$ ) and PDGFRA (weighted  $\kappa$ : inter-observer 0.88, intra-observer 0.98,  $p < 0.0001$ ) (**Supplemental Figure 6.1**)

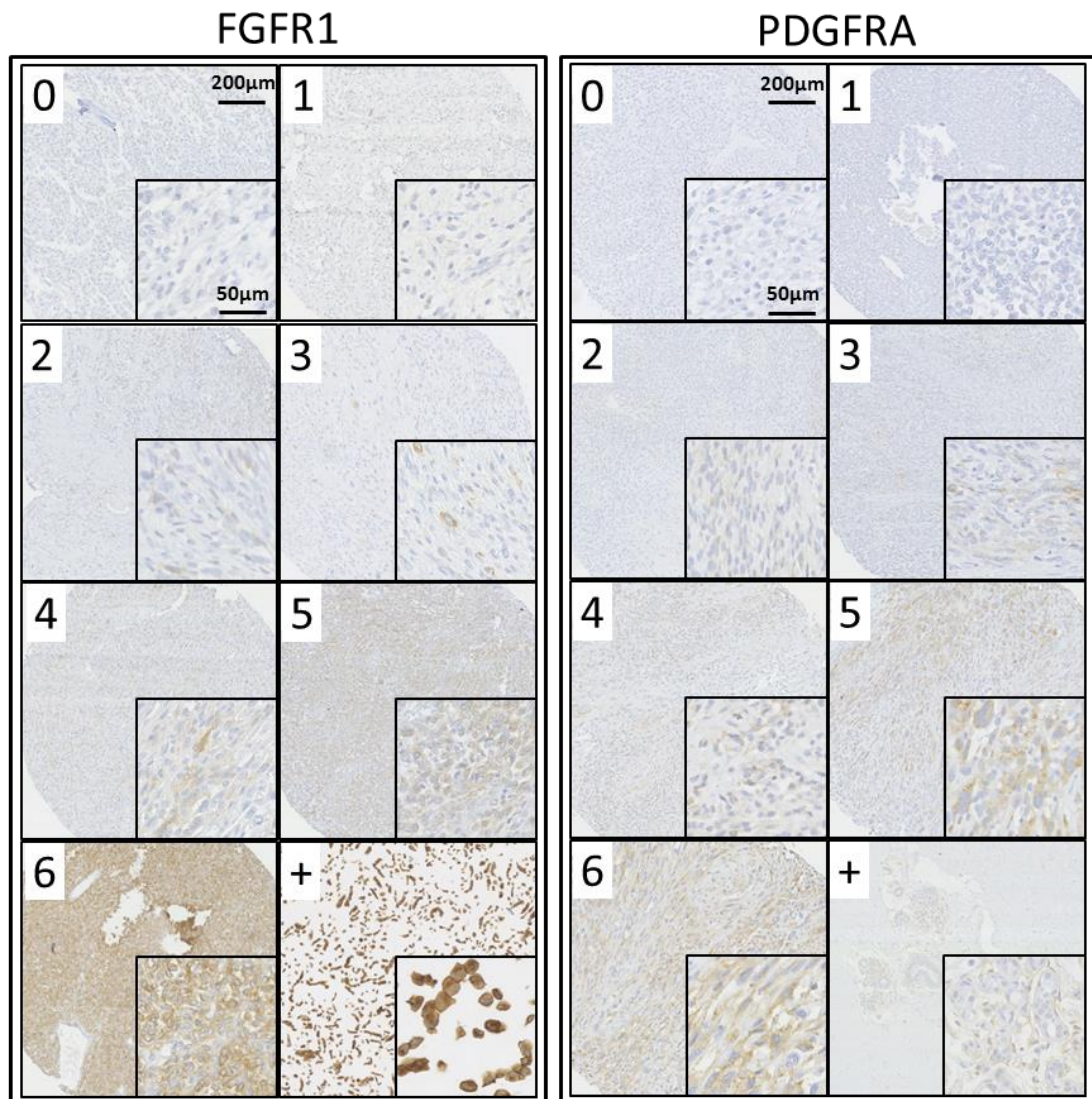


**Figure 6.2: Representative IHC images of FGFR1 and PDGFRA expression levels in pre-pazopanib STS tumour specimen**

FFPE tumour tissue from each case was stained for FGFR1 and PDGFRA. Representative images (x 100 magnification, insert at x400) demonstrate examples of staining scores 0 – 6, derived from the sum of scores for percentage of tumour cells with plasma membrane and/or cytoplasmic staining (0 – absent, 1 – 1-10%, 2 10-50%, 3>50%) and staining intensity (0 – absent, 1 –weak, 2-moderate, 3-strong). For each stain, tumours with a score  $\geq 3$  were classed as ‘high’ expression; tumours with a score  $< 3$  were classed as ‘low expression’ Positive controls T740 cells (FGFR1) and myoepithelial cells within breast tissue (PDGFRA). Digital microscopy images captured with Hamamatsu Nanozoomer at x 40 resolution.

### 6.2.3 TP53 mutations

Sanger sequencing of tumour DNA identified 12 non-synonymous mutations of TP53 (*TP53mut*) in 10 of 38 cases (26%), with the remaining 28 cases showing no detectable *TP53* mutation (*TP53wt*) (**Figure 6.3A, Table 6.2**). 9/12 mutations were single nucleotide missense substitutions identified in 7 tumours – 6 tumours harboured a single substitution, while 1 LMS was found to have 3 different concomitant substitutions. Of the 3 remaining mutations, one was a 2bp deletion resulting in truncating frameshift (R209fs\*6), another was a missense single nucleotide variant at a splice donor site with predicted deleterious effect (X307\_splice) and the last was a previously undescribed 272bp intragenic inversion that introduced a frameshift and early stop codon, resulting in truncation (C275fs\*3) (**Figure 6.3B**).

We searched for reported incidences of the 9 missense mutations within cancer mutation databases, and assessed each mutation using algorithms that predict the consequence of amino acid substitution to protein function (**Figure 6.3C, Table 6.3**). 5 of the 9 substitutions identified in our cohort (V157F, R175H, I195T, R248W, R282W), were highly recurrent mutations in the IARC p53 and/or COSMIC databases, with all 5 previously reported in STS. The remaining 4 missense substitutions are lower frequency mutations with H168R and I232F having been previously observed in STS.. Functional prediction algorithms indicated that all 9 detected missense substitutions were of likely deleterious effects on TP53 function. In the IARC TP53 database, 2/9 of the missense substitutions identified in our cohort (R175H and R248W) are identified as having a consistent dominant negative effects (DNE) on TP53-response (RE) elements, 3/9 (V157F, H168R, R282W) with DNE on some but not all p53-REs, with the remaining 4/9 without DNE data.

Collectively, these findings indicate that 10/38 tumours in our cohort harboured at least one TP53 mutation of confirmed or predicted likely functional consequence.

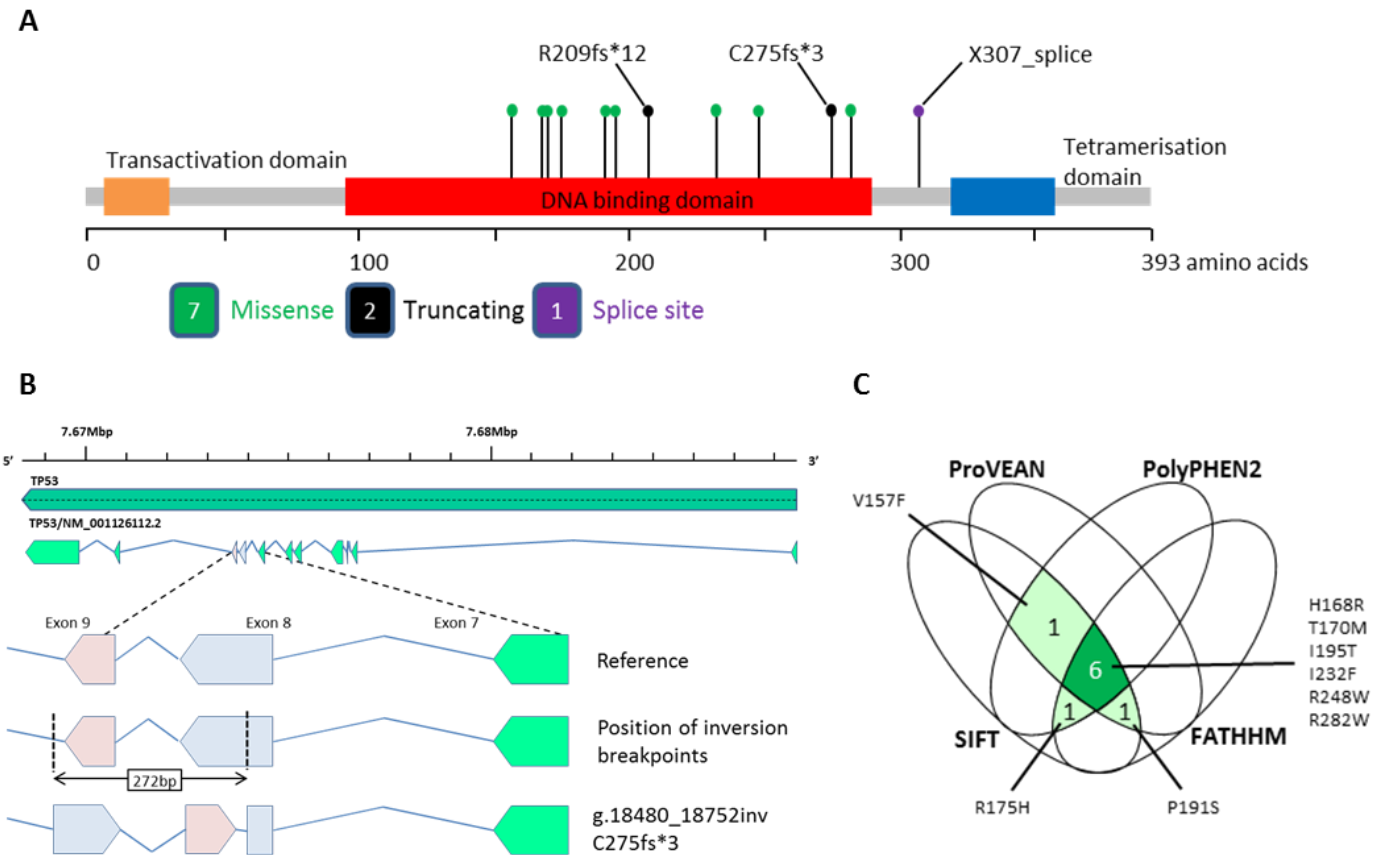


**Figure 6.3: TP53 mutational status in RMH-SARC**

**A.** Lollipop plot showing position of detected mutations within coding exons of *TP53*. **B.** A previously unreported 272bp intragenic inversion resulting in truncating frameshift mutation of *TP53*. Sanger sequencing of exon 8 +9 of *TP53* in a case of high grade UPS identified 272bp sequence, beginning within exon 8, spanning intron 8 and exon 9, and finishing early in intron 9, identical to inverted sequence of complementary (forward) strand, confirmed by sequencing of complementary strand and by amplification using forward primer that spanned sequence breakpoint. Figure shows graphic representation of position of breakpoints in reference gene and orientation of resulting inverted sequence. **C.** Identified *TP53* missense mutations were assessed for functional impact by ProVEAN (predicted deleterious), PolyPHEN2 (predicted probably or possibly damaging), SIFT (predicted damaging) and FATHMM (predicted pathogenic). Venn diagram demonstrates consensus between these 4 separate predictive algorithms (See **Table 6.3** for details).

Cohort ID	Diagnosis	FGFR1	PDGFRA	TP53
RMH015	SFT	High	High	Mutated
RMH030	SFT	High	High	Mutated
RMH004	SFT	High	High	Mutated
RMH061	SFT	High	High	Wildtype
RMH044	SFT	High	High	Wildtype
RMH006	UPS	High	High	Mutated
RMH019	UPS	High	High	Mutated
RMH021	Myxofibrosarcoma	High	High	Wildtype
RMH001	Spindle cell sarcoma	High	High	Wildtype
RMH056	MPNST	High	High	Wildtype
RMH035	LMS (NG)	High	Low	Mutated
RMH008	LMS (NG)	High	Low	Wildtype
RMH032	LMS (G)	High	Low	Wildtype
RMH014	LMS (G)	High	Low	Wildtype
RMH038	LMS (G)	High	Low	Wildtype
RMH029	SFT	High	Low	Wildtype
RMH013	SFT	High	Low	Wildtype
RMH017	Fibrosarcoma	High	Low	Wildtype
RMH040	Granular cell tumour	High	Low	Wildtype
RMH023	Clear cell sarcoma	High	Low	Wildtype
RMH003	LMS (G)	Low	High	Mutated
RMH036	LMS (G)	Low	High	Wildtype
RMH020	Myxofibrosarcoma	Low	High	Wildtype
RMH052	Spindle cell sarcoma	Low	High	Wildtype
RMH049	Myxoid liposarcoma	Low	High	Wildtype
RMH054	EHE	Low	High	Wildtype
RMH012	Myxofibrosarcoma	Low	High	Wildtype
RMH022	LMS (NG)	Low	Low	Mutated
RMH060	LMS (NG)	Low	Low	Mutated
RMH055	LMS (NG)	Low	Low	Wildtype
RMH010	LMS (NG)	Low	Low	Wildtype
RMH028	Spindle cell sarcoma	Low	Low	Mutated
RMH005	Myxoid liposarcoma	Low	Low	Wildtype
RMH025	Angiosarcoma	Low	Low	Wildtype
RMH027	ESMC	Low	Low	Wildtype
RMH011	Myxoid chondrosarcoma	Low	Low	Wildtype
RMH042	ASPS	Low	Low	Wildtype
RMH034	PEComa	Low	Low	Wildtype

**Table 6.2: FGFR1 and PDGFRA IHC expression levels and TP53 mutation status in RMH-SARC cohort**

SFT = solitary fibrous tumour. LMS (NG) = non-gynaecological LMS. LMS (G) = gynaecological LMS. EHE = epithelioid haemangioendothelioma. ESMC = extraskeletal myxoid chondrosarcoma. ASPS = alveolar soft part sarcoma

Cohort ID	RMH022	RMH015	RMH035	RMH060	RMH060	RMH060	RMH028	RMH003	RMH004	RMH019	RMH030	RMH006
Cancer type	LMS	SFT	LMS	LMS	LMS	LMS	SCS	LMS	SFT	UPS	SFT	UPS
Mutation type	Missense	Splice donor site	Frame-shift	Inversion								
gDNA	g.18387 G>T	g.17442 A>G	g.17463 G>A	g.17448 C>T	g.17591 C>T	g.17604 T>C	g.18282 A>T	g.18330 C>T	g.18775 C>T	g.18851 G>T	g.17646_17647 delGA	g.18480_18752inv
cDNA	c.469 G>T	c.503 A>G	c.524 G>A	c.509 C>T	c.571 C>T	c.584 T>C	c.694 A>T	c.742 C>T	c.844 C>T	c.919+1 G>T	c.626-627 delGA	-
Protein	V157F	H168R	R175H	T170M	P191S	I195T	I232F	R248W	R282W	X307_splice	R209fs*6	C275fs*3
Described in STS (TCGA, COSMIC, IARC)	Y	Y	Y	N	N	Y	N	Y	Y	Y	N	N
Occurrences in COSMIC database	162	15	926	7	0	88	11	537	450	-	11	-
IARC somatic count	210	23	1216	11	4	105	11	739	581	17	15	-
SIFT Predictiton	Damaging	-	-	-								
PROVEAN Predictiton	Del	Del	Del	Del	Neut	Del	Del	Del	Del	-	-	-
PolyPHEN2 Prediction	0.9999 PrD	0.865 PoD	0.404 B	0.632 PoD	0.803 PoD	1 PrD	0.974 PrD	1 PrD	1 PrD	-	-	-
FATHMM prediction	0.24 (N)	0.97 (P)	0.99 (P)	0.99 (P)	0.93(P)	0.99 (P)	0.92 (P)	0.94 (P)	0.99 (P)	0.97	-	-
Predicted dominant negative effect (DNE)	Mod	Mod	Yes	N/A	N/A	N/A	N/A	Yes	Mod	-	-	-
Del = deleterious. PrD = probably damaging. PoD=possibly damaging. P= pathogenic. LP = likely pathogenic. N = neutral. U=uncertain significance. C=conflicting interpretations of pathogenicity												

Table 6.3: Description and predicted functional effect of TP53 mutations identified within RMH-SARC cohort

#### **6.2.4 Biclustering analysis identifies biological subgroups variably enriched for histological subtypes or high PDGFRA and low FGFR1 expression**

To identify biologically-defined subgroups within our pazopanib-treated cohort, we generated expression data for a panel of 730 genes annotated as involved in 13 canonical cancer-related pathways. We then performed biclustering analysis of this expression data to identify submatrices of over-expressed genes that could potentially reflect distinct biological processes within patient subgroups.

The first 3 identified biclusters contained between 7 and 11 non-overlapping patients (**Figure 6.4; Supplemental Table 6.1**). Bicluster 1 comprised of 29 genes upregulated in all 7 cases of SFT within our cohort. 11 of these 29 genes are included in a list of genes found to be upregulated in a previously reported study of gene expression profiles of 52 SFT compared to those of over 200 other non-SFT STS<sup>308</sup>. Bicluster 2 was composed of 34 upregulated genes in 11 cases, 9 of which were LMS (82% of all LMS in our cohort). The identification of subgroups consisting largely of cases of the same STS histological subtype is consistent with multiple reports that STS subtypes have distinct gene expression signatures<sup>308–310</sup>, indicating the success and validity of biclustering in rediscovering biologically meaningful patient/gene submatrices.

Unlike biclusters 1 and 2, bicluster 3 did not show enrichment for any histological subtype. This bicluster consisted of a submatrix of elevated expression of 35 genes in 7 samples, including 2 gynaecological LMS, 2 high grade MFS, and single cases of epithelial haemangioendothelioma (EHE), AS and MLPS. Despite a lack of subtype enrichment, 5/7 cases displayed a combination of low FGFR1 and high PDGFRA expression by IHC (F-Lo/P-Hi).

Collectively, biclustering analysis of cancer pathway gene expression in our cohort identified upregulated genes related to distinct histological subtypes as well as a subgroup of patients of different STS subtypes that were enriched with F-Lo/P-Hi IHC pattern.

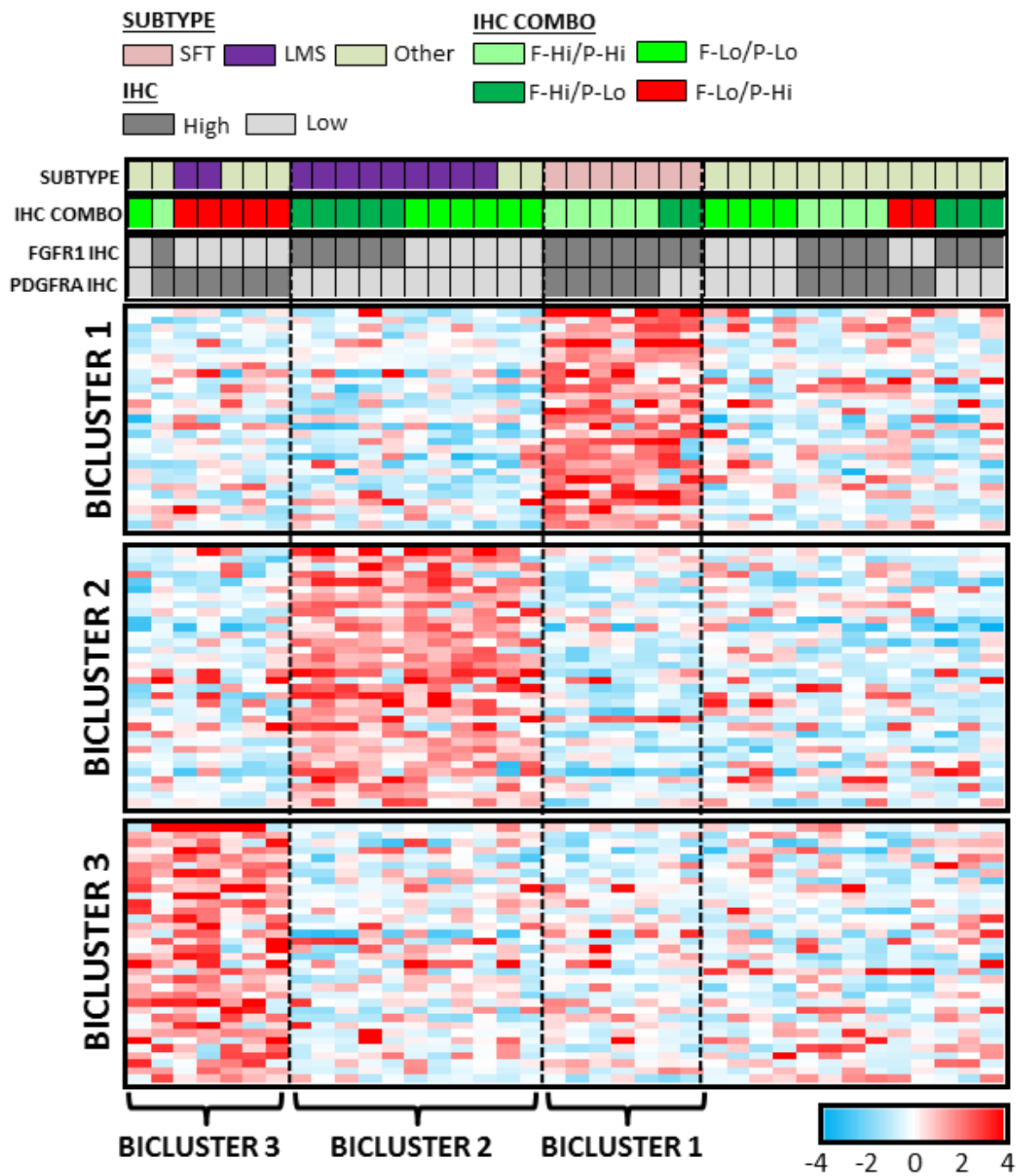


**Figure 6.4: Biclustering analysis of gene expression data from RMH-SARC identifies biology-defined patient subgroups**

Heat map demonstrating first 3 identified bicluster submatrices consisting of upregulated genes within RMH-SARC cohort. Colour bars denote tumour histological subtype, combined and individual FGFR1 and PDGFRA IHC status.

### **6.2.5 High PDGFRA/ Low FGFR1 IHC signature and TP53 mutation are associated with poor outcome following pazopanib therapy**

Given the enrichment of a specific F-Lo/P-Hi IHC signature in bicluster 3, we then examined the post-pazopanib outcomes all 7 patients whose tumours exhibited a F-Lo/P-Hi IHC signature. We found that these patients had significantly worse PFS (median 1.4 vs 4.1 months, HR 9.64; 95% CI 3.58-25.94;  $p < 0.0001$ ) and OS (median 1.7 vs 11.4 months, HR 6.70; 95% CI 2.51-17.91;  $p < 0.0001$ ) compared to all other patients (**Figure 6.5A-B**). When considered individually, FGFR1 expression level alone was not significantly associated with post-pazopanib PFS or OS, while high PDGFRA was associated with worse OS (HR 2.08; 95% CI 1.01-4.35;  $p = 0.04$ ) but no difference in PFS. Interaction test between FGFR1 and PDGFRA expression status for PFS was statistically significant ( $p = 0.001$ ), suggesting that the association of PDGFRA expression with progression depends on FGFR1 and vice versa.

When stratifying the RMH-SARC cohort by tumour *TP53* mutational status, we found that OS was significantly worse in patients with *TP53*-mutated tumours compared to those without identified mutations (median OS 4.8 vs 10.4 months, HR 2.51, 95% CI 1.15-5.51,  $p = 0.02$ ), while PFS was numerically but non-significantly worse in *TP53*mut cases (median PFS 2.9 vs 4.0 months, HR 1.98, 95% CI 0.83-3.76,  $p = 0.14$ ) (**Figure 6.5C-D**).

The association of F-Lo/P-Hi status and *TP53* mutation status with poor outcome was evaluated in multivariable Cox proportional hazard models adjusted for clinico-pathological factors (age, tumour grade, performance status, tumour histological subtype) (**Table 6.4**). F-Lo/P-Hi status (IHCneg vs F-Lo/P-Hi: PFS HR 12.54; 95% CI 3.86—40.72;  $p < 0.001$ ) and *TP53* mutation (*TP53* wt vs mutation: PFS HR 3.97; 95% CI 1.45-10.86;  $p = 0.007$ ) were independently associated with significantly higher risk of progression. F-Lo/P-Hi status (OS HR 22.11; 95% CI 5.90-82.81;  $p < 0.001$ ) and *TP53* mutation (OS HR 7.90; 95% CI 2.56-24.41;  $p < 0.001$ ) also demonstrated independent association with OS. Higher histological grade (HR 3.51; 95% CI 1.40-8.79;  $p = 0.007$ ) and performance status (HR 8.23; 95% CI 2.54-26.69;  $p < 0.001$ ) were independently associated with worse OS but not with PFS. Histological subtype did not demonstrate association with either PFS or OS on univariate or multivariate analysis

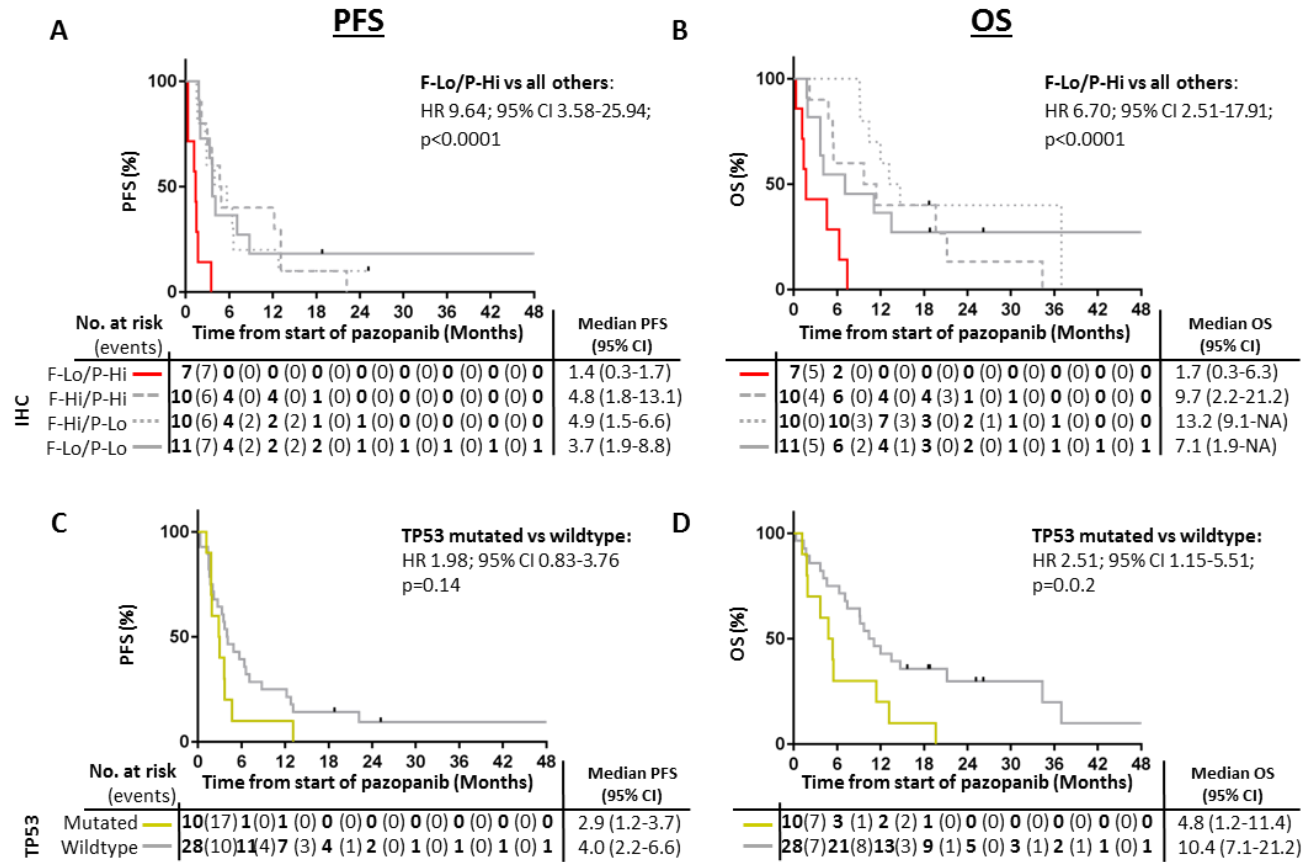


**Figure 6.5: F-Lo/P-Hi and TP53 mutated patient subgroups are associated with worse post-pazopanib outcome**  
 Kaplan Meier plots demonstrating progression-free and overall survival within RMH-SARC cohort when stratified by combined FGFR1 and PDGFRA IHC status (A-B) or TP53 mutational status (C-D). Hazard ratios (HR), 95% confidence intervals (95% CI) and P values from logrank test as stated

	PFS									OS								
	PFS event			Univariate analysis			Multivariable analysis			OS event		Univariate analysis			Multivariable analysis			
	N	N	%	HR	95% CI	P	HR	95% CI	P	N	%	HR	95% CI	P	HR	95% CI	P	
<b>Age (continuous)</b>	38	35	92.1	0.99	0.97–1.02	0.62	0.99	0.96–1.02	0.36	31	81.6	1.01	0.98–1.03	0.65	0.99	0.96–1.03	0.73	
<b>Grade</b>																		
1/2	20	18	90.0	1	-	-	1	-	-	14	70.0	1	-	-	1	-	-	
3	18	17	94.4	1.54	0.79–3.00	0.21	1.18	0.51–2.71	0.70	17	94.0	2.01	0.99–4.09	0.06	3.51	1.40–8.79	<b>0.007</b>	
<b>Performance Status</b>																		
0/1	24	23	95.8	1	-	-	1	-	-	20	83.3	1	-	-	1	-	-	
2	7	7	100.0	1.00	0.42–2.37	0.99	1.17	0.45–3.03	0.75	7	100.0	2.41	0.96–6.09	0.06	8.23	2.54–26.69	<b>&lt;0.001</b>	
NA	7	5	71.4	0.39	0.14–1.06	0.06	0.28	0.08–0.95	<b>0.04</b>	4	57.1	0.49	0.16–1.43	0.19	0.17	0.04–0.73	<b>0.02</b>	
<b>Histological subtype</b>																		
Leiomyosarcoma	11	10	90.1	1	-	-	1	-	-	9	81.8	1	-	-	1	-	-	
Solitary Fibrous Tissue	7	6	85.7	0.48	0.17–1.36	0.17	0.77	0.23–2.62	0.68	5	71.4	0.68	0.22–2.06	0.50	2.06	0.53–7.98	0.56	
Other	20	19	95.0	0.76	0.35–1.66	0.49	1.25	0.47–3.37	0.66	17	85.0	1.06	0.46–2.45	0.89	2.57	0.86–7.67	0.09	
<b>IHC Signature</b>																		
FGFR1-Hi and/or PDGFRA-Lo	31	28	90.3	1	-	-	1	-	-	24	77.4	1	-	-	1	-	-	
FGFR1-Lo and PDGFRA-Hi	7	7	100.0	9.64	3.58–25.94	<b>&lt;0.001</b>	12.54	3.86–40.72	<b>&lt;0.001</b>	7	100.0	6.70	2.51–17.91	<b>&lt;0.001</b>	22.11	5.90–82.81	<b>&lt;0.001</b>	
<b>TP53 status</b>																		
Wildtype	28	25	89.3	1	-	-	1	-	-	21	75.0	1	-	-	1	-	-	
Mutated	10	10	100.0	1.77	0.83–3.76	0.14	3.97	1.45–10.86	<b>0.007</b>	10	100.0	2.51	1.15–5.51	<b>0.02</b>	7.90	2.56–24.41	<b>&lt;0.001</b>	

**Table 6.4: Univariate and multivariate analysis of PFS and OS by clinico-pathological factors, IHC signature and TP53 mutational status**

### **6.2.6 Consensus clustering identifies three subgroups with contrasting post-pazopanib outcomes**

We evaluated the remaining 22 patients with tumours without F-Lo/P-Hi IHC status or *TP53* mutation (henceforth referred to as IHCneg*TP53*wt) for the presence of intrinsic molecular subgroups. Consensus clustering of gene expression data for these 22 cases demonstrated optimal separation into five initial clusters (**Supplemental Figure 6.2**). Visual inspection of these five clusters found that they could be consolidated into three subgroups of equivalent size (subgroups A-C) (**Figure 6.6A**). Multiclass significance analysis of microarrays (SAM – a statistical technique that uses repeated permutations to identify sets of genes in array data whose expression is significantly related to multiclass grouping) identified 229 genes (FDR  $\leq$  10%) showing significant differential expression across these 3 subgroups. We built a standardised centroid for each of the subgroups using these 229 genes. Noting that subgroup B contained all 6 IHCneg*TP53*neg cases of LMS, we sought to ascertain if these tumours shared molecular features with any of three molecular LMS subtypes previously reported in a study by Guo *et al.* by applying these subgroup centroids to gene expression data from the LMS cohort (n=99) used in that same study<sup>32</sup>. We found that the subgroup B shared a subset of upregulated genes with LMS molecular subtype I, described by Guo *et al.* as enriched for genes related to smooth muscle and associated with improved disease-specific survival in extra-uterine tumours. The subgroup B centroid had 100% sensitivity and 69% specificity for identifying LMS subtype I tumours (**Supplemental Table 6.2**), suggesting significant biological overlap with a previously described LMS molecular subtype and providing validation for the use of consensus clustering in the identification of biologically-relevant subgroups.

When assessing post pazopanib outcome in these three subgroups A-C, we found that the patients within subgroup A experienced long-term disease control and survival following pazopanib therapy, with median PFS of 12.8 months and median OS of 34.4 months (**Figure 6.6B-C**). Compared to patients in subgroup B or C, risk of progression (PFS HR 0.27; 95% CI 0.09-0.85; p=0.02) or death (OS HR 0.20; 95% CI 0.04-0.96; p=0.03) was significantly lower in this long term responder subgroup. Subgroup B and C exhibited similar PFS (median PFS 3.3

and 4.1 months, respectively) while subgroup B had an intermediate OS (median 13.5 months) that was not statistically significantly different to subgroup C (median 7.1, B vs C OS  $p=0.22$ ).

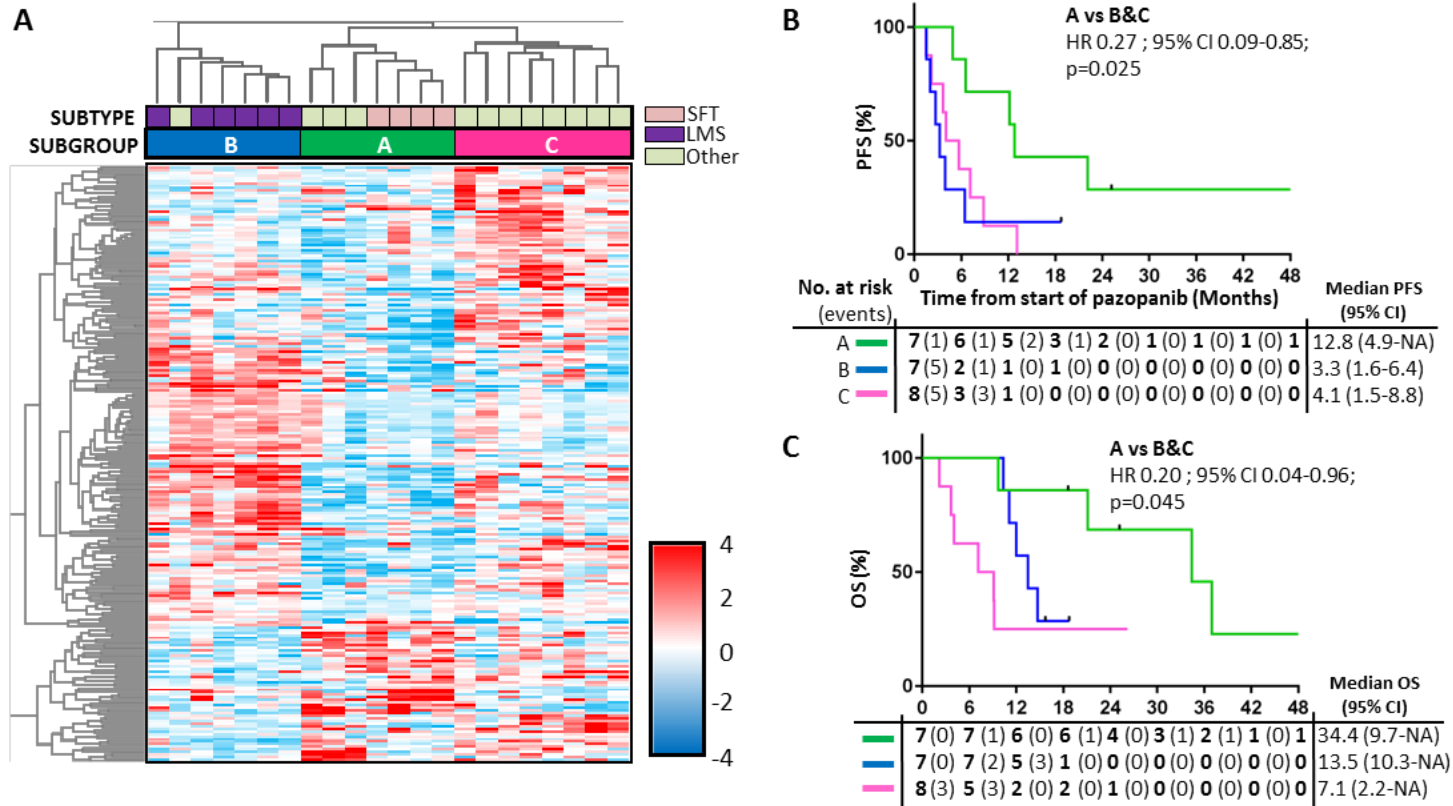


**Figure 6.6: Consensus clustering of gene expression data from IHCnegTP53wt patients identifies biology-defined intrinsic subgroups**

**A.** Consensus clustering identified optimal separation of 22 IHCnegTP53wt patients into 5 clusters, which, after manual inspection, were reduced to 3 subgroups A-C. Shown here is a heatmap of the 22 patients based on expression data of the list of 229 genes which were identified to be significantly different among 3 subgroups using multiclass SAM analysis set at  $\leq 10\%$ FDR. Kaplan Meier plots show **(B)** progression-free and **(C)** overall survival following pazopanib therapy for these three subgroups. Hazard ratios (HR), 95% confidence intervals (95% CI) and P values from logrank test as stated.

### **6.2.7 Integration of molecular subgroups into a candidate risk classification model for pazopanib treatment.**

We conceived a clinical decision tree based on the sequential assessment of FGFR1/PDGFR $\alpha$  IHC, TP53 mutational status and cancer pathway gene expression for molecular risk classification (**Figure 6.7A**). We named this the PARSARC (Pazopanib Activity and Response in SARComa) classifier. We allocated the 38 cases according to this decision tree classifier into one of five molecularly-defined subgroups (F-Lo/P-Hi, TP53 mutated or gene expression-defined subgroups A-C). As already observed, there was significant differential PFS and OS among the five subgroups (**Figure 6.7B-C**). The F-Lo/P-Hi subgroup had the worst PFS and OS overall while subgroup A had significantly superior PFS and OS compared to F-Lo/P-Hi, TP53 mutated and clinical subgroup C.

We used multivariable models to assess the amount of additional prognostic information provided by the integrated decision tree classifier or its constituent parts compared to the use of baseline clinico-pathological variables alone (**Figure 6.7D**). The integrated clinical decision tree classifier provided the largest amount of additional amount of prognostic information compared to a model comprising of clinico-pathological variables only (PFS change in  $\Delta LR\chi^2$  340%; OS change in  $\Delta LR\chi^2$  322%). This significantly outperformed models that included either IHC or TP53 mutational status, and also provided additional prognostic information compared to a model that included both IHC and TP53 status. These findings demonstrate that the use of a decision tree classifier that sequentially integrates F-Lo/P-Hi IHC status, TP53 mutational status and gene expression subgroup analysis provided optimal risk classification of PFS and OS in the RMH-SARC cohort of pazopanib-treated patients. We have named this decision tree the Pazopanib Activity and Response in SARComas (PARSARC) classifier.

To assess whether the PARSARC classifier behaved as a prognostic marker in an independent, mixed STS cohort not defined by pazopanib exposure, we analysed a 261 case STS cohort annotated with genomic and mRNA transcript data that is publically available from TCGA, referred to here as TCGA-SARC. Having established that FGFR1 and PDGFR $\alpha$  mRNA transcript levels could be used to recapitulate the F-Lo/P-Hi IHC group and its survival association in the RMH-SARC cohort (**Supplemental Figure 6.3**), we applied F-Lo/P-Hi, TP53

mutational and PARSARC classifiers to TCGA-SARC dataset using *FGFR1* and *PDGFRA* mRNA level as a surrogate for protein expression (**Figure 6.8**). We found no significant difference in OS when the cohort was stratified by F-Lo/P-Hi gene expression signature (**Figure 6.8A**), *TP53* mutational status (**Figure 6.8B**), or by the PARSARC classifier (**Figure 6.8C**),

Collectively, this analysis finds that while the PARSARC classifier identifies subgroups demonstrating significantly different survival outcomes in a STS cohort defined by pazopanib exposure. No such prognostic association was seen with the PARSARC classifier when applied to a publically available, general STS dataset, suggesting a potential role of the PARSARC classifier as a predictive marker for pazopanib effect.

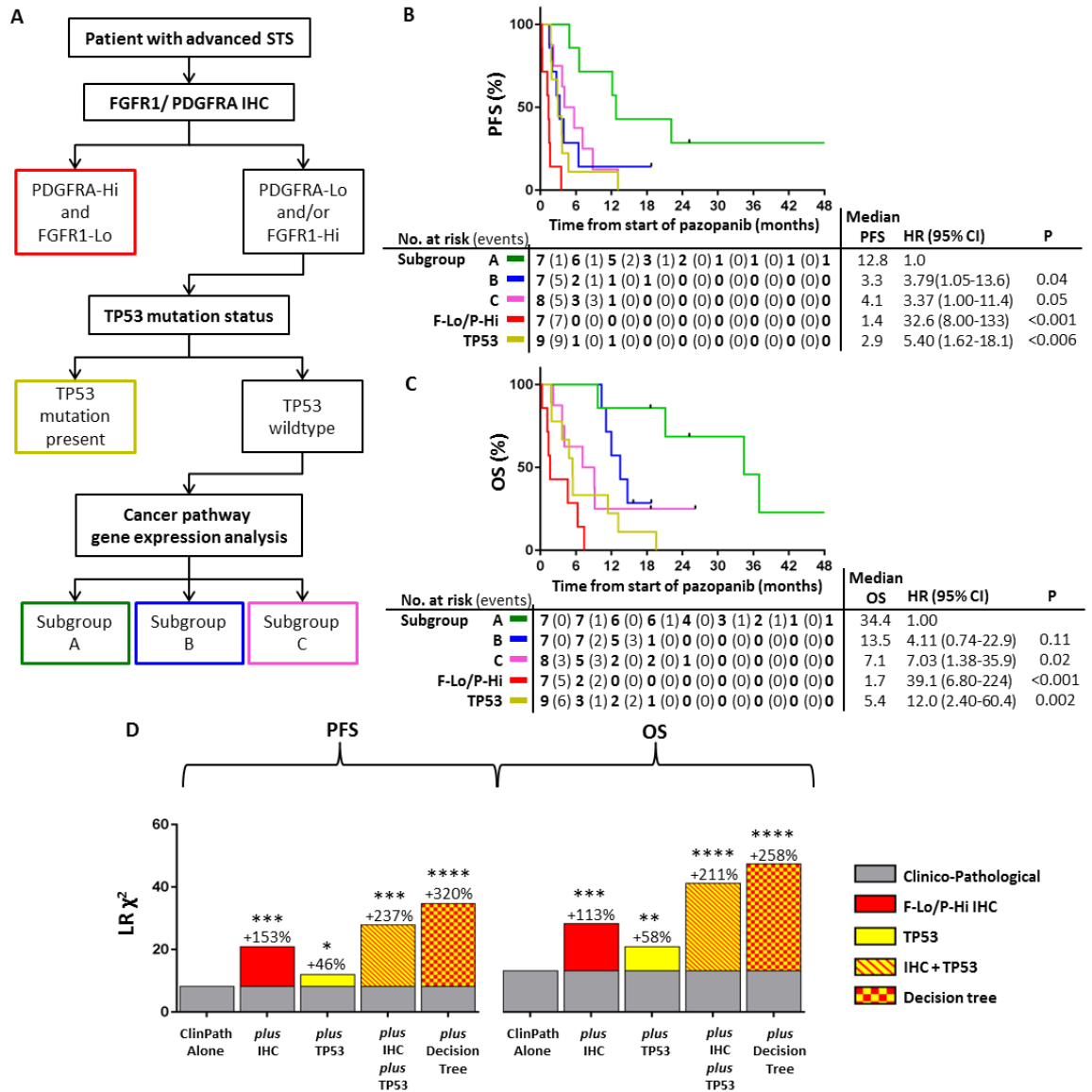


**Figure 6.7: Combination of FGFR1 and PDGFRA IHC, TP53 mutation status and gene expression analysis provides optimal risk classification**

**A.** Decision tree demonstrating sequential integration of molecular risk classifiers. Kaplan Meier curves of the 5 decision tree-defined subgroups for **(B)** PFS and **(C)** OS of 38 patients. **D.** Bar charts showing  $LR\chi^2$  for PFS and OS for 5 proportional hazards regressions. All regression models included baseline clinico-pathological factors (age, tumour grade, performance status, histological subtype), with additional terms being either F-Lo/P-Hi IHC status alone; TP53 mutational status alone; IHC and TP53 mutational status as parallel terms; or decision tree-defined subgroups. Percentage increases in  $LR\chi^2$  compared to regression model using clinico-pathological factors only are stated.  $LR\chi^2$ =Likelihood ratio  $\chi^2$  value. F-Lo/P-Hi = FGFR1-Low/PDGFR A-High. HR=Hazard Ratio, 95% CI (95% Confidence Interval) and P value derive by Cox proportional hazards testing. \*  $p=0.05$  \*\* $p<0.01$  \*\*\* $p<0.001$  \*\*\*\* $p<0.0001$ .

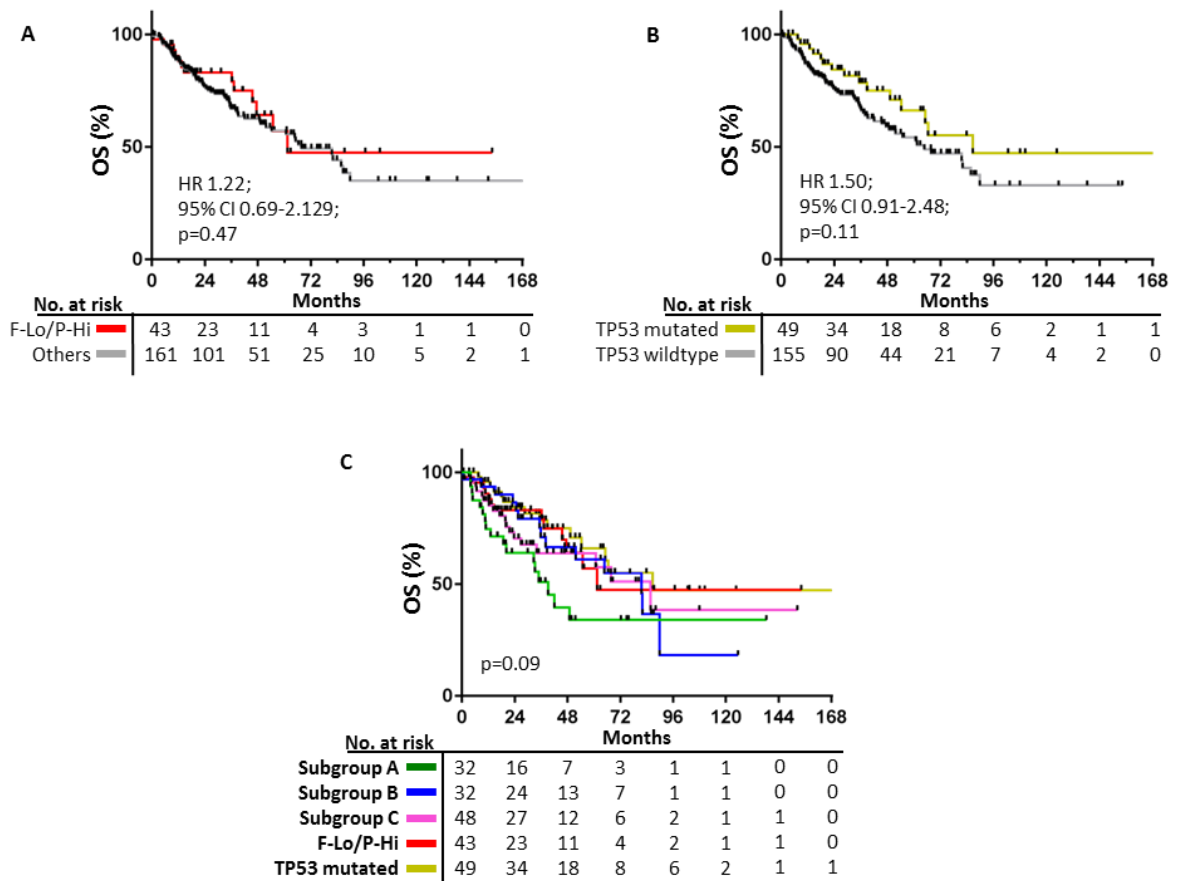


**Figure 6.8: No prognostic association between PARSARC risk classifier and overall survival in TCGA-SARC dataset**

Gene expression data and TP53 mutational status were available for 204 patients within TCGA-SARC dataset. **(A)** Kaplan-Meier curves of F-Lo/P-Hi and all other patient subgroups for OS of 204 cases within TCGA-SARC dataset with available gene expression, TP53 mutational status and survival data. **(B)** Kaplan-Meier curves of TP53 mutated and TP53 wildtype patient subgroups. **(C)** Kaplan-Meier curves of 5 PARSARC classifier-defined subgroups for OS of 204 cases within TCGA-SARC dataset. F-Lo/P-Hi = FGFR1-Low/PDGFR1-High. HR=hazard ratio, 95% CI (95% confidence interval) and P value derive by logrank testing.

### 6.3 Discussion

In this study of a retrospective, heterogeneous cohort of advanced STS treated with pazopanib, advanced STS cohort, we have identified a molecular risk classifier that identifies patient subgroups with distinct PFS and OS following pazopanib therapy. To our knowledge, this is the largest molecular study of a pazopanib-treated STS cohort to date and the first to provide an in-depth examination of multiple aspects of molecular pathology. These findings provide a basis for further development of the PARSARC classifier as a predictive biomarker for pazopanib in the treatment of advanced STS,

The PARSARC classifier is composed of sequential assessment of FGFR1 and PDGFRA expression, TP53 mutational analysis and a 229 gene expression signature. Of notable interest are patients in PARSARC subgroup A which accounted for 7/38 (18%) of the RMH-SARC cohort. This subgroup comprised of 4 different STS subtypes (SFT, high grade spindle cell sarcoma and mesenchymal chondrosarcoma, intermediate grade fibrosarcoma), and demonstrated significantly superior outcomes following pazopanib compared to other PARSARC-defined subgroups. PFS and OS of subgroup A were in keeping with benchmarks for long-term response and survival following pazopanib therapy defined within a retrospective analysis of patients treated within the EORTC phase II and III trials<sup>143</sup>. In this analysis, 22% of 344 patients experienced PFS and OS greater than 6 and 18 months respectively, a subgroup that contained a representative mix of STS subtypes. The similarity in terms of cohort proportion and heterogeneity suggest overlap between this long-term responder/survivor subgroup and subgroup A within RMH-SARC.

In addition to subgroup A, the contrasting PARSARC-defined subgroup with the worst post-pazopanib outcomes (F-Lo/P-Hi IHC status) is similarly composed of heterogeneous STS subtypes. Furthermore, across the RMH-SARC cohort, histological subtype was not associated with post-pazopanib PFS nor OS, consistent with reported subgroup analysis from the EORTC pazopanib trials<sup>142,143</sup>. Our data is in keeping with the recognised limitations of histological classification of STS in selecting patients for specific treatment regimens, as highlighted by a prospective clinical study where generic anthracycline-based chemotherapy outperformed histology-tailored regimens<sup>68</sup>. Our findings

demonstrate that PARSARC provides an unprecedented means of identifying molecularly-defined patient subgroups that are independent of histological classification and are associated with differential benefit from pazopanib therapy. This PARSARC-based decision tree represents a candidate biomarker tool that could be employed in clinic to select the patients most likely to benefit from pazopanib therapy, while identifying those unlikely to respond and thus better suited to alternative management approaches.

Our finding that TP53 mutation was independently associated with worse PFS and OS following pazopanib treatment in our cohort is inconsistent with those reported by Koehler et al<sup>165</sup>. In their study of 19 patients with advanced STS treated with TKI, significantly improved PFS was seen with the 10 tumours with TP53 mutations detected by targeted NGS. The reasons for these conflicting findings are unclear. The STS subtype distribution differed between the studies – notably, patients with SFT accounted for 18% and 0% of our RMH-SARC and Koehler et al.'s cohorts respectively. The higher rate of TP53 mutation seen by Koehler et al. (56% vs 26%) may reflect the greater sensitivity of NGS to detect low frequency mutated subclones. However, the frequency of TP53 mutation as determined by whole exome sequencing in TCGA-SARC was approximately 33%<sup>4</sup>, suggesting that the RMH-SARC cohort may be more representative of a general STS population in terms of frequency of TP53 mutation than the cohort studied by Koehler *et al.* Further investigation of TP53 mutations as a potential biomarker for pazopanib in STS is warranted, including analysis of the possible biological impact of specific mutations on disease biology and treatment sensitivity.

There are several limitations to our study. The study was performed through retrospective analysis of a small, heterogeneous patient cohort treated within a single institution and, as such, is vulnerable to a range of systematic and random biases. While the heterogeneity within our 38 patient cohort reflects the broad range of STS subtypes for which pazopanib is approved, and the age distribution of pazopanib-treated patients in RMH-SARC and the PALETTE trial were very similar (median 54.4 vs 56.7 years respectively), there are key differences that call in to question the degree to which our cohort is representative of patients treated with pazopanib in PALETTE and wider practice. The overrepresentation of SFT, a rare STS subtype of recognised pazopanib sensitivity, in RMH-SARC

could plausibly skew our discovery of intrinsic biological subgroups in a manner that make it difficult to recapitulate PARSARC in a general STS population. Conversely, the absence of any synovial sarcoma, a subtype that accounted for 12% of patients to receive pazopanib in PALETTE in RMH-SARC could mean that there is important subtype-determined biology that is not captured by PARSARC. Median PFS and OS in RMH-SARC was shorter than that of pazopanib-treated patients in PALETTE (respective mPFS 3.7 vs 4.6 months, mOS 9.5 vs 12.6 months), suggesting important differences in the constitution of these cohorts. The larger proportion of patients who experienced disease progression as best response to pazopanib in RMH-SARC compared to the PALETTE cohort (45 vs 23%) indicates that patients in our cohort had less treatment-sensitive, more aggressive disease. Meanwhile, while all patients treated within PALETTE had a performance status of 0-1, 18% of patients within RMH-SARC had baseline PS recorded as 2, with a further 18% with no PS recorded, suggesting that baseline patient fitness was lower in our cohort than the trial population. The archival tissue used for analysis variably consisted of primary, locally recurrent or metastatic lesions, in some cases sampled several years prior to pazopanib initiation, during which patients may have received intervening drug treatment. However, the heterogeneity of the cohort and samples reflects that which is typically encountered in routine practice, with PFS and OS outcomes in our cohort broadly reflecting those in other reported series<sup>93,126,138,141</sup>, supporting the generalisability of our findings. Despite these limitations, we have been able to identify a molecular risk classifier that identifies patient subgroups with significantly distinct post-pazopanib outcome. Although the retrospective nature of our study limits the degree to which we are able to assess whether the PARSARC classifier may act as a predictive rather than prognostic biomarker, we found no prognostic association of the classifier within the pazopanib-naïve TCGA-SARC dataset, indicating that PARSARC may indeed be a pazopanib-specific biomarker. Our findings should be considered as hypothesis generating, with analysis of carefully selected pazopanib-naïve control cohorts and prospective assessment of the identified molecular signature required to provide greater insight into any predictive relationship with pazopanib.

If validated, the PARSARC classifier would assist in the prospective identification of a patient subgroup less likely to benefit from pazopanib (F-Lo/P-Hi) for whom

alternative drugs or best supportive care should be considered. Notably, the PDGFRA-targeting mAb olaratumab recently received accelerated FDA approval for the 1st line treatment of advanced STS in combination with doxorubicin and would represent an avenue of interest in the F-Lo/P-Hi poor prognosis patient group<sup>311</sup>. Furthermore, published results of a randomised phase II trial of regorafenib, a TKI with target selectivity overlap with pazopanib, indicates efficacy in several STS subtypes but not adipocytic tumours<sup>312</sup>. The similarity of these clinical data with those of pazopanib raises the prospect that the identified molecular risk classifiers may also have utility for related TKIs in the same class as pazopanib and that the molecular signature we have identified can also provide risk classification for treatment with regorafenib and other related TKIs of the same class.

Although pazopanib received regulatory approval on the basis of PFS advantage over placebo in a mixed STS cohort, the clinical effectiveness of the drug is limited by a lack of predictive biomarkers and the ubiquity of intrinsic or eventual acquired drug resistance. These factors have contributed to the failure of pazopanib to meet cost-effectiveness benchmarks in certain health economies worldwide, limiting drug availability<sup>107-109</sup>. Our study has established de novo a molecular risk classifier that identifies patients who receive long-term benefit from pazopanib therapy. We propose that further investigation is warranted to establish the utility of this classifier in the prospective stratification of treatment of patients with advanced STS. Our data also provides a new foundation for exploration of the biology that underlies sensitivity and resistance to pazopanib in STS.

## **6.4 Supplementary material**

### ***6.4.1 Supplemental Tables***

**Supplemental Table 6.1:** Upregulated genes identified in biclusters 1-3

**Supplemental Table 6.2.** RMH-SARC subgroup B has a gene expression profile that overlaps with LMS subtype I in Stanford-LMS cohort.

Bicluster 1	Bicluster 2	Bicluster 3
BCOR	CACNA1H	BIRC3
BMP5	CCNE2	BMP4
CACNA1G	CDH1	BMP7
CACNA2D1	COL4A6	CARD11
CACNA2D2	CRLF2	CBLC
CDC14A	FEN1	CCR7
CHAD	FLNA	CD19
DKK1	FOXL2	COL1A1
EFNA2	GADD45G	COL6A6
FGF22	GNG4	CSF2
FZD7	GRIN2A	FIGF
HOXA10	ID4	FOSL1
HOXA11	IDH2	IL11
IGF1	ITGA7	IL13RA2
IL11RA	ITGA8	IL1B
IL1R2	JAG1	IL24
LEFTY2	LAMA3	IL2RA
LIFR	LAMA5	IL6
MAPK8IP2	LEFTY2	IL7R
MMP3	MAPT	IL8
NOG	NKD1	ITGB4
PAX3	NTF3	LIF
PLA2G2A	PLA2G10	MMP7
PTCH1	PPARGC1A	OSM
SIX1	PPP2R2B	PCK1
TLX1	PPP2R2C	PLAG2A
TSPAN7	PRL	PTPRR
WNT2B	PROM1	RELN
ZBTB16	PTPRR	SFN
	RASGRP2	SSX1
	SFN	TMPRSS2
	SOCS2	TNF
	TNC	TNN
	ZAK	WNT2

**Supplemental table 6.1 Upregulated genes identified in biclusters 1-3**

	Assigned Subgroup A	Assigned Subgroup B	Assigned Subgroup C	<u>Total</u>
LMS subtype I	0	31	0	31
LMS subtype II	2	7	29	38
LMS Subtype III	1	13	12	26
Not assigned LMS subtype	1	1	2	4
<u>Total</u>	4	52	43	99

$$\chi^2 = 51.078, \text{ degrees of freedom} = 6, p < 0.0001$$

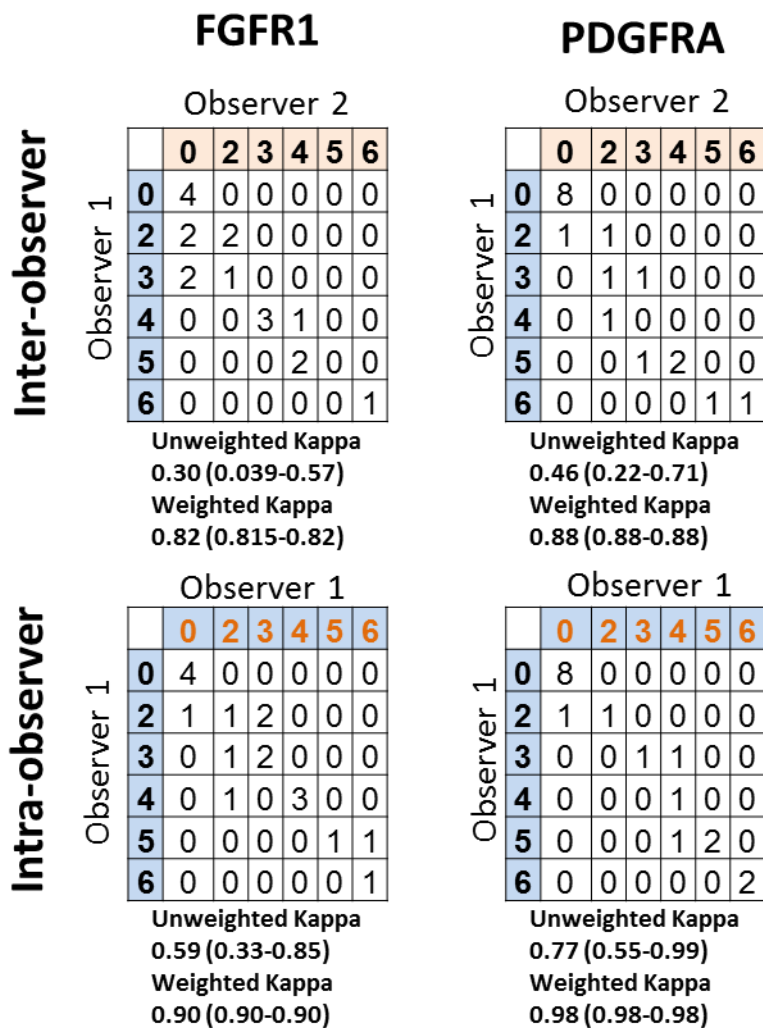
**Supplemental Table 6.2. RMH-SARC subgroup B has a gene expression profile that overlaps with LMS subtype I in Stanford-LMS cohort.** Guo *et al* previously described a cohort of 99 LMS that had been assigned to one of three LMS molecular subtypes based on gene expression analysis (12). Using this gene expression data, we assigned each of the 99 LMS to subgroup A-C through assessment of correlation with subgroup centroids. Contingency table of LMS subtype and subgroup A-C assignment shows significant enrichment of LMS subtype I compared to LMS subtype II and LMS subtype III in cases assigned to gene expression-defined subgroup B. P values derive from Pearson's Chi square test with Monte Carlo simulation of P value (excluding cases not assigned LMS subtype)

#### **6.4.2 Supplemental Figures**

**Supplemental Figure 6.1** IHC-based scoring of tumour FGFR1 and PDGFRA expression exhibits very good inter- and intra-observer agreement.

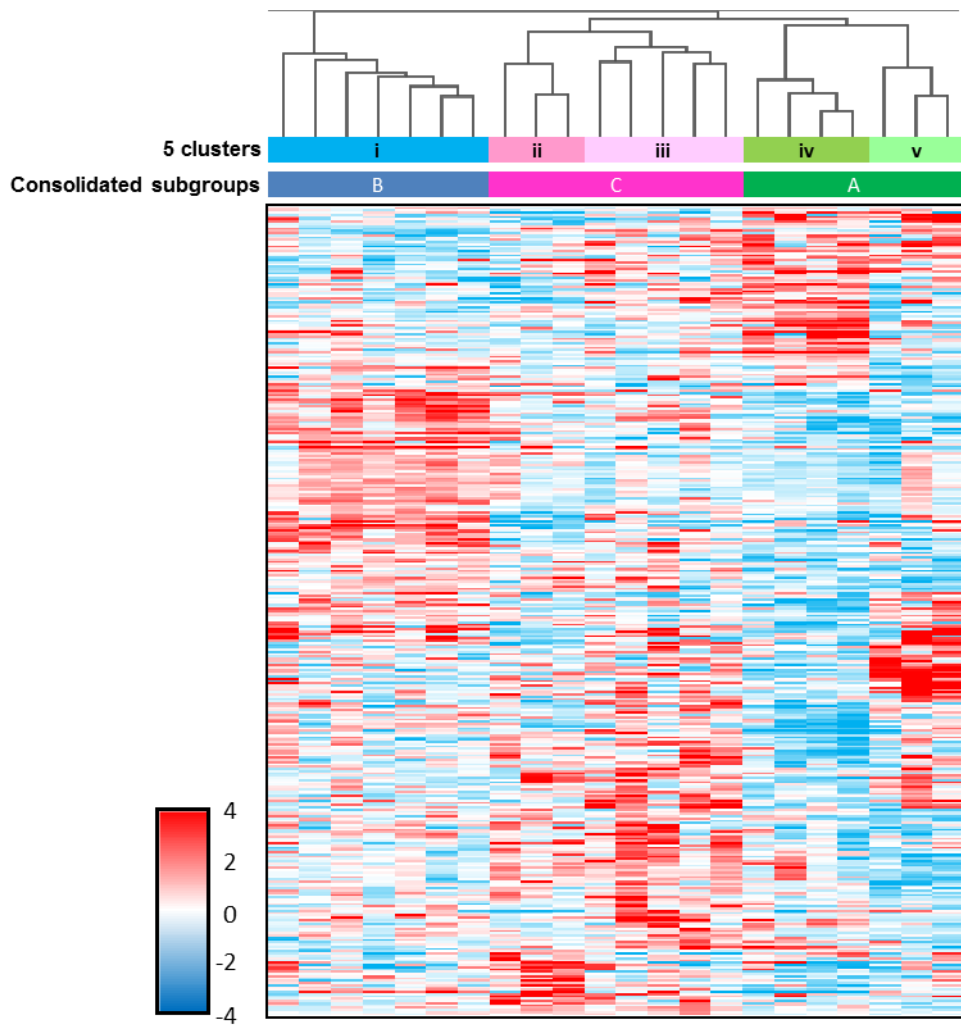
**Supplemental figure 6.2.** Consensus clustering of gene expression data from 22 IHCnegTP53wt patients.

**Supplementary Figure 6.3.** Low FGFR1 and high PDGFRA high gene expression identify a patient subgroup with worse post-pazopanib PFS



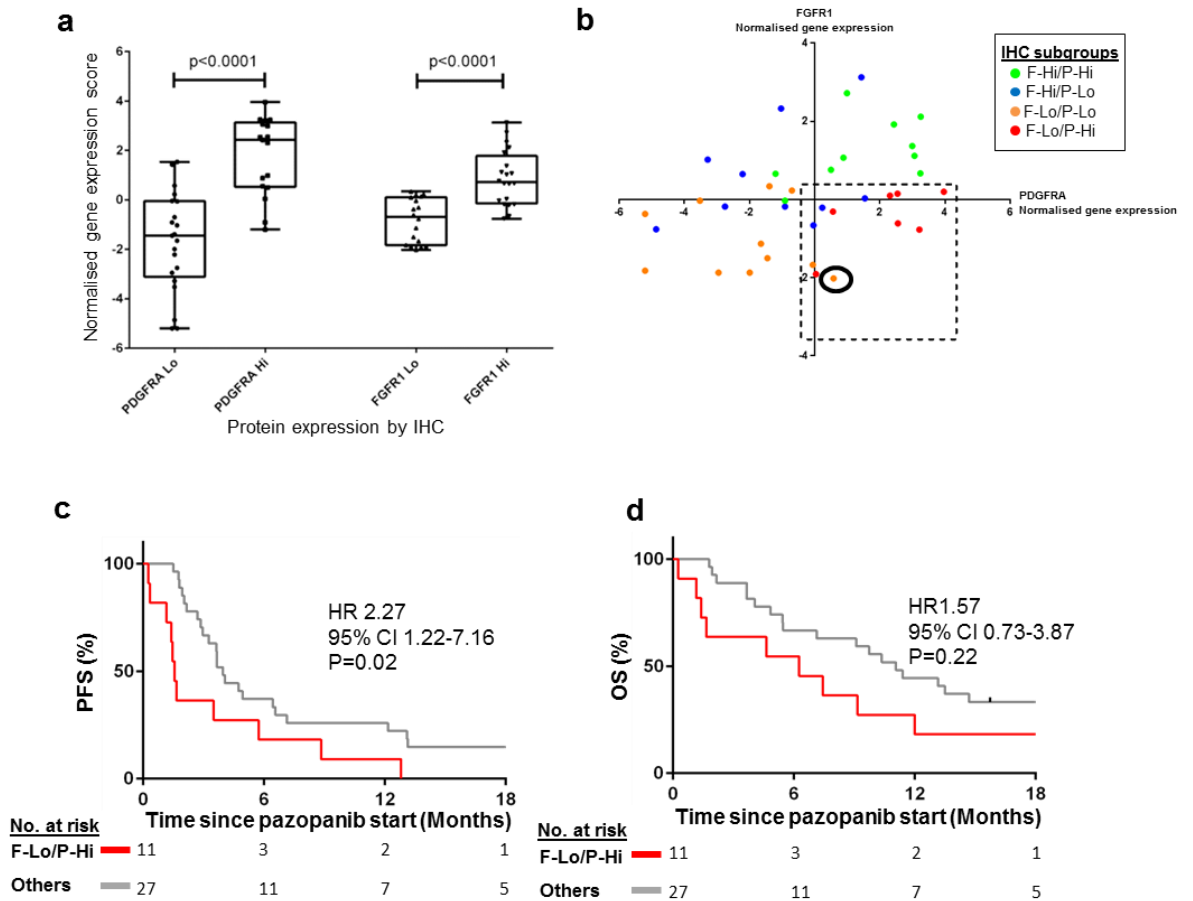
**Supplemental Figure 6.1 IHC-based scoring of tumour FGFR1 and PDGFRA expression exhibits very good inter- and intra-observer agreement.**

A selection of 18 tumours that had been IHC stained for FGFR1 and PDGFRA were independently assessed and scored by two consultant histopathologists (Inter-observer). One of the histopathologists also repeated scoring of the same tumours on a second occasion several months later (Intra-observer). Histopathologists were blinded to the other scores at time of assessment. Cohen's and weighted kappa values were calculated to assess the degree of inter- and intra-observer agreement (95% confidence interval, p value)



**Supplemental figure 6.2. Consensus clustering of gene expression data from 22 IHCnegTP53wt patients.**

Consensus clustering identified optimal separation of 22 IHCnegTP53wt patients into 5 subgroups. (i-v). Shown here is a heatmap of the 22 patients based on expression data of the list of 359 genes which were identified to be significantly differential among the 5 biological subgroups using multiclass SAM analysis set at  $\leq 10\%$  FDR. On manual inspection, we noted shared branches between two pairs of clusters, these five clusters were resolved into 3 subgroups, labelled subgroup A (cluster iv and v), B (cluster i), and C (clusters ii and iii).



**Supplementary Figure 6.3. Low FGFR1 and high PDGFRA high gene expression identify a patient subgroup with worse post-pazopanib PFS.** **A.** Box and tail plot showing normalised gene expression levels for FGFR1 and PDGFRA when grouped by high or low protein expression as assessed by IHC. P values derive from unpaired T test. **B.** Scatter plot of normalised gene expression values for FGFR1 and PDGFRA, grouped by IHC assessment of protein expression. Dotted box denotes cases designated as FGFR-Lo/PDGFR-A-Hi by gene expression analysis. Circled case denotes single case of extraskeletal myxoid chondrosarcoma designated F-Lo/P-Lo by IHC but FGFR-Lo/PDGFR-Hi by gene expression analysis. On IHC review, this case exhibited high PDGFRA expression in intratumour blood vessels but not in tumour cells themselves. As such, this case was re-designated as non-FGFR1-Lo/PDGFR-A-Hi. Kaplan Meier curves of 2 subgroups defined by presence or absence of F-Lo/P-Hi status as determined by gene expression analysis for **(C)** PFS and **(D)** OS for 38 patients. F-Lo = FGFR1-Lo. F-Hi = FGFR1-Hi. P-Lo = PDGFRA-Lo. P-Hi = PDGFRA-Hi. PFS=progression-free survival. OS=overall survival. HR = Hazard ratio, 95% CI (95% Confidence Interval) and P value derive by log-rank testing, comparing FGFR1-Lo/PDGFR-A-Hi subgroup to all other subgroups combined.

## **Chapter 7: Identification of genes associated with pazopanib resistance**

### **7.1 Background and Objectives**

The PARSARC classifier identifies subgroups of patients that are defined by molecular traits and are associated with contrasting treatment outcomes with pazopanib. The subgroups include subgroup A, defined by gene expression profile in the absence of F-Lo/P-Hi IHC pattern or *TP53* mutation, which was associated with long-term response and survival following pazopanib therapy (median PFS 12.8 months, median OS 34.4 months). In contrast, a subgroup defined by high PDGFRA and low FGFR1 expression levels exhibited the worst outcomes in the cohort (median PFS 1.4 months, median OS 1.7 months), indicating that these patients were suffering from rapidly progressing disease that was intrinsically resistant to pazopanib. The mechanisms of differential sensitivity or resistance to pazopanib in STS are currently unknown. However, given that preclinical data have indicated that the drug may deliver anticancer effect through both anti-angiogenic and direct anti-oncogenic mechanisms (**see Chapter 1.4.1 and 1.4.4.5**), it is likely that key determiners of pazopanib response lie within the tumour cell biology and/or TME of individual STS tumours. The characterisation of this biology would further inform the investigation for predictive biomarkers that can prospectively identify baseline sensitivity or resistance to treatment, biomarkers that could be used to monitor patients on treatment for the early detection of emergent resistance, and to identify therapeutic vulnerabilities associated with intrinsic and/or required pazopanib resistance.

In order to investigate for possible mechanisms of pazopanib resistance within the RMH-SARC cohort, we sought to identify genes whose differential expression was enriched in the poor prognosis, intrinsically resistant F-Lo/P-Hi subgroup. We also assessed gene expression data derived from matched pre- and post-pazopanib tumour specimen from a single patient within RMH-SARC who had experienced tumour shrinkage and durable disease control with pazopanib therapy in order to identify genes whose upregulation was associated with acquired resistance as reflected by eventual disease progression.

### **Contributions**

Identification, collection and curation of archival histological material and associated clinic data; analysis of gene set functional annotation; figure generation were the work of the candidate.

SAM analysis of NanoString data was performed by Dr Maggie Cheang and her team in ICR CTSU.

Tumour measurements were performed by the candidate under the supervision of Dr Christina Messiou, consultant radiologist at The Royal Marsden.

## **7.2 Results**

### ***7.2.1 Intrinsic pazopanib resistance is associated with upregulation of cytokine signalling and downregulation of cell cycle control and DNA repair pathways***

To discover genes whose differential association was associated with intrinsic pazopanib resistance in RMH-SARC, we used SAM analysis to compare expression levels of 730 cancer pathway-related genes between the 7 patients identified in the intrinsic resistance F-Lo/P-Hi subgroup and the remaining 31 patients in the cohort. Through this approach we identified 6 and 27 genes whose respective expression was significantly upregulated or downregulated (<10% FDR) in the F-Lo/P-Hi subgroup (**Table 7.1**). Gene ontology functional annotation analysis of the 6 upregulated genes associated with intrinsic pazopanib resistance identified significant enrichment of cytokine signalling pathways (**Table 7.2**), while the 26 downregulated genes were enriched for involvement in DNA damage response and repair (including mismatch and base excision repair pathways) and cell cycle control (**Figure 7.2; Table 7.3**). This finding suggests a role for increased levels of cytokine signalling in conferring intrinsic pazopanib resistance to STS, in a manner which may relate to dysregulation of DNA repair and cell cycle control.

Upregulated (n=6)	Downregulated (n=27)	
IL11	ALKBH3	MLF1
IL8	AMER1	MLH1
LIF	ATR	MSH2
SSX1	BCL2	MUTYH
IL6	CCNO	NPM1
ETV4	CDKN2C	NTHL1
	DAXX	PCNA
	EGF	PPP2CB
	FANCL	PPP2R2C
	GNG7	RAD21
	HDAC11	RBX1
	HDAC5	SKP1
	LIG4	WEE1
	MAPK10	

**Table 7.1: Genes with significantly differential expression in intrinsic resistant F-Lo/P-Hi subgroup within RMH-SARC**

Term	Genes	Fold enrichment	Unadjusted P	FDR (%)
GO:0033138: positive regulation of peptidyl-serine phosphorylation	LIF, IL6, IL11	45.6	0.0010	1.39
GO:0005125: cytokine activity	LIF, IL6, IL8, IL11	10.5	0.0022	1.60
GO:0033135: regulation of peptidyl-serine phosphorylation	LIF, IL6, IL11	40.5	0.0013	1.77
GO:0050731: positive regulation of peptidyl-tyrosine phosphorylation	LIF, IL6, IL11	20.3	0.0055	7.17
GO:0043410: positive regulation of MAPKKK cascade	LIF, IL6, IL11	19.2	0.0061	7.96

**Table 7.2: Biological function analysis of upregulated genes in F-Lo/P-Hi tumours in RMH-SARC**

Gene ontology biological process and molecular function terms identified using DAVID functional annotation tool against 730 gene background. Shown are all enriched ontologies identified at <10% false discover rate

Term	Genes	Fold enrichment	Unadjusted P	FDR(%)
GO:0006281:DNA repair	FANCL, MUTYH, RAD21, MSH2, PCNA, MLH1, ATR, LIG4, ALKBH3, NTHL1, CCNO, RBX1	5.7	0.0000	0.00
GO:0033554:cellular response to stress	FANCL, MUTYH, RAD21, MSH2, BCL2, PCNA, MLH1, ATR, MAPK10, LIG4, ALKBH3, DAXX, NTHL1, CCNO, RBX1	4.0	0.0000	0.00
GO:0006259:DNA metabolic process	FANCL, MUTYH, RAD21, MSH2, PCNA, MLH1, ATR, LIG4, EGF, ALKBH3, NTHL1, CCNO, RBX1	4.3	0.0000	0.01
GO:0032404:mismatch repair complex binding	MUTYH, MSH2, PCNA, MLH1, ATR	24.5	0.0000	0.01
GO:0006974:response to DNA damage stimulus	FANCL, MUTYH, RAD21, MSH2, PCNA, MLH1, ATR, LIG4, ALKBH3, NTHL1, CCNO, RBX1	4.4	0.0000	0.02
GO:0016799:hydrolase activity, hydrolyzing N-glycosyl compounds	MUTYH, PCNA, NTHL1, CCNO	29.4	0.0001	0.14
GO:0019104:DNA N-glycosylase activity	MUTYH, PCNA, NTHL1, CCNO	29.4	0.0001	0.14
GO:0032405:MutLalpha complex binding	MUTYH, MSH2, PCNA, ATR	23.5	0.0003	0.34
GO:0006298:mismatch repair	MUTYH, MSH2, PCNA, MLH1	19.4	0.0006	0.90
GO:0007049:cell cycle	RAD21, CDKN2C, MSH2, BCL2, NPM1, MLH1, SKP1, ATR, LIG4, DAXX, WEE1, MLF1	2.7	0.0011	1.69
GO:0006284:base-excision repair	MUTYH, PCNA, NTHL1, CCNO	14.6	0.0016	2.40
GO:0044265~cellular macromolecule catabolic process	FANCL, MUTYH, PPP2CB, MLH1, SKP1, NTHL1, CCNO, RBX1	3.9	0.0020	3.10
GO:0032407:MutSalpha complex binding	MUTYH, MLH1, ATR	29.4	0.0030	3.50
GO:0009057~macromolecule catabolic process	FANCL, MUTYH, PPP2CB, MLH1, SKP1, NTHL1, CCNO, RBX1	3.6	0.0030	4.54
GO:0009264:deoxyribonucleotide catabolic process	MUTYH, NTHL1, CCNO	29.2	0.0031	4.59
GO:0006285:base-excision repair, AP site formation	MUTYH, NTHL1, CCNO	29.2	0.0031	4.59
GO:0009394:2'-deoxyribonucleotide metabolic process	MUTYH, NTHL1, CCNO	29.2	0.0031	4.59

**Table 7.3: Biological function analysis of downregulated genes in F-Lo/P-Hi tumours in RMH-SARC**

Gene ontology biological process and molecular function terms identified using DAVID functional annotation tool against 730 gene background. Shown are all enriched ontologies identified at <10% false discover rate. Highlighted in blue and red are ontology terms included in Figure 7.2.

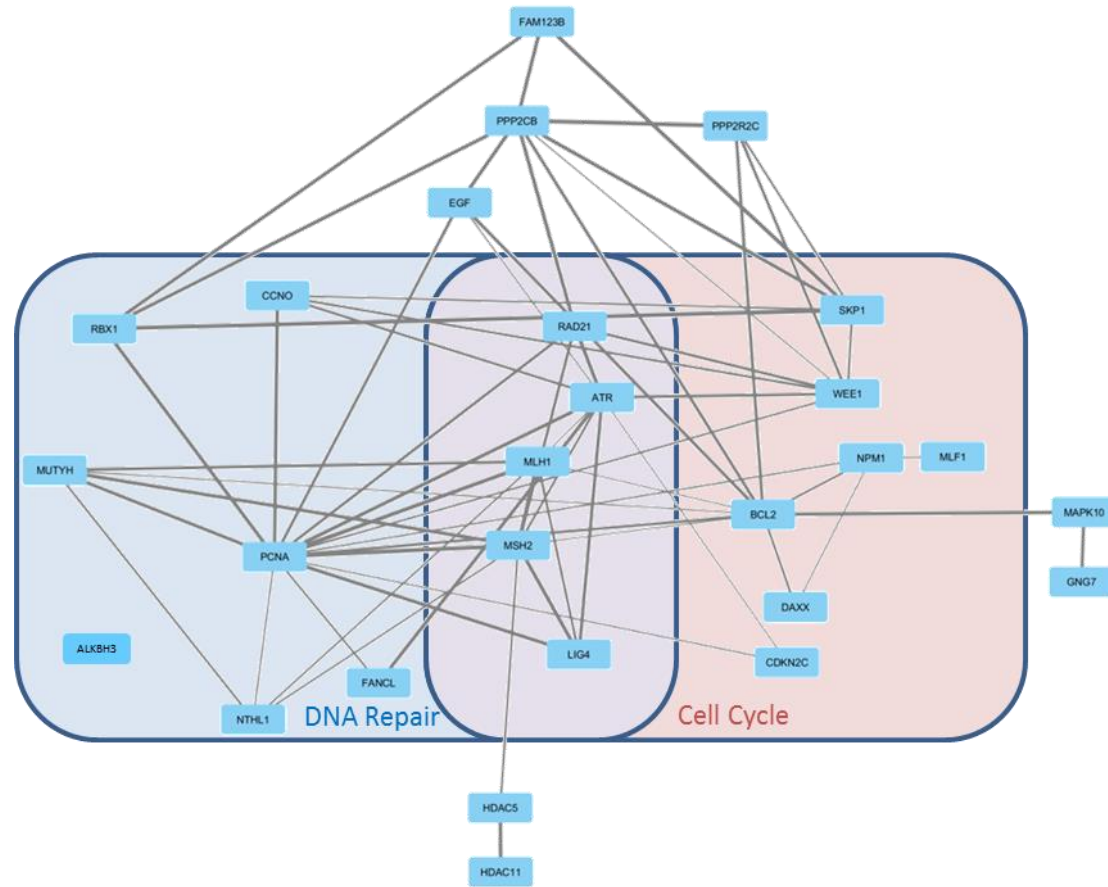


**Figure 7.1: Involvement of genes downregulated in F-Lo/P-Hi tumours in DNA repair and Cell Cycle functional annotation terms**

Association network of 27 genes identified by SAM analysis as being significantly downregulated in F-Lo/P-Hi tumours was produced using the STRING application. Superimposed on this network are boxes indicating membership of subset of genes in DNA repair (GO:0006281) and/or Cell cycle (GO:0007049) functional ontologies. Line thickness portrays the STRING calculated association confidence

### ***7.2.2 Upregulated genes associated with acquired pazopanib resistance in a long-term responding patient***

To assess which genes may be involved in acquired resistance to pazopanib, we further analysed a single patient case study within RMH-SARC (RMH001) who had experienced a long-term response of almost 12 months of disease control with pazopanib therapy (**Figure 7.2**). This female patient in her 30s had experienced early pelvic and abdominal wall recurrence during post-operative radiotherapy following hysterectomy for a high-grade uterine spindle cell sarcoma. Initial control of this recurrent disease was achieved following conversion to radical dose chemoradiation. However, further relapse in the abdominal wall and pelvis necessitated further systemic treatment from month 13. After two cycles of gemcitabine with docetaxel was associated with ongoing disease progression, pazopanib was commenced at month 15 and was associated with marked reduction in tumour dimension on MRI and FDG avidity on PET-CT imaging. Consolidation radiotherapy was delivered in the context of maintained pazopanib response at month 21, with eventual confirmed disease progression and change of therapy at month 27. An excisional biopsy of an abdominal wall metastasis taken 4 months prior to commencing pazopanib (month 11), and a percutaneous needle biopsy of abdominal wall metastasis taken at month 29 served as pazopanib-sensitive pre-treatment and pazopanib-resistant post-treatment tissue samples respectively from which we generated gene expression data. We concentrated on all genes with >1.5 fold increase in expression in the post-pazopanib sample relative to pre-treatment tumour and identified 208 genes.

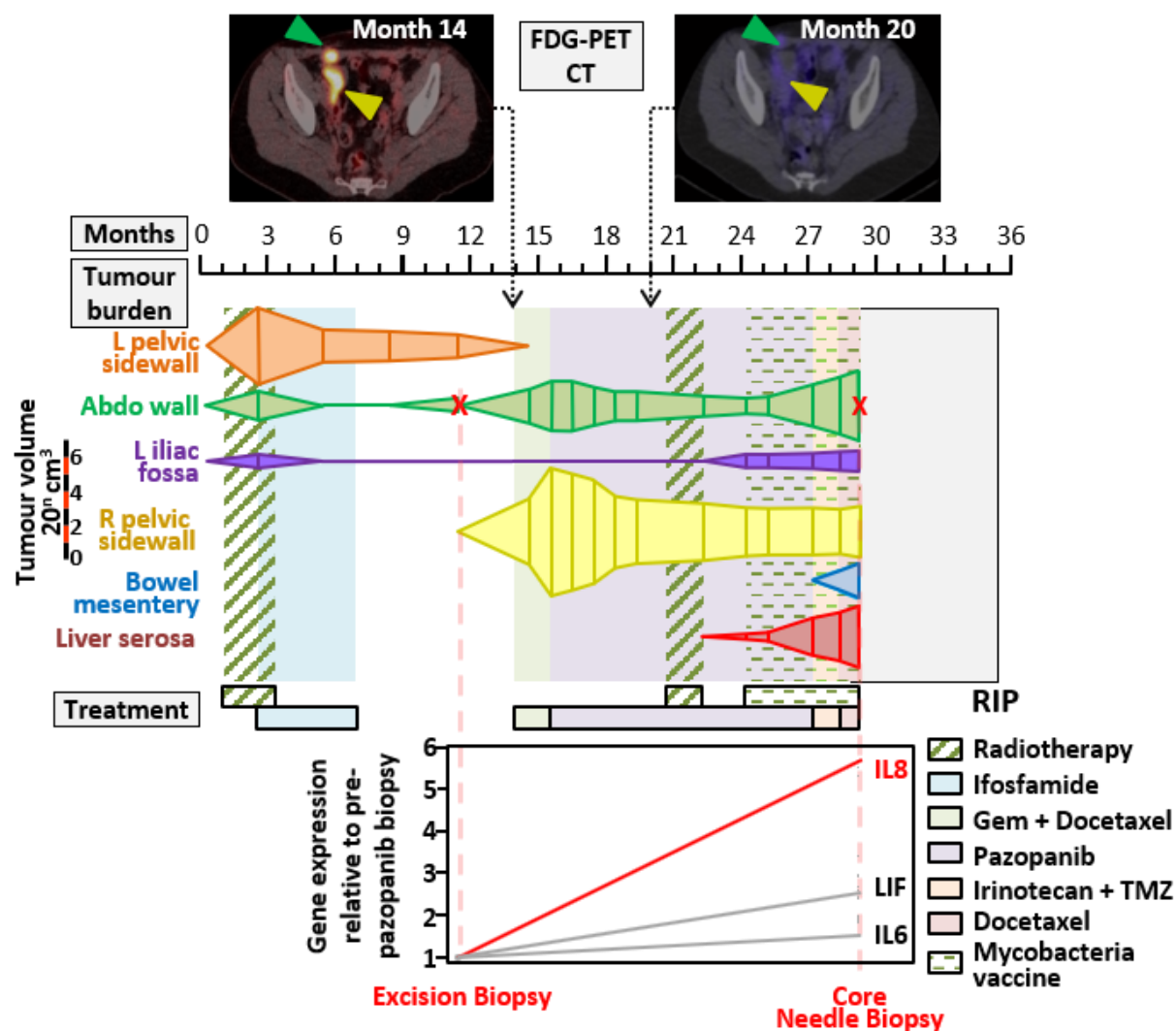


**Figure 7.2: Overview of long-term responder patient treated with pazopanib**

Schematic overview of clinical history of patient RMH001 who experienced durable disease control with pazopanib therapy. Tumour burden at different disease sites as measured by MRI illustrated on exponential scale. Relative pre- and post-pazopanib expression levels shown for three genes with >1.5x increase and that overlapped with upregulated genes in F-Lo/P-Hi tumours in RMH-SARC cohort.

### 7.2.3 Pro-inflammatory cytokine expression is associated with both intrinsic and acquired pazopanib resistance

Three genes were found to overlap between the two gene sets (**Figure 7.3**) and comprise IL-8, IL-6 and LIF, all members of the pro-inflammatory cytokine family. Of these genes, IL-8 showed the greatest fold difference between F-Lo/P-Hi and IHCneg tumours as well as the pre- and post-pazopanib samples in RMH001 (**Figures 7.2**). These genes are to be taken forward for functional validation of their putative role in conferring pazopanib resistance in cell line models of sarcoma in a separate PhD project.

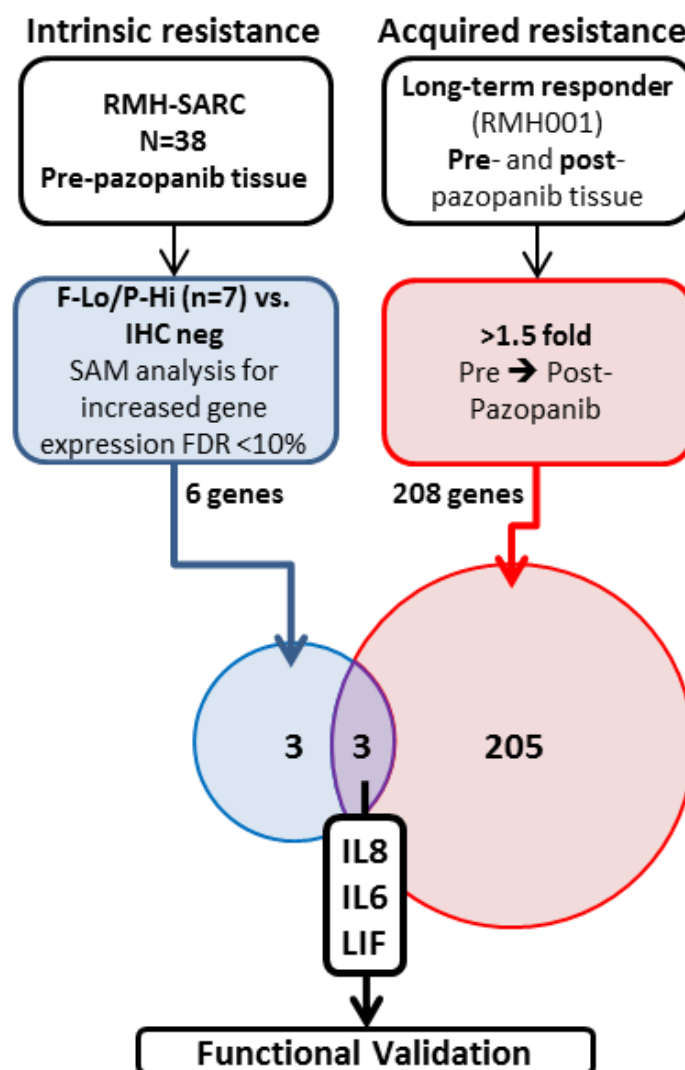


Figure 7.3: Overlap of genes upregulated in F-Lo/P-Hi intrinsic resistant tumours and genes upregulated upon acquisition of pazopanib resistance in a long-term responder (RMH001)

### 7.3 Discussion

The PARSARC classifier includes a subgroup of patients with intrinsic pazopanib resistance that is defined by differential expression of FGFR1 and PDGFRA, both of which are RTKs with documented capacity to activate multiple canonical oncogenic pathways<sup>313,314</sup>. Analysis of genes enriched in this group of patients as well as a case study of acquired resistance in a patient with long-term pazopanib response led to the identification of three cytokines (IL8, IL6 and LIF) as a candidate driver of pazopanib resistance. IL8 exhibiting the strongest association with resistance, in terms of upregulation in F-Lo/P-Hi tumours and in post-progression tumour in the long-term responder case study. Intrinsic resistance to pazopanib was also associated with downregulation of several genes involved in several DNA repair pathways. These findings indicate a potential role for these biological processes in mediating pazopanib resistance and are currently under investigation for functional validation in cell line models of sarcoma, as well as patient-derived xenograft models derived from pre- and post-pazopanib tumour samples from the long-term responder case study.

It is increasingly well recognised that inflammatory cytokines and chemokines including IL-8 and IL-6 can play an important role in modulating the sensitivity of cancers to TKI therapy. This has been best described in EGFR-driven NSCLC, where upregulation of IL-6 or IL-8 in cell line and mouse xenograft models has been shown to confer resistance to EGFR-targeting TKIs<sup>315–318</sup>. IL-8 is a proinflammatory chemokine that attracts granulocytes to inflamed tissues and is also a potent promoter of angiogenesis. IL-6 is an acute phase cytokine that promotes a range of local and systemic pro-inflammatory responses. Both IL-8 and IL-6 have been shown to promote tumorigenesis in multiple tumour types through a range of signalling pathways that mediate cell survival, proliferation, angiogenesis and invasion<sup>319,320</sup>. Pharmaceutical inhibitors of both are currently in clinical development as adjuncts to cytotoxic, molecularly targeted and immunotherapies<sup>321–323</sup>.

While data in STS are limited, a number of studies in other cancer types have indicated that inflammatory mediators are associated with pazopanib resistance<sup>161</sup>. High pre-treatment baseline levels of both IL-8 and IL-6 in serum samples of patients with mRCC were associated with poor outcome in a study

reported by Tran *et al*<sup>158</sup>. In the first stage of this study, a panel of circulating cytokines were assessed for prognostic associations in a single-arm phase II trial cohort of mostly TKI-naïve patients. The cytokines that were found to have significant prognostic associations in this discovery set were then assessed in a validation cohort of uniformly TKI-naïve patients from a randomised phase III trial of pazopanib. Here, high IL-8 was shown to be a negative prognostic but not predictive biomarker for pazopanib therapy in mRCC, whilst IL-6 showed both negative prognostic but positive predictive biomarker for pazopanib. These data suggest that while both high pre-treatment peripheral levels of IL-6 and IL-8 predicted for poor prognosis regardless of treatment exposure, the subgroup of poor prognosis mRCC patients with high pre-treatment levels of IL-6 are enriched for pazopanib effect and may be optimal candidates for pazopanib therapy. In contrast to this, two later studies of pazopanib-treated cohorts of patients with mRCC and urothelial cancer found that pre-treatment baseline levels of IL-6 and IL-8 were not significantly different between pazopanib responders and non-responders<sup>324,325</sup>. However, both these studies found that, in sequential blood samples taken from patients following commencement of pazopanib, increased on-treatment levels of IL-8 in urothelial cancer and both IL-8 and IL-6 in mRCC were found in non-responding patients, while in responding patients, peripheral cytokine levels remained suppressed. These observational studies do not provide evidence of any causative relationship between inflammatory cytokines such as IL-6 and IL-8 and pazopanib resistance but the reported associations are at least in keeping with a possible role of such cytokines in intrinsic and/or acquired drug resistance that is consistent with our data in STS. Investigation of independent cohorts of pazopanib-treated STS is required to confirm our observation of association between overexpression of proinflammatory cytokines and pazopanib resistance, while our ongoing studies in preclinical models aims to confirm a causative role and delineate the molecular mechanisms of such factors in conferring pazopanib resistance. It is possible that such mechanisms may directly involve tumour cells and/or be mediated through indirect effects on immune or vascular compartments of the sarcoma tumour environment – this consideration should inform the design of functional studies. Should a causative mechanism for IL-6 or IL-8-mediated pazopanib resistance be confirmed, the current clinical development of inhibitory mAbs and small molecules that target

IL-6 or IL-8 signalling pathways reflect a potential avenue for therapies that aim to prevent or overcome pazopanib resistance.

Cellular responses to DNA damage have been shown to be modulated by tyrosine kinase (TK) signalling<sup>326–328</sup>. Meanwhile, dysregulation of DNA mismatch repair have been associated with preclinical and clinical resistance to a range of chemotherapy types, including platinum-based drugs, alkylating agents, anthracyclines, antimetabolites and topoisomerase inhibitors<sup>329–333</sup>. While these reports indicate that DNA damage response and repair pathways can interact with TK-mediated signalling, and that therapeutic sensitivity to certain therapeutic agencies can be modulated by deficiencies in DNA repair, the potential contribution of downregulated expression of genes involved in DNA repair and cell cycle control pathways to intrinsic pazopanib resistance is unclear. In tumours where DNA damage and cell cycle checkpoint mechanisms remain intact, pro-survival signals provided by TK-mediated signalling cascades may feasibly promote tumour cell survival during replication stress. In such cases, TKI therapy could disrupt pro-survival stimuli, leading to redirection of replication stress response toward apoptosis. In contrast, the downregulation of DNA repair and cell cycle control mechanisms in other tumours may reflect a state of grossly dysregulated cellular homeostasis where accumulated genomic instability is tolerated. In such cases, a loss of dependence on any TK-mediated signalling for survival during replicative stress would reduce vulnerability to TKIs such as pazopanib. Alternatively, the potentiation and tolerance of genomic instability that may be associated with downregulated DNA repair and cell cycle checkpoint mechanisms could stochastically give rise to clonal aberrations that confer drug resistance - such a mechanism could feasibly give rise to cytokine-mediated pazopanib resistance. Further translational research is required to confirm the association between intrinsic pazopanib resistance and dysregulated DNA repair and cell cycle control that is indicated by our study of gene expression in the F-Lo/P-Hi subgroup within RMH-SARC. Given that defective DNA repair is associated with heightened tumour sensitivity to ionising radiation, such findings would support the use of radiotherapy either as an adjunct to pazopanib therapy or as a means of treating disease with demonstrated pazopanib resistance. A phase II study combining pazopanib with pre-operative radiotherapy in the treatment of high risk STS of the extremities, trunk wall or head and neck areas

is currently recruiting in the UK and Netherlands (NCT02575066), following on from a pilot study in 12 patients that confirmed the safety of the combination and reported encouraging early efficacy signals, with pathological evidence of therapy-induced necrosis in 70% and pathological complete or near-complete response in 40% in the 10 patients who underwent surgery<sup>334</sup>.

In summary, analysis for gene expression associated with clinical evidence of intrinsic and acquired pazopanib resistance with the RMH-SARC cohort has identified proinflammatory cytokines as candidate drivers of drug resistance, and downregulation of DNA repair and/or cell cycle control-related genes as potential mediators of resistance. Given the potential for the therapeutic targeting of these biological processes, further research is indicated to confirm the clinical association and investigate for causative functional mechanisms that may underlie these observations. This could feasibly lead to novel therapeutic avenues for the prevention or targeting of pazopanib-resistant STS.

## **Chapter 8: Conclusions and Future Directions**

The current means of STS classification fail to account for the significant degree of heterogeneity in clinical phenotype that is frequently observed between individual patients with identical histological diagnoses. Novel biomarkers are required to better address this wide variation in disease behaviour, thus providing improved means of risk stratification and selection of optimal management.

My thesis project has involved profiling tumour characteristics within retrospective cohorts in conjunction with associated clinical data. Through this approach, I have increased the evidence characterising the immune microenvironment in 3 STS subtypes, and I have also demonstrated prognostic associations of certain immune characteristics. These findings indicate that the quantitative and qualitative differences in the immune microenvironment of individual tumours could feasibly form the basis for novel prognostic and/or predictive biomarkers. Meanwhile, multi-omic profiling of baseline tumour samples from patients subsequently treated with pazopanib identified a series of molecular traits that identify tumour subgroups with contrasting treatment response. This again provides the basis for further biomarker development.

As detailed in **Chapter 6**, The PARSARC classifier represents a candidate biomarker panel that identifies STS patient subgroups with distinct post-pazopanib outcomes, independent of conventional histological classification. My project represents the discovery phase of this putative predictive biomarker. If successfully validated, this would have direct clinical utility in terms of treatment selection for individual patients, but could also have a potential positive impact on re-evaluation of the cost-effectiveness of pazopanib. Additionally, through comparison of gene expression profiles of tumours that demonstrated clinical pazopanib sensitivity or resistance, we have identified an association between upregulation of pro-inflammatory cytokine signalling and clinical pazopanib resistance (**Chapter 7**). Functional validation of this finding in pre-clinical models is currently underway by other team members, using paired sarcoma cell lines with intrinsic pazopanib sensitivity and induced resistance, and patient-derived xenografts established from pre- and post-pazopanib tumour biopsies taken from the long-term responder case study.

The PARSARC classifier was conceived as a sequential and integrated application of IHC, gene sequencing and gene expression assays. While all three techniques are established as part of routine diagnostic testing, the requirement for three separate assays may present a challenge in the routine application of PARSARC as a predictive biomarker. To address this, we plan to develop the PARSARC panel as a companion diagnostic test, using commercially-available NanoString-based technology to enable the integration of protein, DNA and RNA analysis into a single assay (see below). As a parallel and alternative means of streamlining the PARSARC panel, follow-up investigation by team members has sought to identify a gene expression signature that allows for the stratification of patients into the 5 PARSARC-defined groups without the requirement for IHC or gene sequencing analysis. Using Classification of Nearest Centroid (ClANC)<sup>335</sup> methodology to analyse gene expression data from all 38 cases within RMH-SARC, a set of 225 genes has been identified that is capable of classifying patients into one of the 5 previously described PARSARC subgroups - accuracy of the gene expression-based classifier in relation to the decision tree approach was 92%. A 42 gene predictor was identified to classify patients with intrinsic resistance to pazopanib as defined by the F-Lo/P-Hi HIS PARSARC subgroup. These centroids can now be applied to publicly available gene expression datasets to allocate tumours to one of the PARSARC classes, allowing for validation experiments of the prognostic and/or predictive value of the PARSARC classifier in independent cohorts of STS and other tumour types.

While my investigation of the RMH-SARC cohort encompassed analysis of tumour mutations, gene expression and protein levels, this study adopted a somewhat narrow focus on recognised oncogenic pathways in deriving a candidate biomarker panel. There is further scope for investigation for further potential biomarkers and mechanisms of drug resistance within this cohort. Our study did not investigate for possible associations between post-pazopanib outcome and tumour stromal characteristics (such as angiogenic markers or immune microenvironment). Given the recognised anti-angiogenic action of pazopanib<sup>106</sup> and our observation that pro-inflammatory cytokines are associated with pazopanib resistance (**See Chapter 7**), further evaluation is required to define putative biomarkers based on tumour stromal components. Ongoing work performed by other team members will apply the immune profiling

workflow described in **Chapters 2.2, 4.2.4 and 4.2.5** to the pazopanib-treated RMH-SARC cohort in order to investigate for differences in the immune microenvironment between PARSARC-defined tumour subgroups.

My investigation of putative immune-related prognostic and predictive biomarkers for pazopanib in STS have made use of a rare tissue resource to produce a meaningful contribution to the much-needed development of novel biomarkers and histology-agnostic classification in STS. However, as discussed in **Chapter 6.3**, the retrospective study of a single cohort of limited size and notable heterogeneity gives rise to the possibility of false positive findings and thus represents only an early step toward validated clinical utility. Per revised ASCO Levels of Evidence for tumour biomarker studies<sup>336</sup>, these studies only provide category D/level IV-V evidence. Studies such as these are the most commonly reported tumour marker analyses, making use of specimens that were collected as part of routine care and that are likely subject to variation in processing and storage, and that typically are without prospectively-determined eligibility criteria, power calculations or biomarker cut-point specification. The weight of uncontrolled variables and the strong potential for overfitting of biological parameters to clinical endpoints confer vulnerability to biased conclusions, false-positive results and non-reproducible findings. The gold standard for establishing the clinical utility of a new prognostic or predictive biomarker is the prospective RCT, wherein the benefit of a medical intervention is evaluated according to biomarker status. Prospective design allows for the imposition of tight controls on specimen collection, processing and storage, biomarker assay technique and interpretation, and clinical endpoint data collection. However, the design and conduct of such a trial pose unavoidable challenges in terms of logistics and expense, issues that are compounded by the relative rarity of STS. As such, further retrospective or smaller, non-randomised prospective studies present an avenue for validating findings, that can increase confidence in the scientific rationale of candidate biomarkers prior to embarking on costly randomised trials. Publicly-reported, independent datasets can also be leveraged for this purpose. This is reflected by our use of the TCGA-SARC dataset to assess for the prognostic associations of the PARSARC classifier in pazopanib-naïve STS (see **Chapter 6.2.7**)

Subsequent to the studies reported in this thesis, we have developed and designed the Validation of a Molecular Signature of Pazopanib Response in Advanced Soft Tissue Sarcomas (VMPRASS) study (**Figure 10.1**). The VMPRASS study represents the next phase of development of the PARSARC classifier into a fully validated, readily adoptable predictive biomarker and clinical tool. In VMPRASS, we shall assess the clinical validity of the PARSARC classifier through the analysis of tumour specimens from an independent cohort of pazopanib-treated patients from multiple international institutions and a comparator cohort of pazopanib-naïve patients. In parallel, we seek to develop the constituent parts of the PARSARC classifier into a CE-marked in vitro diagnostic (IVD) assay that is optimised for widespread, standardised application as part of routine patient care. The aims of this study are to:

- (1) Assess the clinical validity of the PARSARC classifier in an independent cohort of pazopanib-treated STS
- (2) Investigate the prognostic value of the PARSARC classifier in a pazopanib-naïve but otherwise equivalent STS cohort
- (3) Develop the three constituent assays of the PARSARC classifier into an integrated IVD

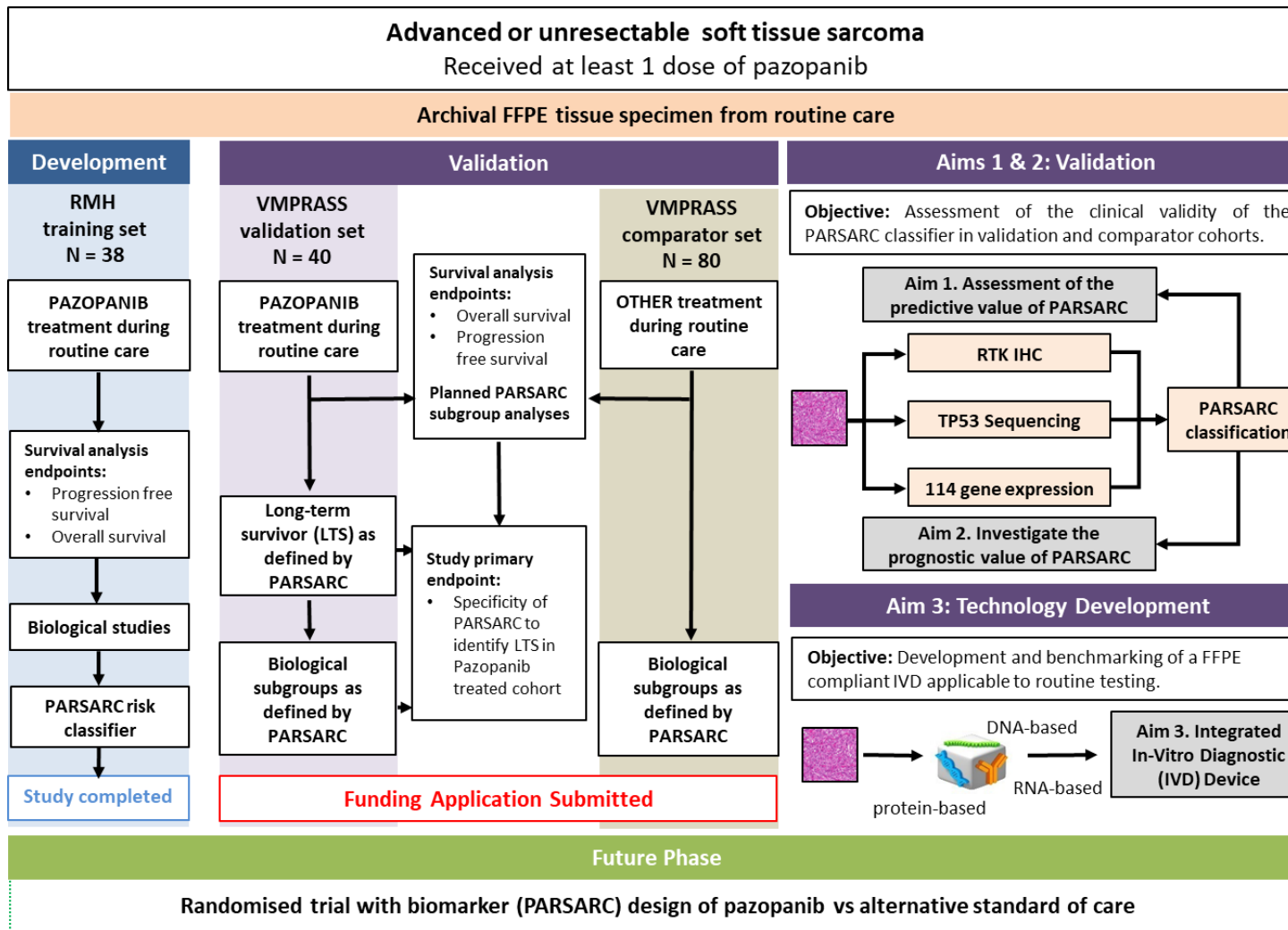


**Figure 8.1: Study overview of VMPRASS (Validation of a Molecular Signature of Pazopanib Response in Advanced Soft Tissue Sarcoma).**  
PFS: Time from first dose of pazopanib to radiological disease progression or death from any cause. OS: Time from first dose of pazopanib to death from any cause. Long-term survivor (LTS): OS ≥ 18 months

The primary research question of the VMPRASS study is to assess if the PARSARC classifier retains the specificity to identify a long-term survivor (LTS) subgroup defined as OS  $\geq$  18 months (PARSARC Subgroup A) when applied to pre-treatment FFPE tumour samples from an independent validation cohort. The ability of the PARSARC classifier to identify patients with distinct survival outcomes will be compared between those treated with pazopanib (training and validation cohorts) and pazopanib-naïve patients with comparable baseline clinico-pathological variables (comparator cohort - patients that meet PZP licensed indication and would be considered for PZP therapy, but were unable to receive treatment due to the lack of NHS drug funding). This analysis will provide an assessment of whether the PARSARC Subgroup A is a predictive marker of good PZP outcome in advanced STS. Meanwhile, we propose to integrate the three constituent assays into a single companion In Vitro Diagnostic (IVD) based on the NanoString 3D biology platform in collaboration with NanoString Technologies (Appendix 1). This IVD removes the need for sequential testing and integrating of data from different platforms while reducing sample input requirements (to the equivalent of 2 FFPE sections).

The VMPRASS study will generate robust evidence and provide a basis to progress the PARSARC classifier into definitive evaluation in a follow-on biomarker-led, randomised clinical trial. I presented the study design at the NCRI Consumer Forum Meeting 'Dragon's Den' in March 2018, with positive feedback received and suggestions incorporated into the revised trial design. The study has also been presented to the NCRI Sarcoma Clinical Studies Group and the NCRI Clinical Trial Pathology Advisory Group in May 2018, both of which provided support. As per revised ASCO Levels of Evidence for tumour biomarker studies<sup>336</sup>, the VMPRASS study will produce analytical and clinical validation for the PARSARC classifier representing Level II evidence. This would provide rationale and justification to advance to a randomised clinical trial with the aim of producing Level I evidence of clinical utility, the pre-requisite for regulatory approval of a biomarker and IVD. The proposed clinical trial would seek to randomise patients on the basis of the PARSARC classifier as determined by the use of the companion IVD.

The key findings of the immune profiling project (Chapters 4 and 5) were that

(i) quantitative variation exists in the extent of immune cell infiltration between individual tumours across 3 STS subtypes typified by karyotypic complexity **(Chapter 4.2.4)**

(ii) subgroups of tumours can be identified based on qualitative and quantitative characteristics of their immune microenvironment at transcriptional and protein expression levels, and that these subgroups are not restricted to conventional histological subtypes **(Chapter 4.2.5)**

(iii) a greater degree of immune cell infiltration and immune gene expression is associated with favourable survival outcome in UPS **(Chapter 5.2.1 to 5.2.3)**

(iv) a subgroup of tumours with the greatest degree of immune cell infiltration and gene expression has longer OS compared to tumours not in this subgroup **(Chapter 5.2.4)**.

In concert with previously reported translational studies and available clinical data regarding the use of immune checkpoint inhibitors in STS<sup>215,235,238,239,241</sup>, these findings suggest that, in a non-trivial proportion of tumours within STS subtypes with typically complex karyotypes, the presence of high levels of immune cell infiltration and immune gene expression identifies a distinct clinical phenotype typified by favourable OS. Our findings support the further development of immune-based biomarkers in STS with complex karyotypes. In addition to providing prognostic information for patients, successfully validated, iTME-based biomarkers would represent a novel means of risk stratification in clinical trials in early stage STS that could feasibly lead to the identification of patient groups that receive greater or lesser benefit from peri-operative treatment. Our findings also suggest that further investigation for underlying causative mechanisms between iTME characteristics, underlying tumour biology and prognosis in STS would be worthwhile. This might involve the generation of an integrated multi-omic dataset that provides both broader coverage of immune microenvironment components at cellular, functional and gene expression levels. This could include the use of TCR clonality and epitope prediction analysis to identify the presence of antigen-specific anti-tumour responses within STS, and analysis for association between immune microenvironment characteristics with genomic, transcriptomic and/or proteomic traits. A selection of tumours from within our cohort have already undergone mass spectrometry-based proteomic profiling, using an optimised

workflow for the extraction and analysis of FFPE tissue-derived protein (manuscript submitted). Tumour RNA and DNA are available for all 266 tumours, and a more in-depth assessment of immune-related gene expression, utilising a curated NanoString-based panel, is underway by other members of our team.

The limitations of my study investigating the iTME as a source of prognostic biomarkers in STS subtypes with complex karyotypes are discussed in **Chapters 4.3 and 5.3**. Many of the limitations of this study overlap with those of the PARSARC discovery study, among them a retrospective design that has produced results yet to be validated in independent cohorts. The process required for developing and validating any immune-based prognostic biomarker in STS might reflect that of the Immunoscore in colorectal cancer (**see Chapter 1.5.1**). This involved both the retrospective and prospective enrolment of several thousand colorectal cancer patients across several continents. It took 12 years from the initial report of the proposed biomarker to the publication of definitive prospective validation and the proposal for a new TNM-Immune risk classification to be adopted in routine care<sup>174,176</sup>. The notion of repeating a similar undertaking in STS would require exhaustive and committed international collaboration over many years. The initial steps of this process would involve the development of a technically and analytically replicable immune-based score. This could potentially take the form of an IHC-based score derived from optimised cutoff values for infiltrating cell density. As has been the case in the development of the Immunoscore, the deployment of digital histopathological approaches would offer a range of benefits in this regard. In addition or as an alternative to an IHC-based score, a gene expression centroid-based single sample predictor could be developed to enable the allocation of individual tumours to one of several subgroups with qualitatively distinct immune gene expression profiles. This is an approach analogous to the CINSARC classifier, a panel of 67 genes associated with maintenance of genomic stability and mitotic control that has been validated as a prognostic biomarker in STS (**see Chapter 1.2.4**). The clinical applicability of the CINSARC classifier has been enhanced through the successful demonstration of the equivalence of NanoString-based analysis of FFPE-derived tumour RNA with the original RNA-Seq-based tumour analysis<sup>337</sup>. The development of the CINSARC classifier as a biomarker began with initial discovery and validation studies first reported in 2010<sup>22</sup>. Further validation was

then provided by the application of the classifier to two prospectively-collected gene expression datasets (collected from the ISG-STS 1001 trial of subtype-guided pre-operative chemotherapy and the STRASS trial of pre-operative radiation in retroperitoneal sarcomas)<sup>68</sup>. Currently, prospective validation of the marker is underway in the NEOSarcomics trial of pre-operative chemotherapy (NCT02789384). In addition, prospective studies that base treatment decisions upon the CINSARC risk classifier are in development (NCT03805022). The CINSARC project not only demonstrates the feasibility of the clinical development of candidate prognostic and/or predictive biomarkers within a reasonable timeframe, but will also provide a data resource upon which different candidate biomarkers can be validated.

In conclusion, my studies have identified two novel avenues for biomarker development in sarcomas. The first identifies the immune TME of localised STS as a source of prognostic biomarkers, while the second provides the means to select patients with advanced STS with greater or lesser chance of benefit from pazopanib. Both approaches are independent of conventional STS histological classification and contribute toward much-needed efforts to develop new means of identifying groups of patients with shared tumour behaviour upon whom existing and novel therapeutic approaches might be focussed. Such advances are likely to be crucial to improved understanding and outcomes for these rare cancers.

## **References**

1. Fletcher, C. D. M., Hogendoorn, P. C. W., Mertens, F. & Bridge, J. A. *WHO Classification of Tumours of Soft Tissue and Bone*. (IARC Press, 2013).
2. Lee, A. T. J., Pollack, S. M., Huang, P. & Jones, R. L. Phase III Soft Tissue Sarcoma Trials: Success or Failure? *Curr. Treat. Options Oncol.* **18**, 19 (2017).
3. Dangoor, A. *et al.* UK guidelines for the management of soft tissue sarcomas. *Clin. Sarcoma Res.* **6**, 20 (2016).
4. Abeshouse, A. *et al.* Comprehensive and Integrated Genomic Characterization of Adult Soft Tissue Sarcomas. *Cell* **171**, 950-965.e28 (2017).
5. Italiano, A. *et al.* Clinical effect of molecular methods in sarcoma diagnosis (GENSARC): a prospective, multicentre, observational study. *Lancet Oncol.* **17**, 532–538 (2016).
6. Oppelt, P. J., Hirbe, A. C. & Van Tine, B. A. Gastrointestinal stromal tumors (GISTs): point mutations matter in management, a review. *J. Gastrointest. Oncol.* **8**, 466–473 (2017).
7. Penzel, R. *et al.* The location of KIT and PDGFRA gene mutations in gastrointestinal stromal tumours is site and phenotype associated. *J. Clin. Pathol.* **58**, 634–9 (2005).
8. Fletcher, C. D. M. *et al.* Diagnosis of gastrointestinal stromal tumors: A consensus approach. *Hum. Pathol.* **33**, 459–465 (2002).
9. Antonescu, C. R. *et al.* Association of KIT Exon 9 Mutations with Nongastric Primary Site and Aggressive Behavior. *Clin. Cancer Res.* **9**, 3329–3337 (2003).
10. Miettinen, M., El-Rifai, W., H L Sobin, L. & Lasota, J. Evaluation of malignancy and prognosis of gastrointestinal stromal tumors: a review. *Hum. Pathol.* **33**, 478–83 (2002).

11. Demetri, G. D. *et al.* Efficacy and Safety of Imatinib Mesylate in Advanced Gastrointestinal Stromal Tumors. *N. Engl. J. Med.* **347**, 472–480 (2002).
12. Antonescu, C. R. *et al.* Sarcomas With CIC-rearrangements Are a Distinct Pathologic Entity With Aggressive Outcome: A Clinicopathologic and Molecular Study of 115 Cases. *Am. J. Surg. Pathol.* **41**, 941–949 (2017).
13. Steele, C. D. *et al.* Undifferentiated Sarcomas Develop through Distinct Evolutionary Pathways. *Cancer Cell* **35**, 441-456.e8 (2019).
14. George, S., Serrano, C., Hensley, M. L. & Ray-Coquard, I. Soft Tissue and Uterine Leiomyosarcoma. *J. Clin. Oncol.* **36**, 144–150 (2018).
15. Fletcher, C. D. Pleomorphic malignant fibrous histiocytoma: fact or fiction? A critical reappraisal based on 159 tumors diagnosed as pleomorphic sarcoma. *Am. J. Surg. Pathol.* **16**, 213–28 (1992).
16. Fletcher, C. D., Gustafson, P., Rydholm, A., Willén, H. & Akerman, M. Clinicopathologic re-evaluation of 100 malignant fibrous histiocytomas: prognostic relevance of subclassification. *J. Clin. Oncol.* **19**, 3045–50 (2001).
17. Nakayama, R. *et al.* Gene expression analysis of soft tissue sarcomas: characterization and reclassification of malignant fibrous histiocytoma. *Mod. Pathol.* **20**, 749–759 (2007).
18. Widemann, B. C. & Italiano, A. Biology and Management of Undifferentiated Pleomorphic Sarcoma, Myxofibrosarcoma, and Malignant Peripheral Nerve Sheath Tumors: State of the Art and Perspectives. *J. Clin. Oncol.* **36**, 160–167 (2018).
19. Lee, A. T. J., Thway, K., Huang, P. H. & Jones, R. L. Clinical and Molecular Spectrum of Liposarcoma. *J. Clin. Oncol.* **36**, 151–159 (2018).
20. Singer, S., Antonescu, C. R., Riedel, E. & Brennan, M. F. Histologic subtype and margin of resection predict pattern of recurrence and survival for retroperitoneal liposarcoma. *Ann. Surg.* **238**, 358–70; discussion 370-1 (2003).
21. Forus, A. *et al.* Comparative genomic hybridization analysis of human

- sarcomas: I. Occurrence of genomic imbalances and identification of a novel major amplicon at 1q21-q22 in soft tissue sarcomas. *Genes, Chromosomes Cancer* **14**, 8–14 (1995).
22. Chibon, F. *et al.* Validated prediction of clinical outcome in sarcomas and multiple types of cancer on the basis of a gene expression signature related to genome complexity. *Nat. Med.* **16**, 781–7 (2010).
  23. Lagarde, P. *et al.* Chromosome Instability Accounts for Reverse Metastatic Outcomes of Pediatric and Adult Synovial Sarcomas. *J. Clin. Oncol.* **31**, 608–615 (2013).
  24. Lesluyes, T., Delespaul, L., Coindre, J.-M. & Chibon, F. The CINSARC signature as a prognostic marker for clinical outcome in multiple neoplasms. *Sci. Rep.* **7**, 5480 (2017).
  25. Lesluyes, T. *et al.* RNA sequencing validation of the Complexity INDEX in SARCOMAS prognostic signature. *Eur. J. Cancer* **57**, 104–111 (2016).
  26. Bertucci, F., Finetti, P., Sabatier, R. & Birnbaum, D. The CINSARC signature: Prognostic and predictive of response to chemotherapy? *Cell Cycle* (2010). doi:10.4161/cc.9.19.13463
  27. Beck, A. H. *et al.* Discovery of molecular subtypes in leiomyosarcoma through integrative molecular profiling. *Oncogene* **29**, 845–54 (2010).
  28. Gibault, L. *et al.* New insights in sarcoma oncogenesis: a comprehensive analysis of a large series of 160 soft tissue sarcomas with complex genomics. *J. Pathol.* **223**, 64–71 (2011).
  29. Agaram, N. P. *et al.* Targeted exome sequencing profiles genetic alterations in leiomyosarcoma. *Genes, Chromosom. Cancer* **55**, 124–130 (2016).
  30. Mäkinen, N. *et al.* Exome Sequencing of Uterine Leiomyosarcomas Identifies Frequent Mutations in TP53, ATRX, and MED12. *PLOS Genet.* **12**, e1005850 (2016).
  31. Chudasama, P. *et al.* Integrative genomic and transcriptomic analysis of leiomyosarcoma. *Nat. Commun.* **9**, 144 (2018).

32. Guo, X. *et al.* Clinically Relevant Molecular Subtypes in Leiomyosarcoma. *Clin. Cancer Res.* **21**, 3501–11 (2015).
33. Svarvar, C. *et al.* Do DNA copy number changes differentiate uterine from non-uterine leiomyosarcomas and predict metastasis? *Mod. Pathol.* **19**, 1068–1082 (2006).
34. Larramendy, M. L., Kaur, S., Svarvar, C., Böhling, T. & Knuutila, S. Gene copy number profiling of soft-tissue leiomyosarcomas by array-comparative genomic hybridization. *Cancer Genet. Cytogenet.* **169**, 94–101 (2006).
35. Ganjoo, K. N. *et al.* The prognostic value of tumor-associated macrophages in leiomyosarcoma: a single institution study. *Am. J. Clin. Oncol.* **34**, 82–6 (2011).
36. Carneiro, A. *et al.* Indistinguishable genomic profiles and shared prognostic markers in undifferentiated pleomorphic sarcoma and leiomyosarcoma: different sides of a single coin? *Lab. Investig.* **89**, 668–675 (2009).
37. Pérot, G. *et al.* Constant p53 Pathway Inactivation in a Large Series of Soft Tissue Sarcomas with Complex Genetics. *Am. J. Pathol.* **177**, 2080–2090 (2010).
38. Lee, J.-C. *et al.* Alternative lengthening of telomeres and loss of ATRX are frequent events in pleomorphic and dedifferentiated liposarcomas. *Mod. Pathol.* **28**, 1064–1073 (2015).
39. Matushansky, I. *et al.* Derivation of sarcomas from mesenchymal stem cells via inactivation of the Wnt pathway. *J. Clin. Invest.* **117**, 3248–57 (2007).
40. Harvey, K. F., Zhang, X. & Thomas, D. M. The Hippo pathway and human cancer. *Nat. Rev. Cancer* **13**, 246–257 (2013).
41. Conyers, R., Young, S. & Thomas, D. M. Liposarcoma: Molecular genetics and therapeutics. *Sarcoma* **2011**, (2011).
42. Singer, S. *et al.* Gene expression profiling of liposarcoma identifies

- distinct biological types/subtypes and potential therapeutic targets in well-differentiated and dedifferentiated liposarcoma. *Cancer Res.* **67**, 6626–6636 (2007).
43. Binh, M. B. N. *et al.* MDM2 and CDK4 immunostainings are useful adjuncts in diagnosing well-differentiated and dedifferentiated liposarcoma subtypes: a comparative analysis of 559 soft tissue neoplasms with genetic data. *Am. J. Surg. Pathol.* **29**, 1340–7 (2005).
  44. Italiano, A. *et al.* Clinical and biological significance of CDK4 amplification in well-differentiated and dedifferentiated liposarcomas. *Clin. Cancer Res.* **15**, 5696–5703 (2009).
  45. Lee, S. *et al.* CDK4 amplification predicts recurrence of well-differentiated liposarcoma of the abdomen. *PLoS One* **9**, 1–9 (2014).
  46. Meza-Zepeda, L. A. *et al.* Ectopic sequences from truncated HMGI-C in liposarcomas are derived from various amplified chromosomal regions. *Genes. Chromosomes Cancer* **31**, 264–73 (2001).
  47. Fedele, M. *et al.* Truncated and chimeric HMGI-C genes induce neoplastic transformation of NIH3T3 murine fibroblasts. *Oncogene* **17**, 413–8 (1998).
  48. Meltzer, P. S. *et al.* Identification and cloning of a novel amplified DNA sequence in human malignant fibrous histiocytoma derived from a region of chromosome 12 frequently rearranged in soft tissue tumors. *Cell Growth Differ.* **2**, 495–501 (1991).
  49. Kanojia, D. *et al.* Genomic landscape of liposarcoma. *Oncotarget* **6**, 42429–44 (2015).
  50. Barretina, J. *et al.* Subtype-specific alterations define new targets for soft tissue sarcoma therapy. *Nat. Rev. Genet.* **42**, 715–721 (2010).
  51. Asano, N. *et al.* Frequent amplification of receptor tyrosine kinase genes in well-differentiated/ dedifferentiated liposarcoma. *Oncotarget* **8**, 12941–12952 (2017).
  52. McGwire, G. B. & Skidgel, R. A. Extracellular conversion of epidermal

- growth factor (EGF) to des-Arg53-EGF by carboxypeptidase M. *J. Biol. Chem.* **270**, 17154–8 (1995).
53. Beird, H. C. *et al.* Genomic profiling of dedifferentiated liposarcoma compared to matched well-differentiated liposarcoma reveals higher genomic complexity and a common origin. *Cold Spring Harb. Mol. case Stud.* **4**, a002386 (2018).
  54. Chibon, F. *et al.* A subgroup of malignant fibrous histiocytomas is associated with genetic changes similar to those of well-differentiated liposarcomas. *Cancer Genet. Cytogenet.* **139**, 24–29 (2002).
  55. Chibon, F. *et al.* ASK1 (MAP3K5) as a potential therapeutic target in malignant fibrous histiocytomas with 12q14-q15 and 6q23 amplifications. *Genes. Chromosomes Cancer* **40**, 32–7 (2004).
  56. Mariani, O. *et al.* JUN oncogene amplification and overexpression block adipocytic differentiation in highly aggressive sarcomas. *Cancer Cell* **11**, 361–74 (2007).
  57. Dass, C. R., Galloway, S. J., Clark, J. C. M., Khachigian, L. M. & Choong, P. F. M. Involvement of c-jun in human liposarcoma growth: supporting data from clinical immunohistochemistry and DNazyme efficacy. *Cancer Biol. Ther.* **7**, 1297–301 (2008).
  58. American Joint Committee on Cancer. Soft Tissue Sarcoma of the Trunk and Extremities. in *AJCC Cancer Staging Manual* 507 (Springer, 2017).
  59. Williard, W. C., Hajdu, S. I., Casper, E. S. & Brennan, M. F. Comparison of amputation with limb-sparing operations for adult soft tissue sarcoma of the extremity. *Ann. Surg.* **215**, 269–75 (1992).
  60. Gronchi, a. *et al.* Frontline extended surgery is associated with improved survival in retroperitoneal low- to intermediate-grade soft tissue sarcomas. *Ann. Oncol.* **23**, 1067–1073 (2012).
  61. Derbel, O. *et al.* Survival impact of centralization and clinical guidelines for soft tissue sarcoma (A prospective and exhaustive population-based cohort). *PLoS One* **12**, e0158406 (2017).

62. Beane, J. D. *et al.* Efficacy of adjuvant radiation therapy in the treatment of soft tissue sarcoma of the extremity: 20-year follow-up of a randomized prospective trial. *Ann. Surg. Oncol.* **21**, 2484–9 (2014).
63. O’Sullivan, B. *et al.* Preoperative versus postoperative radiotherapy in soft-tissue sarcoma of the limbs: a randomised trial. *Lancet* **359**, 2235–2241 (2002).
64. Baldini, E. H. *et al.* Treatment guidelines for preoperative radiation therapy for retroperitoneal sarcoma: Preliminary consensus of an international expert panel. *Int. J. Radiat. Oncol. Biol. Phys.* **92**, 602–612 (2015).
65. Collins, R. *et al.* Adjuvant chemotherapy for localised resectable soft-tissue sarcoma of adults: meta-analysis of individual data. Sarcoma Meta-analysis Collaboration. *Lancet (London, England)* **350**, 1647–54 (1997).
66. Pervaiz, N. *et al.* A systematic meta-analysis of randomized controlled trials of adjuvant chemotherapy for localized resectable soft-tissue sarcoma. *Cancer* **113**, 573–81 (2008).
67. Woll, P. J. *et al.* Adjuvant chemotherapy with doxorubicin, ifosfamide, and lenograstim for resected soft-tissue sarcoma (EORTC 62931): a multicentre randomised controlled trial. *Lancet Oncol.* **13**, 1045–1054 (2012).
68. Gronchi, A. *et al.* Histotype-tailored neoadjuvant chemotherapy versus standard chemotherapy in patients with high-risk soft-tissue sarcomas (ISG-STS 1001): an international, open-label, randomised, controlled, phase 3, multicentre trial. *Lancet Oncol.* 1–11 (2017). doi:10.1016/S1470-2045(17)30334-0
69. Lindner, L. H. *et al.* Prognostic factors for soft tissue sarcoma patients with lung metastases only who are receiving first-line chemotherapy: An exploratory, retrospective analysis of the European Organization for Research and Treatment of Cancer-Soft Tissue and Bone Sarcoma Group (EORTC-STBSG). *Int. J. cancer* **142**, 2610–2620 (2018).
70. Judson, I. *et al.* Doxorubicin alone versus intensified doxorubicin plus

- ifosfamide for first-line treatment of advanced or metastatic soft-tissue sarcoma: A randomised controlled phase 3 trial. *Lancet Oncol.* **15**, 415–423 (2014).
71. Young, R. J. *et al.* Predictive and prognostic factors associated with soft tissue sarcoma response to chemotherapy: a subgroup analysis of the European Organisation for Research and Treatment of Cancer 62012 study. *Acta Oncol. (Madr)*. 1–8 (2017).  
doi:10.1080/0284186X.2017.1315173
  72. Tap, W. D. *et al.* Olaratumab and doxorubicin versus doxorubicin alone for treatment of soft-tissue sarcoma: an open-label phase 1b and randomised phase 2 trial. *Lancet* **388**, 488–497 (2016).
  73. Antoniou, G., Lee, A. T. J., Huang, P. H. & Jones, R. L. Olaratumab in soft tissue sarcoma - Current status and future perspectives. *Eur. J. Cancer* **92**, 33–39 (2018).
  74. Redondo, A. *et al.* ANNOUNCE 2: An open-label phase 1b, and a randomized, double-blind phase 2 study of olaratumab with gemcitabine plus docetaxel in the treatment of patients with advanced soft tissue sarcoma (STS). *Ann. Oncol.* **27**, (2016).
  75. Maki, R. G. *et al.* Randomized Phase II Study of Gemcitabine and Docetaxel Compared With Gemcitabine Alone in Patients With Metastatic Soft Tissue Sarcomas : Results of Sarcoma Alliance for Research Through Collaboration Study 002. *J. Clin. Oncol.* **25**, 2755–2764 (2009).
  76. Pautier, P. *et al.* Randomized Multicenter and Stratified Phase II Study of Gemcitabine Alone Versus Gemcitabine and Docetaxel in Patients with Metastatic or Relapsed Leiomyosarcomas: A Fédération Nationale des Centres de Lutte Contre le Cancer (FNCLCC) French Sarcoma Group. *Oncologist* **17**, 1213–1220 (2012).
  77. Garcia-del-Muro, X. *et al.* Randomized Phase II Study Comparing Gemcitabine Plus Dacarbazine Versus Dacarbazine Alone in Patients With Previously Treated Soft Tissue Sarcoma: A Spanish Group for Research on Sarcomas Study. *J. Clin. Oncol.* **29**, 2528–2533 (2011).

78. Skubitz, K. M. & Haddad, P. A. Paclitaxel and pegylated-liposomal doxorubicin are both active in angiosarcoma. *Cancer* **104**, 361–366 (2005).
79. Penel, N. *et al.* Phase II Trial of Weekly Paclitaxel for Unresectable Angiosarcoma: The ANGIOTAX Study. *J. Clin. Oncol.* **26**, 5269–5274 (2008).
80. Schlemmer, M. *et al.* Paclitaxel in patients with advanced angiosarcomas of soft tissue: A retrospective study of the EORTC soft tissue and bone sarcoma group. *Eur. J. Cancer* **44**, 2433–2436 (2008).
81. Schöffski, P. *et al.* Activity of eribulin mesylate in patients with soft-tissue sarcoma: a phase 2 study in four independent histological subtypes. *Lancet. Oncol.* **12**, 1045–52 (2011).
82. Schöffski, P. *et al.* Eribulin versus dacarbazine in previously treated patients with advanced liposarcoma or leiomyosarcoma: a randomised, open-label, multicentre, phase 3 trial. *Lancet (London, England)* **387**, 1629–1637 (2016).
83. Demetri, G. D. *et al.* Activity of Eribulin in Patients With Advanced Liposarcoma Demonstrated in a Subgroup Analysis from a Randomized Phase III Study of Eribulin Versus Dacarbazine. *J. Clin. Oncol.* In Press (2017).
84. Demetri, G. D. *et al.* Efficacy and safety of trabectedin or dacarbazine for metastatic liposarcoma or leiomyosarcoma after failure of conventional chemotherapy: Results of a phase III randomized multicenter clinical trial. *J. Clin. Oncol.* **34**, 786–793 (2016).
85. Cesne, A. Le *et al.* Results of a prospective randomized phase III T-SAR trial comparing trabectedin vs best supportive care (BSC) in patients with pretreated advanced soft tissue sarcoma (ASTS). *Ann. Oncol.* **27**, 1396O (2016).
86. Kawai, A. *et al.* Trabectedin monotherapy after standard chemotherapy versus best supportive care in patients with advanced, translocation-related sarcoma: a randomised, open-label, phase 2 study. *Lancet.*

- Oncol.* **16**, 406–16 (2015).
87. PDQ Adult Treatment Editorial Board, P. A. T. E. *Levels of Evidence for Adult and Pediatric Cancer Treatment Studies (PDQ®): Health Professional Version. PDQ Cancer Information Summaries* (National Cancer Institute (US), 2002).
  88. Bramwell, V. H. C., Anderson, D. & Charette, M. L. Doxorubicin-based chemotherapy for the palliative treatment of adult patients with locally advanced or metastatic soft-tissue sarcoma: a meta-analysis and clinical practice guideline. *Sarcoma* **4**, 103–112 (2000).
  89. Lorigan, P. *et al.* Phase III trial of two investigational schedules of ifosfamide compared with standard-dose doxorubicin in advanced or metastatic soft tissue sarcoma: A European Organisation for Research and Treatment of Cancer Soft Tissue and Bone Sarcoma Group study. *J. Clin. Oncol.* **25**, 3144–3150 (2007).
  90. van Oosterom, A. T. *et al.* Results of randomised studies of the EORTC Soft Tissue and Bone Sarcoma Group (STBSG) with two different ifosfamide regimens in first- and second-line chemotherapy in advanced soft tissue sarcoma patients. *Eur. J. Cancer* **38**, 2397–406 (2002).
  91. Bramwell, V. H. *et al.* Cyclophosphamide versus ifosfamide: a randomized phase II trial in adult soft-tissue sarcomas. The European Organization for Research and Treatment of Cancer [EORTC], Soft Tissue and Bone Sarcoma Group. *Cancer Chemother. Pharmacol.* **31 Suppl 2**, S180-4 (1993).
  92. Seddon, B. *et al.* GeDDiS: A prospective randomised controlled phase III trial of gemcitabine and docetaxel compared with doxorubicin as first-line treatment in previously untreated advanced unresectable or metastatic soft tissue sarcomas (EudraCT 2009-014907-29). *J. Clin. Oncol.* **33**, (2015).
  93. van der Graaf, W. T. *et al.* Pazopanib for metastatic soft-tissue sarcoma (PALETTE): a randomised, double-blind, placebo-controlled phase 3 trial. *Lancet* **379**, 1879–1886 (2012).

94. Zucali, P. A. *et al.* The “old drug” dacarbazine as a second/third line chemotherapy in advanced soft tissue sarcomas. *Invest. New Drugs* **26**, 175–181 (2008).
95. Buesa, J. M. *et al.* High-dose DTIC in advanced soft-tissue sarcomas in the adult. A phase II study of the E.O.R.T.C. Soft Tissue and Bone Sarcoma Group. *Ann. Oncol. Off. J. Eur. Soc. Med. Oncol.* **2**, 307–9 (1991).
96. Skubitz, K. M. Phase II trial of pegylated-liposomal doxorubicin (Doxil) in sarcoma. *Cancer Invest.* **21**, 167–76 (2003).
97. Judson, I. *et al.* Randomised phase II trial of pegylated liposomal doxorubicin (DOXIL/CAELYX) versus doxorubicin in the treatment of advanced or metastatic soft tissue sarcoma: a study by the EORTC Soft Tissue and Bone Sarcoma Group. *Eur. J. Cancer* **37**, 870–7 (2001).
98. Benson, C. *et al.* A retrospective study of patients with malignant PEComa receiving treatment with sirolimus or temsirolimus: the Royal Marsden Hospital experience. *Anticancer Res.* **34**, 3663–8 (2014).
99. Wagner, A. J. *et al.* Clinical activity of mTOR inhibition with sirolimus in malignant perivascular epithelioid cell tumors: Targeting the pathogenic activation of mTORC1 in tumors. *J. Clin. Oncol.* **28**, 835–840 (2010).
100. Butrynski, J. E. *et al.* Crizotinib in ALK-rearranged inflammatory myofibroblastic tumor. *N. Engl. J. Med.* **363**, 1727–33 (2010).
101. Rutkowski, P. *et al.* Imatinib Mesylate in Advanced Dermatofibrosarcoma Protuberans: Pooled Analysis of Two Phase II Clinical Trials. *J. Clin. Oncol.* **28**, 1772–1779 (2010).
102. Kitagawa, D. *et al.* Activity-based kinase profiling of approved tyrosine kinase inhibitors. *Genes to Cells* **18**, 110–122 (2013).
103. Ku, X., Heinzlmeir, S., Helm, D., Médard, G. & Kuster, B. New Affinity Probe Targeting VEGF Receptors for Kinase Inhibitor Selectivity Profiling by Chemical Proteomics. *J. Proteome Res.* **13**, 2445–2452 (2014).
104. Kumar, R. *et al.* Pharmacokinetic-pharmacodynamic correlation from

- mouse to human with pazopanib, a multikinase angiogenesis inhibitor with potent antitumor and antiangiogenic activity. *Mol. Cancer Ther.* **6**, 2012–21 (2007).
105. Noujaim, J., Payne, L. S., Judson, I., Jones, R. L. & Huang, P. H. Phosphoproteomics in translational research: a sarcoma perspective. *Ann. Oncol. Off. J. Eur. Soc. Med. Oncol.* **27**, 787–94 (2016).
  106. Podar, K. *et al.* The small-molecule VEGF receptor inhibitor pazopanib (GW786034B) targets both tumor and endothelial cells in multiple myeloma. *Proc. Natl. Acad. Sci.* **103**, 19478–19483 (2006).
  107. Amdahl, J. *et al.* Cost-effectiveness of pazopanib in advanced soft tissue sarcoma in the United kingdom. *Sarcoma* **2014**, 481071 (2014).
  108. Delea, T. E. *et al.* Cost-effectiveness of pazopanib in advanced soft-tissue sarcoma in Canada. *Curr. Oncol.* **21**, 748 (2014).
  109. Villa, G., Hernández-Pastor, L. J., Guix, M., Lavernia, J. & Cuesta, M. Cost-effectiveness analysis of pazopanib in second-line treatment of advanced soft tissue sarcoma in Spain. *Clin. Transl. Oncol.* **17**, 24–33 (2014).
  110. Harris, P. A. *et al.* Discovery of 5-[[4-[(2,3-Dimethyl-2 *H*-indazol-6-yl)methylamino]-2-pyrimidinyl]amino]-2-methyl-benzenesulfonamide (Pazopanib), a Novel and Potent Vascular Endothelial Growth Factor Receptor Inhibitor †. *J. Med. Chem.* **51**, 4632–4640 (2008).
  111. Gril, B. *et al.* Pazopanib Reveals a Role for Tumor Cell B-Raf in the Prevention of HER2+ Breast Cancer Brain Metastasis. *Clin. Cancer Res.* **17**, 142–153 (2011).
  112. Gril, B. *et al.* Pazopanib inhibits the activation of PDGFR $\beta$ -expressing astrocytes in the brain metastatic microenvironment of breast cancer cells. *Am. J. Pathol.* **182**, 2368–79 (2013).
  113. Gril, B. *et al.* The B-Raf Status of Tumor Cells May Be a Significant Determinant of Both Antitumor and Anti-Angiogenic Effects of Pazopanib in Xenograft Tumor Models. *PLoS One* **6**, e25625 (2011).

114. Hurwitz, H. I. *et al.* Phase I Trial of Pazopanib in Patients with Advanced Cancer. *Clin. Cancer Res.* **15**, 4220–4227 (2009).
115. Glade Bender, J. L. *et al.* Phase I Pharmacokinetic and Pharmacodynamic Study of Pazopanib in Children With Soft Tissue Sarcoma and Other Refractory Solid Tumors: A Children's Oncology Group Phase I Consortium Report. *J. Clin. Oncol.* **31**, 3034–3043 (2013).
116. Sternberg, C. N. *et al.* Pazopanib in Locally Advanced or Metastatic Renal Cell Carcinoma: Results of a Randomized Phase III Trial. *J. Clin. Oncol.* **28**, 1061–1068 (2010).
117. Motzer, R. J. *et al.* Pazopanib versus Sunitinib in Metastatic Renal-Cell Carcinoma. *N. Engl. J. Med.* **369**, 722–731 (2013).
118. Sleijfer, S. *et al.* Pazopanib, a multikinase angiogenesis inhibitor, in patients with relapsed or refractory advanced soft tissue sarcoma: a phase II study from the European organisation for research and treatment of cancer-soft tissue and bone sarcoma group (EORTC study 620. *J. Clin. Oncol.* **27**, 3126–32 (2009).
119. Coens, C. *et al.* Health-related quality-of-life results from PALETTE: A randomized, double-blind, phase 3 trial of pazopanib versus placebo in patients with soft tissue sarcoma whose disease has progressed during or after prior chemotherapy-a European Organization for res. *Cancer* **121**, 2933–2941 (2015).
120. Kawai, A. *et al.* A randomized, double-blind, placebo-controlled, Phase III study of pazopanib in patients with soft tissue sarcoma: results from the Japanese subgroup. *Jpn. J. Clin. Oncol.* **46**, 248–253 (2016).
121. Guo, J. *et al.* Safety of pazopanib and sunitinib in treatment-naive patients with metastatic renal cell carcinoma: Asian versus non-Asian subgroup analysis of the COMPARZ trial. *J. Hematol. Oncol.* **11**, 69 (2018).
122. Inada-Inoue, M. *et al.* Phase 1 study of pazopanib alone or combined with lapatinib in Japanese patients with solid tumors. *Cancer Chemother. Pharmacol.* **73**, 673–683 (2014).

123. Kalow, W. Interethnic variation of drug metabolism. *Trends Pharmacol. Sci.* **12**, 102–7 (1991).
124. Phan, V. H. *et al.* Ethnic differences in drug metabolism and toxicity from chemotherapy. *Expert Opin. Drug Metab. Toxicol.* **5**, 243–257 (2009).
125. Benson, C. *et al.* Outcome of uterine sarcoma patients treated with pazopanib: A retrospective analysis based on two European Organisation for Research and Treatment of Cancer (EORTC) Soft Tissue and Bone Sarcoma Group (STBSG) clinical trials 62043 and 62072. *Gynecol. Oncol.* **142**, 89–94 (2016).
126. Gelderblom, H. *et al.* Treatment patterns and clinical outcomes with pazopanib in patients with advanced soft tissue sarcomas in a compassionate use setting: results of the SPIRE study\*. *Acta Oncol. (Madr)*. **56**, 1769–1775 (2017).
127. Samuels, B. L. *et al.* Results of a prospective phase 2 study of pazopanib in patients with advanced intermediate-grade or high-grade liposarcoma. *Cancer* **123**, 4640–4647 (2017).
128. Subbiah, V. *et al.* Phase Ib/II Study of the Safety and Efficacy of Combination Therapy with Multikinase VEGF Inhibitor Pazopanib and MEK Inhibitor Trametinib In Advanced Soft Tissue Sarcoma. *Clin. Cancer Res.* **23**, 4027–4034 (2017).
129. Dembla, V. *et al.* Outcomes of patients with sarcoma enrolled in clinical trials of pazopanib combined with histone deacetylase, mTOR, Her2, or MEK inhibitors. *Sci. Rep.* **7**, 15963 (2017).
130. Munhoz, R. R. *et al.* A Phase Ib/II Study of Gemcitabine and Docetaxel in Combination With Pazopanib for the Neoadjuvant Treatment of Soft Tissue Sarcomas. *Oncologist* **20**, 1245–1246 (2015).
131. Fu, S. *et al.* Phase I study of pazopanib and vorinostat: a therapeutic approach for inhibiting mutant p53-mediated angiogenesis and facilitating mutant p53 degradation. *Ann. Oncol.* **26**, 1012–1018 (2015).
132. Frezza, A. *et al.* Pazopanib in advanced desmoplastic small round cell

- tumours: a multi-institutional experience. *Clin. Sarcoma Res.* **4**, 7 (2014).
133. Maruzzo, M. *et al.* Pazopanib as first line treatment for solitary fibrous tumours: the Royal Marsden Hospital experience. *Clin. Sarcoma Res.* **5**, 5 (2015).
134. Frezza, A. M. *et al.* Anthracycline, Gemcitabine, and Pazopanib in Epithelioid Sarcoma. *JAMA Oncol.* **4**, e180219 (2018).
135. Jones, R. L. *et al.* Clinical benefit of antiangiogenic therapy in advanced and metastatic chondrosarcoma. *Med. Oncol.* **34**, 167 (2017).
136. Kollár, A. *et al.* Pazopanib in advanced vascular sarcomas: an EORTC Soft Tissue and Bone Sarcoma Group (STBSG) retrospective analysis. *Acta Oncol. (Madr)*. **56**, 88–92 (2017).
137. Menegaz, B. A. *et al.* Clinical Activity of Pazopanib in Patients with Advanced Desmoplastic Small Round Cell Tumor. *Oncologist* **23**, 360–366 (2018).
138. Nakamura, T. *et al.* The clinical outcome of pazopanib treatment in Japanese patients with relapsed soft tissue sarcoma: A Japanese Musculoskeletal Oncology Group (JMOG) study. *Cancer* **122**, 1408–16 (2016).
139. Nakano, K. *et al.* Differences in the responses to pazopanib and the prognoses of soft tissue sarcomas by their histological eligibility for the PALETTE study. *Jpn. J. Clin. Oncol.* **45**, 449–455 (2015).
140. Stacchiotti, S. *et al.* Preclinical and clinical evidence of activity of pazopanib in solitary fibrous tumour. *Eur. J. Cancer* **50**, 3021–8 (2014).
141. Yoo, K. H. *et al.* Efficacy of pazopanib monotherapy in patients who had been heavily pretreated for metastatic soft tissue sarcoma: a retrospective case series. *BMC Cancer* **15**, 154 (2015).
142. Van Der Graaf, W. T. A. *et al.* PALETTE: Final overall survival (OS) data and predictive factors for OS of EORTC 62072/GSK VEG110727, a randomized double-blind phase III trial of pazopanib versus placebo in advanced soft tissue sarcoma (STS) patients. *ASCO Meet. Abstr.* **30**,

10009 (2012).

143. Kasper, B. *et al.* Long-term responders and survivors on pazopanib for advanced soft tissue sarcomas: subanalysis of two European Organisation for Research and Treatment of Cancer (EORTC) clinical trials 62043 and 62072. *Ann. Oncol.* **25**, 719–24 (2014).
144. Choi, H. *et al.* Correlation of Computed Tomography and Positron Emission Tomography in Patients With Metastatic Gastrointestinal Stromal Tumor Treated at a Single Institution With Imatinib Mesylate: Proposal of New Computed Tomography Response Criteria. *J. Clin. Oncol.* **25**, 1753–1759 (2007).
145. Benjamin, R. S. *et al.* We Should Desist Using RECIST, at Least in GIST. *J. Clin. Oncol.* **25**, 1760–1764 (2007).
146. Stacchiotti, S. *et al.* High-Grade Soft-Tissue Sarcomas: Tumor Response Assessment—Pilot Study to Assess the Correlation between Radiologic and Pathologic Response by Using RECIST and Choi Criteria. *Radiology* **251**, 447–456 (2009).
147. Stacchiotti, S. *et al.* Tumor response assessment by modified Choi criteria in localized high-risk soft tissue sarcoma treated with chemotherapy. *Cancer* **118**, 5857–5866 (2012).
148. Ronellenfitsch, U. *et al.* Preoperative therapy with pazopanib in high-risk soft tissue sarcoma: a phase II window-of-opportunity study by the German Interdisciplinary Sarcoma Group (GISG-04/NOPASS). *BMJ Open* **6**, e009558 (2016).
149. Van Der Graaf, W. T. A. *et al.* Early metabolic response as predictor for treatment outcome of pazopanib in patients with metastatic soft tissue sarcomas (the PREDICT study). *J. Clin. Oncol.* **36**, 11555–11555 (2018).
150. Narahara, H. *et al.* 508P Prognostic factors of soft tissue sarcoma (STS) treated with pazopanib from Nishinomiya Sarcoma Cohort Study (NSCS). *Ann. Oncol.* **27**, (2016).
151. Suttle, A. B. *et al.* Relationships between pazopanib exposure and clinical

- safety and efficacy in patients with advanced renal cell carcinoma. *Br. J. Cancer* **111**, 1909–16 (2014).
152. Mir, O. *et al.* Pazopanib plus best supportive care versus best supportive care alone in advanced gastrointestinal stromal tumours resistant to imatinib and sunitinib (PAZOGIST): a randomised, multicentre, open-label phase 2 trial. *Lancet. Oncol.* **17**, 632–41 (2016).
153. Lankheet, N. A. G. *et al.* Optimizing the dose in cancer patients treated with imatinib, sunitinib and pazopanib. *Br. J. Clin. Pharmacol.* **83**, 2195–2204 (2017).
154. Goldstein, D. *et al.* Is change in blood pressure a biomarker of pazopanib and sunitinib efficacy in advanced/metastatic renal cell carcinoma? *Eur. J. Cancer* **53**, 96–104 (2016).
155. Duffaud, F. *et al.* Hypertension (HTN) as a potential biomarker of efficacy in pazopanib-treated patients with advanced non-adipocytic soft tissue sarcoma. A retrospective study based on European Organisation for Research and Treatment of Cancer (EORTC) 62043 and 62072 trials. *Eur. J. Cancer* **51**, 2615–2623 (2015).
156. Verheijen, R. B. *et al.* Exposure-survival analyses of pazopanib in renal cell carcinoma and soft tissue sarcoma patients: opportunities for dose optimization. *Cancer Chemother. Pharmacol.* **80**, 1171–1178 (2017).
157. Rodriguez-Vida, A., Strijbos, M. & Hutson, T. Predictive and prognostic biomarkers of targeted agents and modern immunotherapy in renal cell carcinoma: Table 1. *ESMO Open* **1**, e000013 (2016).
158. Tran, H. T. *et al.* Prognostic or predictive plasma cytokines and angiogenic factors for patients treated with pazopanib for metastatic renal-cell cancer: A retrospective analysis of phase 2 and phase 3 trials. *Lancet Oncol.* **13**, 827–837 (2012).
159. Verbiest, A. *et al.* Molecular Subtypes of Clear Cell Renal Cell Carcinoma Are Associated With Outcome During Pazopanib Therapy in the Metastatic Setting. *Clin. Genitourin. Cancer* **16**, e605–e612 (2018).

160. Choueiri, T. K. *et al.* The Role of Aberrant VHL/HIF Pathway Elements in Predicting Clinical Outcome to Pazopanib Therapy in Patients with Metastatic Clear-Cell Renal Cell Carcinoma. *Clin. Cancer Res.* **19**, 5218–5226 (2013).
161. Sleijfer, S. *et al.* Cytokine and angiogenic factors associated with efficacy and toxicity of pazopanib in advanced soft-tissue sarcoma: an EORTC-STBSG study. *Br. J. Cancer* **107**, 639–45 (2012).
162. Templeton, A. J. *et al.* Prognostic Role of Neutrophil-to-Lymphocyte Ratio in Solid Tumors: A Systematic Review and Meta-Analysis. *JNCI J. Natl. Cancer Inst.* **106**, dju124 (2014).
163. De Maio, E. *et al.* Evolution in neutrophil-to-lymphocyte ratio (NLR) among advanced soft tissue sarcoma (STS) patients treated with pazopanib within EORTC 62043/62072 trials. *Ann. Oncol.* **28**, (2017).
164. Kobayashi, H. *et al.* Neutrophil-to-lymphocyte ratio after pazopanib treatment predicts response in patients with advanced soft-tissue sarcoma. *Int. J. Clin. Oncol.* **23**, 368–374 (2018).
165. Koehler, K., Liebner, D. & Chen, J. L. TP53 mutational status is predictive of pazopanib response in advanced sarcomas. *Ann. Oncol.* **26**, 2361–2362 (2015).
166. Wong, J. P. *et al.* Dual Targeting of PDGFR $\alpha$  and FGFR1 Displays Synergistic Efficacy in Malignant Rhabdoid Tumors. *Cell Rep.* **17**, 1265–1275 (2016).
167. Vyse, S. *et al.* Quantitative phosphoproteomic analysis of acquired cancer drug resistance to pazopanib and dasatinib. *J. Proteomics* **170**, 130–140 (2018).
168. Qiao, Z. *et al.* Proteomic approach toward determining the molecular background of pazopanib resistance in synovial sarcoma. *Oncotarget* **8**, 109587–109595 (2017).
169. Dunn, G. P., Old, L. J. & Schreiber, R. D. The three Es of cancer immunoediting. *Annu. Rev. Immunol.* **22**, 329–60 (2004).

170. Binnewies, M. *et al.* Understanding the tumor immune microenvironment (TIME) for effective therapy. *Nat. Med.* **24**, 541–550 (2018).
171. Chen, D. S. & Mellman, I. Elements of cancer immunity and the cancer-immune set point. *Nature* **541**, 321–330 (2017).
172. Gooden, M. J. M., de Bock, G. H., Leffers, N., Daemen, T. & Nijman, H. W. The prognostic influence of tumour-infiltrating lymphocytes in cancer: a systematic review with meta-analysis. *Br. J. Cancer* **105**, 93–103 (2011).
173. Fridman, W. H., Pagès, F., Sautès-Fridman, C. & Galon, J. The immune contexture in human tumours: impact on clinical outcome. *Nat. Rev. Cancer* **12**, 298–306 (2012).
174. Galon, J. *et al.* Type, Density, and Location of Immune Cells Within Human Colorectal Tumors Predict Clinical Outcome. **313**, 1960–1965 (2006).
175. Anitei, M.-G. *et al.* Prognostic and Predictive Values of the Immunoscore in Patients with Rectal Cancer. *Clin. Cancer Res.* **20**, 1891–1899 (2014).
176. Pagès, F. *et al.* International validation of the consensus Immunoscore for the classification of colon cancer: a prognostic and accuracy study. *Lancet* **391**, 2128–2139 (2018).
177. Malka, D. *et al.* Impact of the Immunoscore® assay on adjuvant chemotherapy decision making in patients with resected stage II-III colon cancer: A prospective, multicenter study (PROSCORE). *Ann. Oncol.* **29**, (2018).
178. Denkert, C. *et al.* Tumor-associated lymphocytes as an independent predictor of response to neoadjuvant chemotherapy in breast cancer. *J. Clin. Oncol.* **28**, 105–113 (2010).
179. Salgado, R. *et al.* Tumor-Infiltrating Lymphocytes and Associations With Pathological Complete Response and Event-Free Survival in HER2-Positive Early-Stage Breast Cancer Treated With Lapatinib and Trastuzumab. *JAMA Oncol.* **1**, 448 (2015).

180. Hodi, F. S. *et al.* Improved Survival with Ipilimumab in Patients with Metastatic Melanoma. *N. Engl. J. Med.* **363**, 711–723 (2010).
181. Darvin, P., Toor, S. M., Sasidharan Nair, V. & Elkord, E. Immune checkpoint inhibitors: recent progress and potential biomarkers. *Exp. Mol. Med.* **50**, 165 (2018).
182. Andrews, L. P., Marciscano, A. E., Drake, C. G. & Vignali, D. A. A. LAG3 (CD223) as a cancer immunotherapy target. *Immunol. Rev.* **276**, 80–96 (2017).
183. Du, W. *et al.* TIM-3 as a Target for Cancer Immunotherapy and Mechanisms of Action. *Int. J. Mol. Sci.* **18**, 645 (2017).
184. MacGregor, H. L. & Ohashi, P. S. Molecular Pathways: Evaluating the Potential for B7-H4 as an Immunoregulatory Target. *Clin. Cancer Res.* **23**, 2934–2941 (2017).
185. Zhang, Y. *et al.* TIM-3 is a potential prognostic marker for patients with solid tumors: A systematic review and meta-analysis. *Oncotarget* **8**, 31705–31713 (2017).
186. Podojil, J. R. & Miller, S. D. Potential targeting of B7-H4 for the treatment of cancer. *Immunol. Rev.* **276**, 40–51 (2017).
187. Soliman, H., Mediavilla-Varela, M. & Antonia, S. Indoleamine 2,3-Dioxygenase. *Cancer J.* **16**, 354–359 (2010).
188. Holmgaard, R. B., Zamarin, D., Munn, D. H., Wolchok, J. D. & Allison, J. P. Indoleamine 2,3-dioxygenase is a critical resistance mechanism in antitumor T cell immunotherapy targeting CTLA-4. *J. Exp. Med.* **210**, 1389–1402 (2013).
189. Chester, C., Sanmamed, M. F., Wang, J. & Melero, I. Immunotherapy targeting 4-1BB: mechanistic rationale, clinical results, and future strategies. *Blood* **131**, blood-2017-06-741041 (2017).
190. Jenkins, R. W., Barbie, D. A. & Flaherty, K. T. Mechanisms of resistance to immune checkpoint inhibitors. *Br. J. Cancer* **118**, 9–16 (2018).

191. Shen, X. & Zhao, B. Efficacy of PD-1 or PD-L1 inhibitors and PD-L1 expression status in cancer: meta-analysis. *BMJ* **362**, k3529 (2018).
192. Passiglia, F. *et al.* PD-L1 expression as predictive biomarker in patients with NSCLC: a pooled analysis. *Oncotarget* **7**, 19738–47 (2016).
193. Larkin, J. *et al.* Combined Nivolumab and Ipilimumab or Monotherapy in Untreated Melanoma. *N. Engl. J. Med.* **373**, 23–34 (2015).
194. Udall, M. *et al.* PD-L1 diagnostic tests: a systematic literature review of scoring algorithms and test-validation metrics. *Diagn. Pathol.* **13**, 12 (2018).
195. Teixidó, C., Vilariño, N., Reyes, R. & Reguart, N. PD-L1 expression testing in non-small cell lung cancer. *Ther. Adv. Med. Oncol.* **10**, 1758835918763493 (2018).
196. Merok, M. A. *et al.* Microsatellite instability has a positive prognostic impact on stage II colorectal cancer after complete resection: results from a large, consecutive Norwegian series. *Ann. Oncol. Off. J. Eur. Soc. Med. Oncol.* **24**, 1274–82 (2013).
197. Chan, T. A. *et al.* Development of tumor mutation burden as an immunotherapy biomarker: utility for the oncology clinic. *Ann. Oncol.* **30**, 44–56 (2019).
198. Lyu, G.-Y., Yeh, Y.-H., Yeh, Y.-C. & Wang, Y.-C. Mutation load estimation model as a predictor of the response to cancer immunotherapy. *npj Genomic Med.* **3**, 12 (2018).
199. Goodman, A. M. *et al.* Tumor Mutational Burden as an Independent Predictor of Response to Immunotherapy in Diverse Cancers. *Mol. Cancer Ther.* **16**, 2598–2608 (2017).
200. Marcus, L., Lemery, S. J., Keegan, P. & Pazdur, R. FDA Approval Summary: Pembrolizumab for the treatment of microsatellite instability-high solid tumors. *Clin. Cancer Res.* clincanres.4070.2018 (2019). doi:10.1158/1078-0432.CCR-18-4070
201. Thorsson, V. *et al.* The Immune Landscape of Cancer. *Immunity* **48**, 812-

830.e14 (2018).

202. Kim, J. R. *et al.* Tumor Infiltrating PD1-Positive Lymphocytes and the Expression of PD-L1 Predict Poor Prognosis of Soft Tissue Sarcomas. *PLoS One* **8**, e82870 (2013).
203. D'Angelo, S. P. *et al.* Prevalence of tumor-infiltrating lymphocytes and PD-L1 expression in the soft tissue sarcoma microenvironment. *Hum. Pathol.* **46**, 357–365 (2015).
204. van Erp, A. E. M. *et al.* Expression and clinical association of programmed cell death-1, programmed death-ligand-1 and CD8+ lymphocytes in primary sarcomas is subtype dependent. *Oncotarget* **8**, 71371–71384 (2017).
205. Honda, Y. *et al.* Infiltration of PD-1-positive cells in combination with tumor site PD-L1 expression is a positive prognostic factor in cutaneous angiosarcoma. *Oncoimmunology* **6**, e1253657 (2017).
206. Movva, S. *et al.* Multi-platform profiling of over 2000 sarcomas: Identification of biomarkers and novel therapeutic targets. *Oncotarget* **6**, (2015).
207. Paydas, S., Bagir, E. K., Deveci, M. A. & Gonlusen, G. Clinical and prognostic significance of PD-1 and PD-L1 expression in sarcomas. *Med. Oncol.* **33**, 93 (2016).
208. Pollack, S. M. *et al.* T-cell infiltration and clonality correlate with programmed cell death protein 1 and programmed death-ligand 1 expression in patients with soft tissue sarcomas. *Cancer* 1–14 (2017). doi:10.1002/cncr.30726
209. Que, Y. *et al.* PD-L1 Expression Is Associated with FOXP3+ Regulatory T-Cell Infiltration of Soft Tissue Sarcoma and Poor Patient Prognosis. *J. Cancer* **8**, 2018–2025 (2017).
210. Boxberg, M. *et al.* PD-L1 and PD-1 and characterization of tumor-infiltrating lymphocytes in high grade sarcomas of soft tissue—prognostic implications and rationale for immunotherapy. *Oncoimmunology* **7**,

- (2018).
211. Patel, K. R. *et al.* Increase in PD-L1 expression after pre-operative radiotherapy for soft tissue sarcoma. *Oncoimmunology* **7**, e1442168 (2018).
  212. Kostine, M. *et al.* Increased infiltration of M2-macrophages, T-cells and PD-L1 expression in high grade leiomyosarcomas supports immunotherapeutic strategies. *Oncoimmunology* **7**, e1386828 (2018).
  213. Shurell, E. *et al.* Characterizing the immune microenvironment of malignant peripheral nerve sheath tumor by PD-L1 expression and presence of CD8+ tumor infiltrating lymphocytes. *Oncotarget* **7**, 64300 (2016).
  214. Toulmonde, M. *et al.* Integrative assessment of expression and prognostic value of PDL1, IDO, and kynurenine in 371 primary soft tissue sarcomas with genomic complexity. *J. Clin. Oncol.* **34**, 11008–11008 (2016).
  215. Toulmonde, M. *et al.* Use of PD-1 Targeting, Macrophage Infiltration, and IDO Pathway Activation in Sarcomas. *JAMA Oncol.* **4**, 93 (2018).
  216. Sorbye, S. W. *et al.* Prognostic Impact of Lymphocytes in Soft Tissue Sarcomas. *PLoS One* **6**, e14611 (2011).
  217. Biswas, S. K. & Mantovani, A. Macrophage plasticity and interaction with lymphocyte subsets: cancer as a paradigm. *Nat. Immunol.* **11**, 889–96 (2010).
  218. Poh, A. R. & Ernst, M. Targeting Macrophages in Cancer: From Bench to Bedside. *Front. Oncol.* **8**, 49 (2018).
  219. Lee, C.-H. *et al.* Prognostic significance of macrophage infiltration in leiomyosarcomas. *Clin. Cancer Res.* **14**, 1423–30 (2008).
  220. Espinosa, I. *et al.* Coordinate expression of colony-stimulating factor-1 and colony-stimulating factor-1-related proteins is associated with poor prognosis in gynecological and nongynecological leiomyosarcoma. *Am. J. Pathol.* **174**, 2347–56 (2009).

221. Nabeshima, A. *et al.* Tumour-associated macrophages correlate with poor prognosis in myxoid liposarcoma and promote cell motility and invasion via the HB-EGF-EGFR-PI3K/Akt pathways. *Br. J. Cancer* **112**, 547–55 (2015).
222. Patwardhan, P. P. *et al.* Sustained inhibition of receptor tyrosine kinases and macrophage depletion by PLX3397 and rapamycin as a potential new approach for the treatment of MPNSTs. *Clin. Cancer Res.* **20**, 3146–58 (2014).
223. Liu, J. *et al.* Pre-Clinical Development of a Humanized Anti-CD47 Antibody with Anti-Cancer Therapeutic Potential. *PLoS One* **10**, e0137345 (2015).
224. Germano, G. *et al.* Role of Macrophage Targeting in the Antitumor Activity of Trabectedin. *Cancer Cell* **23**, 249–262 (2013).
225. Lutsiak, M. E. C. *et al.* Inhibition of CD4+25+ T regulatory cell function implicated in enhanced immune response by low-dose cyclophosphamide. *Blood* **105**, 2862–2868 (2005).
226. Newman, A. M. *et al.* Robust enumeration of cell subsets from tissue expression profiles. *Nat. Methods* **12**, 453–457 (2015).
227. Bertucci, F. *et al.* PDL1 expression is a poor-prognosis factor in soft-tissue sarcomas. *Oncoimmunology* **6**, 1–11 (2017).
228. Budczies, J. *et al.* PD-L1 (CD274) copy number gain, expression, and immune cell infiltration as candidate predictors for response to immune checkpoint inhibitors in soft-tissue sarcoma. *Oncoimmunology* **6**, e1279777 (2017).
229. Gross, E., Sunwoo, J. B. & Bui, J. D. Cancer Immunosurveillance and Immunoediting by Natural Killer Cells. *Cancer J.* **19**, 483–489 (2013).
230. Ellyard, J. I., Simson, L. & Parish, C. R. Th2-mediated anti-tumour immunity: friend or foe? *Tissue Antigens* **70**, 1–11 (2007).
231. Mariathasan, S. *et al.* TGF $\beta$  attenuates tumour response to PD-L1 blockade by contributing to exclusion of T cells. *Nature* **554**, 544–548

- (2018).
232. Bierie, B. & Moses, H. L. Transforming growth factor beta (TGF- $\beta$ ) and inflammation in cancer. *Cytokine Growth Factor Rev.* **21**, 49–59 (2010).
  233. Patnaik, A. *et al.* Phase I Study of Pembrolizumab (MK-3475; Anti-PD-1 Monoclonal Antibody) in Patients with Advanced Solid Tumors. *Clin. Cancer Res.* **21**, 4286–4293 (2015).
  234. George, S. *et al.* Loss of PTEN Is Associated with Resistance to Anti-PD-1 Checkpoint Blockade Therapy in Metastatic Uterine Leiomyosarcoma. *Immunity* **46**, 197–204 (2017).
  235. Ben-Ami, E. *et al.* Immunotherapy with single agent nivolumab for advanced leiomyosarcoma of the uterus: Results of a phase 2 study. *Cancer* (2017). doi:10.1002/cncr.30738
  236. Tawbi, H. A.-H. *et al.* Safety and efficacy of PD-1 blockade using pembrolizumab in patients with advanced soft tissue (STS) and bone sarcomas (BS): Results of SARC028--A multicenter phase II study. *ASCO Meet. Abstr.* **34**, 11006 (2016).
  237. Groisberg, R. *et al.* Characteristics and outcomes of patients with advanced sarcoma enrolled in early phase immunotherapy trials. *J. Immunother. Cancer* **5**, 100 (2017).
  238. D'Angelo, S. P. *et al.* Nivolumab with or without ipilimumab treatment for metastatic sarcoma (Alliance A091401): two open-label, non-comparative, randomised, phase 2 trials. *Lancet Oncol.* **19**, 416–426 (2018).
  239. Tawbi, H. A. *et al.* Pembrolizumab in advanced soft-tissue sarcoma and bone sarcoma (SARC028): a multicentre, two-cohort, single-arm, open-label, phase 2 trial. *Lancet. Oncol.* **18**, 1493–1501 (2017).
  240. Tseng, W. W. *et al.* Analysis of the Intratumoral Adaptive Immune Response in Well Differentiated and Dedifferentiated Retroperitoneal Liposarcoma. *Sarcoma* **2015**, 1–9 (2015).
  241. Maki, R. G. *et al.* A Pilot Study of Anti-CTLA4 Antibody Ipilimumab in Patients with Synovial Sarcoma. *Sarcoma* **2013**, 168145 (2013).

242. Lewin, J. *et al.* Response to Immune Checkpoint Inhibition in Two Patients with Alveolar Soft-Part Sarcoma. *Cancer Immunol. Res.* **6**, 1001–1007 (2018).
243. Conley, A. P. *et al.* Positive Tumor Response to Combined Checkpoint Inhibitors in a Patient With Refractory Alveolar Soft Part Sarcoma: A Case Report. *J. Glob. Oncol.* **4**, 1–6 (2018).
244. Salah, S. *et al.* Immunoprofiling in alveolar soft part sarcoma. *J. Clin. Oncol.* **35**, 11059–11059 (2017).
245. Jungbluth, A. A. *et al.* Monophasic and biphasic synovial sarcomas abundantly express cancer/testis antigen NY-ESO-1 but not MAGE-A1 or CT7. *Int. J. Cancer* **94**, 252–6 (2001).
246. Pollack, S. *et al.* NY-ESO-1 is a Ubiquitous Immunotherapeutic Target Antigen for Patients with Myxoid/ Round Cell Liposarcoma. *Cancer* **118**, 4564–4570 (2013).
247. Pollack, S. M. *et al.* Tetramer guided, cell sorter assisted production of clinical grade autologous NY-ESO-1 specific CD8(+) T cells. *J. Immunother. cancer* **2**, 36 (2014).
248. D'Angelo, S. P. *et al.* Antitumor Activity Associated with Prolonged Persistence of Adoptively Transferred NY-ESO-1 <sup>c259</sup> T Cells in Synovial Sarcoma. *Cancer Discov.* **8**, 944–957 (2018).
249. D'Angelo, S. P. *et al.* Pilot study of NY-ESO-1 <sup>c259</sup> T cells in advanced myxoid/round cell liposarcoma. *J. Clin. Oncol.* **36**, 3005–3005 (2018).
250. Robbins, P. F. *et al.* A pilot trial using lymphocytes genetically engineered with an NY-ESO-1-reactive T-cell receptor: long-term follow-up and correlates with response. *Clin. Cancer Res.* **21**, 1019–27 (2015).
251. Mackall, C. *et al.* Open label, non-randomized, multi-cohort pilot study of genetically engineered NY-ESO-1 specific NY-ESO-1 <sup>c259</sup> t in HLA-A2 + patients with synovial sarcoma (NCT01343043). *J. Clin. Oncol.* **35**, 3000–3000 (2017).
252. Pender, A., Jones, R. L. & Pollack, S. Optimising Cancer Vaccine Design

- in Sarcoma. *Cancers (Basel)*. **11**, (2018).
253. Lee, A., Huang, P., DeMatteo, R. P. & Pollack, S. M. Immunotherapy for Soft Tissue Sarcoma: Tomorrow Is Only a Day Away. *Am. Soc. Clin. Oncol. Educ. B.* **35**, 281–290 (2016).
254. Kyzas, P. A., Loizou, K. T. & Ioannidis, J. P. A. Selective Reporting Biases in Cancer Prognostic Factor Studies. *JNCI J. Natl. Cancer Inst.* **97**, 1043–1055 (2005).
255. Ioannidis, J. P. A. Why Most Discovered True Associations Are Inflated. *Epidemiology* **19**, 640–648 (2008).
256. Cooke, T., Reeves, J., Lanigan, A. & Stanton, P. HER2 as a prognostic and predictive marker for breast cancer. *Ann. Oncol. Off. J. Eur. Soc. Med. Oncol.* **12 Suppl 1**, S23-8 (2001).
257. Picca, A., Berzero, G., Di Stefano, A. L. & Sanson, M. The clinical use of IDH1 and IDH2 mutations in gliomas. *Expert Rev. Mol. Diagn.* **18**, 1041–1051 (2018).
258. Duffy, M. J., O'Donovan, N., McDermott, E. & Crown, J. Validated biomarkers: The key to precision treatment in patients with breast cancer. *The Breast* **29**, 192–201 (2016).
259. Gold, J. S. *et al.* Development and validation of a prognostic nomogram for recurrence-free survival after complete surgical resection of localised primary gastrointestinal stromal tumour: a retrospective analysis. *Lancet. Oncol.* **10**, 1045–52 (2009).
260. Taniguchi, M. *et al.* Effect of c-kit mutation on prognosis of gastrointestinal stromal tumors. *Cancer Res.* **59**, 4297–300 (1999).
261. Joensuu, H. *et al.* Effect of *KIT* and *PDGFRA* Mutations on Survival in Patients With Gastrointestinal Stromal Tumors Treated With Adjuvant Imatinib. *JAMA Oncol.* **3**, 602 (2017).
262. Frampton, G. M. *et al.* Development and validation of a clinical cancer genomic profiling test based on massively parallel DNA sequencing. *Nat. Biotechnol.* **31**, 1023–1031 (2013).

263. Schindelin, J. *et al.* Fiji: an open-source platform for biological-image analysis. *Nat. Methods* **9**, 676–682 (2012).
264. Wolak, M. E., Fairbairn, D. J. & Paulsen, Y. R. Guidelines for estimating repeatability. *Methods Ecol. Evol.* **3**, 129–137 (2012).
265. IARC. Detection of TP53 mutations by direct sequencing. 2010 Available at: [http://p53.iarc.fr/Download/TP53\\_DirectSequencing\\_IARC.pdf](http://p53.iarc.fr/Download/TP53_DirectSequencing_IARC.pdf). (Accessed: 15th December 2016)
266. Kumar, P., Henikoff, S. & Ng, P. C. Predicting the effects of coding non-synonymous variants on protein function using the SIFT algorithm. *Nat. Protoc.* **4**, 1073–1081 (2009).
267. Choi, Y., Sims, G. E., Murphy, S., Miller, J. R. & Chan, A. P. Predicting the functional effect of amino acid substitutions and indels. *PLoS One* **7**, e46688 (2012).
268. Adzhubei, I. A. *et al.* A method and server for predicting damaging missense mutations. *Nat. Methods* **7**, 248–249 (2010).
269. Shihab, H. A. *et al.* An integrative approach to predicting the functional effects of non-coding and coding sequence variation. *Bioinformatics* **31**, 1536–43 (2015).
270. Bouaoun, L. *et al.* TP53 Variations in Human Cancers: New Lessons from the IARC TP53 Database and Genomics Data. *Hum. Mutat.* **37**, 865–76 (2016).
271. Desmet, F.-O. *et al.* Human Splicing Finder: an online bioinformatics tool to predict splicing signals. *Nucleic Acids Res.* **37**, e67–e67 (2009).
272. Shabalin, A. A., Weigman, V. J., Perou, C. M. & Nobel, A. B. Finding large average submatrices in high dimensional data. *Ann. Appl. Stat.* **3**, 985–1012 (2009).
273. Wilkerson, M. D. & Hayes, D. N. ConsensusClusterPlus: a class discovery tool with confidence assessments and item tracking. *Bioinformatics* **26**, 1572–1573 (2010).

274. Tusher, V. G., Tibshirani, R. & Chu, G. Significance analysis of microarrays applied to the ionizing radiation response. *Proc. Natl. Acad. Sci. U. S. A.* **98**, 5116–21 (2001).
275. Huang, D. W., Sherman, B. T. & Lempicki, R. A. Systematic and integrative analysis of large gene lists using DAVID bioinformatics resources. *Nat. Protoc.* **4**, 44–57 (2008).
276. Huang, D. W., Sherman, B. T. & Lempicki, R. A. Bioinformatics enrichment tools: paths toward the comprehensive functional analysis of large gene lists. *Nucleic Acids Res.* **37**, 1–13 (2009).
277. Tibshirani, R., Hastie, T., Narasimhan, B. & Chu, G. Diagnosis of multiple cancer types by shrunken centroids of gene expression. *Proc. Natl. Acad. Sci.* **99**, 6567–6572 (2002).
278. Parker, J. S. *et al.* Supervised Risk Predictor of Breast Cancer Based on Intrinsic Subtypes. *J. Clin. Oncol.* **27**, 1160–1167 (2009).
279. Benito, M. *et al.* Adjustment of systematic microarray data biases. *Bioinformatics* **20**, 105–14 (2004).
280. Kononen, J. *et al.* Tissue microarrays for high-throughput molecular profiling of tumor specimens. *Nat. Med.* **4**, 844–7 (1998).
281. Bedard, P. L., Hansen, A. R., Ratain, M. J. & Siu, L. L. Tumour heterogeneity in the clinic. *Nature* **501**, 355–364 (2013).
282. Camp, R. L., Neumeister, V. & Rimm, D. L. A decade of tissue microarrays: Progress in the discovery and validation of cancer biomarkers. *J. Clin. Oncol.* **26**, 5630–5637 (2008).
283. Kallioniemi, O. P., Wagner, U., Kononen, J. & Sauter, G. Tissue microarray technology for high-throughput molecular profiling of cancer. *Hum. Mol. Genet.* **10**, 657–662 (2001).
284. Camp, R. L., Charette, L. a & Rimm, D. L. Validation of tissue microarray technology in breast carcinoma. *Lab. Invest.* **80**, 1943–1949 (2000).
285. Rubin, M. A., Dunn, R., Strawderman, M. & Pienta, K. J. Tissue

- microarray sampling strategy for prostate cancer biomarker analysis. *Am. J. Surg. Pathol.* **26**, 312–9 (2002).
286. Kaur, H. B. *et al.* Association of tumor-infiltrating T-cell density with molecular subtype, racial ancestry and clinical outcomes in prostate cancer. *Mod. Pathol.* (2018). doi:10.1038/s41379-018-0083-x
287. Baras, A. S. *et al.* The ratio of CD8 to Treg tumor-infiltrating lymphocytes is associated with response to cisplatin-based neoadjuvant chemotherapy in patients with muscle invasive urothelial carcinoma of the bladder. *Oncoimmunology* **5**, e1134412 (2016).
288. Wei, J. S. *et al.* Clinically Relevant Cytotoxic Immune Cell Signatures and Clonal Expansion of T Cell Receptors in High-risk MYCN -not-amplified Human Neuroblastoma. *Clin. Cancer Res.* clincanres.0599.2018 (2018). doi:10.1158/1078-0432.CCR-18-0599
289. Kluger, H. M. *et al.* Characterization of PD-L1 Expression and Associated T-cell Infiltrates in Metastatic Melanoma Samples from Variable Anatomic Sites. *Clin. Cancer Res.* **21**, 3052–3060 (2015).
290. Schalper, K. A. *et al.* Objective Measurement and Clinical Significance of TILs in Non–Small Cell Lung Cancer. *JNCI J Natl Cancer Inst* **107**, (2015).
291. Jiménez-Sánchez, A. *et al.* Heterogeneous Tumor-Immune Microenvironments among Differentially Growing Metastases in an Ovarian Cancer Patient. *Cell* **170**, 927-938.e20 (2017).
292. Shi, L. *et al.* Multi-omics study revealing the complexity and spatial heterogeneity of tumor-infiltrating lymphocytes in primary liver carcinoma. *Oncotarget* **8**, 34844–34857 (2017).
293. Li, M. *et al.* Heterogeneity of PD-L1 expression in primary tumors and paired lymph node metastases of triple negative breast cancer. *BMC Cancer* **18**, 1–9 (2018).
294. Rehman, J. A. *et al.* Quantitative and pathologist-read comparison of the heterogeneity of programmed death-ligand 1 (PD-L1) expression in non-

- small cell lung cancer. *Mod. Pathol.* **30**, 340–349 (2017).
295. Mlecnik, B. *et al.* Comprehensive Intrametastatic Immune Quantification and Major Impact of Immunoscore on Survival. *JNCI J. Natl. Cancer Inst.* **110**, 97–108 (2018).
296. Zlobec, I., Koelzer, V. H., Dawson, H., Perren, A. & Lugli, A. Next-generation tissue microarray (ngTMA) increases the quality of biomarker studies: an example using CD3, CD8, and CD45RO in the tumor microenvironment of six different solid tumor types. *J. Transl. Med.* **11**, 104 (2013).
297. Botti, G., Scognamiglio, G. & Cantile, M. PD-L1 immunohistochemical detection in tumor cells and tumor microenvironment: Main considerations on the use of tissue micro arrays. *Int. J. Mol. Sci.* **17**, 8–10 (2016).
298. Khan, A. M. & Yuan, Y. Biopsy variability of lymphocytic infiltration in breast cancer subtypes and the ImmunoSkew score. *Sci. Rep.* **6**, 2–11 (2016).
299. Davoli, T., Uno, H., Wooten, E. C. & Elledge, S. J. Tumor aneuploidy correlates with markers of immune evasion and with reduced response to immunotherapy. *Science (80-. )*. **355**, eaaf8399 (2017).
300. Rao, U. N. M. *et al.* Presence of tumor-infiltrating lymphocytes and a dominant nodule within primary melanoma are prognostic factors for relapse-free survival of patients with thick (t4) primary melanoma: pathologic analysis of the e1690 and e1694 intergroup trials. *Am. J. Clin. Pathol.* **133**, 646–653 (2010).
301. Geng, Y. *et al.* Prognostic Role of Tumor-Infiltrating Lymphocytes in Lung Cancer: a Meta-Analysis. *Cell. Physiol. Biochem.* **37**, 1560–1571 (2015).
302. Hendry, S. *et al.* Assessing Tumor-Infiltrating Lymphocytes in Solid Tumors. *Adv. Anat. Pathol.* **24**, 311–335 (2017).
303. Lewis, J. J., Leung, D., Woodruff, J. M. & Brennan, M. F. Retroperitoneal soft-tissue sarcoma: analysis of 500 patients treated and followed at a single institution. *Ann. Surg.* **228**, 355–65 (1998).

304. Chen, D. S. *et al.* Oncology Meets Immunology: The Cancer-Immunity Cycle. *Immunity* **39**, 1–10 (2013).
305. Büttner, R. *et al.* Programmed Death-Ligand 1 Immunohistochemistry Testing: A Review of Analytical Assays and Clinical Implementation in Non–Small-Cell Lung Cancer. *J. Clin. Oncol.* **35**, 3867–3876 (2017).
306. Lu, S. *et al.* Comparison of Biomarker Modalities for Predicting Response to PD-1/PD-L1 Checkpoint Blockade: A Systematic Review and Meta-analysis. *JAMA Oncol.* **5**, 1195 (2019).
307. Budczies, J. *et al.* Cutoff Finder: A Comprehensive and Straightforward Web Application Enabling Rapid Biomarker Cutoff Optimization. *PLoS One* **7**, e51862 (2012).
308. Bertucci, F. *et al.* Gene Expression Profiling of Solitary Fibrous Tumors. *PLoS One* **8**, e64497 (2013).
309. Segal, N. H. *et al.* Classification and subtype prediction of adult soft tissue sarcoma by functional genomics. *Am. J. Pathol.* **163**, 691–700 (2003).
310. Nielsen, T. O. *et al.* Molecular characterisation of soft tissue tumours: a gene expression study. *Lancet* **359**, 1301–1307 (2002).
311. Tap, W. D. *et al.* Doxorubicin plus evofosfamide versus doxorubicin alone in locally advanced, unresectable or metastatic soft-tissue sarcoma (TH CR-406/SARC021): an international, multicentre, open-label, randomised phase 3 trial. *Lancet. Oncol.* **18**, 1089–1103 (2017).
312. Mir, O. *et al.* Safety and efficacy of regorafenib in patients with advanced soft tissue sarcoma (REGOSARC): a randomised, double-blind, placebo-controlled, phase 2 trial. *Lancet Oncol.* **17**, 1732–1742 (2016).
313. Demoulin, J.-B. & Essaghir, A. PDGF receptor signaling networks in normal and cancer cells. *Cytokine Growth Factor Rev.* **25**, 273–283 (2014).
314. Katoh, M. & Nakagama, H. FGF Receptors: Cancer Biology and Therapeutics. *Med. Res. Rev.* **34**, 280–300 (2014).

315. Yao, Z. *et al.* TGF-beta IL-6 axis mediates selective and adaptive mechanisms of resistance to molecular targeted therapy in lung cancer. *Proc. Natl. Acad. Sci. U. S. A.* **107**, 15535–40 (2010).
316. Kim, S. M. *et al.* Activation of IL-6R/JAK1/STAT3 Signaling Induces De Novo Resistance to Irreversible EGFR Inhibitors in Non-Small Cell Lung Cancer with T790M Resistance Mutation. *Mol. Cancer Ther.* **11**, 2254–2264 (2012).
317. Liu, Y.-N. *et al.* IL-8 confers resistance to EGFR inhibitors by inducing stem cell properties in lung cancer. *Oncotarget* **6**, 10415–31 (2015).
318. Fernando, R. I. *et al.* IL-8 signaling is involved in resistance of lung carcinoma cells to erlotinib. *Oncotarget* **7**, 42031–42044 (2016).
319. Johnson, D. E., O’Keefe, R. A. & Grandis, J. R. Targeting the IL-6/JAK/STAT3 signalling axis in cancer. *Nat. Rev. Clin. Oncol.* **15**, 234–248 (2018).
320. Waugh, D. J. J. & Wilson, C. The Interleukin-8 Pathway in Cancer. *Clin. Cancer Res.* **14**, 6735–6741 (2008).
321. Schott, A. F. *et al.* Phase Ib Pilot Study to Evaluate Reparixin in Combination with Weekly Paclitaxel in Patients with HER-2–Negative Metastatic Breast Cancer. *Clin. Cancer Res.* **23**, 5358–5365 (2017).
322. Collins, J. M. *et al.* Phase I trial of BMS-986253, an anti-IL-8 monoclonal antibody, in patients with metastatic or unresectable solid tumors. *J. Clin. Oncol.* **36**, 3091–3091 (2018).
323. Rossi, J.-F., Lu, Z.-Y., Jourdan, M. & Klein, B. Interleukin-6 as a Therapeutic Target. *Clin. Cancer Res.* **21**, 1248–1257 (2015).
324. Pal, S. K. *et al.* Pazopanib as third line therapy for metastatic renal cell carcinoma: Clinical efficacy and temporal analysis of cytokine profile. *J. Urol.* **193**, 1114–1121 (2015).
325. Necchi, A. *et al.* Analysis of plasma cytokines and angiogenic factors in patients with pretreated urothelial cancer receiving Pazopanib: The role of circulating interleukin-8 to enhance the prognostic accuracy. *Br. J. Cancer*

- 110**, 26–33 (2014).
326. Meyn, R. E., Munshi, A., Haymach, J. V., Milas, L. & Ang, K. K. Receptor signaling as a regulatory mechanism of DNA repair. *Radiother. Oncol.* **92**, 316–322 (2009).
327. Dent, P., Yacoub, A., Fisher, P. B., Hagan, M. P. & Grant, S. MAPK pathways in radiation responses. *Oncogene* **22**, 5885–5896 (2003).
328. Hayakawa, J., Depatie, C., Ohmichi, M. & Mercola, D. The activation of c-Jun NH2-terminal kinase (JNK) by DNA-damaging agents serves to promote drug resistance via activating transcription factor 2 (ATF2)-dependent enhanced DNA repair. *J. Biol. Chem.* **278**, 20582–92 (2003).
329. Martin, L. P., Hamilton, T. C. & Schilder, R. J. Platinum Resistance: The Role of DNA Repair Pathways. *Clin. Cancer Res.* **14**, 1291–1295 (2008).
330. Christmann, M. & Kaina, B. MGMT—a critical DNA repair gene target for chemotherapy resistance. *DNA Repair Cancer Ther.* 55–82 (2016). doi:10.1016/B978-0-12-803582-5.00002-4
331. Rosell, R. *et al.* Nucleotide Excision Repair Pathways Involved in Cisplatin Resistance in Non-Small-Cell Lung Cancer. *Cancer Control* **10**, 297–305 (2003).
332. Bouwman, P. & Jonkers, J. The effects of deregulated DNA damage signalling on cancer chemotherapy response and resistance. *Nat. Rev. Cancer* **12**, 587–98 (2012).
333. Kaplan, E. & Gündüz, U. Expression analysis of TOP2A, MSH2 and MLH1 genes in MCF7 cells at different levels of etoposide resistance. *Biomed. Pharmacother.* **66**, 29–35 (2012).
334. Haas, R. L. M. *et al.* A phase I study on the combination of neoadjuvant radiotherapy plus pazopanib in patients with locally advanced soft tissue sarcoma of the extremities. *Acta Oncol. (Madr)*. **54**, 1195–1201 (2015).
335. Dabney, A. R. ClaNC: point-and-click software for classifying microarrays to nearest centroids. *Bioinformatics* **22**, 122–123 (2006).

336. Simon, R. M., Paik, S. & Hayes, D. F. Use of Archived Specimens in Evaluation of Prognostic and Predictive Biomarkers. *JNCI J. Natl. Cancer Inst.* **101**, 1446–1452 (2009).
337. Le Guellec, S. *et al.* Validation of the Complexity INdex in SARComas prognostic signature on formalin-fixed, paraffin-embedded, soft-tissue sarcomas. *Ann. Oncol.* **29**, 1828–1835 (2018).

## **Appendix 1 – PROSPECTUS study protocol**

Title: **PROgnoStic and PrEdiCTive ImmUnoprofiling of Sarcomas**

Short title: **PROSPECTUS**

Chief Investigator:	Dr Robin L Jones, Consultant Oncologist The Royal Marsden NHS Foundation Trust
Principal Investigator:	Dr Robin L Jones, Consultant Oncologist
Co-investigators:	Professor Ian Judson, Royal Marsden NHS Foundation Trust Dr Seth Pollack, Fred Hutchinson Cancer Research Center Dr Paul Huang, The Institute of Cancer Research Dr Khin Thway, Royal Marsden NHS Foundation Trust Prof Cyril Fisher, Royal Marsden NHS Foundation Trust Dr Aisha Miah, Royal Marsden NHS Foundation Trust Dr Charlotte Benson, Royal Marsden NHS Foundation Trust Dr Winette van der Graaf, Royal Marsden NHS Foundation Trust Dr Shane Zaidi, Royal Marsden NHS Foundation Trust Dr Alexander Lee, Royal Marsden NHS Foundation Trust
Collaborators	Professor Eva Wardelmann, University Hospital Munster Professor Adrienne Flanagan, University College London
Statistician:	Bernice Asare

### **Sponsor:**

The Royal Marsden NHS Foundation Trust

### **Address:**

The Royal Marsden NHS Foundation Trust, Fulham Road, London SW3 6JJ  
The Institute of Cancer Research, 123 Old Brompton Road, London SW7 3RP

### **Management:**

Clinical Research & Development, The Royal Marsden NHS Foundation Trust, Downs Road,  
Sutton, Surrey SM2 5PT

### **Site Address:**

The Institute of Cancer Research, 15 Cotswold Road, Sutton, Surrey SM2 5NG  
The Royal Marsden NHS Foundation Trust, Downs Road, Sutton, Surrey SM2 5PT

<b>Protocol Reference:</b>	CCR4371 - PROSPECTUS
<b>Version Number &amp; Date:</b>	V3.1 21/04/2018
<b>Effective Date:</b>	01//05/2018
<b>Superseded Version Number &amp; Date (If applicable)</b>	V2.2 14/07/2016

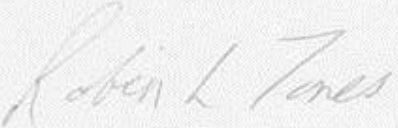
**PROTOCOL SIGNATURE PAGE**

**Study title:** Prognostic and predictive immunoprofiling of Sarcomas (PROSPECTUS)

**Protocol version:** 3.1

**Version date:** 21/04/2018

Approved by Chief Investigator:



---

(Dr Robin Jones)

---

(Dr Robin Jones)

Date:

## **Table of Contents**

1. STUDY OBJECTIVES	3
2. BACKGROUND	4
3. RATIONALE	7
4. STUDY DESIGN -	
4.1. Overview	9
4.2. Patient identification and screening	10
4.3. Patient accrual and study duration	10
4.4. Study Sites	10
5. ELIGIBILITY	
5.1. Inclusion criteria	12
5.2. Exclusion criteria	12
6. STUDY PROCEDURES	
6.1 Patient and sample identification	13
6.2 Collection and storage of archival tumour material	13
6.3 Sample processing	13
6.4 Sample analysis	13
6.5 Data analysis	14
7. STATISTICAL CONSIDERATIONS	
7.1 Statistical endpoints	15
7.2 Analysis section	15
7.3 Sample size	17
8. STUDY ORGANISATION	
8.1 Regulatory & ethics committee approval	18
8.2 Informed consent	18
8.3 Patient confidentiality	18
8.4 Data Handling and record keeping	18
8.5 Financing, indemnity and insurance	18
	321

8.6 Publication policy 18

9. REFERENCES 19

## **1: STUDY OBJECTIVES**

1. To establish the rate and level of expression of PD-1 and PD-L1, two recognised protein markers of tumour-immunity interaction well characterised in other cancer types, in soft tissue sarcomas, and to investigate any possible association between marker expression and prognosis.

2. To establish an 'immunoscore' - a measure of the different components of the immune system that can be found in the microscopic tumour environment - that is of prognostic value in primary and advanced soft tissue sarcoma.

3. To isolate DNA, RNA and protein from tissue samples to explore at genomic, gene expression and protein expression level, markers that add prognostic value to a STS Immunoscore

4. To investigate the possible impact of intra-tumoral heterogeneity on the validity of the use of tissue microarrays in the study of the immune microenvironment of STS

5. To investigate the differences in tumour immune microenvironment between paired tissue samples from primary and metastatic sites of STS, and from pre- and post-cytotoxic and radiotherapy samples.

## **2: BACKGROUND**

Soft tissue sarcomas (STS) are a rare and heterogenous group of malignancies arising from mesenchymal tissue. Accounting for around 1% of all adult cancers, STS represents a grouping of over 80 different diagnoses which are variably defined by morphological, genetic or molecular characteristics. STS often presents with localised disease, for which the mainstay of radical treatment is surgery. Despite the addition of radiotherapy and cytotoxic therapies as adjuvant or neoadjuvant modalities, recurrence is frequent and associated with generally poor prognosis, with a median survival consistently reported around 12 months. The current standard management for advanced sarcoma is cytotoxic chemotherapy with doxorubicin and/or ifosfamide and these treatments have a response rate of about 15-35%, which has not increased in the last 15 years. The identification of specific molecular abnormalities, such as mutations of KIT in GIST and TSC in PEComa, have led to the successful deployment of targeted therapies in some disease subtypes, but the absence of identified predictive biomarkers in the large majority of advanced STS has resulted in the significant limitation of successful development of novel treatments<sup>1–4</sup>

The concept of therapeutically exploiting cancers potential vulnerability to attack by the host's immune system has existed for over 100 years. A wide variety of immunotherapy techniques, including high dose cytokine therapy, vaccines derived from tumour-specific material, and the adoptive transfer of autologous immune cells primed against tumour, have been employed in many tumour types, including some STS, with generally limited success<sup>5</sup>. More recently, a number of therapeutic monoclonal antibodies that produce targeted inhibition of negative regulators of T lymphocyte anticancer response – the so-called immune checkpoint inhibitors – have produced previously unseen rates of success in clinical trials across a range of advanced solid tumours, and are now approved for the treatment of metastatic melanoma and NSCLC. There is currently little clinical data to inform the potential efficacy of these new agents in STS but, given the broad efficacy of these novel immunotherapeutics across tumour types, it is hoped that STS subtypes can be identified that will stand to benefit from the current wave of preclinical and clinical research into the therapeutic anticancer immune response.

Published preclinical and clinical data support the notion of an active anti-tumour immune response in at least some sarcoma subtypes. The high levels of expression of cancer testis antigens (CTAs) in synovial sarcomas (SS) and liposarcomas present a tumour-specific antigenic target, as do the novel proteins that result from the pathognomonic chromosomal translocations found in SS, Ewing sarcoma and rhabdomyosarcoma, amongst others. The high mutational burden of other sarcoma subtypes raises the possibility of the creation of large number of cancer neoantigens. The use of CTA or fusion

protein-targeting adoptive lymphocyte therapy has been associated with incidences of dramatic clinical responses in sarcoma patients<sup>6</sup>.

It has been demonstrated in a number of tumours that the immune microenvironment, i.e. the nature and extent of the infiltrating lymphocytes and myeloid cells, is of prognostic significance. This was first observed more than 20 years ago in melanoma patients and has now been recognized in multiple cancer types including pancreatic cancer, ovarian cancer, lung cancer, breast cancer and others<sup>7–11</sup>. The presence of large numbers of infiltrating lymphocytes in pre-treatment samples has been shown to predict for response to neoadjuvant chemotherapy in triple-negative breast cancer and, increasingly, the tumour immune microenvironment is being scrutinised as a potential source of other predictive biomarkers, particularly for newer immunotherapies<sup>12</sup>. Prominent amongst these putative immune biomarkers is the expression of Programmed Death Ligand 1 (PD-L1) within the tumour. PD-L1 is one of two ligands for Programmed Cell Death Protein (PD-1), a cell surface receptor protein that results in downregulation of cytotoxic activation of CD8<sup>+</sup> T lymphocytes present in the tumour microenvironment.. The inhibition of this receptor-ligand interaction with therapeutic monoclonal antibodies has produced dramatic clinical benefit in a number of tumour types. The level of PD-L1 expression has been heavily investigated as a potential predictive biomarker for benefit from these drugs. However the predictive performance of many assays has been limited, with heterogeneous methodologies in terms of antibodies used, positive/negative staining cut-offs and which TME compartment is scored all likely contributing to conflicting reports of the application of PD-L1 as a biomarker.

A prognostic 'Immunoscore' has been proposed by researchers who have demonstrated, via highly reproducible IHC techniques and digital quantitative imaging methodologies used across hundreds of clinical FFPE tumour samples, a score derived from numbers of CD3<sup>+</sup> and CD8<sup>+</sup> lymphocyte infiltrates at the tumour core and invasive margin of localised colorectal cancers. In a 415 patient series, the Immunoscore was shown to outperform conventional TNM staging in the prediction of disease-free survival, a finding confirmed by validation against two large external datasets<sup>13</sup>. An international effort is on-going to validate the "immunoscore" in thousands of patients with respect to its reproducibility, prognostic value and predictive value for established treatments and novel immunotherapies<sup>14</sup>. The establishment of a widely accepted "immunoscore" in colorectal cancer with prognostic and predictive value would be a milestone for both oncology and immunotherapy.

The prognostic significance of the tumour immune microenvironment in STS has been investigated in several studies in recent years. Sorbye et al reported that, from a cohort of 249 patients with non-GIST primary STS, high numbers of infiltrating CD20<sup>+</sup> lymphocytes was an independent prognostic

indicator for patients with a wide resection margin<sup>15</sup>. A follow-up study into the same cohort found that conversely, high CD20+ lymphocytes in the peritumoral capsule was an independent predictor of worse disease-specific survival<sup>16</sup>. Increased levels of intratumoral CD8+ T lymphocytes have been associated with improved outcome in series of Ewing sarcoma and cutaneous angiosarcoma, whilst intratumoral tertiary lymphoid aggregates was associated with worse outcomes in a small series of well-differentiated and dedifferentiated liposarcoma<sup>17–19</sup>. The presence of intratumoral macrophages exhibiting an anti-immunity 'M2' polarization phenotype was associated with worse outcomes in non-gynaecological leiomyosarcoma and myxoid liposarcomas<sup>20,21</sup>. Kim et al reported a series of 105 non-GIST primary STS where high levels of infiltrating PD-1 expressing lymphocytes and intratumoral PD-L1 expression both were associated with shorter event-free and overall survival.<sup>22</sup> Conversely, a later series of 50 patients with either primary or metastatic STS found no association between outcome and PD-1 or PD-L1, whilst survival analysis indicated that lower levels of lymphocyte infiltration were associated with better outcomes.<sup>23</sup>

If a fully validated Immunoscore is adopted for clinical prognostication of early colorectal cancer, it is unlikely that such a method would be readily transferable to other disease types. There remains much to be understood as to the factors that govern tumour immunogenicity and it is highly probable that variation in anti-tumour immune response will be associated with differences in tissue of origin, specific molecular signatures and baseline host factors. Existing data suggests a degree of heterogeneity in terms of different immunogenicity, immune evasion mechanisms and levels of immune response within that mirrors the extent of clinical, histopathological and molecular variety. As such, much more work is required to characterise the tumour immune microenvironment of STS subtypes.

The cellular component of the tumour immune microenvironment can be partly appreciated by bright light microscopy, where the experienced histopathologist can discriminate between the characteristic nuclear morphology of infiltrating lymphocytes and, to some extent, polymorphic leukocytes against tumour and native tissue cells. This approach cannot however discriminate between the broad functional differences of leukocyte subtype. Immunohistochemical analysis of fixed tissue sections is a widely available, affordable and well-validated method for characterising immune cells of differing functional subtype via the qualitative and quantitative assessment of characteristic protein expression signatures. The use of tissue microarrays (TMA) is a scalable and cost-effective method that allows high throughput analysis of protein expression by immunohistochemistry across a large number of individual tissue samples. The validity of tissue sampling for TMA construction compared to full tissue

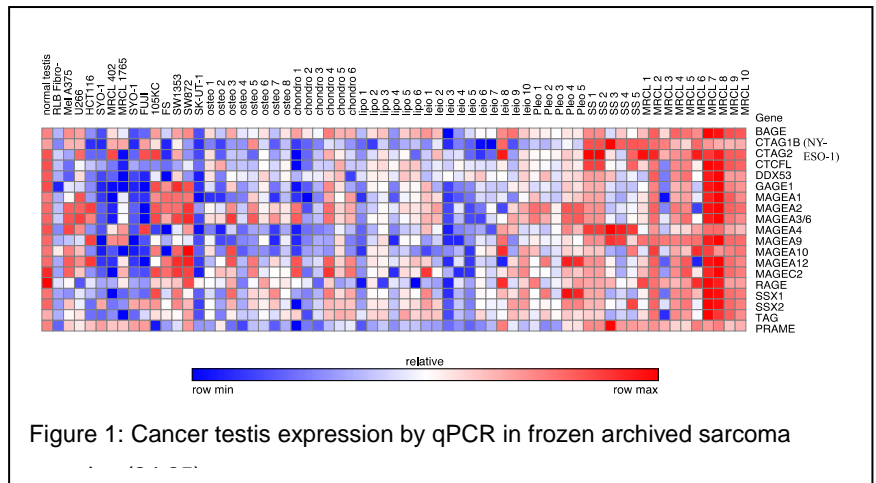
mount sections has been established for the study of molecular phenotype of tumour cells in a range of cancer types.

Whilst TMAs have been widely used in studies of tumour microenvironment, there has been little work to demonstrate that the sampling of tissue cores typically 0.6-2.0mm in diameter can be representative of immune infiltrates that can exhibit significant intra-tumoral spatial heterogeneity. Studies in an increasing number of tumour types have demonstrated the importance of where in the tumour the immune microenvironment is examined, in terms of macroscopic position (e.g. core vs. invasive margin) and microscopic tumoral compartment (e.g. intra-tumoral vs stromal infiltrate). Gene expression studies on mRNA extracted from whole tissue samples take into account heterogeneity by encompassing a more representative tissue area, but results in the loss of resolution in terms of defining which genes are expressed which component of the tumour immune microenvironment, and in terms of the specific spatial relationships between component cells which has been shown to provide additional prognostic information. Additionally, the cost of such technologies as well as the challenges of extracting sufficient quantities of non-degraded RNA from FFPE samples makes it likely that IHC techniques will be the mainstay of any widely applicable clinical immune scores.

Whilst an IHC-based approach to immune profiling as proven to be clinically useful in other cancer contexts, the addition of different molecular analysis modalities offers the opportunity to produce complementary data that can be integrated with IHC to produce a more detailed picture of the complex biology of a tumour's immune microenvironment. Modern genomic sequencing, gene expression analysis and proteomic techniques represent high resolution, multiplex approaches for the in-depth characterisation of both host and tumour biology in the TME. Exploratory studies that are able to identify molecular correlates with the cellular TME are likely to offer insight into the mechanisms that link the TME with cancer phenotype and provide valuable information for the development of immunotherapies in advanced STS.

### 3: RATIONALE

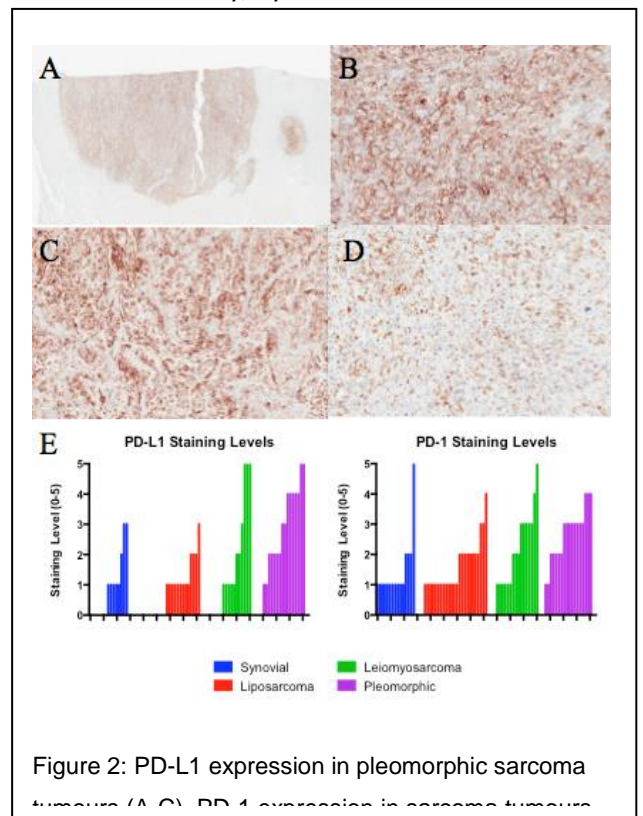
The Royal Marsden sarcoma tissue archive represents one of the largest STS banks in the world, containing samples from approximately 700 unique patients with corresponding clinical details. This represents a valuable resource for the investigation of STS immune microenvironment in



terms of sufficient patient numbers to provide the statistical power for findings that can be generalised in a subtype-specific fashion. Such findings will add substantially to the evidence of STS immunity and provide a basis for patient stratification in clinical trials of immunotherapies and other treatment modalities.

Sarcomas are a highly heterogeneous group of malignancies and our data suggests that different sarcoma subtypes have different immunogenicities, immune evasion mechanisms and levels of immune response. For example, certain sarcomas are highly mutated and are, therefore, quite likely to express numerous inflammatory neoantigens while other sarcomas may be driven by a single translocation and, therefore, have few immunogenic mutations. Conversely, synovial sarcoma and myxoid round cell liposarcoma, both translocation-associated sarcoma subtypes with relatively low mutational burden, have been shown to express immunogenic self antigens such as cancer testis antigens at high levels<sup>24,25</sup>. (Fig 1.)

There is also variability in the mechanisms of immune evasion employed by individual sarcoma subtypes. In a small pilot study, we observed that detectable PD-L1 was seen in thirteen (48%) liposarcoma tumours, 11 (58%) leiomyosarcoma, 16 (80%) pleomorphic sarcomas and 7 (47%) synovial sarcoma (10). PD-1 expressing lymphocytes were also seen in a majority of tumours in each subtype, 24 (89%) in liposarcoma, 18 (90%) pleomorphic sarcoma, 16 (84%) leiomyosarcoma, 15



(100%) synovial sarcoma (10). However, pleomorphic sarcomas had higher levels of PD-L1 ( $p = 0.03$ ) and PD-1 ( $p = 0.05$ ) (Fig. 2).

The purpose of this study is to expand on this work and add to the limited clinical data on the prognostic significance of PD-1 and PD-L1 expression within sarcoma FFPE tumour samples drawn from the RMH sarcoma tissue bank. These results will be combined with those from similar studies performed at the Royal National Orthopaedic Hospital and the university of Munster.

We also wish to develop a sarcoma 'immunoscore', based on statistical correlation of IHC-based assessment of the tumour immune microenvironment of samples in the RMH tissue bank and clinical outcome. We would then validate this 'immunoscore' against large validation cohorts from RNOH, the University of Munster and the University of Seattle.

In order to validate a sampling methodology for use across the entire sample population, a pilot study will be performed to examine the degree of heterogeneity in the tumour immune microenvironment between spatially separate areas of the same tumour. Additionally, the validity of taking sample cores for TMAs will be investigated by comparison of immune microenvironment as assessed by TMA or corresponding whole tissue mount. This pilot study will focus on patients for whom surgical specimen samples are available from a primary tumour excised in the absence of demonstrable metastatic disease – this measure is to ensure the availability of two or more tumour-containing FFPE blocks representing discrete areas of the same tumour. Synovial sarcoma and leiomyosarcoma will be used in the pilot study as exemplars of translocation-associated and mutationally complex STS subtypes, respectively – both subtypes are sufficiently common to ensure availability of an adequate number of cases within the tissue bank.

DNA, RNA and protein will be extracted from a representative sample of FFPE blocks and be used to investigate exploratory endpoints that will investigate the relationship between the tumour immune microenvironment. mRNA extracted from tumour immune microenvironment will be used to assess expression levels of immune-related genes to provide a wider reaching overview of the immune milieu of individual tumours and provide more detailed understanding of inter-tumour variability in immune context and pro- or anti-tumour immune response. Extracted protein will be used as input for unbiased quantitative mass spectrometry-based assessment of immune-related proteins and other potential correlates with IHC, genomic and mRNA-based immune readouts.

## 4: STUDY DESIGN

### **4.1: Overview**

This is an observational retrospective case series study of patients treated for soft tissue sarcoma in the Royal Marsden. Assessment of archived diagnostic FFPE sample by immunohistochemistry will be used to investigate the rate of expression of the putative immune biomarkers PD-1 and PD-L1 within the tumour immune microenvironment across a range of STS subtypes. PD-1 and PD-L1 expression will be correlated with clinical patient outcome to investigate any prognostic association. The same samples will also be assessed for IHC markers of different component cells of the immune infiltrate (infiltrating T cell subsets [CD3, CD4, CD8, FoxP3], natural killer cells [CD56], B Cells [CD20], Dendritic Cells [CD11c] and type I/II macrophages [CD68, CD206, CD163]), with the relative expression of different cell types used to explore by multivariate analysis a possible prognostic 'Immunoscore'.

A pilot study to validate tissue sampling from blocks will be performed to provide insight into the possible effect of spatial heterogeneity in immune infiltrates in STS and to inform methodology for the main study. A randomly selected cohort of 30 surgical specimens taken from two STS subtypes will be examined to provide insight into the degree of heterogeneity of immune infiltrates between different areas of the same tumour. The degree of observed heterogeneity will inform the method of sampling tumour cores for the construction of TMAs for the immune profiling of the full 700 patient 'training set', with a view to designing a methodology that is reproducible in a 'real world' setting that can incorporate percutaneous core biopsy samples.

A training set of 700 sarcoma patients will be used in the initial analysis including over 100 samples for each of the most common sarcoma subtypes and a combined pool of 200 patients with more rare subtypes. A nanozoomer 2.0-HT microscopic scanner as well as automated quantification software (HistoQuest, ImageJ) will be used for standardized digital quantification of IHC staining. A multivariate Cox model will be created incorporating the quantitative data from all of the IHC markers and subsequently eliminating markers without significant independent predictive value. This analysis will be performed for both STS as a disease group and also within individual sarcoma subtypes. If there is a single "immunoscore" with significance in most sarcoma subtypes this would be preferable to having multiple scoring systems (even if there are certain markers with redundancy for individual sarcoma subtypes) as this would have wider applicability

Once a scoring system with prognostic value has been developed, it would be tested on a separate validation set of 700 randomly selected STS patients, obtained from the data bases of the Royal National Orthopedic Hospital, the University of Münster and the University of Washington, both to

validate its prognostic significance but also to test its ability to predict response to individual cytotoxic chemotherapies as well as the small molecule VEGFR inhibitor pazopanib. Individual IHC results will also be tested in this analysis as there could be an individual marker not prognostic for outcome, but predictive for response to a particular agent.

Extracted DNA, RNA and protein will be collected from representative FFPE samples to provide material for substudies with exploratory endpoints that will provide complementary molecular information on the sarcoma immune microenvironment. These substudies will involve:

- i) mRNA analysis of expression of a panel of immune-related genes in the microenvironment
- ii) quantitative mass spectrometry-based proteomic profiling of immune-related proteins

A follow on study would aim to utilize a novel mass spectrometry platform for characterisation of the phosphoproteome to map activated signalling pathways in sarcoma and to identify a potential predictive signature of response to systemic therapy (funding for this study is not requested in this proposal).

#### **4.2: Patient identification and study duration**

Patients will be identified from the prospectively maintained RMH sarcoma patient database. Cross-referencing of this patient list with histopathology archive records will identify a cohort of patients treated at RMH for STS for whom there are accessible FFPE tumour samples. Patients will then be divided into one or several groups stratified on the basis of diagnosis and tissue availability. These groupings will include:

- Histological diagnosis
- Stage of disease at time of sample extraction
- Availability of paired primary/metastasis tissue samples
- Availability of paired pre/post-treatment tissue samples

Patient and sample details will be held on a specifically designed, secure database to allow for identification of specific cohorts.

It is anticipated that tissue samples and clinical details are available for approximately 700 patients. As patient sub-cohorts based on the above groupings are identified, sample processing and analysis will be batched. The aim is to complete collection of data on PD-1/PD-L1 expression and Immunoscore in all relevant subcohorts within 12 months, with analysis of validation sets occurring between months 12-24.

### **4.3: Study sites**

All patient data and FFPE samples for the primary cohort will be identified and processed with the Royal Marsden Hospital. Data collection and analysis will occur between the Royal Marsden and Institute of Cancer Research. Validation cohorts will be identified, processed and analysed at Royal National Orthopaedic Hospital, University of Munster and University of Washington.

## 5: ELIGIBILITY

### **5.1 Inclusion Criteria**

- Patient age >18 years at point of study commencement
- Histopathologically confirmed diagnosis of soft tissue sarcoma
- FFPE block(s) available within RMH tissue bank
- Details of clinical follow-up available
- Provided generic informed consent for tissue storage and use in future research

*Additional criteria for pilot study:*

- Surgical resection specimen of primary tumour available
- 2 or more tumour-containing blocks available from same specimen, representative of gross spatial separation
- Absence of clinically apparent metastatic disease at time of surgery

*10 randomly selected cases of each synovial sarcoma, gynaecological leiomyosarcoma and non-gynaecological leiomyosarcoma that meet the above criteria will be included in pilot study.*

### **5.2 Exclusion Criteria**

- FFPE tumour samples contain insufficient tumour sample for analysis
- Insufficient clinical details available

## 6: STUDY PROCEDURES

### **6.1: Patient and sample identification**

A list of all potentially eligible patients will be identified from the prospectively maintained RMH sarcoma patient database. All patients who have received management for STS at RMH will be eligible, pending sample availability. Patient identification will be stratified by histological subtype and date of diagnosis to allow for focused identification of samples within tissue archive. All patient personal data will be anonymized by use of a unique numerical ID at the point of extraction from database

Eligible patient lists will be cross-referenced with tumour bank records to identify FFPE samples. Available samples will then be recorded against corresponding anonymized patient details along with pre-specified parameters

### **6.2: Collection and storage of archival tissue samples**

Identified samples will be collected by research team by AL and stored in separate area of RMH tissue bank or within secure FFPE storage facilities within protein networks laboratory, ICR. FFPE slides and TMAs will be kept in sample storage facility at ICR. Both RMH and ICR are HTA licensed premises, with transfer of significant material between sites covered by overarching MTA. FFPE block and slide locations will be prospectively logged in RMH histopathology database and researcher database at ICR. All FFPE blocks will be returned to RMH tissue bank following use and no later than end of study. Extracted DNA, RNA and protein will be kept in freezer facilities at ICR, with sample location recorded in researcher maintained database.

### **6.3: Sample processing**

FFPE tissue section slides, TMA assembly and IHC staining will be carried out by ICR Breakthrough laboratory.

Review of H&E slides and mark-up for TMA core position will be performed in RMH histopathology department by specialist sarcoma consultant histopathologist (KT/CF)

- If prespecified level of acceptable heterogeneity and TMA representativeness is met within pilot study, single area of representative viable tumour will be identified on tumour-containing blocks from 700 patient training set and marked for core extraction to use in TMA assembly

Extraction of DNA and RNA from FFPE slides will be via use of Qiagen AllPrep DNA/RNA FFPE kit. Extraction of protein from FFPE slides will be via use of Qiagen QProteome protein FFPE kit. Quality of extracted nucleic acid/protein will be assessed by spectrophotometric and fluorescence analysis.

#### **6.4: Sample analysis**

Digital images of all FFPE whole tissue section and TMA slides will be taken at x40 magnification on Hamamatsu Nanozoomer 2.0HT microscopic scanner.

Slides images from pilot study samples will be assessed by a consultant histopathologist with staining scored as per a standardised method. Pilot study samples will also be analysed via optimised digital quantification technique on HistoQuest and ImageJ software platforms. If prespecified degree of agreement between manual and digital IHC scoring is met, digital quantification will be utilised for main training set.

IHC analysis scoring for each marker will be recorded in study database via use of data entry forms

#### **6.5: Data analysis**

Data will be anonymised using a unique patient identification number. According to Caldecott principles only relevant information will be collected. Patients will only be identifiable to researchers by anonymised patient number. Clinical tissue samples will be allocated unique identifiers and linked to corresponding patient number. A secure link file will be maintained to allow for reconnection of research material to patient in the unlikely event of new potentially clinically relevant findings arising (for example, disagreement in histopathological diagnosis between researchers and prospective clinical opinion). In such an event, the patient's normal care team will be alerted and will hold responsibility for adjudging clinical significance and according action. A secure database for the study will be housed on a password protected server at the host institution. Demographic, pathology and treatment data will be recorded on this database which will remain on the RMH NHS network.

## 7. STATISTICAL CONSIDERATIONS

### 7.1: Statistical endpoints

- **Primary Endpoint**

- *Pilot study*

- establish the degree of variability in CD3+ lymphocyte infiltrate between tumour blocks taken from the same tumour specimen

- *Main study*

- to establish the proportion of patients with detectable PD-1 and PD-L1 in all STS subtypes and in all STS patients

- **Secondary Endpoints**

- to establish any correlation between tumour PD-1 and/or PD-L1 expression and patient prognosis
  - to evaluate expression of a range of immune markers within STS samples with the aim of deriving a prognostic 'Immunoscore' that is associated with overall survival and recurrence-free survival in a training set (Royal Marsden patients).
  - To validate the Immunoscore through application to validation patient sets from 3 sarcoma referral centre (Royal Orthopaedic Hospital, the University of Munster and the University of Washington) to test Immunoscore's ability to identify discrete prognostic groups. This will be performed for both STS as a disease group and also within individual sarcoma subtypes.

- **Exploratory Endpoints**

- to evaluate the degree of heterogeneity in the immune microenvironment between spatially separated areas of the same tumour
  - to validate the representativeness in terms of immune microenvironment of cores sampled for TMA construction compared to whole tissue sections
  - to investigate any differences in the tumour immune microenvironment between areas of morphological heterogeneity within the same tumour block
  - to validate the use of digital imaging pathology quantification of IHC staining
  - to extract DNA, mRNA and protein from FFPE samples and to establish sample quality for downstream applications
  - **to assess for correlations between expression values of immune-related genes/proteins as assessed by IHC, mRNA transcript quantification and quantitative mass spectrometry-based proteomics**
  - **to identify immune-defined tumour subgroups through unsupervised clustering of integrated IHC, mRNA and mass-spec proteomic data**
  - to compare differences in the patterns of tumour immune microenvironment between primary and metastatic tumour sites, and between pre- and post-neoadjuvant tumour samples, both within paired samples from individual patients and across patient cohorts

## 7.2: Analysis section

### • Primary analyses

- The proportion of patients with detectable PD-1 and PD-L1 will be presented in all individual sarcoma subtypes and in for STS as a whole. The 95% confidence intervals will be presented where appropriate.

### • Secondary Analyses

- Training set:
  - Royal Marsden patients only (700 patients). All IHC markers that are identified (including PD-1, PD-L1, CD3 and CD20) will be tested to check whether they affect overall survival. It is not known which biomarkers will be identified but it is estimated to be around 5-10. Univariate Cox regression analyses will be performed to identify any markers affecting overall survival. Any markers with a p value of less than 0.2 will be entered into multivariate model along with known prognostic variables (age, tumour grade and size of tumour) in a forward stepwise manner with a 5% significance level. A Bonferroni correction will be applied to allow for multiple test of significance. This analysis will be performed for both STS as a disease group and also within individual sarcoma subtypes.
- Validation set:
  - Royal National Orthopaedic Hospital, the University of Munster and University of Washington (700 patients). The above will be repeated to validate the training set in all sarcoma types and in individual types.

### • Exploratory Analyses

This will be analysed in a small sample of 30 patients as below:

#### Heterogeneity in pilot study

3-6 FFPE blocks will be selected from the same tumour specimen to reflect spatially discrete tumour areas from both tumour core and invasive margin. Sections from these blocks will be stained with H&E, anti-CD3, anti-CD20 and anti-PD-L1 and compared to interrogate possible intratumoral heterogeneity of immune infiltrate. There will be descriptive analysis with proportions and 95% confidence intervals where appropriate, and analysed with a Bland Altman plot. For comparison of dichotomised expression values (split into 'high' and 'low' staining based on median values) between tumour blocks, and between digital and manual IHC, proportion of discordance will be calculated together with 95% confidence intervals, as well as the Cohen's  $\kappa$  coefficient of agreement.

#### Representativeness of TMAs in pilot study

3 x 0.6mm cores taken from an area of viable tumour pre-marked by a histopathologist and incorporated into a tissue microarray. TMAs will be stained for CD3, CD20 and PD-L1, with scores compared to a gold standard of scoring of the parent whole tissue section.

The % agreement will be presented between score from the 3 cores and the score from the histopathologist. The % agreement will also be presented between score from the 3 cores and the score from the histopathologist. The 95% confidence intervals will be presented where appropriate.

#### Changes in immune microenvironment between primary/metastatic samples, pre/post neoadjuvant therapy samples

The differences in IHC scoring primary/metastatic samples, pre/post neoadjuvant will be presented as proportions with the appropriate 95% confidence intervals.

Digital imaging quantification

The digital IHC scoring will be compared against the scoring performed manually by a consultant histopathologist. This data will be categorical and % agreement will be presented with the 95% confidence interval.

Heterogeneity between areas of morphological heterogeneity within single tumour blocks

We want to see the differences in IHC profiles between different areas of clear morphological variation. This will be a purely descriptive analysis with proportions and 95% confidence intervals where appropriate.

A fully detailed Statistical Analysis Plan will be written and approved prior to the analysis.

**7.3 Sample Size**

There have been approximately 700 patients identified from the Royal Marsden. From a previous pilot study, the rates of the PD-L1 and PD-1 are as follows:

Histological subtype	PD-L1	PD-1
Liposarcoma	48%	89%
Leiomyosarcoma	58%	90%
Pleomorphic sarcoma	80%	84%
Synovial sarcoma	47%	100%

There is estimated to be 100 patients who have liposarcoma, 100 patients who have leiomyosarcoma, 100 patients who have pleomorphic sarcoma, 100 patients who have synovial sarcoma and a further 300 patients who will be defined as “other”.

The below table shows the widths of the 95% confidence intervals given the rate of PD-L1 or PD-1 by subtype or overall.

	95% confidence interval widths (%) given rate of PD-L1 or PD-1				
N	10 or 90%	20 or 80%	30 or 70%	40 or 60%	50%
100	+/-5.9	+/-7.8	+/-9.0%	+/-9.6	+/-9.8
300	+/-3.4	+/-4.5	+/-5.2	+/-5.3	+/-5.7
700	+/-2.2	+/-3.0	+/-3.4	+/-3.6	+/-3.7

There have been a further 700 patients from Royal National Orthopaedic Hospital, the University of Munster and University of Washington who will be used as the validations set.

There will be a small pilot study which will be purely descriptive. For this there will be roughly 30 patients included. The plan is for 10 of each of the 3 chosen subtypes (synovial sarcoma, gynae leiomyosarcoma, non-gynae leiomyosarcoma) which will be chosen at random.

Eligible patients for pilot study will have:

- Available surgical specimens consisting >1 tumour-containing block
- Localised disease at time of tumour resection

## 8. STUDY ORGANISATION

### **8.1: Regulatory & Ethics Committee Approval**

Local R&D approval will be obtained at each site. Ethical approval will be obtained from the Research Ethics Committee before commencing recruitment and the trial carried out in accordance with the Declaration of Helsinki (1996). The study will be conducted in accordance with the conditions of ethical approval.

### **8.2: Informed Consent**

Informed consent will be obtained in accordance with the following trust policies, all available on RMH intranet:

*Consent to Examination or Treatment Policy (325)*

*Generic Bio banking and Sample Access Policy (2061)*

*Removal, Storage, Use and Disposal of Human Tissue for Research (1691)*

The study will be conducted in accordance with the Human Tissue Act 2004 and Codes of Practice for consent issued by the Human Tissue Authority.

### **8.3: Patient Confidentiality**

Confidential patient information will be treated in accordance with the Data Protection Act 1998 and also in accordance with the CONFIDENTIALITY CODE OF PRACTICE AND DATA PROTECTION POLICY AND PROCEDURE (277)

### **8.4. Data Handling and Record Keeping**

Patient records relating to the study will be kept in a locked filing cabinet in a secure office at the Royal Marsden Hospital. Data will be kept in accordance to the Data Protection Policy (102).

Data will be anonymised using unique Patient Identification numbers. No other patient identifiable information will be kept. Data will be stored in a CRSWeb database.

### **8.5 Financing, Indemnity & Insurance**

BRC grant has been awarded to fund the cost of this study (BRC reference A77Resub)

Where the Royal Marsden NHS Foundation Trust is either sponsoring or collaborating with externally sponsored research the NHS Litigation Authority will cover standard clinical negligence by employees, staff and health professionals employed by the Royal Marsden NHS Foundation Trust.

There is unlimited liability and no excess. Insurance is provided under the Clinical Negligence Scheme for Trusts and there is no cover for non-negligence claims.

For all notification of claims please contact the Board Secretariat.

### **8.6 Publication Policy**

Results from the project will be presented at national and international meetings, e.g. British Sarcoma Group, NCRI, Connective Tissue Oncology Society. We will be in dialogue with our partners in the NCRI Sarcoma Clinical Studies Group regarding the design of future clinical trials.

## 9. REFERENCES

1. Linch, M., Miah, A. B., Thway, K., Judson, I. R. & Benson, C. Systemic treatment of soft-tissue sarcoma-gold standard and novel therapies. *Nat. Rev. Clin. Oncol.* 11, 187–202 (2014).
2. Judson, I. et al. Doxorubicin alone versus intensified doxorubicin plus ifosfamide for first-line treatment of advanced or metastatic soft-tissue sarcoma: a randomised controlled phase 3 trial. *Lancet. Oncol.* 15, 415–23 (2014).
3. Karavasilis, V. et al. Significant clinical benefit of first-line palliative chemotherapy in advanced soft-tissue sarcoma: retrospective analysis and identification of prognostic factors in 488 patients. *Cancer* 112, 1585–91 (2008).
4. Le Cesne, A. et al. Randomized phase III study comparing conventional-dose doxorubicin plus ifosfamide versus high-dose doxorubicin plus ifosfamide plus recombinant human granulocyte-macrophage colony-stimulating factor in advanced soft tissue sarcomas: A trial of the Europe. *J. Clin. Oncol.* 18, 2676–84 (2000).
5. Burgess, M., Gorantla, V., Weiss, K. & Tawbi, H. Immunotherapy in Sarcoma: Future Horizons. *Curr. Oncol. Rep.* 17, 52 (2015).
6. Robbins, P. F. et al. Tumor Regression in Patients With Metastatic Synovial Cell Sarcoma and Melanoma Using Genetically Engineered Lymphocytes Reactive With NY-ESO-1. *J. Clin. Oncol.* 29, 917–924 (2011).
7. Clemente, C. G. et al. Prognostic value of tumor infiltrating lymphocytes in the vertical growth phase of primary cutaneous melanoma. *Cancer* 77, 1303–10 (1996).
8. Aust, S. et al. Determination of tumor-infiltrating CD8+ lymphocytes in human ovarian cancer. *Int. J. Gynecol. Pathol.* 32, 269–276 (2013).
9. Bachmayr-Heyda, A. et al. Prognostic impact of tumor infiltrating CD8+ T cells in association with cell proliferation in ovarian cancer patients--a study of the OVCAD consortium. *BMC Cancer* 13, 422 (2013).
10. Adams, S. et al. Prognostic Value of Tumor-Infiltrating Lymphocytes in Triple-Negative Breast Cancers From Two Phase III Randomized Adjuvant Breast Cancer Trials: ECOG 2197 and ECOG 1199. *J. Clin. Oncol.* 32, 2959–2966 (2014).
11. Fridman, W. H., Pagès, F., Sautès-Fridman, C. & Galon, J. The immune contexture in human tumours: impact on clinical outcome. *Nat. Rev. Cancer* 12, 298–306 (2012).
12. Issa-Nummer, Y., Loibl, S., von Minckwitz, G. & Denkert, C. Tumor-infiltrating lymphocytes in breast cancer: A new predictor for responses to therapy. *Oncoimmunology* 3, e27926 (2014).
13. Galon, J. et al. Type, Density, and Location of Immune Cells Within Human Colorectal Tumors Predict Clinical Outcome. 313, 1960–1965 (2006).
14. Galon, J. et al. Towards the introduction of the 'Immunoscore' in the classification of malignant tumours. *J. Pathol.* 232, 199–209 (2014).

15. Sorbye, S. W. et al. Prognostic Impact of Lymphocytes in Soft Tissue Sarcomas. *PLoS One* 6, e14611 (2011).
16. Sorbye, S. W. et al. Prognostic impact of peritumoral lymphocyte infiltration in soft tissue sarcomas. *BMC Clin. Pathol.* 12, 5 (2012).
17. Berghuis, D. et al. Pro-inflammatory chemokine-chemokine receptor interactions within the Ewing sarcoma microenvironment determine CD8(+) T-lymphocyte infiltration and affect tumour progression. *J. Pathol.* 223, 347–357 (2011).
18. Fujii, H. et al. CD8 + tumor-infiltrating lymphocytes at primary sites as a possible prognostic factor of cutaneous angiosarcoma. *Int. J. Cancer* 134, 2393–2402 (2014).
19. Tseng, W. W. et al. Analysis of the Intratumoral Adaptive Immune Response in Well Differentiated and Dedifferentiated Retroperitoneal Liposarcoma. *Sarcoma* 2015, 1–9 (2015).
20. Lee, C.-H. et al. Prognostic significance of macrophage infiltration in leiomyosarcomas. *Clin. Cancer Res.* 14, 1423–30 (2008).
21. Nabeshima, A. et al. Tumour-associated macrophages correlate with poor prognosis in myxoid liposarcoma and promote cell motility and invasion via the HB-EGF-EGFR-PI3K/Akt pathways. *Br. J. Cancer* 112, 547–55 (2015).
22. Kim, J. R. et al. Tumor Infiltrating PD1-Positive Lymphocytes and the Expression of PD-L1 Predict Poor Prognosis of Soft Tissue Sarcomas. *PLoS One* 8, e82870 (2013).
23. D'Angelo, S. P. et al. Prevalence of tumor-infiltrating lymphocytes and PD-L1 expression in the soft tissue sarcoma microenvironment. *Hum. Pathol.* 46, 357–65 (2015).
24. Pollack, S. M., Loggers, E. T., Rodler, E. T., Yee, C. & Jones, R. L. Immune-Based Therapies for Sarcoma. 2011, (2011).
25. Pollack, S. et al. NY-ESO-1 is a Ubiquitous Immunotherapeutic Target Antigen for Patients with Myxoid/ Round Cell Liposarcoma. *Cancer* 118, 4564–4570 (2013).